CONSERVED AND DIVERGENT ROLES OF DELLA PROTEINS IN *PHYSCOMITRIUM (PHYSCOMITRELLA) PATENS*

by

ALEXANDROS PHOKAS

A thesis submitted to the University of Birmingham

for the degree of

DOCTOR OF PHILOSOPHY

School of Biosciences

College of Life and Environmental Sciences

University of Birmingham

March 2021

Statement regarding the publication of work in this thesis

This is to state that the majority of the content of Chapter 1, parts from the introduction of Chapters 3 and 4, and parts from Chapter 6 have already been published as a synthetic review in the peer-reviewed journal *Evolution & Development* in January 2021 (**https://doi.org/10.1111/ede.12365**). The two authors of the published review declare that the content of the present thesis belongs solely to Alexandros Phokas, who is the first author of the review. Dr Juliet Coates contributed by providing constructive feedback throughout the writing process, discussing structure and figure development and making minor corrections on the manuscript. There is no possibility of retrospective dispute regarding the ownership of this work.

Alexandros Phokas
First Author

Dr Juliet Coates
Senior Author

Abstract

DELLA proteins are master growth regulators that repress responses to the phytohormones gibberellins (GAs). Manipulation of DELLA signalling was instrumental in the development of high-yielding crop varieties that saved millions from starvation during the “Green Revolution”. In order to infer how DELLA signalling has evolved within the land plant lineage, the functions of DELLA proteins in the bryophyte *Physcomitrium (Physcomitrella) patens* were examined in the present study. It was found that *Pp*DELLAs are regulated differently from flowering DELLA proteins, as they are not degraded by diterpenes, they do not interact with GID1 homologues, they are not directly regulated by the 26S proteasome and they do not regulate abiotic stress responses. However, similarly to flowering plant DELLAs, they are involved in the regulation of reproductive development and they act as transcriptional ‘hubs’, possibly interacting with transcription factors belonging to similar families as flowering plant DELLA interactors. Using IP-MS and yeast two-hybrid, three photoreceptors were identified as *Pp*DELLA protein-protein interactors, however no involvement of *Pp*DELLAs in light responses was observed. In addition, while the Arabidopsis DELLA *At*RGA1 did not interact with the seed dormancy regulator *At*DOG1, *Pp*DELLAs interacted with *Pp*DOG1s, and the two proteins displayed similar functions in spore germination. This work shows that DELLA proteins in *P. patens* have both conserved and divergent functions. Unravelling how *Pp*DELLAs function at the molecular level may provide novel ways of genetic modification that can be used to engineer better crops and contribute towards mitigating the effects of global warming and achieving global food security.

Acknowledgements

I would like to thank my supervisor Dr Juliet Coates for her immense support throughout the course of this PhD, from the application process back in 2016 to thesis submission in 2021. Her role has been instrumental in my development as a scientist, an educator, and a human being.

I am also grateful to Professor Dan Gibbs for always providing support eagerly when asked, for constructive discussions on experimental design and especially for providing feedback on my thesis manuscript.

In addition, I would like to thank all the fantastic people from the Plant Science theme at the University of Birmingham, who provided both emotional and technical support to me over the past five years. Especially my fellow Coates lab members Xulyu Cao and Dr Clare Clayton, the Gibbs lab members Dr Mark Bailey, Dr Anne Marie Labandera and Ross Etherington, as well as Dr Alice Darbyshire and Dr Andrew Plackett. Their support has been vital for my wellbeing and my work. Also, a big thank you to the staff from Central Services, Stores, the Glasshouse facility, the BALM facility and the Proteomics and Genomics Facilities for their important contributions.

I am also grateful to Professor Stefan Rensing and Dr Rabea Meyberg from the University of Marburg, for collaborative work included in Chapters 3 and 5, Professor Miguel Blázquez, Dr Asier Briones-Moreno and Jorge Hernández-García from the Institute for Plant Molecular and Cell Biology (IBMCP, Valencia) for collaborative work

included in Chapter 4, Professor Peter Hedden from Rothamsted Research for provision of diterpene supplies, as well as Professor Nicholas Harberd from the University of Oxford for provision of mutant lines.

Last but not least, I would like to thank the Biotechnology and Biological Sciences Research Council (BBSRC) for their generous financial support and for granting me an extension due to the unprecedented circumstances created by the pandemic, as well as the Society of Experimental Biology (SEB) for providing funding for me to attend the SEB Conference in Florence in 2018, which I will always remember as one of the most beautiful experiences of my life.

Contents

List of figures

List of tables

CHAPTER 1: Introduction

1.1 Introduction

Global food security and global warming are two interlinked critical issues that the world is facing at present. Current projections suggest that global food production will need to increase by at least 50% by 2050 if an estimated world population of 9-10 billion is to be fed (Smith and Gregory, 2013). Increased flooding, heat stress and chilling injuries resulting from current and future global warming, are also expected to have detrimental effects on crop yields (The Royal Society, 2009). Improving yields and sustainability of crops by genetic modification has the potential to contribute towards the goal of achieving food security and alleviating the effects of global warming (Qaim and Kouser, 2013).

In the 1960s and 1970s, a similar food crisis was managed by the "Green Revolution", an initiative that was characterised by increased application of fertilisers and pesticides as well as the production of semi-dwarf wheat and rice varieties with higher grain yields, reduced lodging and higher tolerance to large amounts of fertiliser (Gale and Youssefian, 1985; Hedden, 2003). As a consequence of the "Green Revolution", crop yields in developing countries increased initially by 21% and after the 1970s by 50%, global food prices fell significantly, and millions of people were saved from starvation (Evenson and Gollin, 2003). Subsequent research led to the identification of the alleles of genes responsible for conferring those semi-dwarf phenotypes. Among these, were the wheat alleles *REDUCED HEIGHT (TaRHT)-B1b* and *TaRHT-D1b*, whose corresponding genes encode DELLA proteins (Peng *et al*., 1999).

Given that current crop varieties are unlikely to be able to withstand future climatic and edaphic changes, a similar 'revolution' will need to happen again to

address the need for increased food production (Ribeiro *et al.,* 2012). As DELLA proteins have a key role in integrating environmental signals to regulate growth responses, manipulation of DELLA signalling by genetic modification constitutes one of the potential avenues via which food insecurity can be tackled (Claeys *et al*., 2014). Unravelling how DELLA proteins function at the molecular level in response to environment signals and how their signalling mechanisms have evolved can enable us to engineer better crops in an attempt to contribute towards mitigating the effects of global warming and achieving global food security.

1.2 DELLA proteins: repressors of vascular plant gibberellin (GA) responses

DELLA proteins are master growth repressors belonging to the GRAS (named after GIBBERELLIN INSENSITIVE (GAI), REPRESSOR OF GA1-3 (RGA) and SCARECROW (SCR)) family of putative transcriptional regulators (Peng *et al*., 1997; Pysh *et al*., 1999). They are present exclusively in land plants and they vary in numbers between species (Hernández-García *et al*., 2019). Some species have just a single DELLA protein, such as rice (SLENDER RICE1, *Os*SLR1), barley (SLENDER1, *Hv*SLN1) and tomato (PROCERA, *Sl*PRO or *Sl*DELLA) (Ikeda *et al*., 2001; Gubler *et al*., 2002; Jasinski *et al*., 2008), while others have more than one; for example *Arabidopsis thaliana* has five: *At*GAI1, *At*RGA1, *At*RGA-LIKE1 (*At*RGL1), *At*RGL2 and *At*RGL3, which have distinct and overlapping functions (Peng and Harberd 1993; Silverstone *et al*., 1997; Sánchez-Fernández *et al*., 1998; Dill and Sun, 2001).

DELLA proteins get their name from five conserved amino acids (aspartic acid, glutamic acid, leucine, leucine, and alanine), present in their N-terminal domain. This domain is important for their regulatory function and is absent in other GRAS family

proteins such as *At*SCR. The primary role of DELLA proteins in vascular plants is to repress responses to a group of structurally related plant hormones, gibberellins (GAs), which promote many major developmental responses in plants, such as germination, stem elongation, leaf expansion and flowering (Olszewski *et al.,* 2002). As DELLAs do not possess a DNA-binding domain, they exert their repression on GA responses by interacting mainly with transcription factors that regulate these responses (Feng *et al*., 2008).

1.3 The evolution of DELLA proteins in land plants: An overview

The evolution of DELLA proteins in land plants has attracted the attention of researchers for over a decade now. With the recent increase in the availability of genomic and transcriptomic data, we are now starting to get a clearer picture of how DELLA proteins evolved in the different land plant lineages. Independent phylogenetic analyses have suggested that two duplication events have occurred in the history of DELLA protein-encoding genes: the first one in the ancestor of vascular plants and the second one in eudicot flowering plants (Figure **1.1**) (Van De Velde *et al*., 2017; Hernández-García *et al.*, 2019). Consequently, non-vascular plants (bryophytes) possess a single DELLA clade, termed DELLA1/2/3 (Hernández-García *et al.*, 2020), vascular plants (excluding eudicots) possess a DELLA1/2 clade and a DELLA3 clade, and eudicots have three DELLA clades termed DELLA1 or RGA, DELLA2 or RGL and DELLA3 or DGLLA (Figure **1.1**) (Van De Velde *et al*., 2017; Hernández-García *et al.*, 2019).

Interestingly, ferns appear to lack the DELLA1/2 clade and several flowering plant species have lost clades or have undergone further DELLA duplications

(Hernández-García *et al.*, 2019). For example, in tomato, a eudicot flowering plant, the DELLA1 and DELLA3 clades have been lost, while in rice, a monocot flowering plant, DELLA3 clade proteins have lost their N-terminal DELLA domains, but have retained their ability to repress growth (Jasinski *et al*., 2008; Itoh *et al*., 2005b). It has been suggested that rice DELLA3 clade proteins may be part of a mechanism that evolved to inhibit growth under certain conditions where levels of the rice DELLA1/2 clade protein (*Os*SLR1) are low (Itoh *et al*., 2005b; Van De Velde *et al*., 2017). Whether this is a common property among DELLA3 clade proteins remains unknown.

In addition, the increased number of DELLA proteins found in some flowering plant species does not correlate with increased diversity of DELLA functions, as single DELLA proteins in rice or tomato perform the same functions as the five Arabidopsis DELLAs collectively (Blázquez *et al*., 2020). Instead, it appears that the diversification of DELLA functions in species with multiple DELLA proteins, such as Arabidopsis, is a consequence of the diversification in their expression patterns, rather than the ability of different DELLAs to interact with different partners (Gallego-Bartolomé *et al.*, 2010). This conclusion is based on the fact that (i) transcription factors or regulators that interact with DELLA proteins mostly do not discriminate between the different DELLA proteins within a species (e.g. Lantzouni *et al*., 2020; Gallego-Bartolomé *et al.*, 2010) and that (ii) DELLAs such as *At*RGA1 and *At*RGL2, which mostly regulate hypocotyl elongation and germination respectively, can perform exchangeable functions when expressed under each other's promoter (Gallego-Bartolomé *et al.*, 2010). Under this hypothesis, DELLA proteins would have started with a general growth repressive function, which would have then been refined in a tissue-specific manner, for example the repression of germination by *At*RGL2 in Arabidopsis seeds.

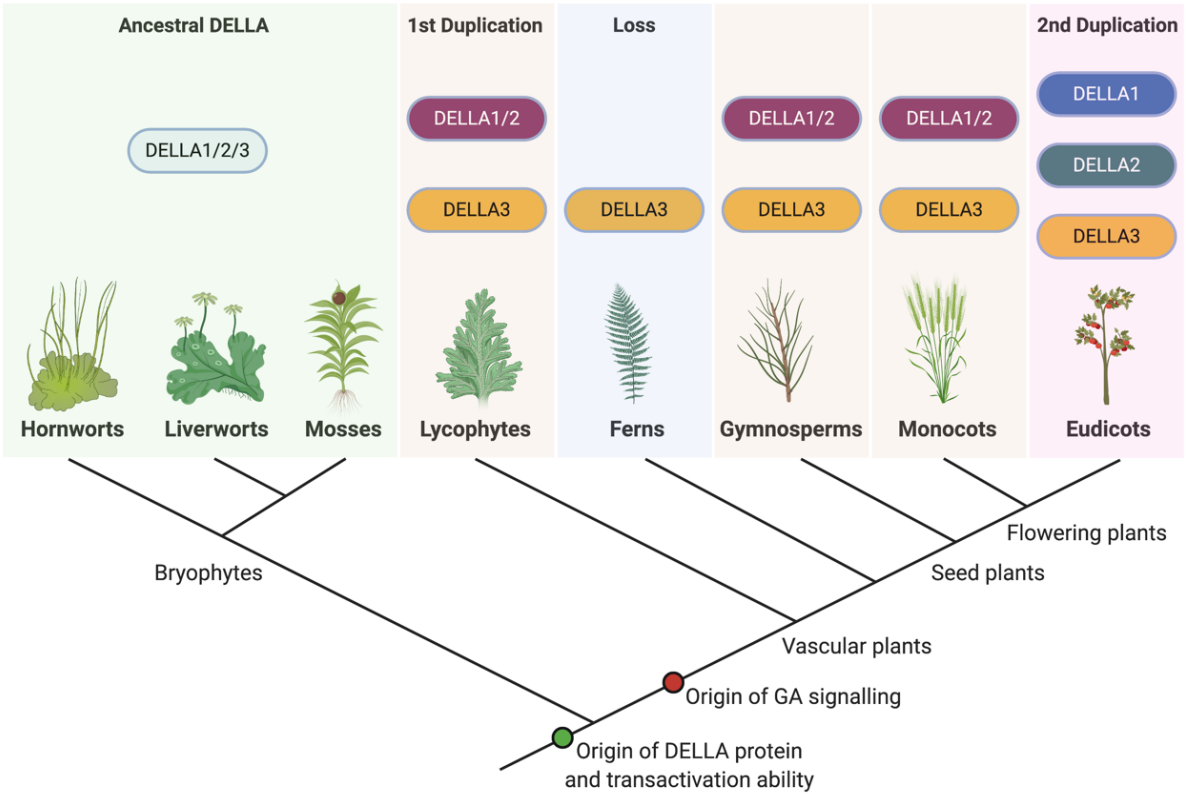

Figure 1.1. The evolution of DELLA proteins in land plants. DELLA protein-encoding genes (DELLA1/2/3 clade) appeared in the ancestor of land plants and were maintained in bryophytes without any major duplications. The first major duplication of DELLA-encoding genes occurred in the ancestor of vascular plants, giving rise to the DELLA1/2 and DELLA3 clades, which were maintained in gymnosperms and monocot flowering plants. In ferns, the DELLA3 clade was retained, but DELLA1/2 was lost. The second major duplication of DELLA-encoding genes happened in eudicot flowering plants, where the DELLA1/2 clade gave rise to the DELLA1 and DELLA2 clades, while DELLA3 was retained. Further duplications and/or losses have also occurred in several flowering plant species or families. DELLA transactivation ability originated in the ancestor of land plants and canonical gibberellin (GA) signalling in the ancestor of vascular plants (Figure created with BioRender.com; hornwort icon drawn by Debbie Maizels).

1.4 Lifting the growth repressive function of DELLAs via GA signalling

DELLA-induced repression of GA responses can be overcome by GAs themselves in a dose-dependent manner (Itoh *et al.*, 2002). GAs are perceived by GA-INSENSITIVE DWARF1 (GID1) receptors, which bind GAs in a pocket-like structure (Figure **1.2**) (Ueguchi-Tanaka *et al.*, 2005; Murase *et al.*, 2008). This interaction triggers a GID1 N-terminal extension to fold back and form a lid-like structure that

secures GA into the GID1 pocket, preventing the former from coming into contact with DELLAs (Ueguchi-Tanaka *et al*., 2005; Murase *et al*. 2008; Shimada *et al*., 2008). The GA-GID1 complex formed is then able to sequester DELLA proteins in the nucleus, an interaction that requires the N-terminal DELLA domain (Ueguchi-Tanaka *et al*., 2005, 2007). Binding of the DELLA domain to the GID1 lid stabilises the GA-GID1 complex further and presumably triggers a conformational change in the C-terminal GRAS domain of DELLA, allowing F-box proteins, such as *Os*GID2 in rice, or SLEEPY1 (*At*SLY1) in Arabidopsis, which form part of an SKP1-CUL1-F-box (SCF) E3 ligase complex, to bind DELLAs and polyubiquitinate them (McGinnis *et al*., 2003; Sasaki *et al*., 2003; Ueguchi-Tanaka *et al*., 2007; Hirano *et al*., 2010). Polyubiquitinated DELLAs are then degraded by the 26S proteasome and repression on GA responses is lifted (Figure **1.2**) (Fu *et al*., 2002; Sasaki *et al*., 2003).

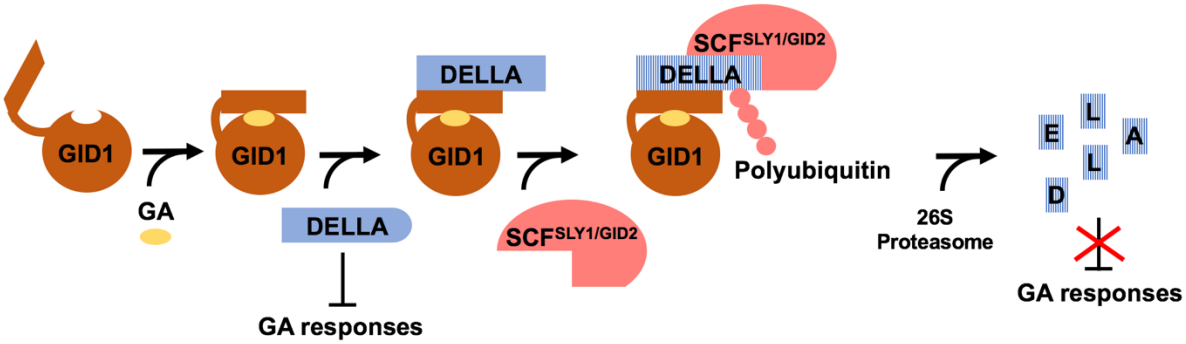

Figure 1.2. DELLA proteins repress gibberellin (GA) responses in vascular plants and DELLA repression is lifted by GAs via DELLA degradation. The GA receptor, GID1, perceives GA and secures it within its GA-binding pocket using its N-terminal lid-like structure. The GA–GID1 complex can then sequester DELLA protein, enabling an SKP1-CUL1-F-box (SCF) E3 ligase complex containing an F-box protein such as SLEEPY1 (SLY1) in *Arabidopsis thaliana* or GID2 in rice, to induce DELLA polyubiquitination and subsequent degradation via the 26S proteasome. DELLA degradation then releases GA responses from repression.

DELLA repression can also be overcome in a proteolysis-independent manner via interaction with the GA-GID1 complex, which reduces DELLA repression in *Atsly1*

mutants where *At*GID1 has been overexpressed (Ariizumi *et al*., 2008). Furthermore, a recent study has demonstrated that the DELLA interaction with *At*GID1 can be inhibited by the circadian clock component GIGANTEA (*At*GI), which can bind and stabilise DELLA during daytime under short-day conditions, thus regulating the diurnal rhythmic accumulation pattern of DELLA proteins (Nohales and Kay, 2019). In addition, *At*GID1 expression levels are also regulated by the circadian clock under short-day conditions, promoting DELLA degradation and increased GA sensitivity during the night (Arana *et al*., 2011).

1.5 DELLA protein function and regulation: implications for evolution

DELLA proteins possess a characteristic domain structure that appears largely conserved across land plants (Hernández-García *et al.*, 2019). How has DELLA protein function diversified throughout land plant evolution? The evidence from flowering plants suggests that DELLAs can indirectly regulate transcription via different mechanisms involving interactions with transcription factors (e.g. Feng *et al*., 2008; de Lucas *et al*., 2008). However, the transcriptional targets of DELLA-transcription-factor complexes are only characterised in a few flowering plants. In addition, there are multiple ways in which DELLA proteins themselves are post-translationally modified to regulate their function, and these have also only been characterised in flowering plants. The following sections outline the variety of known DELLA functions and regulatory mechanisms and propose ways in which the degree of their conservation across land plants can be examined. This knowledge will be relevant for understanding how DELLA function diversified from the ancestral land plant DELLA protein.

1.5.1 DELLA proteins: structure and function

DELLA proteins are made up of an N-terminal DELLA domain and a C-terminal GRAS domain, which are linked together by a homopolymeric region rich in serine, threonine and valine (polyS/T/V), a site for post-translational modifications that affect the stability and activity of DELLA proteins (Figure **1.3**) (Itoh *et al*., 2002; Fu *et al*., 2002; Itoh *et al*., 2005a). Plant *della* gene mutants have been widely studied over the past three decades in order to shed light on the precise role of the different subdomains and motifs that make up these domains. These mutants can be divided into two categories: (i) dominant gain-of-function mutants, which render the DELLA protein unable to be degraded and give rise to GA-insensitive dwarf plants, and (ii) loss-of-function mutants lacking DELLA activity, which give rise to slender plants with constitutively activated GA responses (Peng *et al*., 1997; Silverstone *et al*., 1998). The "Green Revolution" mutants *Tarht-B1b* and *Tarht-D1b* belong to former category (Peng *et al*., 1999).

Functional characterisation of *Tarht-B1b* and *Tarht-D1b* revealed that they have nucleotide substitutions that generate a stop codon in the N-terminal domain (Peng *et al*., 1999). Due to a translation initiation site downstream of the generated stop codon, these genes give rise to active proteins lacking the DELLA domain (Peng *et al*., 1999; Van de Velde *et al*., 2021). Similar gain-of-function mutants have also been identified in *Arabidopsis thaliana*, for example *Atgai-1*, which synthesises a DELLA that lacks 17 amino acids in its N-terminus corresponding to the DELLA domain (Peng *et al*., 1997). These mutants produce active truncated DELLA proteins that can no longer interact with the GA-GID1 complex, are resistant to GA-induced degradation and are therefore

constitutively repressing GA responses, yielding semi-dwarf phenotypes (Dill *et al*., 2001; Itoh *et al*., 2002).

Several lines of evidence have confirmed that the DELLA, LEQLE and VHYNP motifs within the DELLA domain are necessary for GA-dependent interaction with GID1 and GA-induced degradation (Figure **1.3**) (Itoh *et al*., 2002; Ueguchi-Tanaka *et al*., 2007). In addition, the N-terminal DELLA domain is also responsible for the conserved transactivation activity of DELLA proteins that ultimately represses GA responses (Hirano *et al*., 2012; Hernández-García *et al.*, 2019). This transactivation activity can be suppressed by interaction with GID1 (Hirano *et al*., 2012). It has been demonstrated that DELLA transactivation activity is conserved at least in bryophytes and lycophytes, however the targets of transactivation have not yet been elucidated (Hernández-García *et al.*, 2019).

The repressive function of DELLA proteins on GA responses by means other than transactivation has been attributed to their C-terminal GRAS domain (Figure **1.3**) (Hirano *et al*., 2010). This domain is necessary for the interaction of DELLA with *At*SLY1 or *Os*GID2 and subsequent DELLA degradation (Dill *et al*., 2004; Muangprom *et al*., 2005). Removal of the GRAS domain from the VHIID subdomain to the end of the protein sequence results in the induction of a loss-of-function slender phenotype, indicating that the GRAS domain is responsible for growth suppression (Itoh *et al*., 2002). A similar slender phenotype is also observed with single amino acid changes in the PFYRE or SAW subdomains located at the C-terminal end of the GRAS domain, indicating that these subdomains have key roles in growth repression (Figure **1.3**) (Itoh *et al*., 2002). Studies have also demonstrated that apart from PFYRE and SAW, the other three major GRAS subdomains, VHIID and two leucine heptad repeat (LHR)

subdomains: LHR1 and LHR2, are also involved in growth repression, although presumably VHIID and LHR2 to a lesser extent (Figure **1.3**) (Bassel *et al*., 2008; Hirano *et al*., 2010; 2012).

The growth repression activity of the GRAS domain is mediated by DELLA protein-protein interactions (e.g. de Lucas *et al*., 2008; Bai *et al*., 2012). These interactions have almost exclusively been characterised in flowering plants, therefore the degree of their conservation remains elusive (see section **1.5.4** and Chapter 4, section **4.1**).

DELLA interaction with *At*SLY1/*Os*GID2 requires the VHIID and LHR2 domains, as amino acid substitutions in those subdomains abolish the interaction, even in the presence of GID1 and GA (Hirano *et al*., 2010). In addition to their involvement in growth suppression, the PFYRE and SAW subdomains have also been shown to interact with GID1, contributing to the stabilisation of the GA-GID1-DELLA complex and facilitating DELLA recognition by *At*SLY1/*Os*GID2 (Hirano *et al*., 2010). The LHR1 subdomain enables DELLA dimer formation and is required for protein-protein interactions with transcription factors regulating GA responses (Itoh *et al*., 2002; de Lucas *et al*., 2008; Bai *et al*., 2012). Another conserved motif on the GRAS domain is the nuclear localisation signal (NLS) motif, which is responsible for the localisation of DELLA proteins in the nucleus (Figure **1.3**) (Silverstone *et al*., 1998).

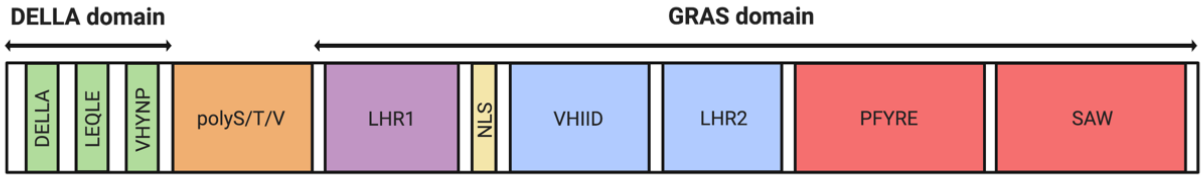

Figure 1.3. DELLA protein domain structure. The N-terminal DELLA domain contains the DELLA, LEQLE, and VHYNP motifs required for interaction with GA-GID1 and GA-dependent degradation. The C-terminal GRAS domain consists of two leucine heptad repeat (LHR) subdomains: LHR1, which is required for protein–protein interactions mediating repression on GA responses, and LHR2, which along with the VHIID subdomain are required for DELLA interaction with SLEEPY1 or GID2. The C-terminal PFYRE and SAW subdomains are involved in repression on GA responses and interaction with GID1. The GRAS domain also contains a nuclear localization signal (NLS) motif. The N-terminal and C-terminal domains are linked with a homopolymeric region rich in serine, threonine, and valine (polyS/T/V), which is involved in post-translational modifications (Figure created with BioRender.com).

1.5.2 DELLA post-translational modifications (PTMs)

DELLA proteins are known to undergo several types of PTMs (reviewed in Blanco-Touriñán *et al*., 2020b), namely polyubiquitination (Sasaki *et al.*, 2003), phosphorylation (Wang *et al*., 2014), glycosylation (Zentella *et al*., 2017) and Small Ubiquitin-like Modifier (SUMO)-ylation (Conti *et al*., 2014). Due to its agronomic relevance, the most well-characterised post-translational modification of DELLA proteins is polyubiquitination, which occurs via the $SCF^{SLY1/GID2}$ complex and is necessary for proteasomal degradation of DELLAs (Sasaki *et al.*, 2003). In addition, it has been demonstrated that DELLA degradation can also be induced by the E3 ubiquitin ligase CONSTITUTIVE PHOTOMORPHOGENIC1 (*At*COP1) via ubiquitination in a GA-independent manner upon exposure to warm temperatures or shade (Blanco-Touriñán *et al*., 2020a). A recent study has also suggested that DELLA ubiquitination and degradation can be induced by the E3 ubiquitin ligase FLAVIN-BINDING KELCH REPEAT F-BOX1 (*At*FKF1) to promote flowering under long-day conditions (Yan *et al*., 2020). However, the involvement of *At*FKF1 in direct

polyubiquitination of DELLA proteins has not been confirmed by *in vitro* assays, as in Blanco-Touriñán *et al*. (2020a), neither has it been demonstrated that the mechanism acts in a GA/GID1-independent manner, for example by showing whether *At*FKF1 affects the stability of *At*gai-1 or *At*rgaΔ17.

Other DELLA modifications affecting DELLA stability, such as phosphorylation, have also been described. Sasaki *et al.* 2003 demonstrated that *Os*SLR1 phosphorylation increases upon GA application in an *Osgid2* mutant background. This was initially supported by the observation that *Os*GID2 interacts only with phosphorylated *Os*SLR1 in an *in vitro* binding assay (Gomi *et al*., 2004); however it was later shown that neither GA-induced *Os*SLR1 degradation nor *Os*SLR1-*Os*GID2 interaction require *Os*SLR1 phosphorylation and that *Os*SLR1 phosphorylation can be induced independently of GA (Itoh *et al*., 2005a).

Studies in barley have shown that GA-induced *Hv*SLN1 degradation can be inhibited with the application of phosphatase inhibitors or tyrosine kinase inhibitors, suggesting a role for phosphorylation in GA signalling (Fu *et al*., 2002). In line with these observations, it was also demonstrated that GA-induced *At*RGL2 or *At*RGA1 degradation can be inhibited by treatment with serine/threonine phosphatase inhibitors, indicating that dephosphorylated DELLA is less stable in barley and Arabidopsis (Hussain *et al*., 2005; Wang *et al*., 2009). Further support for a role of phosphorylation in GA signalling was provided by Dai and Xue (2010), who showed that phosphorylation of *Os*SLR1 by a casein kinase I, EARLIER FLOWERING1 (*Os*EL1), makes the rice DELLA more stable, and that lack of *Os*SLR1 phosphorylation in an *Osel1* mutant reduces DELLA repression on GA responses. Similarly, overexpressing *At*RGA1 with six serine or threonine residues substituted with alanine,

to mimic constitutive dephosphorylation, induces early flowering and a slender phenotype in wild-type Arabidopsis, suggesting that dephosphorylated DELLAs are less capable of repressing GA responses (Wang *et al*., 2014). When the same residues are substituted with aspartic acid, to mimic constitutive phosphorylation, dwarfing and sterility is induced and *At*RGA1 is much more stable under GA treatment, suggesting that phosphorylation increases DELLA stability (Wang *et al*., 2014).

Recent evidence also suggests that apart from phosphorylation, DELLA proteins undergo *O*-fucosylation by SPINDLY (*At*SPY), a post-translational modification that potentially induces an open confirmation on DELLAs, enhancing binding to interacting transcription factors and thus promoting growth repression (Zentella *et al*., 2017). An *At*SPY paralogue, SECRET AGENT (*At*SEC), has also been identified in Arabidopsis, whose role is to catalyse DELLA *O*-linked N-acetylglucosamine modification (*O*-GlcNAcylation), which reduces interactions with transcription factors such as PHYTOCHROME INTERACTING FACTORS (*At*PIFs) (Zentella *et al*., 2016). Major overlap between the sites of *O*-fucosylation and *O*-GlcNAcylation in the polyS/T/V domain and an N-terminal LSN peptide suggests that *At*SEC-induced *O*-GlcNAcylation antagonises *At*SPY-induced *O*-fucosylation by potentially promoting a closed DELLA conformation, which weakens binding to interacting transcription factors, thus enhancing growth derepression (Zentella *et al*., 2017).

Another way that DELLA proteins appear to be regulated post-translationally is by SUMOylation (Conti *et al*., 2014). Conjugation of SUMO to DELLA protein enables binding to *At*GID1 in a GA-independent manner. This in turn reduces the availability of free *At*GID1 receptors and by extension the degradation of non-SUMOylated DELLA

proteins, enabling increased growth repression, especially under salt stress conditions. The fact that DELLA proteins can be both polyubiquitinated and SUMOylated allows us to speculate that the two mechanisms may be counteracting each other, as they commonly do in other pathways; for example ABSCISIC ACID INSENSITIVE5 (*At*ABI5) SUMOylation inhibits abscisic acid (ABA)-induced polyubiquitination (Miura *et al.*, 2009). However, both SUMOylated and non-SUMOylated forms of DELLA can be degraded upon GA application, suggesting that SUMOylation cannot prevent GA-induced DELLA polyubiquitination and subsequent degradation (Conti *et al*., 2014). Furthermore, DELLA SUMOylation is mediated by a lysine (K) residue in the N-terminal DELLA domain (e.g. *At*RGA1^{K65}, *At*GAI^{K49}), which is involved in binding to the GID1 lid upon formation of the GA-GID1 complex, and is thus unlikely to be a site for polyubiquitination (Murase *et al*., 2008; Conti *et al*., 2014).

While all DELLA PTMs have been extensively characterised in Arabidopsis and few other flowering plants, their relevance within non-flowering plant DELLAs is currently unknown. In the case of SCF$^{SLY1/GID2}$ induced polyubiquitination, although lycophyte and fern DELLAs can be degraded in a GA-dependent manner (Yasumura *et al*., 2007; Tanaka *et al*., 2014) and species belonging to these plant lineages possess *At*SLY1 homologues (Hernández-García *et al.*, 2019), fern or lycophyte DELLA polyubiquitination has not yet been experimentally confirmed.

In bryophytes, it appears that only liverworts have *At*SLY1 homologues (Hernández-García *et al.*, 2019), but it is currently unknown if these homologues can induce DELLA polyubiquitination and degradation. Even more intriguing is the case of mosses and hornworts, which appear to lack *At*SLY1 homologues (Hernández-García *et al.*, 2019), and therefore if DELLA polyubiquitination is present, it is mediated by

other proteins. As bryophytes do not synthesise GAs (Hernández-García *et al.*, 2020) and *At*COP1 can induce DELLA polyubiquitination in a GA-independent manner in Arabidopsis (Blanco-Touriñán *et al*., 2020a), *At*COP1 orthologues might be good candidates for bryophyte DELLA polyubiquitination. Bryophytes, such as *Physcomitrella patens (*now *Physcomitrium patens*; Rensing *et al*., 2020), have orthologues of *At*COP1 (Ranjan *et al*., 2014). It would be interesting to test whether *Pp*COP1 proteins can interact with *Pp*DELLA and induce polyubiquitination, to investigate whether this important PTM is conserved in bryophytes and infer whether it was a property of the ancestral DELLA protein that was maintained during evolution.

1.5.3 DELLA downstream transcriptional targets

Flowering plant DELLA proteins have numerous and diverse transcriptional targets. Transcriptomic analyses using overexpression of DELLA proteins or mutants in GA biosynthesis or signalling (reviewed in Locascio *et al*., 2013b) have been carried out, in order to elucidate the mechanisms by which DELLAs repress GA responses. Cao *et al.*, (2006) used microarray hybridisation in a quadruple *della* mutant line in an *Atga1-3* (GA biosynthesis) mutant background (*Atgai-t6 Atrga-t2 Atrgl1-1 Atrgl2-1 Atga1-3*) and compared gene expression with an *Atga1-3* mutant line, to identify DELLA-induced transcriptional changes occurring in imbibed seeds and unopened flower buds. As germination in Arabidopsis is regulated by *At*RGL2 primarily as well as *At*GAI and *At*RGA1, and flowering by *At*RGL1, *At*RGL2 and *At*RGA1, the choice of the quadruple knockout should have been sufficient to enable identification of gene targets regulated by DELLAs during these developmental stages (Cao *et al*, 2006). Collectively, transcriptional changes were observed in the expression of genes

involved in cell growth and cell wall loosening, such as pectinesterases and expansins (most of which were repressed by DELLA), genes involved in protein phosphorylation, genes encoding transcription factors belonging to the MYB, bHLH, WRKY and MADS-box families, and genes regulating responses to disease, stress and hormones (Cao *et al.*, 2006). Some overlap was observed between DELLA-induced gene expression in imbibed seeds and unopened flower buds, but a significant amount of transcriptional changes were tissue-specific, suggesting that DELLA function is tightly linked to its expression patterns in the different tissues (Cao *et al.*, 2006; Gallego-Bartolomé *et al.*, 2010).

Zentella *et al*. (2007) attempted to identify direct DELLA targets using microarray analysis after treating *Atga1-3* seedlings with GA and thus inducing rapid degradation of all DELLAs. In addition, in the same genetic background, they overexpressed *At*rgaΔ17, which lacks the DELLA domain and is resistant to GA-induced degradation, using a dexamethasone (DEX)-inducible system. This experiment stimulated rapid and high induction of stable *At*RGA1, aiming to identify early transcriptional changes that are more likely to be directly induced by *At*RGA1 (Zentella *et al*., 2007). Among the genes that were differentially expressed in both datasets were GA biosynthesis and perception genes, such as *AtGID1* and GA-oxidase-encoding genes, nuclear transcription factors or regulators, such as *SCR-LIKE3* (*AtSCL3*), *WRKY27*, members of the bHLH and MYB families, as well as genes encoding E2 conjugating enzymes and E3 ligases, such as *AtXERICO*, which is activated by DELLA to induce ABA biosynthesis (Zentella *et al*., 2007). All these genes were induced by *At*rgaΔ17 and repressed by GA.

Early transcriptional responses to DELLA induction were also identified by Gallego-Bartolomé *et al.* (2011b) using etiolated seedlings overexpressing either *At*gai-1 under the control of a heat-shock promoter or a translational fusion between *At*gai-1 and the glucocorticoid receptor domain under the control of the *At*GAI1 promoter. Activation of expression by either heat shock induction or treatment with DEX and cycloheximide (CHX), led to the identification of early transcriptional targets involved in processes such as GA homeostasis, stress responses, and hormone signalling and biosynthesis (Gallego-Bartolomé *et al.*, 2011b). Most notably, the promoters of DELLA downstream target genes were statistically enriched in the *cis* elements recognised by transcription factors that were later shown to interact with DELLA proteins, such as DNA BINDING1 ZINC FINGER6 (*At*DOF6), regulating seed dormancy (Ravindran *et al*., 2017) and ARABIDOPSIS RESPONSE REGULATOR1 (*At*ARR1) regulating root meristem identity (Marín-de la Rosa *et al*., 2015) (see also Chapter 4, section **4.1**).

A subsequent meta-analysis of transcriptomic datasets by Locascio *et al*. (2013b) identified genes involved in GA metabolism to be regulated by DELLAs under most physiological contexts in most tissue types. This confirms the previously described role of DELLAs in regulating the feedback response to maintain GA homeostasis (Dill and Sun, 2001; Wen and Chang, 2002; Itoh *et al*., 2002). Furthermore, transcriptomic analyses have demonstrated that DELLA proteins exert their repression on plant size by interfering with two main cellular processes: cell expansion, by regulating cell wall biogenesis and modification, and cell division, by regulating cell-cycle genes (Locascio *et al*., 2013b).

Many of the flowering plant DELLA target genes regulate processes conserved in non-flowering plants, such as cell wall biogenesis (e.g. Shibaya and Sugawara, 2007) and cell cycle regulation (e.g. Nishihama *et al*., 2015). Therefore, future studies should investigate the putative role of DELLA proteins in these processes using non-flowering plant model species.

Very recently, a study has revealed that *Mp*DELLA protein overexpression in *Marchantia polymorpha* induces upregulation of genes involved in stress responses and secondary metabolism, such as phenylpropanoid and flavonoid biosynthesis genes (Hernández-García *et al.*, 2021). Furthermore, the role of *Mp*DELLA in promoting oxidative stress tolerance has been demonstrated experimentally, suggesting that stress response regulation may have been a function of the ancestral DELLA protein (Hernández-García *et al.*, 2021). Characterising further the *Mp*DELLA targets elucidated by the Hernández-García *et al.*, 2021 transcriptome might reveal more insights into the mechanism via which *Mp*DELLA protein functions and by extension the ancestral DELLA. In addition, comparative transcriptomic analyses in land plants from different lineages, in response to induction or impairment of DELLA signalling, will provide more insights into whether DELLA transcriptional targets are conserved in land plants.

1.5.4 DELLA protein-protein interactions

Several attempts have been made to identify direct DELLA binding to gene promoters via chromatin immunoprecipitation (ChIP), however DELLAs have not shown any direct DNA-binding (Feng *et al*., 2008) Instead, it was demonstrated that DELLA protein function relies on protein-protein interactions having direct or indirect

effects on transcription (e.g. Feng *et al*., 2008; de Lucas *et al*., 2008; Hou *et al*., 2010). Marín-de la Rosa *et al*., (2014) carried out a large yeast two-hybrid screen using the GRAS domain of *At*GAI and identified 57 unique transcription factors as DELLA interactors. These belonged to 15 different transcription factor families regulating a big range of plant growth responses, including germination, vegetative growth, reproductive development, light signalling, stress responses and hormone signalling. However, this screen did not identify all the possible DELLA interactions as the Arabidopsis transcription factor library used was only ~75% complete and a truncated version of DELLA (containing only the GRAS domain) was used as bait (Marín-de la Rosa *et al*., 2014).

A more recent study used truncated versions of *At*RGA1 and *At*GAI1 (containing the GRAS domain) as bait to screen a library of 1956 Arabidopsis transcriptional regulators for DELLA interaction using yeast two-hybrid (Lantzouni *et al*., 2020). *At*RGA1 and *At*GAI1 interactor sets showed ~87% overlap, supporting the hypothesis that DELLA function is tightly linked to its expression patterns in the different tissues rather than its ability to interact with different transcription factors (Gallego-Bartolomé *et al.*, 2010; Lantzouni *et al*., 2020). Furthermore, the screen identified more than 250 DELLA interaction partners, raising the total number of putative DELLA interactors to more than 350 (Lantzouni *et al*., 2020). A number of these interactions have been confirmed by more than one method and their biological significance and functional mechanism have been elucidated. The vast majority of DELLA interactions regulate transcription, however there are few cases where they also regulate other processes. For example, DELLAs interact with and sequester the co-chaperone PREFOLDIN5 (*At*PFD5) in the nucleus to prevent the formation of tubulin heterodimers required for

microtubule organisation regulating cell expansion (Locascio *et al.*, 2013a). The four main mechanisms by which DELLA interactions regulate transcription are outlined in detail in Chapter 4.

1.6 The evolution of DELLA signalling: a case of molecular exploitation

Over the past two decades, several studies have been conducted to identify how DELLA signalling evolved. The current dogma suggests that only vascular plants possess the characterised DELLA signalling pathway regulating GA responses, and that the functionality of the mechanism components was acquired gradually during the course of land plant evolution (Yasumura *et al.*, 2007). This hypothesis is supported by biochemical studies demonstrating that the only land plant groups which possess bioactive GAs are angiosperms, gymnosperms and some ferns and lycophytes (MacMillan, 2001; Aya *et al.*, 2011; Tanaka *et al.*, 2014). Consequently, this raises the question of how DELLA proteins are regulated in bryophytes, where bioactive GAs are not present, and whether they are able to repress growth responses in a similar manner. The following sections discuss older and more recent findings regarding the molecular and biochemical properties of DELLA proteins in non-seed plants and the insights that they provide about DELLA evolution. This information is summarised in Figure **1.4**.

Land plant group	Synthesise bioactive GAs	Have DELLA orthologues	Have GID1 orthologues	Have SLY1 orthologues	DELLA interacts with GID1 orthologues in GA-dependent manner	DELLA can be degraded by GAs	DELLA can induce dwarfism in Arabidopsis
 Angiosperms	✓	✓	✓	✓	✓	✓	✓
 Gymnosperms	✓	✓	✓	✓	✓	✓	?
 Ferns	✓	✓	✓	✓	✓	✓	?
 Lycophytes	✓	✓	✓	✓	✓	✓	✓
 Mosses	✗ Only bioactive diterpenes	✓	✗	✗	✗	✗ Only tested in Arabidopsis	✓
 Liverworts	✗	✓	✗	✓	✗	?	?
 Hornworts	✗	✓	✗ Some may have	✗	✓	?	?

Figure 1.4. Properties related to DELLA signalling that are present or absent in the different land plant groups. Check marks (✓) or X marks may be based on evidence gathered from only one species within that plant group. Question marks indicate absence of evidence (Figure created with BioRender.com; hornwort icon drawn by Debbie Maizels).

1.6.1 DELLA orthologues are present throughout the land plant lineage

Bioinformatic analyses using species from all three bryophyte groups, including mosses such as *P. patens* and *Sphagnum fallax*, liverworts such as *Marchantia polymorpha* and hornworts such as *Nothoceros vincentianus* and the recently sequenced *Anthoceros agrestis* and *Anthoceros punctatus*, have suggested that DELLA orthologues are present in all three bryophyte groups, while *At*SLY1 orthologues are only found in liverworts (Hernández-García *et al.*, 2019; Li *et al.*, 2020). Despite the confirmed presence of GRAS family proteins in two charophyte families, Zygnematales and Coleochaetales, DELLA proteins appear to be absent from algae,

suggesting that they evolved in the common ancestor of land plants (Hernández-García *et al.*, 2019).

GID1 homologues have been identified in bryophytes, such as GID1-like (*Pp*GLPs) in *P. patens*, however these proteins lack the defining features of true flowering plant GID1s, such as the catalytic triad forming the GA pocket or the N-terminal lid required for interaction with DELLA (Hirano *et al*., 2007). Similarly, these features are absent in *Mp*GLPs, suggesting that *Marchantia* does not possess canonical GA signalling, despite the presence of an *AtSLY* orthologue (Hernández-García *et al.*, 2019). It appears that *At*GID1 orthologues are exclusively found in vascular plants, including ferns and lycophytes such as *Selaginella moellendorffii*, although partial sequences from bryophytes such as *Phaeoceros carolinianus* and *Paraphymatoceros halli* suggest that GID1 orthologues may be present in some hornworts (Hernández-García *et al.*, 2019). It would be interesting to examine whether these putative hornwort GID1 orthologues possess the biochemical properties of true GID1s, to provide more evidence for the presence or absence of GID1 orthologues from bryophytes.

Despite the fact that bryophyte DELLAs have a highly conserved GRAS domain, the N-terminal DELLA domain, which is necessary for interaction with GID1, is more divergent in mosses such as *P. patens* (Hirano *et al.*, 2007; Hernández-García *et al.*, 2019). Interestingly, this is not the case for a number of hornworts, including *Nothoceros vincentianus* and *Anthoceros* species, which have DELLAs with highly conserved N-terminal domains, a number of liverworts, including *Marchantia*, as well as other mosses, such as *Takakia lepidozioides*, whose DELLA has a highly conserved DELLA and VHYNP motif, but lacks the LEQLE motif within the wider DELLA domain

(Hernández-García *et al.*, 2019; Li *et al*., 2020). Ancestral protein reconstruction has also suggested that the predicted ancestral DELLA peptide sequence displays a highly conserved N-terminal domain (Hernández-García *et al.*, 2019). These observations imply that the ancestral DELLA, as well as a number of bryophyte DELLAs, were most probably already equipped for interaction with GID1 homologues (Hernández-García *et al.*, 2019).

Following from the above observations, it is unclear why the majority of mosses studied so far display a more divergent N-terminal domain and what selective forces might have brought about those amino acid changes. Interestingly, a similar pattern of peptide sequence conservation has been observed in DELLA-like proteins in rice, such as *Os*SLR1-like1 (*Os*SLRL1), which appears to have lost the DELLA domain, but is still able to induce dwarfism and remain stable in the presence of GA (Itoh *et al*., 2005b). This observation implied that moss DELLAs with a divergent N-terminal domain such as *Pp*DELLAs might still be able to repress growth in a GA-independent manner (see section **1.6.3**). *In silico* comparative gene co-expression network analysis using putative orthologues of DELLA-interacting transcription factors in Arabidopsis, tomato (two flowering plants), *P. patens* (bryophyte) and *Chlamydomonas reinhardtii* (green alga), suggested that the function of *Pp*DELLAs was most likely to regulate stress responses, and that coordination between the functions regulated by DELLAs increased during the course of evolution (Briones-Moreno *et al*., 2017). This suggests that bryophyte DELLAs may be able to repress growth in response to stress in a GA-independent manner, although this hypothesis awaits experimental confirmation.

It is also interesting to note that bryophyte genomes encode the enzymes catalysing the first committed biochemical reactions involved in GA biosynthesis, such

as *ent*-copalyl diphosphate synthase (CPS) and *ent*-kaurene synthase (KS) - although bryophytes possess bifunctional enzymes (CPS/KS) - that catalyse the conversion of *trans*-geranylgeranyl diphosphate (GGPP) into *ent*-kaurene, as well as *ent*-kaurene oxidase (KO), which oxidises *ent*-kaurene into *ent*-kaurenoic acid (Hayashi *et al.*, 2010; Bowman *et al*., 2017; Li *et al*., 2020). In addition, hornworts and liverworts have one more enzyme required for GA biosynthesis, *ent*-kaurenoic acid oxidase (KAO), which is not encoded by the *P. patens* or *S. fallax* genomes (Li *et al*., 2020). Nevertheless, it appears that bryophytes lack orthologues of GA20ox and GA3ox, required for the biosynthesis of bioactive GAs, or GA2ox, required for GA catabolism, in contrast to vascular plants, including lycophytes and ferns, where the complete biosynthesis pathway can be found (Tanaka *et al*., 2014; Li *et al*., 2020; Hernández-García *et al.*, 2020). Whether the endogenous diterpenes found in bryophytes have a role in DELLA signalling remains elusive (see section **1.6.4**).

1.6.2 The GID1-binding ability of DELLAs was most likely present in bryophytes

Several attempts have been made to test whether bryophyte or lycophyte DELLA and GID1 homologues are able to interact in a GA-dependent manner. Yeast two-hybrid assays demonstrated that *Sm*DELLAs could interact with *Sm*GID1s in a GA-dependent manner and this was further supported by *in vitro* binding assays showing that *Sm*GID1 proteins could bind GA_4 in the presence of *Sm*DELLA1 (Hirano *et al*., 2007). Similarly, Yasumura *et al.* (2007) demonstrated that proteins from a different lycophyte, *Sellaginella kraussiana*, *Sk*GID1 and *Sk*DELLA, could interact in yeast cells in the absence of GAs, but much more strongly in the presence of GA_3, suggesting that canonical GA signalling is present in lycophytes.

In contrast, homologous proteins in moss, *Pp*GLP1 and *Pp*DELLAs, were not able to interact in the presence or absence of GAs, and *Pp*GLP1 could not bind GA_4 or other GAs *in vitro* in either the presence or absence of *Sm*DELLA1 (Yasumura *et al*., 2007; Hirano *et al*., 2007). Interestingly, *Pp*GLP1 was able to interact with *Sk*DELLA in the presence of GA_3, however, interaction of similar magnitude was also observed in the absence of GA_3, indicating that the interaction was GA-independent (Yasumura *et al*., 2007). This finding was not supported by Hirano *et al.* (2007) who observed that *Pp*GLP1 could not interact with DELLAs from a different *Selaginella* species, *Selaginella moellendorffii*. Furthermore, *Pp*DELLAs were not able to interact with any GID1 homologue (Hirano *et al*., 2007). These observations suggested that bryophyte GLPs probably possessed affinity for DELLAs that was maintained during GID1 evolution - although this was only supported by the observation that *Pp*GLP1 could interact with *Sk*DELLA - whereas DELLA affinity for GID1 most likely arose after the bryophyte divergence (Yasumura *et al*., 2007).

This hypothesis was later challenged by Hernández-García *et al.* (2019) who demonstrated that while *Pp*DELLAa, the DELLA from *Takakia lepidozioides* (*Tl*DELLA) and *Mp*DELLA could not interact with *At*GID1s in yeast cells in a GA-dependent manner, DELLA from the hornwort *Nothoceros vincentianus* was able to interact with *At*GID1s in a GA-dependent manner, suggesting that DELLA affinity for GID1 homologues may have evolved as early as the hornwort divergence. As hornworts appear to be sister to liverworts and mosses (Li *et al*., 2020), it is possible that the ancestral land plant DELLA probably possessed GID1 affinity and it was later lost in mosses and liverworts. Furthermore, the fact that *Mp*DELLA or *Tl*DELLA have fairly conserved N-terminal domains but are still unable to interact with *At*GID1s, suggests

that conservation of the DELLA N-terminal domains is not sufficient for interaction with GID1 homologues and that conservation of other regions might be necessary to enable this interaction (Hernández-García *et al.*, 2019). It is also worth noting that the *Nv*DELLA-*At*GID1 interaction as well as all other interactions described in this section have only been tested in the yeast two-hybrid system, and therefore further *in vivo* interaction assays will need to be carried out to confirm these findings, before drawing any major conclusions.

In addition, yeast two-hybrid assays by Yasumura *et al*. (2007) showed that *Sk*DELLA was also able to interact with *At*GID1c in a GA-dependent manner, whereas *At*RGA1 was not able to interact with *Sk*GID1 at all. This led to the conclusion that DELLA specificity for GID1 became more tight during the course evolution (Yasumura *et al.,* 2007). Measurements of β-galactosidase activity have also indicated that the DELLA-GID1 interaction in Arabidopsis is much more GA-dependent than in *Selaginella kraussiana*, suggesting that GA potentiation increased with land plant evolution (Yasumura *et al*., 2007). This hypothesis was further supported by biochemical studies showing that GID1 affinity for bioactive GAs increased with land plant evolution (Hirano *et al*., 2007; Yoshida *et al.*, 2018). In addition, studies using the fern *Lygodium japonicum* have shown that minute concentrations of GA_4 enable *Lj*GID1 and *Lj*DELLA proteins to interact in yeast cells and that GID1 affinity for GA_4 is much greater than that of seed plant GID1s, suggesting an increase in GA potentiation in the ancestor of ferns (Tanaka *et al*., 2014). The exceptional affinity of *Lj*GID1 for GA_4 in this case is probably a consequence of the very specific function of GA_4 (sex determination) in a very specific tissue type (young prothalli), where selection would favour tight specificity of *Lj*GID1 for GA_4 to ensure proper sex organ development.

1.6.3 DELLA-induced growth repression evolved before GA signalling

Complementation assays have shown that *Sm*GID1s were able to complement the function of *Os*GID1 in the *Osgid1-3* mutant and *Sm*DELLAs were able to repress growth in wild-type rice, whereas *P. patens* homologues could not (Hirano *et al*., 2007). In contrast, overexpression of *Pp*DELLAa-GFP in the Arabidopsis slender *Atgai-t6 Atrga-24 Atga1-3* mutant induced dwarfism (Yasumura *et al*., 2007). The discrepancy between the two observations on the effect of *Pp*DELLA overexpression on growth in rice and Arabidopsis has been attributed to the fact that wild-type rice was used in one study, where *Os*SLR1 was still actively suppressing growth responses, whereas the Arabidopsis line in the other study was a double *della* mutant in a GA-deficient background, and thus DELLA-induced vegetative growth suppression had already been eliminated (Hirano *et al*., 2007).

Application of GA_3 to Arabidopsis plants overexpressing *pRGA::GFP-SkDELLA* resulted in the loss of the fluorescence signal, presumably due to GA_3-induced degradation of *Sk*DELLA, whereas loss of fluorescence was not observed when plants overexpressing *pRGA::GFP-Pp*DELLAa were treated with GA_3 (Yasumura *et al*., 2007). These observations support the hypothesis that bryophyte DELLAs have the capacity to induce growth repression in a GA-independent manner. In fact, the recent study on the functions of DELLA protein in *M. polymorpha* demonstrated that *Mp*DELLA overexpression induces vegetative growth inhibition by reducing the rate of cell division (Hernández-García *et al*., 2021). This suggests DELLA-induced growth repression predated GA signalling and that regulating plant size might have been one of the roles of the ancestral DELLA protein. In the case of *P. patens*, as has been pointed out by Yasumura *et al.* (2007), it is highly likely that *Pp*DELLA was able to

induce vegetative growth repression in Arabidopsis and not in *P. patens*, because downstream gene expression regulating growth has evolved the ability to respond to DELLA proteins in angiosperms, but not in *P. patens*. Comparative *in vivo* transcriptomic analyses will need to be carried out to test the validity of this hypothesis.

1.6.4 *P. patens* possesses a diterpene signalling mechanism that might be uncoupled from DELLA signalling

Experiments have provided evidence that a putative GA-like/diterpene signalling pathway is present in mosses. As pointed out earlier, *P. patens* possesses GA signalling and biosynthesis orthologues, such as *Pp*DELLAs, *Pp*CPS/KS, and *Pp*KO, and produces the diterpenes *ent*-kaurene, *ent*-kaurenoic acid and the recently discovered *ent*-3β-hydroxy-kaurenoic acid (3OH-KA) (Hayashi *et al*., 2006; Hayashi *et al*., 2010; Miyazaki *et al*., 2018). *Ppdella* mutants do not display any obvious defects in vegetative growth (Yasumura *et al*., 2007), however further analysis is necessary to establish if they produce phenotypes at different developmental points that have been overlooked. In fact, recent experiments in the Coates lab have demonstrated that loss of either *PpDELLAa* or *PpDELLAb* or both, results in a faster germination rate in spores of *P. patens*, demonstrating that *Pp*DELLAs are involved in the inhibition of spore germination (Vesty, unpublished).

Disruption of *PpCPS/KS* results in the suppression of chloronema to caulonema differentiation, required for normal vegetative growth in *P. patens*, and the phenotype can be rescued with exogenous application of *ent*-kaurene or *ent*-kaurenoic acid, which are naturally synthesised by *P. patens*, as well as by application of the fern antheridiogen GA_9 methyl-ester (GA_9-ME) (Hayashi *et al*., 2010; Tanaka *et al*., 2014).

In addition, loss of *PpCPS/KS* in *P. patens* results in a decrease in the rate of spore germination, a phenotype that can be partially rescued by application of exogenous *ent*-kaurene or GA_9-ME (Vesty *et al*., 2016), as well as a decrease in total dry weight when grown in liquid cultures (Pan *et al*., 2015).

Wild-type *P. patens* is also responsive to the exogenous application of diterpenes. Application of *ent*-kaurene to moss protonemata results in increased production of caulonemata as well as a faster spore germination rate (Hayashi *et al*., 2010; Vesty *et al.*, 2016). A similarly faster germination rate is also induced upon application of exogenous GA_9-ME on wild-type moss spores (Vesty *et al*., 2016). In the case of *Selaginella moellendorffii*, exogenous application of GA_4 induces an increase in outer exospore projection heights in microspores, demonstrating GA bioactivity (Aya *et al*., 2011). Uniconazole, which inhibits the conversion of *ent*-kaurene into *ent*-kaurenoic acid, induces growth repression in *Selaginella moellendorffii* and produces defects in microspore outer exospore walls, however only the latter be rescued by exogenous application of GA_4 (Hirano *et al.,* 2007; Aya *et al*., 2011). Similarly, in *P. patens*, paclobutrazol (PAC), which also inhibits the biosynthesis of *ent*-kaurenoic acid, induces a growth phenotype that cannot be rescued by exogenous application of GA_3, suggesting that a diterpene signalling pathway regulating growth exists in *P. patens* (Yasumura *et al*., 2007). This pathway is probably uncoupled from DELLA signalling, as the *PpdellaAB* mutant does not display faster vegetative growth and is sensitive to exogenous application of PAC at the vegetative stage (Yasumura *et al*., 2007).

As mentioned earlier, overexpression of *PpDELLAa* driven by the *pRGA* promoter in the Arabidopsis slender *Atgai-t6 Atrga-24 Atga1-3* mutant induces dwarfism, demonstrating that *Pp*DELLAs possess the ability to inhibit growth in

Arabidopsis (Yasumura *et al*., 2007). It has also demonstrated both in yeast and *Nicotiana benthamiana* that the N-terminal domain of *PpDELLAa*, as well as other bryophyte DELLAs, possesses the ability to induce transactivation, despite being more divergent compared to other bryophyte DELLAs, suggesting that *Pp*DELLAs may share functional homology with vascular plant DELLAs (Hernández-García *et al.*, 2019).

Collectively, these observations suggest that a diterpene signalling mechanism involving a molecule similar to GA_9-ME is present in *P. patens* regulating germination and morphogenesis. The recently identified 3OH-KA is suggested to be the end-product of the moss diterpene biosynthesis pathway and its exogenous application can rescue the defects in caulonemal differentiation observed in the moss *Ppcps/ks* mutant (Miyazaki *et al*., 2018). It would therefore be interesting to test if 3OH-KA can potentiate the interaction between *Pp*GLPs and *Pp*DELLAs or induce *Pp*DELLA degradation. The absence of a GID1 orthologue in *P. patens* makes it unlikely that moss diterpene and *Pp*DELLA signalling are linked, however it cannot be ruled out that *P. patens* has a completely novel receptor for perceiving the bioactive diterpene. More detailed characterisation of *Ppdella* mutants as well as more *in vivo* interaction assays in *P. patens* and other bryophytes will be necessary to shed more light on the evolution of DELLA signalling in *P. patens* and other non-vascular plants.

1.7 Summary and future perspectives

DELLA proteins originated in land plants (Hernández-García *et al.*, 2019). Some bryophyte DELLAs (the *Pp*DELLAs) do not seem able to induce growth repression within their species (Yasumura *et al*., 2007), while others (*Mp*DELLA) do (Hernández-

García *et al.*, 2021). All bryophyte DELLAs tested can induce transactivation via their N-terminal domain, suggesting that bryophyte DELLAs may be functioning as transcriptional 'hubs' (Yasumura *et al*., 2007; Hernández-García *et al.*, 2019). Although some bryophyte DELLAs, such as the hornwort *Nv*DELLA, can bind *At*GID1s in a GA-dependent manner, this property is absent from the majority of bryophyte DELLAs examined so far (Hernández-García *et al.*, 2019). Whether GA-dependent *At*GID1 interaction is universal among hornwort DELLA orthologues remains elusive.

Intriguingly, *P. patens* possesses a diterpene signalling pathway, but it is unclear whether this pathway is linked in any way with the *Pp*DELLA signalling pathway (Yasumura *et al*., 2007; Hayashi *et al*., 2010). It would be useful to investigate whether any other bryophytes have similar diterpene signalling pathways regulating growth responses and whether DELLA proteins are involved in those pathways. In addition, *M. polymorpha* and other liverworts appear to be the only bryophytes that have an *At*SLY1 orthologue (Hernández-García *et al.*, 2019). Thus, it would be interesting to examine whether *Mp*DELLA is linked in any way with *Mp*SLY1, for example by investigating the stability of *Mp*DELLA in an *Mpsly1* mutant.

Collectively, the evidence so far suggests that canonical GA signalling involving DELLA, GID1 and SLY1/GID2 proteins appeared with the evolution of vascular plants, where bioactive GAs first appeared, exploiting the transactivation domain of DELLA proteins to enable DELLA interaction with the GA-GID1 complex (Figure **1.1**) (Hernández-García *et al.*, 2019). As DELLA signalling predates GA signalling, it is likely that GAs exploited the already established DELLA signalling mechanisms in order to control growth-regulating transcription (Hernández-García *et al.*, 2019), and DELLA functions were refined in different species according to their expression

patterns (Gallego-Bartolomé *et al.*, 2010) and perhaps by post-translational modifications too.

The question of how DELLA proteins arose in the very first land plants, and what the selection pressures were that retained them during early land plant evolution, still remains unanswered. *In silico* comparative gene co-expression network analysis has suggested the hypothesis that the function of *Pp*DELLAs is likely to regulate stress responses (Briones-Moreno *et al*., 2017). To validate this hypothesis, it is necessary to test how the *PpdellaAB* mutant performs under various forms of stress. Experiments by Yasumura *et al*. (2007) have shown that *PpdellaAB* is sensitive to salt stress. Whether this is the case for other forms of stresses is unknown. Interestingly in *M. polymorpha*, *Mp*DELLA promotes oxidative stress tolerance, providing further support for a putative role of the ancestral DELLA in regulating stress responses. Future studies should concentrate on using bryophyte species with sequenced genomes as well as other emerging model species, to carry out more *in vivo* genetic and biochemical studies to shed more light on the evolution of DELLA signalling in land plants. Analysis of additional bryophyte and charophyte genomes or transcriptomes may pinpoint the emergence of DELLAs more accurately.

1.8 Using *P. patens* to elucidate the evolution of DELLA signalling

In the past few decades, the moss *P. patens* has emerged as an important model species for studying land plant evolution. It is currently believed that transition to land from a freshwater algal ancestor belonging to the charophytes occurred as early as the Middle Cambrian-Early Ordovician, approximately 500 million years ago (MYA), with all main plant groups diverging by the late Silurian (425MYA) (Morris *et*

al., 2018). The evolution of land plants was a milestone in the Earth's history, as it completely changed the composition of the atmosphere, leading to a decrease in carbon dioxide levels and an increase in oxygen levels that enabled the divergence of multicellular plant and animal species (Lenton *et al.,* 2012; Lenton *et al.,* 2016). Understanding how plants managed to make the transition to land is important but also challenging. Comparative studies between different groups of plant species are among the key means that enable inferences to be made on the evolution of land plants and terrestrial life on Earth, and by extension the evolution from simple to complex form.

Among bryophytes, the moss *P. patens* was until recently the only species with a sequenced genome, due to a number of features that made it a very attractive model organism. These include the haploidy of the dominant gametophyte phase, which makes mutant screens easy, as well as a high frequency of homologous recombination (higher than 90%) – most probably a consequence of its predominantly selfing nature (Rensing *et al*., 2020) –, which place *P. patens* in a unique position among multicellular eukaryote model species (Schaefer 2002). Furthermore, its simple body structure allows the tracking of biological responses at the cellular and subcellular level (Rensing *et al*., 2020) and its phylogenetic position, half way between charophytes and flowering plants, make it important in addressing questions on the evolution of land plants (Arif *et al*., 2019).

The draft genome sequence of the 'Gransden' ecotype (500 Mbp, 27 chromosomes) was published in 2008 and revealed important insights into the genomic changes that allowed plant transition to land to take place (Rensing *et al*., 2008). Among these, were an increase in the number of genes associated with desiccation tolerance, such as ABA signalling-related genes, and the loss of genes

required for survival in aquatic habitats (Rensing *et al*., 2008). Hormone signalling, such as ABA and auxin signalling, which are key to morphogenesis and growth regulation in land plants, have been well-studied in *P. patens* over the past decades (Komatsu *et al*., 2009; Khandelwal *et al*., 2010; Prigge *et al*., 2010; Tao & Estelle *et al*., 2018); however a lot less is known about diterpene and DELLA signalling and whether their evolution was instrumental for plant transition to land.

1.9 Project aims and objectives

1.9.1 Aims

The overarching aim of the current work was to use the resources available for studying the molecular genetics of *P. patens* to (i) investigate whether *Pp*DELLA proteins are part of a diterpene-signalling pathway in moss and (ii) elucidate the roles of *Pp*DELLA proteins at the molecular level and examine whether they have conserved functions compared to DELLA proteins from Arabidopsis. Addressing those aims will be essential in answering the question whether DELLA protein emergence was important in the transition to land and understanding how DELLAs have evolved in the different land plant lineages in response to selection pressures.

1.9.2 Objectives

In order to examine the hypothesis that *Pp*DELLA proteins are involved in a diterpene-signalling pathway, the following objectives were set:

1. Generation of *pHSP::PpDELLA-GFP* overexpression moss lines to test whether *Pp*DELLAs can be degraded by diterpenes or stabilised by the 26S proteasome inhibitor MG132.

2. Employment of a yeast two-hybrid assay and a Co-Immunoprecipitation to test whether *Pp*DELLAs interact with GID1 homologues in the presence of diterpenes.
3. Performance of a spore germination assay of *Ppdella* mutants under treatment with GA_9-ME.

In addition, in order to investigate how *Pp*DELLA proteins function at the molecular level, the following objectives were set:

1. Examination of how *Ppdella* mutants respond under conditions of salt stress, oxidative stress or desiccation.
2. Use of *pHSP::PpDELLA-GFP* overexpression moss lines to perform an immunoprecipitation coupled to mass spectrometry (IP-MS) in order to identify *Pp*DELLA protein interactors.
3. Analysis of the transcriptome of the *PpdellaAB* mutant.

CHAPTER 2: Materials and methods

2.1 *Physcomitrium (Physcomitrella) patens* tissue culture

2.1.1 Preparation of growth media

BCD minimal medium (Appendix) for growth of *P. patens* was prepared as in Moody *et al.* (2012). For chloronema-enriched tissue production, minimal BCD was supplemented with 1mM $CaCl_2$ and 5mM ammonium tartrate (BCDAT) and for spore germination it was supplemented with 5mM $CaCl_2$ and 5mM ammonium tartrate. For phenotyping, BCDAT was supplemented with 0.5% glucose (BCDATG) to speed up tissue growth. For selection plates, BCDAT was supplemented with 50µg/ml G418 (Sigma-Aldrich, A1720). For sporophyte induction or long-term storage of tissue, minimal BCD was supplemented with 1mM $CaCl_2$. The medium was poured in autoclaved 77mm x 77mm x 97mm magenta vessels (Sigma-Aldrich) for sporophyte induction or in 90mm petri dishes for tissue culture or storage.

Hormone treatment plates were prepared by cooling BCD medium for spore germination or BCDATG to 50^{o}C and then adding the required hormone or solvent before pouring into 90mm petri dishes. Abscisic acid (ABA) (Sigma-Aldrich, A1049), norflurazon (Sigma-Aldrich, 34364), gibberellin A_3 (GA_3) (Sigma-Aldrich, 48880), gibberellin A_9 methyl-ester (GA_9-ME), *ent*-kaurene and *ent*-kaurenoic acid were dissolved in methanol and concentrated stock solutions were stored at -20^{o}C or -80^{o}C for long-term storage. Equivalent solvent-only controls were included alongside hormone treatments in all assays. Supplies of GA_9-ME, *ent*-kaurene and *ent*-kaurenoic acid were kindly provided by Professor Peter Hedden (Rothamsted Research).

Protoplast regeneration medium bottom layer medium (PRMB) contained BCD minimal medium supplemented with 5mM ammonium tartrate, 10mM $CaCl_2$, 60g/L mannitol and 0.5% glucose. Solid protoplast regeneration medium top layer (PRMT)

contained BCD minimal medium supplemented with 5mM ammonium tartrate, 10mM $CaCl_2$, 80g/l mannitol, 0.5% glucose and 5g/L agar. Protoplast liquid regeneration medium for overnight incubation of transformed protoplasts contained minimal BCD medium supplemented with 1mM $CaCl_2$, 80g/L mannitol, and 0.5% glucose.

All agar-containing media were poured in 90mm petri dishes and overlaid with sterile cellophanes (A.A. Packaging Limited, UK), which had been autoclaved between moist filter papers (Whatman plc) in glass petri dishes, and applied to the solidified medium in a laminar flow hood using sterile forceps.

2.1.2 Tissue culture growth conditions

The 'Gransden 2004' and 'Reute' wild-type ecotypes of *P. patens* were kindly provided by Dr Andrew Cuming (University of Leeds), and Professor Stefan Rensing, (University of Marburg), respectively. Mutant strains were kindly provided by Professor Henrik Toft Simonsen (Technical University of Denmark) (*Ppcps/ks* KO, Pan *et al*. 2015; *Ppglp1glp2* KO, unpublished), Professor Nicholas Harberd (University of Oxford) (*PpdellaA* KO*, PpdellaB* KO*, PpdellaAB* KO, Yasumura *et al.*, 2007*)* and Professor Stefan Rensing (University of Marburg) (*Ppdog1* KOs: *Pp3c13_11750*, *Pp3c26_14620* and *Pp3c3_9650*, unpublished).

Fresh protonemal tissue was generated by homogenising protonemata in 5-10ml sterile water in a sterile glass vial for 30-60 seconds at 17-19,000rpm using a polytron tissue tearer (IKA® T25 digital Ultra-Turrax) and pipetting 1ml of the suspension onto cellophane-overlaid solid BCDAT or BCDATG plates subsequently sealed with micropore tape (3M Healthcare, Germany). Tissue was cultured at 22±1^{o}C under a 16h light/8h dark regime with a light intensity of 50-70µmol$m^{-2}s^{-1}$.

In order to induce reproductive organ formation and sporulation, 4-8ml homogenised protonemal tissue was pipetted onto sterile peat plugs (LBS Worldwide Ltd) or onto BCD minimal medium in sterile magenta vessels or glass jars. The vessels or jars were then incubated for 4-6 weeks at 22±1°C under a 16h light/8h dark regime, followed by incubation at 15°C for 3-4 weeks under an 8h light/16h dark regime. As soon as reproductive organs were formed, the vessels or jars were returned to 22±1°C for an additional 6-12 weeks under a 16h light/8h dark regime. Mature (dark brown, slightly 'sparkly') sporophytes were harvested using forceps under an SMZ645 light dissecting microscope (Nikon, Tokyo, Japan) and air-dried for one week in Eppendorf tubes (with open lid) at room temperature before being used or stored in the dark at room temperature. Tissue for long-term storage was incubated on minimal BCD agar plates at 8°C under a 2h light/22h dark regime or at 4°C in darkness for up to 6 months. For experiments testing the effect of different light wavelengths on growth, moss was incubated at 22±1°C under a 16h light/8h dark or a continuous light regime, inside cardboard boxes illuminated from the top by white LED lights filtered using neutral density or colour filters, or by far-red LED lights (Lumitronix®, Germany). White light was adjusted to 63µmolm^{-2}s^{-1} intensity using single layers of neutral density filters No. 209 and No. 298 (LEE filters, UK) overlaid together, red light (640-695nM) was adjusted to 26µmolm^{-2}s^{-1} intensity using a double layer of Deep golden amber filter No. 135 (LEE filters, UK) and blue light (445-490nM) was adjusted to 16µmolm^{-2}s^{-1} intensity using a triple layer of Moonlight blue filter No. 183 (LEE filters, UK). Far-red light (730nM) was set to 16µmolm^{-2}s^{-1} intensity by adjusting the distance of the petri dishes from the source of illumination.

2.2 *P. patens* PEG-mediated transformation

2.2.1 Protoplast isolation

P. patens protoplast isolation was performed as described in Schaefer *et al.* (1991). Essentially, 60-90mg Driselase™ (Sigma-Aldrich, D9515) was dissolved in 6ml 8% mannitol in a 14ml round-bottom polypropylene tube (Fisher Scientific) for 15-20 minutes at room temperature. The enzyme solution was gently inverted to mix at 5-minute intervals and centrifuged for 3 minutes at 3,000 g. The supernatant was filter sterilised through a 0.2µM Acrodisc® syringe filter and collected in a 50ml Falcon tube. 1.5-2 plates of 5- or 6-day old protonemal tissue was added to the enzyme solution.

The tissue was digested for 1h at room temperature with gentle agitation. The suspension was then filtered through a sterile 40µm cell strainer (Fisher Scientific) and incubated at room temperature for 5-10 minutes. The solution was then transferred to a 14ml round-bottom polypropylene tube (Fisher Scientific) and centrifuged for 3 minutes at 120 g. The supernatant was removed and cells were resuspended in 6ml 8% mannitol and centrifuged for 3 minutes at 120 g. Following an additional wash and centrifugation step, cells were resuspended in 6ml 8% mannitol. Protoplast yield was estimated using a haemocytometer.

2.2.2 Protoplast transformation by heat shock

Protoplast transformation was performed according to Moody *et al.* (2018). 2g polyethylene glycol (PEG) 6000 (Sigma-Aldrich) was melted for 2 minutes in a microwave in a flat-bottomed autoclavable glass vial, added to 5ml mannitol/$Ca(NO_3)_2$ solution (0.8% mannitol, 100mM $Ca(NO_3)_2$, 10mM Tris pH 8.0) and incubated for 2-3h at room temperature.

Protoplasts were centrifuged at 140 g for 3 minutes and then resuspended very gently in an appropriate volume of MMM solution (9.1% mannitol, 150mM $MgCl_2$, 0.1% MES pH 5.6) to obtain a protoplast density of ~$1.5x10^6$/ml. 10-15µg linearised plasmid DNA was added to 14ml round-bottom polypropylene tubes (Fisher Scientific) as required and 300µl protoplasts in MMM solution was added to each tube by slowly pipetting down the side of the tube. 300µl PEG solution was added to the protoplast mixture in drops and swirled to mix after each addition. Tubes were covered in aluminium foil to prevent photo-oxidative DNA damage. The samples were then heat-shocked for 5 minutes at 45°C and incubated at room temperature for 5 minutes. 300µl 8% mannitol was added to each tube, 5 times at 4-6 minute intervals, followed by addition of 1ml 8% mannitol 5 times at 4-6 minute intervals. Tubes were tilted gently to mix after each addition. Cells were centrifuged for 4 minutes at 140 g, the supernatant was removed and pellets were resuspended in 5ml protoplast liquid regeneration medium (see section **2.1.1**) and incubated overnight at 22±1°C. All centrifugation steps were carried out with rotor brakes off.

Following overnight incubation, protoplasts were centrifuged for 4 minutes at 120 g and resuspended in 500µl 8% mannitol. Autoclaved PRMT was maintained at 37°C and 2.5ml was added to cell suspensions. 1ml of suspension was immediately plated onto cellophane-overlaid PRMB plates, which were then sealed with micropore tape (3M Healthcare, Germany).

Plates were incubated at 22±1°C under a 16h light/8h dark regime for 5 days, after which time, cellophane discs were transferred onto selection plates using sterile forceps. Plates were sealed with micropore tape and incubated at 22±1°C under a 16h light/8h dark regime for 2 weeks. On day 21, cellophane discs were transferred onto

non-selective plates, which were sealed with micropore tape and incubated at 22±1°C in a 16h light/8h dark regime for another 2 weeks. On day 35, cellophane discs were transferred onto selection plates, but this time, they were turned upside down so that the aerial part of the moss faced down into the agar plate. Moss was pushed into the agar using a sterile spatula and plates were sealed with micropore tape and incubated for at least 7 days at 22±1°C under a 16h light/8h dark regime to enable selection of stable transformants.

2.2.3 DNA extraction from moss transformants

DNA was extracted from transformants as described in Yasumura *et al.* (2005). Essentially, transformed moss plants (a half of each plant) were collected 14-21 days after being transferred onto selective plates for the second time (Day 35, section **2.2.2**) and ground up in an Eppendorf tube using sterile micropestles. Tissue was resuspended in 700µl cetyltrimethyl ammonium bromide (CTAB) DNA extraction buffer (100mM Tris-HCl (pH 8.0), 20mM EDTA (pH 8.0), 1.4M NaCl, 2% (w/v) CTAB, 1% polyvinyl pyrrolidone (PVP) 40,000) and incubated at 65°C for 1h. This was followed by addition of 1 volume of chloroform and vigorous shaking. The mixture was centrifuged for 10 minutes at 14,000 g and 500µl of the upper aqueous layer was transferred into a 2ml Eppendorf tube, followed by the addition of 0.8 volumes of isopropanol, to precipitate the DNA. The mixture was incubated for at least 2h (sometimes overnight) at -20°C and then centrifuged at 14,000 g or 20 minutes. Pellets were washed with 100µl 70% ethanol twice (10 minutes each) and air-dried for 8-10 minutes. DNA was eluted in 30-50µl nuclease free water and stored at −20°C.

2.2.4 Genotyping of moss transformants

Transformants were screened for the presence of *pHSP::PpDELLA-GFP* by PCR, using the primers *pHSP_F* and *mGFP_R* (for both *PpDELLAa* and *PpDELLAb*) and *XhoI-PpDELLAa_pHSP-F* and *mGFP_R* (for *PpDELLAa*) (see section **2.9.8** for primer sequences). To confirm integration of the construct into the inert *108* genomic locus, plants were genotyped by PCR using *nptII_F* and *108locus5'_R* (see section **2.9.8** for primer sequences). Transformants were screened for the presence of *pHSP::GFP* by PCR using *pHSP_F* and *35STer_R* and for integration of the construct into the 108 locus using *nptII_F* and *108locus5'_R* (see section **2.9.8** for primer sequences).

2.3 Phenotypic analysis of *P. patens*

2.3.1 Spore germination assays

Spore germination assays were carried out as described in Vesty *et al.* (2016). In summary, sporangia were sterilised in 25% Parozone^{TM} (Jeyes Group, Thetford, UK) for 10-15 minutes on a turning wheel at room temperature and washed 3 times (lasting 10 minutes each) with sterile distilled water (dH_2O). Sporangia were then perforated with a sterile pipette tip into 200µl dH_2O to release the spores, which were diluted down in sufficient dH_2O to allow plating of 500µl of spore-containing suspension per cellophane-overlaid plate of BCD spore germination medium. Plates were air-dried in a laminar flow hood, sealed with micropore tape (3M Healthcare, Germany) and incubated at 22±1^{o}C under a 16h light/8h dark regime with a light intensity of 50-70µmolm^{-2}s^{-1}. For thermoinhibition assays, sealed plates were incubated at 35^{o}C under a 16h light/8h dark regime with a light intensity of 50-70µmolm^{-2}s^{-1} for 7 days

and returned to 22±1°C under the same light conditions for a further 7 days.

For assays testing the effect of *Pp*DELLA overexpression, plates containing spores from the *pHSP::PpDELLA-GFP* or *pHSP::GFP* overexpression lines were incubated under normal conditions, but were transferred to 37°C in the dark for 1h every day to enable continuous overexpression of the construct. Plates containing the same spores from the *pHSP::PpDELLA-GFP* or *pHSP::GFP* overexpression lines were also incubated continuously at 22±1°C as a control (uninduced *Pp*DELLA-GFP or GFP protein expression).

Germinated (first deformation of the spore coat by emerging protonemal filament) and ungerminated spores were counted daily or every few days over a period of 7-20 days under a 4x objective of a Leica compound microscope with a 10x eyepiece. At least 200 spores per plate originating from at least 3 sporangia were counted to calculate the number of germinated spores as a percentage of the total spores counted. At least three plates for each treatment and genotype were used (technical replicates) and the experiment was repeated three times on different days using spores from different batches of sporangia (biological replicates).

2.3.2 Vegetative tissue growth assays

Protonemata of *P. patens* were homogenised as described in section **2.1.2** and transferred onto cellophane-overlaid plates containing BCDAT agar medium. The plants were left to grow for 7-14 days and then 4-5 individual moss plants (at the protonemal stage of their life cycle) of similar size were transferred using sterile forceps onto cellophane-overlaid plates containing only BCDATG agar or BCDATG agar supplemented with NaCl or methylviolagen (Sigma-Aldrich, 856177) or Indole-3-acetic

acid (IAA; Duchefa Biochemie, I0901), or A-Naphthalene acetic acid (NAA; Duchefa Biochemie, N0903) or solvent (control). Plates were incubated at 22±1ºC under a 16h light/8h darkness regime for 11-21 days. For experiments testing the effect of *Pp*DELLA overexpression on vegetative growth under various treatments, moss plants from transgenic lines carrying the *pHSP::PpDELLA-GFP* or *pHSP::GFP* construct were grown under normal conditions but were incubated at 37ºC for 1h in the dark once a day over the total duration of the experiment. As a control, wild-type plants were also incubated under the same conditions and in addition, plants from the same transgenic lines were incubated continuously at 22±1ºC, without undergoing a daily heat shock (uninduced *Pp*DELLA-GFP or GFP protein expression). Plates were photographed using a Nikon D40 SLR camera.

Vegetative tissue growth was assayed by quantifying moss plant area. This was calculated by subtracting the plant area measured at the start of the experiment from that measured at the end of the experiment. Plant area was measured using the polygon function in Fiji software. For experiments testing the effect of different light wavelengths or drought stress on moss vegetative growth, growth was assayed qualitatively by observing effects on plant physical appearance, e.g. development of gametophores, wilting, etc.

Drought stress assays were performed by transferring cellophanes carrying 7-day old protonemata growing on BCDAT agar medium onto fresh BCDAT plates supplemented with ABA or methanol and incubating them overnight at normal growth conditions. Cellophanes were then transferred into empty petri dishes (drought stress conditions) and incubated at normal growth conditions for one week, after which time they were transferred onto BCDAT agar medium for 7 days to allow tissue recovery.

Performance under drought stress was assayed qualitatively by observing plant appearance following the recovery period.

2.3.3 Sporophyte development assays

P. patens protonemata were homogenised as described in section **2.1.2** and transferred onto cellophane-overlaid plates containing BCDAT agar medium. Plants were left to grow for 7-14 days and then 5 individual moss plants (at the protonemal stage of their life cycle) of similar size were transferred using sterile forceps onto cellophane-overlaid BCDATG agar plates. Plates were incubated at 22±1^{o}C under a 16h light/8h darkness regime for 4 weeks and then transferred using sterile forceps onto minimal BCD agar medium inside magenta pots (one plant per pot) and incubated at 15^{o}C under an 8h light/16h darkness regime for 7 weeks in order to induce sex organ development, fertilisation and sporophyte development. To estimate sporophyte density, the number of sporophytes per plant tissue area in each pot was counted.

2.4 *Arabidopsis thaliana* growth and transformation

2.4.1 Preparation of growth media

½ Murashige and Skoog (½ MS) medium was prepared by adding 2.2g MS basal medium (Sigma-Aldrich, M0404) and 8g/L agar to 1L dH_2O. The pH was adjusted to 5.7 using 1M KOH.

2.4.2 Tissue culture growth conditions

The 'Columbia-0 (Col-0)' and the 'Landsberg *erecta* (L*er*)' wild-type ecotypes of *Arabidopsis thaliana* were used. The *pRGA::GFP-AtRGA1* overexpression line in the L*er* background (Achard *et al*., 2006) was kindly provided by Professor Nicholas Harberd (University of Oxford). Seed of *Atdog1-2* in the Col-0 background (Nakabayashi *et al*., 2012) was kindly provided by Professor Stefan Rensing (University of Marburg).

Seeds were sterilised in 20% Parozone^{TM} (Jeyes Group, Thetford, UK) for 10-15 minutes on a turning wheel at room temperature and washed 3 times (each lasting 10 minutes) with dH_2O. They were then plated onto ½ MS plates, sealed with micropore tape (3M Healthcare, Germany) and stratified for 48-72h at 4^{o}C. Following stratification, plates were incubated at 22±1^{o}C under a 16h light/8h dark regime. For transformant selection, plates were supplemented with 50µg/ml kanamycin.

2.4.3 Growth of Arabidopsis in soil

Seeds were sown on a Levington M3 compost, vermiculite and perlite mix (ratio of 4:2:1) in the glasshouse at 22±1^{o}C under a 16h light/8h dark regime.

2.4.4 Transformation of Arabidopsis by floral dip

Transformation of Arabidopsis was carried out as described in Clough and Bent (1998). Arabidopsis seeds were grown on soil for 4-6 weeks until the first buds on the main inflorescence spike began to open. A single colony of *Agrobacterium tumefaciens* containing the construct of interest was used to inoculate a 5ml low salt liquid LB (Appendix) culture supplemented with 50µg/ml kanamycin and 25 µg/ml rifampicin.

The culture was incubated at 28°C for 24-48h on an orbital shaker with agitation (200rpm) and was then used to inoculate 250ml low salt liquid LB culture supplemented with 50µg/ml kanamycin and 25 µg/ml rifampicin. The culture was incubated for an additional 24-48h at 28°C on an orbital shaker with agitation (200rpm). The bacterial pellet was harvested by centrifuging the culture at 3500-4500 g for 20 minutes and thoroughly resuspended in 250ml 5% sucrose. 100µl Silwet L-77 was then added to the suspension. The suspension was transferred to a 500ml beaker in the glasshouse and plants were inverted, dipped into the suspension and gently agitated for 1 minute. The suspension was applied to individual flowers that could not be dipped using a Pasture pipette. Plants were laid down and placed between two layers of cling film in the dark for 24-48h. Plants were then transferred to normal growth conditions in the glasshouse until seeds were ready to be harvested.

2.4.5 Screening of Arabidopsis transformants

T1 generation seeds were harvested and dried by incubation at 30°C for 3-4 days in glassine bags. Seeds were left to after-ripen for 2-3 weeks at room temperature and sterilised as described in section **2.4.2**. Seeds were then incubated in 1% Plant Preservative Mixture (PPM; Sigma-Aldrich) supplemented with autoclaved 100µM $MgCl_2$ on a turning wheel overnight at 4°C. Following overnight incubation, seeds were washed 3 times with dH_2O and resuspended in autoclaved 0.7% agarose maintained at 55°C and poured immediately onto ½ MS plates (140mm diameter) supplemented with 50µg/ml kanamycin. Plates were sealed with micropore tape (3M Healthcare, Germany), stratified for 48h at 4°C and then grown under standard conditions for 10-14 days, until transformants could be identified. Green transformants were transferred

to soil (see section **2.4.3**) and allowed to set T2 seed. The T2 generation of seeds was harvested, left to after-ripen, sterilised and plated onto ½ MS plates supplemented with 50µg/ml kanamycin. Lines segregating with a 3:1 ratio were transferred to soil. T3 seed was harvested, left to after-ripen, sterilised and plated onto ½ MS plates supplemented with 50µg/ml kanamycin and screened for 100% transformation success.

The *Atdog1-2* mutant (Nakabayashi *et al.*, 2012) was genotyped by amplifying *Atdog1* from gDNA using Phusion® polymerase (NEB) according to manufacturer's instructions with *NdeI-AtDOG1_F* and *EcoRI-AtDOG1_R* (see section **2.9.8** for primer sequences) (52ºC Tm, 4 minutes extension time, 35 cycles), and sequencing the amplicon with the PCR primers (Eurofins, Germany).

2.5 *Nicotiana benthamiana* growth and infiltration

2.5.1 Growth of *N. benthamiana* in soil

Seeds were sown on a Levington M3 compost, vermiculite and perlite mix (ratio of 4:2:1) in the glasshouse at 22±1ºC under a 16h light/8h dark regime.

2.5.2 Infiltration of *N. benthamiana* with *Agrobacterium tumefaniens* for Co-Immunoprecipitation (Co-IP)

Infiltration of *N. benthamiana* was performed as described in Sparkes *et al*., 2006 with minor adaptations. Essentially, *Agrobacterium tumefaciens* strain GV3101 transformed with the required plasmids (see section **2.8.3.2** for method) was cultured overnight at 28ºC in low salt LB liquid medium (Appendix) supplemented with 50µg/ml kanamycin and 25µg/ml rifampicin. 2-4ml culture was centrifuged and resuspended in infiltration buffer (50mM MES, 200µM Acetosyringone (3', 5'-Dimethoxy-4-

hydroxyacetophenon; Sigma-Aldrich, D134406) in DMSO, 2mM Na_3PO_4-$12H_2O$). OD_{600} was measured and appropriate volumes of resuspended Agrobacterium containing the two plasmids to be co-inserted were mixed to give a final OD_{600} of 2.5. Leaves were infiltrated using a 1ml sterile syringe, dried with tissue and the infiltration zone was marked on the leaf with a marker pen. Plants were returned to normal growth conditions and leaves were collected 3 days post infiltration for protein extraction (see section **2.12**) and Co-IP (see section **2.15.2**).

2.6 Bioinformatics

Genomic DNA, cDNA and peptide sequences for *PpDELLA* from the *P. patens* genome (version 3.3) and peptide sequences for DELLA or other GRAS homologues from *Marchantia polymorpha* (version 3.1), *Sphagnum fallax* (version 0.5; theoretical peptide sequence), *Selaginella moellendorffii* (version 1.0), *Amborella trichopoda* (version 1.0), *Oryza sativa* (version 7_JGI), *Solanum lycopersicum* (iTAG2.4), *Medicago truncatula* (Mt4.0v1), *Hordeum vulgare* (version r1), *Arabidopsis thaliana* (TAIR10) and *Selaginella moellendorffii* (version 1.0) were obtained from Phytozome (http://www.phytozome.net/) (Goodstein *et al.*, 2012) using BLASTP. The peptide sequences for *Triticum aestivum* (taxid:4565), *Pinus tabuliformis* (taxid:88731) and *Selaginella kraussiana* (taxid:81964) were obtained from NCBI (www.ncbi.nlm.nih.gov/BLAST/) using standard protein BLAST. The peptide sequences of *Encalypta streptocarpa, Hedwigia ciliata, Timmia autriaca* and *Schwetschkeopsis fabronia* were obtained using BLASTP from the oneKP database (One thousand plant transcriptomes initiative, 2019; https://db.cngb.org/onekp/). The

peptide sequences of *Anthoceros punctatus and Anthoceros agrestis* were obtained from Li *et al*. (2020) and those of *Ceratopteris richardii* from Marchant *et al.* (2019). The *At*RGA1 peptide sequence was used as a query for all BLAST searches.

Peptide sequences were aligned using SeaView software (version 4.7) (Gouy *et al*., 2010) and presented using BoxShade (version 3.2) (https://embnet.vital-it.ch/software/BOX_form.html) with default settings. DNA sequences were aligned using Clustal Omega (https://www.ebi.ac.uk/Tools/msa/clustalo/) with default settings. Phylogenetic trees of DELLA land plant homologues were generated using the maximum likelihood algorithm with 100 bootstrap replicates or the BioNJ algorithm with 1000 bootstrap replicates in SeaView on default settings, and presented using iTOL (https://itol.embl.de/). Primers were designed using the NCBI primer designing tool (https://www.ncbi.nlm.nih.gov/tools/primer-blast/).

GO term enrichment analysis for RNA-sequencing data was performed in PlantRegMap (Tian *et al.*, 2020) using the topGO package (Alexa and Rahnenfuhrer, 2020) and Fisher's exact test. Transcription factor enrichment analysis was performed in PlantRegMap using the Fisher's exact test and transcription factor prediction was also performed PlantRegMap using the family assignment rules and thresholds of the website. GO term enrichment analysis for proteomics data was performed in the Gene Ontology AmiGO database (Carbon *et al*., 2009) using the PANTHER overrepresentation test (Fisher's exact test with Bonferroni correction).

2.7 Nucleic acid isolation and analysis

2.7.1 Genomic DNA isolation

7-14-day old protonemata from *P. patens* were harvested and dried using filter paper. DNA was extracted as described in section **2.2.3** or using an Isolate II genomic DNA kit (Bioline) as per manufacturer's instructions. Essentially, tissue was ground up in an Eppendorf tube using a sterile micropestle and resuspended in lysis buffer. The lysate was then loaded on a spin column to allow binding of DNA to a silica membrane by means of hydrogen bonding, before being washed with an ethanol-based buffer. DNA was eluted from the membrane using nuclease free water (Qiagen), quantified using a NanoDrop spectrophotometer (Thermo Fisher Scientific) and stored at -20°C prior to PCR.

2.7.2 PCR and Colony PCR

PCR for cloning DNA was carried out using the proofreading high-fidelity DNA polymerases Q5® (New England Biolabs (NEB)) or Phusion® (NEB) according to manufacturer's instructions. 35 cycles were normally used as a starting point. For genotyping, HS Taq Mix Red (PCRBiosystems) was used according to manufacturer's instructions using 20µl reactions. To carry out colony PCR, single bacterial colonies were picked up using sterile 10µl pipette tips and diluted in 10µl dH_2O. 1µl of suspension was used as template DNA to carry out a PCR with HS Taq Mix Red (PCRBiosystems) using 20µl reactions. In the case of *Agrobacterium tumefaciens*, diluted colonies were incubated at 95^{o}C for 5 minutes before addition to the PCR mix, to enable efficient release of plasmid DNA from bacterial cells.

2.7.3 Agarose gel electrophoresis

0.6-1.0% agarose was made in 1xTBE (90mM Tris, 90mM boric acid, 2.5mM EDTA) and poured in gel trays containing gel combs. 6x gel loading dye (NEB) containing 1:1500 GelRed nucleic acid stain (Biotium) was added to the DNA samples and the 1kb or 100bp DNA ladder (NEB/PCRBiosystems), which were then loaded into wells in the gels. DNA was visualized with the Molecular Imager Gel Doc XR+ system using the Image Lab software (BioRad).

2.7.4 Gel extraction

PCR products used for cloning were loaded on 0.6% agarose gel and extracted from gel and purified using the Isolate II Gel extraction and purification kit (Bioline) as per manufacturer's instructions. Essentially, the gel band containing the DNA of interest was excised using a scalpel under UV light and then solubilised in buffer with high ionic strength at 50^{o}C. DNA in solution was then run through a spin column to allow binding of DNA to a silica membrane and subsequently washed using an ethanol-based buffer to clean from contaminants, before being eluted in 30µl dH_2O prewarmed at 50^{o}C. For optimal yields, multiple bands from PCRs run using the same template and conditions were loaded on the same column and eluted together.

2.7.5 Ligation

Ligations were performed using T4 DNA ligase as per manufacturer's instructions (NEB) with a 3:1 molar ratio of insert:vector, calculated using NEBioCalculator. If that did not work, ratios of 1:1, 2:1, 5:1 or 7:1 were used. Ligation

reactions were either incubated at 16°C or room temperature overnight or at 22°C for 2-3h.

2.7.6 Plasmid DNA extraction

Bacterial mini cultures were set up by inoculating 5-10ml LB liquid (Appendix) cultures containing the appropriate antibiotics with single transformed colonies picked up using sterile 10µl pipette tips. Liquid cultures were incubated in an orbital incubator for 16-20h at 37°C and plasmid DNA was extracted using Isolate II Plasmid Mini Kit (Bioline) as per manufacturer's instructions. In summary, this involved centrifugation of bacterial cells, cell lysis in an SDS/NaOH-based buffer, which allows denaturation and separation of plasmid DNA from chromosomal DNA, and neutralisation. Following centrifugation, the clear solution containing plasmid DNA was run through a spin column to allow binding of DNA to a silica membrane, washed twice with an ethanol-based buffer and eluted in 30µl dH_2O.

2.7.7 Restriction enzyme digests

Plasmid DNA was digested in CutSmart® buffer using restriction enzymes (NEB) as per manufacturer's instructions. In general, 20-30µl reactions were used for diagnostic digests, 30µl reactions for linearising plasmids for moss transformations, and 50µl reactions for cloning. 10 units of each restriction enzyme were used for digesting up to 5µg DNA for cloning or 30 units of a single enzyme for digesting up to 20µg DNA for plasmid linearisation. Digests were normally carried out for 2-3 hours or overnight at 37°C.

2.7.8 RNA isolation

RNA was extracted using the *Quick*-RNA^{TM} Plant Miniprep Kit (Zymo Research, California, USA) or the Isolate II RNA Plant Kit (Bioline, London, UK) as per manufacturer's instructions. This involved grinding up 100mg frozen tissue in liquid nitrogen using a mortar and a pestle pretreated with 70% ethanol or in sterile Eppendorf tubes using a frozen micropestle, followed by cell lysis in a lysis buffer, filtration through a spin column and mixing with ethanol. The resulting solution was then passed through a spin column to enable RNA binding to a silica membrane, followed by desalting, on-column DNA digestion, RNA clean-up with wash buffers and elution in 50µl RNAse-free water. RNA was visualised by agarose gel electrophoresis, quantified using a NanoDrop spectrophotometer (Thermo Fisher Scientific) and stored at -80°C.

2.7.9 cDNA synthesis

The Tetro cDNA synthesis kit (Bioline) was used to synthesise cDNA from RNA as per manufacturer's instructions. Oligo $(dT)_{18}$ were normally used in the reaction.

2.8 Bacterial and yeast methods

2.8.1 Bacterial and yeast strains

2.8.1.1 *Escherichia coli* DH5α

*SupE*44, Δ*lac*U169 (Φ80*lac*ZΔM15), *hsd*R17, *recA*1, *endA*1, *gyrA*96, *thi*-1, *relA*1.

2.8.1.2 *Agrobacterium tumefaciens* GV3101

A disarmed *Agrobacterium* strain produced in a C58 background with a rifampicin resistance gene and a pMP90 Ti virulence plasmid (pTiC5ΔT-DNA) carrying a gentamycin resistance gene.

2.8.1.3 *Saccharomyces cerevisiae* AH109

MATa, *trp*1-901, *leu*2-3, 112, *ura*3-52, *his*3-200, gal4., gal80., LYS2::$Gal1_{UAS}$-$GAL1_{TATA}$-HIS3, $Gal2_{UAS}$-$GAL2_{TATA}$-ADE2, URA3::$MEL1_{UAS}$-$MEL1_{TATA}$-lacZ MEL 1

2.8.2 Bacterial and yeast culture, transformation and protein extraction

2.8.2.1 *E. coli*

E. coli were cultured on LB agar medium (Appendix) in 90mm petri dishes or in liquid LB cultures (Appendix) in glass vials or conical flasks. Cultures were supplemented with 50-100µg/ml ampicillin or 50-100µg/ml carbenicillin or 50µg/ml zeocin (low salt LB, Appendix) or 50µg/ml kanamycin. LB agar plates were grown inverted at 37°C for 16-20h and liquid cultures were grown at 37°C with agitation (200rpm). Glycerol stocks were prepared by adding 500µl culture to 500µl of 50% glycerol and were then stored at -80°C.

2.8.2.2 *A. tumefaciens*

Agrobacterium cells were cultured on low salt LB agar medium (Appendix) or in low salt liquid LB (Appendix) as described for *E.coli* in section **2.8.2.1**. Cultures were supplemented with 50µg/ml kanamycin (for plasmid selection) and 25µg/ml rifampicin (selects for Agrobacterium). LB agar plates were grown inverted at 28-30°C for 48h and liquid cultures were grown at 28-30°C for 24-48h with agitation (200rpm). Glycerol

stocks were prepared by adding 500µl culture to 500µl of 50% glycerol and were then stored at -80°C.

2.8.2.3 *S. cerevisiae*

S. cerevisiae (AH109 strain) were cultured on YPAD agar medium (20g/L bacto-peptone, 10g/L bacto-yeast extract, 20g/L dextrose, 40mg/L adenine sulfate, 20g/L bacto-agar). Plates were grown inverted at 30°C for 2-3 days. Transformed yeast was cultured on -LW Drop-Out media (Appendix). Colonies growing on -LW plates were picked up and used to inoculate 5-10ml cultures of -LW, which were then incubated in an orbital incubator at 30°C with agitation (200rpm) for 24h. Glycerol stocks were prepared by adding 500µl culture to 500µl of 50% glycerol and were then stored at -80°C.

2.8.3 Bacterial and yeast transformations

2.8.3.1 Transformation of *E. coli*

50-100µl chemically competent DH5α *E. coli* cells (prepared by Xulyu Cao, University of Birmingham) were thawed on ice for 10 minutes and 5-20µl of completed ligation reaction or 1-2µl plasmid DNA (up to 1µg) was added and gently mixed with it. The mixture was incubated for 30 minutes on ice, heat shocked for 45-90 seconds at 42°C and returned to ice for 2-5 minutes. 250-700µl LB liquid medium (Appendix) was added to the mixture and was then incubated for 1-3h at 37°C with agitation (200rpm) to allow bacteria to recover from the heat shock and express the antibiotic resistance gene. The mixture was then centrifuged for 4 minutes at 3500 g and the supernatant was discarded so that ~150µl suspension was left in the tube. The bacterial pellet was

resuspended in the remaining supernatant, before being spread onto LB agar (Appendix) plates containing the appropriate antibiotic using a sterile plastic spreader (Thermofisher). Plates were sealed with micropore tape (3M Healthcare, Germany) and grown inverted at 37°C overnight. Successful incorporation of constructs was confirmed by colony PCR as described in section **2.7.2** and/or diagnostic digests as described in section **2.7.7** and sequencing.

2.8.3.2 Transformation of *A. tumefaciens*

Electrocompetent *A. tumefaciens* cells were prepared by Xulyu Cao (University of Birmingham). Briefly, a 250ml culture of *A. tumefaciens* was incubated at 28°C until an OD of 0.5-1.0 was reached. The culture was then incubated on ice for 15-30 minutes and centrifuged at 3000rpm for 10 minutes. The pelleted cells were washed with 250ml refrigerated water twice, resuspended in 10ml ice-cold 10% glycerol, centrifuged at 3000rpm for 10 minutes and finally resuspended in 2ml ice-cold 10% glycerol. Aliquots were frozen in liquid nitrogen and stored at -80°C.

100µl electrocompetent *A. tumefaciens* cells were thawed on ice for 10 minutes. 100-500ng binary transformation vector was added to the cells and gently mixed with them. The mixture was incubated on ice for 30 minutes and then transferred into a pre-chilled electroporation cuvette. The mixture was electroporated using a micropulser (BioRad) at 2.2kV for 5ms and then resuspended in 600µl low salt LB liquid (Appendix). The suspension was then transferred into an Eppendorf tube and incubated at 28-30°C for 3-4h with agitation (200rpm). This was followed, by centrifugation for 4 minutes at 3500 g and the discarding of the supernatant so that ~150µl liquid remained in the tube. Bacteria were resuspended in the remaining supernatant, before being spread

onto low salt LB agar (Appendix) plates containing the appropriate antibiotics using a sterile plastic spreader (Thermo Fisher Scientific). Plates were sealed with micropore tape (3M Healthcare, Germany) and grown inverted at 28-30ºC for 48h. Successful incorporation of constructs was confirmed by colony PCR as described in section **2.7.2** and/or diagnostic digests as described in section **2.7.7**.

2.8.3.3 Transformation of *S. cerevisiae*

Yeast transformation for yeast two-hybrid assays was performed as described in Bailey *et al*. (2021). Single yeast colonies were picked up with sterile 10µl inoculation loops (Sigma-Aldrich) and resuspended in 100µl transformation buffer (2:1 50% PEG 3350MW, 1M lithium acetate, 0.6% β-mercaptoethanol). 2µg of each plasmid containing the construct of interest was added to the mixture, which was then vortexed briefly and given a pulse in the centrifuge. Tubes containing the mixture were mounted at a 45º and incubated at 37ºC for 45 minutes on an orbital shaker (200rpm), before being plated on -LW Drop-Out medium (Appendix) to select for co-transformed plasmids. Plates were sealed with micropore tape (3M Healthcare, Germany) and incubated inverted at 30ºC for 2-4 days or at room temperature for 7 days.

2.8.4 *S. cerevisiae* protein extraction

Yeast was grown overnight in liquid cultures as described in section **2.8.2.3**. Concentration was adjusted to OD_{600} of 8 and 1ml culture was pelleted by centrifuging for 4 minutes at 12000 g. The supernatant was removed and the pellet was resuspended in 50µl Buffer A (0.1M NaOH, 50mM EDTA, 2% SDS, 2% β-mercaptoethanol) and incubated for 10 minutes at 90ºC. 0.67µl 3M acetic acid was

added to the suspension, which was then vortexed for 30s on a Titrtek and 1 minute on the vortex. The suspension was then incubated for 10 minutes at 90^{o}C and 12.5µl of Buffer B (250mM Tris pH6.8, 50% glycerol, 0.05% bromophenol blue) was added to it, followed by vortexing for 2 seconds. The mixture was centrifuged at 12000 g for 5 minutes and 55µl supernatant was transferred to a new tube. The tube containing the supernatant was boiled for 1 minute at 98^{o}C before being stored at -20^{o}C or analysed by SDS-PAGE (see section **2.18**).

2.9 Cloning of *PpDELLA* and other genes in *P. patens*, Arabidopsis and *S. cerevisiae*

2.9.1 Vectors

pGreenII 0029 and pSoup

The 4.6kb disarmed T-DNA pGreenII 0029 plasmid contains two aminoglycoside phosphotransferase cassettes conferring kanamycin resistance in both plants and bacteria, a MCS within the 35S promoter and a *GFP* gene, enabling GFP fusion proteins to be synthesised. The pSoup plasmid confers gentamycin resistance and encodes the RecA protein, which allows pGreenII 0029 to replicate in *A. tumefaciens*.

pBI121 (Li *et al*., 2015)

A 12.9kb modified pBI121 plasmid containing two aminoglycoside phosphotransferase cassettes conferring resistance to kanamycin in bacteria and plants and a MCS located within a NOS cassette.

pDONR^{TM}/Zeo (ThermoFisher Scientific)

The 4.3kb Gateway^{TM} plasmid contains a zeocin resistance cassette for selection in bacteria and attP sites enabling directional cloning of PCR products via BP recombination.

pEarleyGate-104 (Earley *et al*., 2006)

The 12.5kb Gateway^{TM} plasmid contains an aminoglycoside phosphotransferase cassette conferring resistance to kanamycin in bacteria and an enhanced YFP (eYFP) gene under the control of the CaMV 35S promoter, enabling generation of N-terminal fusion proteins via LR recombination.

pGBKT7 (Clontech)

The 7.3kb plasmid contains a neomycin phosphotransferase cassette conferring resistance to kanamycin in bacteria and a *TRP1* marker for nutritional selection in yeast. A MCS is located downstream of the *GAL4* DNA binding domain (BD), which is under the control of the yeast *ADH1* promoter, enabling generation of GAL4-BD-protein fusions in yeast. A T7 promoter site and a MYC epitope tag are found downstream of the *GAL4-BD* domain, allowing the *in vitro* synthesis of (N-terminal) epitope tagged proteins.

pGADT7 (Clontech)

The 8.0kb plasmid contains a *bla* gene encoding beta-lactamase which confers resistance to ampicillin and carbenicillin in bacteria and a *LEU2* marker for nutritional selection in yeast. A MCS is located downstream of the *GAL4* activation domain (AD), which is under the control of the yeast *ADH1* promoter enabling generation of GAL4-

AD-protein fusions in yeast. A T7 promoter site and a HA epitope tag are found downstream of the GAL4-AD domain, allowing the *in vitro* synthesis of (N-terminal) epitope tagged proteins.

pHSP-MCS-GFP-108-35SNPT (GenBank: KP893621.1; Moody *et al*., 2016)

The 8.22kb plasmid contains a multiple cloning site (MCS) within a heat-shock promoter, an *mGFP* gene enabling GFP fusion proteins to be synthesised, a neomycin phosphotransferase cassette conferring resistance to kanamycin and G418 in plant cells, and a 1.9kb sequence homologous to the inert genomic 108 locus. It also has a *bla* gene encoding beta-lactamase which confers resistance to ampicillin and carbenicillin in bacteria.

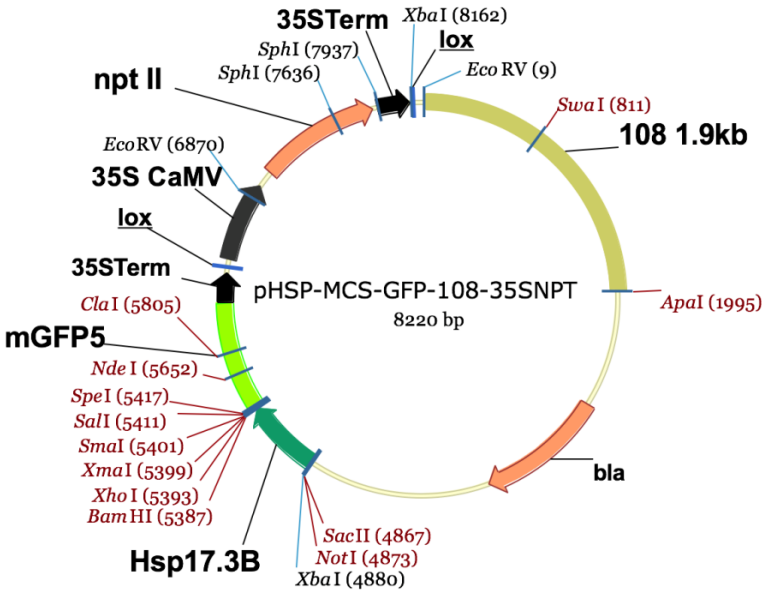

pHSP-MCS-GFP-108-35SHYGR (Generated during the course of this research)

The 8.711kb plasmid contains a multiple cloning site (MCS) within a heat-shock promoter, a *mGFP* gene, enabling GFP fusion proteins to be synthesised, an aminoglycoside phosphotransferase cassette conferring resistance to hygromycin B in plant cells, and a 1.9kb sequence homologous to the inert genomic 108 locus. It also has a *bla* gene encoding beta-lactamase which confers resistance to ampicillin and carbenicillin in bacteria. The plasmid was generated by replacing the neomycin phosphotransferase cassette from pHSP-MCS-GFP-108-35SNPT with an aminoglycoside phosphotransferase cassette, taken from pGWB14 (provided by Dr Mark Bailey, University of Birmingham). The neomycin phosphotransferase cassette was digested out of pHSP-MCS-GFP-108-35SNPT plasmid using EcoRV restriction endonucleases and the aminoglycoside phosphotransferase cassette was amplified from pGWB14 using *p35S-HygR-NOS_F* and *p35S-HygR-NOS_R* (see section **2.9.8** for primer sequences), using Q5® High-Fidelity DNA polymerase as per manufacturer's instructions (NEB), an annealing temperature of 53^{o}C, 90 seconds' extension time and 35 cycles. The PCR product was gel extracted and purified as described in section **2.7.4**, ligated with pCR-blunt using the Zero Blunt PCR cloning kit (Thermo Fisher Scientific) as per manufacturer's instructions, and subsequently incorporated into competent DH5α *E. coli* by transformation as described in section **2.8.3.1**. Transformation mixtures were plated out onto LB agar (Appendix) plates containing 50µg/ml kanamycin and incubated for 16-20h at 37^{o}C. 4 colonies were selected for colony PCR (see section **2.7.2**) with the primers used to amplify the construct. Positive colonies were used to inoculate individual 5-10ml LB liquid (Appendix) cultures supplemented with 50µg/ml kanamycin, which were then

incubated in an orbital incubator overnight at 37°C (200rpm). Plasmid DNA was extracted as described in section **2.7.6** and screened for correct integration of the PCR product via diagnostic digests using EcoRV. Inserts were then sequenced (Eurofins, Germany) from both ends using the universal primers *M13_F* and *M13_R* as well as *p35S-HygR-NOS_R* (see section **2.9.8** for primer sequences).

The *p35S::HygR-NOS* construct was digested out of pCR-blunt using EcoRV for 2h at 37°C. Digested pHSP-MCS-GFP-108-35S and *p35S::HygR-NOS* constructs were gel extracted and purified as described in section **2.7.4** and ligated together using T4 DNA ligase, as per manufacturer's instructions (NEB). Chemically competent DH5α *E. coli* were transformed with the ligation reactions as described in section **2.8.3.1**. Transformation mixtures were plated out onto LB agar plates containing 50µg/ml carbenicillin and incubated for 16-20h at 37°C. 12 colonies were selected for colony PCR (see section **2.7.2**) with the primers used to amplify the construct. Positive colonies were used to inoculate individual 5-10ml LB liquid cultures supplemented with 50µg/ml carbenicillin and cultures were then incubated in an orbital incubator overnight at 37°C (200rpm). Plasmid DNA was extracted as described in section **2.7.6** and screened for correct integration of the PCR product via diagnostic digests using XhoI and AatII. The *pHSP::PpDELLAb-GFP-108-35SHYGR* plasmid identity was only confirmed by colony PCR and not by diagnostic digests, as after various attempts, plasmid extractions from liquid cultures did not produce sufficient yields in order to carry out diagnostic digests or to transform moss protoplasts.

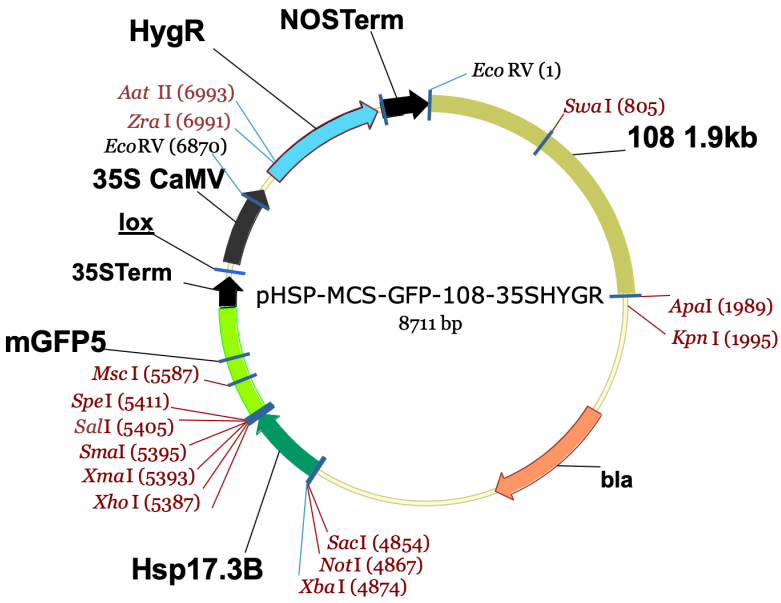

2.9.2 Cloning of *PpDELLAa* and *PpDELLAb* in pHSP::MCS-GFP-108 for inducible overexpression in *P. patens*

Genomic DNA extracted from 10-day old *P. patens* protonemata as described in section **2.7.1** was used as template in PCR reactions using Q5® High-Fidelity DNA polymerase as per manufacturer's instructions (NEB). The *PpDELLAa* coding sequence (excluding the stop codon) was amplified using *XhoI-PpDELLAa_pHSP-F* and *SalI-PpDELLAa_pHSP-R*, and *Pp*DELLAb coding sequence (excluding the stop codon) was amplified using *XhoI-PpDELLAb_pHSP-F* and *SalI-PpDELLAb_pHSP-R* (see section **2.9.8** for primer sequences), with an annealing temperature of 60ºC, 90 seconds' extension time and 35 cycles.

PCR products were gel extracted and purified as described in section **2.7.4**, ligated with pCR-blunt using the Zero Blunt PCR cloning kit (Thermo Fisher Scientific) as per manufacturer's instructions, and the ligation reaction was subsequently used to transform competent DH5α *E. coli* as described in section **2.8.3.1**. Transformation mixtures were plated out onto LB agar (Appendix) plates containing 50µg/ml

kanamycin and incubated for 16-20h at 37°C. 2-6 colonies were selected for colony PCR (see section **2.7.2**) with the primers used to amplify the construct. Positive colonies were used to inoculate individual 5-10ml LB liquid (Appendix) cultures supplemented with 50µg/ml kanamycin, which were then incubated in an orbital incubator overnight at 37°C (200rpm). Plasmid DNA was extracted as described in section **2.7.6** and screened for correct integration of the PCR product via diagnostic digests using XhoI and SalI. Inserts were then sequenced (Eurofins, Germany) from both ends using the universal primers *M13_F* and *M13_R* as well as *XhoI-PpDELLAa_pHSP-F* and *PpDELLAa_internal_F* or *XhoI-PpDELLAb_pHSP-F* and *PpDELLAb_internal_F* for *PpDELLAa* and *PpDELLAb* respectively (see section **2.9.8** for primer sequences).

Destination plasmids pHSP::MCS-GFP-108 (*nptII* or *HygR*) and pCR-blunt containing *PpDELLA* construct were digested using XhoI and SalI for 2h at 37°C. 0.5U/µg Calf Intestinal Alkaline Phosphatase (CIP) (NEB) was added to pHSP::MCS-GFP-108 digest mixture for a further hour at 37°C to prevent vector self-ligation. Digested pHSP::MCS-GFP-108 (nptII or HygR) and *PpDELLA* constructs were gel extracted and purified as described in section **2.7.4** and ligated together using T4 DNA ligase as per manufacturer's instructions (NEB). Chemically competent DH5α *E. coli* were transformed with the ligation reactions as described in section **2.8.3.1**. Transformation mixtures were plated out onto LB agar plates containing 50µg/ml carbenicillin and incubated for 16-20h at 37°C. 2-6 colonies were selected for colony PCR (see section **2.7.2**) with the primers used to amplify the construct. Positive colonies were used to inoculate individual 5-10ml LB liquid cultures supplemented with 50µg/ml carbenicillin, which were then incubated in an orbital incubator overnight at

37°C (200rpm). Plasmid DNA was extracted and screened for correct integration of *PpDELLA* via diagnostic digests using XhoI and SalI.

2.9.3 Cloning of *PpDELLAa* and *PpDELLAb* in the pGreenII 0029 vector for constitutive overexpression in Arabidopsis

The *p35S::PpDELLA-GFP-Ter* constructs were generated in pGreenII 0029 by replacing *SELAGIDILLO* in the *p35S::SELAGIDILLO-GFP-Ter* construct (Moody *et al*., 2016). *PpDELLAa* and *PpDELLAb* coding sequences (excluding stop codons) were amplified from the previously generated *pHSP::PpDELLA-GFP-108-35SNPT* vector using *BamHI-PpDELLAa_pGreen-F* with *NotI-PpDELLAa_pGreen-R* and *XbaI-PpDELLAb_pGreen-F* with *NotI-PpDELLAb_pGreen-R* for *PpDELLAa* and *PpDELLAb* respectively (see section **2.9.8** for primer sequences). PCR was performed using Q5® High-Fidelity DNA polymerase as per manufacturer's instructions (NEB), with an annealing temperature of 60°C, 90 seconds' extension time and 35 cycles. PCR products were gel extracted and purified as described in section **2.7.4** and ligated with pCR-blunt using the Zero Blunt PCR cloning kit (Thermo Fisher Scientific) as per manufacturer's instructions. Ligations were subsequently used to transform competent DH5α *E. coli* as described in section **2.8.3.1**. Transformation mixtures were plated out onto LB agar (Appendix) plates containing 50µg/ml kanamycin and incubated for 16-20h at 37°C. 2-6 colonies were selected for colony PCR (see section **2.7.2**) with the primers used to amplify the construct. Positive colonies were used to inoculate individual 5-10ml LB liquid (Appendix) cultures supplemented with 50µg/ml kanamycin which were then incubated in an orbital incubator overnight at 37°C (200rpm). Plasmid DNA was extracted and purified as described in section **2.7.4** and screened for correct

integration of the PCR product via diagnostic digests using BamHI/NotI or XbaI/NotI for *PpDELLAa* or *PpDELLAb* respectively. Inserts were then sequenced (Eurofins, Germany) from both ends using the universal primers M13_F and M13_R, as well as *BamHI-PpDELLAa_pGreen-F* and *PpDELLAa_internal_F* or *XbaI-PpDELLAb_pGreen-F* and *PpDELLAb_internal_F* (see section **2.9.8** for primer sequences) for *PpDELLAa* or *PpDELLAb* respectively.

The vector pGreenII 0029 containing *p35S::SELAGIDILLO-GFP-Ter* construct was digested using BamHI/NotI or XbaI/NotI for 2h at 37°C to remove *SELAGIDILLO*. This was followed by treatment with 0.5U/µg Calf Intestinal Alkaline Phosphatase (CIP) (NEB) for 1h and subsequent gel extraction and purification as described in section **2.7.4**. *PpDELLAa* and *PpDELLAb* were digested out of the pCR-blunt vector using BamHI/NotI or XbaI/NotI respectively and ligated with digested pGreenII 0029 using T4 DNA ligase as per manufacturer's instructions (NEB). Ligated products were used to transform chemically competent DH5α *E. coli* as described in section **2.8.3.1**. Transformation mixtures were plated out onto LB agar plates containing 50µg/ml kanamycin and incubated for 16-20h at 37°C. 2-6 colonies were selected for colony PCR (see section **2.7.2**) with the primers used to amplify the construct. Positive colonies were used to inoculate individual 5-10ml LB liquid cultures supplemented with 50µg/ml kanamycin which were then incubated in an orbital incubator overnight at 37°C (200rpm). Plasmid DNA was extracted and purified as described in section **2.7.4** and screened for correct integration of *PpDELLA* via diagnostic digests using BamHI/NotI for *PpDELLAa* or XbaI/NotI for *PpDELLAb*.

2.9.4 Cloning of *PpPHY5B, PpPHOTA2*, *PpPHOTB1, PpDOG1*s and *AtDOG1* in the pGBKT7 vector for constitutive overexpression in *S. cerevisiae*

PpDELLAs and *AtRGA1* cloned in pGADT7 (Yasumura *et al*., 2007) were kindly provided by Professor Nicholas Harberd (University of Oxford). In order to test the interaction between *Pp*DELLA proteins and a number of different candidate interaction partners, the genes encoding those candidate proteins were cloned in pGBKT7. These genes were: *PpPHY5B (Pp3c12_9240), PpPHOTA2 (Pp3c21_21410), PpPHOTB1 (Pp3c2_10380)*, three *PpDOG1* genes: *Pp3c13_11750*, *Pp3c26_14620* and *Pp3c3_9650*, *AtDOG1* and truncated versions of *PpDOG1*s. *PpGLP1* and *AtGID1c* cloned in pGBKT7 (Yasumura *et al*., 2007) were also kindly provided by Professor Nicholas Harberd (University of Oxford).

P. patens cDNA was synthesised from RNA isolated from gametophore tissue as described in sections **2.7.8** and **2.7.9**, and used as template in PCR reactions using Phusion® High-Fidelity DNA polymerase (NEB) as per manufacturer's instructions. *PpDOG1* cDNA (excluding the start codons) was amplified using *NdeI-Pp3c13_11750_F* with *SalI-Pp3c13_11750_R*, *NdeI-Pp3c26_14620_F* with *SalI-Pp3c26_14620_R*, and *NdeI-Pp3c3_9650_F* with *SalI-Pp3c3_9650_R* (see section **2.9.8** for primer sequences), using an annealing temperature of 55ºC, 3 minutes' extension time and 35 cycles. PCR products were gel extracted and purified as described in section **2.7.4** and ligated with pCR-blunt using the Zero Blunt PCR cloning kit (Thermo Fisher Scientific) as per manufacturer's instructions. The ligation reaction was subsequently used to transform competent DH5α *E. coli* as described in section **2.8.3.1**. Transformation mixtures were plated out onto LB agar (Appendix) plates containing 50µg/ml kanamycin and incubated for 16-20h at 37ºC. 2-8 colonies were

selected for colony PCR (see section **2**.**7.2**) with the primers used to amplify the cDNAs. Positive colonies were used to inoculate individual 5-10ml LB liquid (Appendix) cultures supplemented with 50µg/ml kanamycin, which were then incubated in an orbital incubator overnight at 37°C (200rpm). Plasmid DNA was extracted as described in section **2.7.6** and screened for correct integration of the cDNAs via diagnostic digests using NdeI and SalI. Inserts were then sequenced (Eurofins, Germany) from both ends using the universal primers *M13_F* and *M13_R* (see section **2.9.8** for primer sequences). Sequencing showed that for *Pp3c26_14620*, *Pp3c26_14620V3.3* cDNA was cloned instead of *Pp3c26_14620V3.1* due to their high sequence similarity, therefore *Pp3c26_14620V3.3* was used in all subsequent cloning steps.

The three *PpDOG1* genes were digested out of pCR-blunt using NdeI and SalI for 2h at 37°C and pGBKT7 was also digested with the same enzymes using the same conditions. 0.5U/µg Calf Intestinal Alkaline Phosphatase (CIP) (NEB) was added to the pGBKT7 digest mixture for a further hour at 37°C to dephosphorylate the vector. Digested pGBKT7 and *PpDOG1* constructs were gel extracted and purified as described in section **2.7.4** and ligated together using T4 DNA ligase (NEB), as per manufacturer's instructions. Chemically competent DH5α *E. coli* were transformed with the ligation reactions as described in section **2.8.3.1**. Transformation mixtures were plated out onto LB agar plates containing 50µg/ml kanamycin and incubated for 16-20h at 37°C. 2-8 colonies were selected for colony PCR (see section **2**.**7.2**) using *T7_F* and either *SalI-Pp3c13_11750_R* or *SalI-Pp3c26_14620_R* or *SalI-Pp3c3_9650_R* (see section **2.9.8** for primer sequences). Positive colonies were used to inoculate individual 5-10ml LB liquid cultures supplemented with 50µg/ml kanamycin, which were then incubated in an orbital incubator overnight at 37°C (200rpm). Plasmid DNA

was extracted as described in section **2.7.6** and screened for correct integration of the constructs via diagnostic digests using NdeI and SalI. Plasmids were re-sequenced using *T7_F* and *M13_R* (see section **2.9.8** for primer sequences).

Truncated *PpDOG1* genes encoding either the DOG1 domain (N-terminal) or the ankyrin domain (C-terminal) were amplified from pGBKT7 containing cDNA from the three *PpDOG1* genes. Truncations of *Pp3c13_11750* were amplified using *NdeI-Pp3c13_11750_F* with *SalI- Pp3c13_11750_DOG_R* (DOG1 domain, encoding amino acids 1-280) and *NdeI-Pp3c13_11750_ANK_F with SalI-Pp3c13_11750_R* (ankyrin domain, encoding amino acids 281-512) (see section **2.9.8** for primer sequences), using an annealing temperature of 55^{o}C, 3 minutes' extension time and 35 cycles. Truncations of *Pp3c3_9650* were amplified using *NdeI-Pp3c3_9650_F* with *SalI-Pp3c3_9650_DOG_R* (DOG1 domain, encoding amino acids 1-296) and *NdeI-Pp3c3_9650_ANK_F* with *SalI-Pp3c3_9650_R* (Ankyrin domain, encoding amino acids 297-531) (see section **2.9.8** for primer sequences), using an annealing temperature of 55^{o}C, 3 minutes' extension time and 35 cycles. Truncations of *Pp3c26_14620* were amplified using *NdeI-Pp3c26_14620_F* with *SalI-Pp3c26_14620_DOG_R* (DOG1 domain, encoding amino acids 1-278) and *NdeI-Pp3c26_14620_ANK_F* with *SalI-Pp3c26_14620V3.3_R* (Ankyrin domain, encoding amino acids 279-512) (see section **2.9.8** for primer sequences), using an annealing temperature of 55^{o}C, 3 minutes' extension time and 35 cycles. All PCR products were gel extracted and purified as described in section **2.7.4**, digested using NdeI and SalI for 2h at 37^{o}C and directly ligated with digested pGBKT7 using T4 DNA ligase (NEB), as per manufacturer's instructions. The ligation reactions were subsequently used to transform competent DH5α *E. coli* as described in section **2.8.3.1**. Transformation

mixtures were plated out onto LB agar (Appendix) plates containing 50µg/ml kanamycin and incubated for 16-20h at 37ºC. 8-12 colonies were selected for colony PCR (see section **2.7.2**) using *T7_F* and the reverse primer used to amplify each insert (see section **2.9.8** for primer sequences). Positive colonies were used to inoculate individual 5-10ml LB liquid (Appendix) cultures supplemented with 50µg/ml kanamycin, which were then incubated in an orbital incubator overnight at 37ºC (200rpm). Plasmid DNA was extracted as described in section **2.7.6** and sequenced (Eurofins, Germany) using *T7_F* (see section **2.9.8** for primer sequence).

The *AtDOG1* CDS (excluding the start codon) was cloned from cDNA from Col-0 Arabidopsis seedlings kindly provided by Dr Mark Bailey (University of Birmingham). The cDNA was used as template in a PCR reaction using Phusion® High-Fidelity DNA polymerase (NEB) as per manufacturer's instructions. *AtDOG1* was amplified using *NdeI-AtDOG1_F* and *EcoRI-AtDOG1_R* (see section **2.9.8** for primer sequences), using an annealing temperature of 50ºC, 4 minutes' extension time and 38 cycles. The PCR product was gel extracted and purified as described in section **2.7.4**, and directly digested using NdeI and EcoRI for 2h at 37ºC. After being gel extracted and purified as described in section **2.7.4**, the digested PCR product was ligated with pGBKT7 that had been digested with NdeI and EcoRI under the same conditions, dephosphorylated for a further hour with 0.5U/µg Calf Intestinal Alkaline Phosphatase (CIP) (NEB) and gel extracted and purified as described in section **2.7.4***.* The ligation reaction was subsequently used to transform competent DH5α *E. coli* as described in section **2.8.3.1**. Transformation mixtures were plated out onto LB agar (Appendix) plates containing 50µg/ml kanamycin and incubated for 16-20h at 37ºC. 8 colonies were selected for colony PCR (see section **2.7.2**) using *T7_F* and *EcoRI-AtDOG1_R* (see

section **2.9.8** for primer sequences). Positive colonies were used to inoculate individual 5-10ml LB liquid (Appendix) cultures supplemented with 50µg/ml kanamycin, which were then incubated in an orbital incubator overnight at 37ºC (200rpm). Plasmid DNA was extracted as described in section **2.7.6** and sequenced (Eurofins, Germany) from both ends using the universal primers *T7_F* and *M13_R* (see section **2.9.8** for primer sequences).

PpPHY5B, PpPHOTA2 and *PpPHOTB1* cDNA (excluding the start codons) was amplified in PCR reactions using Phusion® High-Fidelity DNA polymerase (NEB) as per manufacturer's instructions, using *NdeI-PpPHY5B_F* with *NotI-PpPHY5B_R*, *SalI-PpPHOTA2_F* (including an additional TT after the restriction site to enable in-frame cloning) with *NotI- PpPHOTA2_R*, and *NdeI-PpPHOTB1_F* with *NotI-PpPHOTB1_R* (see section **2.9.8** for primer sequences), using an annealing temperature of 55ºC, 5 minutes' extension time and 35 cycles. PCR products were gel extracted and purified as described in section **2.7.4** and ligated with pCR-blunt using the Zero Blunt PCR cloning kit (Thermo Fisher Scientific) as per manufacturer's instructions. The ligation reaction was subsequently used to transform competent DH5α *E. coli* as described in section **2.8.3.1**. Transformation mixtures were plated out onto LB agar plates containing 50µg/ml kanamycin and incubated for 16-20h at 37ºC. 2-8 colonies were selected for colony PCR (see section **2.7.2**) with the primers used to amplify the cDNAs. Positive colonies were used to inoculate individual 5-10ml LB liquid cultures supplemented with 50µg/ml kanamycin, which were then incubated in an orbital incubator overnight at 37ºC (200rpm). Plasmid DNA was extracted as described in section **2.7.6** and screened for correct integration of the cDNAs via diagnostic digests using NdeI and NotI or SalI and NotI in the case of *PpPHOTA2*. Inserts were then

sequenced (Eurofins, Germany) from both ends using the universal primers *M13_F* and *M13_R* (see section **2.9.8** for primer sequences).

PpPHY5B, PpPHOTA2 and *PpPHOTB1* cDNA (excluding the start codons) was amplified using plasmid (pCR-blunt) DNA as template and *NdeI-PpPHY5B_F* with *NotI-PpPHY5B_R*, *SalI-PpPHOTA2_F* with *NotI-PpPHOTA2_R*, and *NdeI-PpPHOTB1_F* with *NotI-PpPHOTB1_R* (see section **2.9.8** for primer sequences), using an annealing temperature of 55°C, 5 minutes' extension time and 35 cycles. PCR products were gel extracted and purified as described in section **2.7.4**, and directly digested using either NdeI and NotI or SalI and NotI in the case of *PpPHOTA2* for 2-3h at 37°C. The plasmid pGBKT7 was also digested using the same enzyme combinations for 2h at 37°C and treated with 0.5U/µg Calf Intestinal Alkaline Phosphatase (CIP) (NEB) for a further hour. Digested *PpPHY5B*, *PpPHOTA2* and *PpPHOTB1* were gel extracted and purified as described in section **2.7.4** and then ligated with digested pGBKT7 using T4 DNA ligase (NEB), as per manufacturer's instructions. Chemically competent DH5α *E. coli* were transformed with the ligation reactions as described in section **2.8.3.1**. Transformation mixtures were plated out onto LB agar plates containing 50µg/ml kanamycin and incubated for 16-20h at 37°C. 2-8 colonies were selected for colony PCR (see section **2.7.2**) using *T7_F* and either *NotI-PpPHY5B_R*, or *NotI- PpPHOTA2_R* or *NotI-PpPHOTB1_R* (see section **2.9.8** for primer sequences). Positive colonies were used to inoculate individual 5-10ml LB liquid cultures supplemented with 50µg/ml kanamycin, which were then incubated in an orbital incubator overnight at 37°C (200rpm). Plasmid DNA was extracted as described in section **2.7.6** and screened for correct integration of the constructs via diagnostic digests using either NdeI and NotI or SalI and NotI in the case of *PpPHOTA2*.

Plasmids were sequenced (Eurofins, Germany) using a number of primers due to the large size of the inserted constructs. To confirm the presence of *PpPHY5B*, the following primers were used for sequencing: *T7_F*, *NdeI-PpPHY5B_F, PpPHY5B-Seq_F, PpPHY5B-Seq2_F, PpPHY5B-Seq3_F* (see section **2.9.8** for primer sequences). To confirm the presence of *PpPHOTA2* the following primers were used for sequencing: *T7_F*, *M13_R*, *SalI-PpPHOTA2_F, PpPHOTA2-Seq_F, PpPHOTA2-Seq2_F, PpPHOTA2-Seq3_F* (see section **2.9.8** for primer sequences). Finally, to confirm the presence of *PpPHOTB1* the following primers were used for sequencing: *T7_F*, *M13_R*, *NdeI-PpPHOTB1_F, PpPHOTB1-Seq_F, PpPHOTB1-Seq2_F, PpPHOTB1-Seq3_F* (see section **2.9.8** for primer sequences).

2.9.5 Cloning of *PpDOG1*s and *AtDOG1* in the binary vector pBI121 for constitutive overexpression in *A. thaliana* or *N. benthamiana*

PpDOG1 genes were first cloned in pGBKT7 as described in section **2.9.4** in order to acquire the N-terminal MYC epitope and were then used as templates in PCR reactions using Q5® High-Fidelity DNA polymerase (NEB) or Phusion® High-Fidelity DNA polymerase (NEB) as per manufacturer's instructions. *MYC-PpDOG1* genes were amplified using *KpnI-MYC_F* and either *SalI-Pp3c13_11750_R* or *SalI-Pp3c26_14620_R* or *SalI-Pp3c3_9650_R* (see section **2.9.8** for primer sequences), with an annealing temperature of 55^{o}C, 3 minutes' extension time and 35 cycles. To amplify a shorter splicing variant of *Pp3c26_14620*, *KpnI-MYC_F* was used with *SalI-Pp3c26_14620_SHR_R* (see section **2.9.8** for primer sequences) under the same PCR conditions. PCR products were gel extracted and purified as described in section **2.7.4** and directly digested using KpnI and SalI for 2h at 37^{o}C. The plasmid pBI121 was also

digested using the same enzymes for 2h at 37ºC and treated with 0.5U/µg Calf Intestinal Alkaline Phosphatase (CIP) (NEB) for a further hour. Digested *MYC-PpDOG1*s and pBI121 were gel extracted and purified as described in section **2.7.4** and then ligated together using T4 DNA ligase (NEB), as per manufacturer's instructions. Chemically competent DH5α *E. coli* were transformed with the ligation reactions as described in section **2.8.3.1**. Transformation mixtures were plated out onto LB agar plates containing 50µg/ml kanamycin and incubated for 16-20h at 37ºC. 3-12 colonies were selected for colony PCR (see section **2.7.2**) using *p35S_F* and either *SalI-Pp3c13_11750_R* or *SalI-Pp3c26_14620_R* or *SalI-Pp3c3_9650_R* or *SalI-Pp3c26_14620_SHR_R* (see section **2.9.8** for primer sequences) with an annealing temperature of 55ºC, 2.5-3 minutes' extension time and 35 cycles. Positive colonies were used to inoculate individual 5-10ml LB liquid cultures supplemented with 50µg/ml kanamycin, which were then incubated in an orbital incubator overnight at 37ºC (200rpm). Plasmid DNA was extracted as described in section **2.7.6** and sequenced (Eurofins, Germany) using *p35S_F* and *pBI121-Seq_R* or *p35S_F* and *NdeI-Pp3c26_14620_ANK_F* (see section **2.9.8** for primer sequences).

AtDOG1 cDNA was first cloned in pGBKT7 as described in section **2.9.4** in order to acquire the N-terminal MYC epitope and were then used as template in a PCR reaction using Phusion® High-Fidelity DNA polymerase (NEB) as per manufacturer's instructions. *MYC-AtDOG1* was amplified using *KpnI-MYC_F* and *EcoRI-AtDOG1_R* (see section **2.9.8** for primer sequences), with an annealing temperature of 55ºC, 3 minutes' extension time and 35 cycles. The PCR product was gel extracted and purified as described in section **2.7.4** and directly digested using KpnI and EcoRI overnight at 37ºC. The plasmid pBI121 was also digested using the same enzymes

overnight at 37°C and treated with 0.5U/µg Calf Intestinal Alkaline Phosphatase (CIP) (NEB) for a further hour. Digested *MYC-AtDOG1* and pBI121 were gel extracted and purified as described in section **2.7.4** and then ligated together using T4 DNA ligase (NEB), as per manufacturer's instructions. The ligation reaction was subsequently used to transform competent DH5α *E. coli* as described in section **2.8.3.1**. Transformation mixtures were plated out onto LB agar (Appendix) plates containing 50µg/ml kanamycin and incubated for 16-20h at 37°C. 8 colonies were selected for colony PCR (see section **2.7.2**) with the primers used to amplify the insert. Positive colonies were used to inoculate individual 5-10ml LB liquid (Appendix) cultures supplemented with 50µg/ml kanamycin, which were then incubated in an orbital incubator overnight at 37°C (200rpm). Plasmid DNA was extracted as described in section **2.7.6** and screened for correct integration of the insert via diagnostic digests using KpnI and EcoRI. The insert was then sequenced (Eurofins, Germany) using *p35S_F* (see section **2.9.8** for primer sequence).

AtDOG1 gDNA was also cloned in pGBKT7 in order to acquire the MYC tag. Genomic DNA from Col-0 Arabidopsis seedlings kindly provided by Tumie Akintewe (University of Birmingham) was used as template in a PCR reaction using Phusion® High-Fidelity DNA polymerase (NEB) as per manufacturer's instructions to amplify the genomic sequence of *At*DOG1 (excluding the start codon). *AtDOG1* was amplified using *NdeI-AtDOG1_F* with *EcoRI-AtDOG1_R* (see section **2.9.8** for primer sequences), using an annealing temperature of 50°C, 4 minutes' extension time and 38 cycles. The PCR product was gel extracted and purified as described in section **2.7.4**, and directly digested using NdeI and EcoRI for 2h at 37°C. After being gel extracted and purified as described in section **2.7.4**, the digested PCR product was

ligated with pGBKT7 that had been digested with NdeI and EcoRI under the same conditions, dephosphorylated for a further hour with 0.5U/µg Calf Intestinal Alkaline Phosphatase (CIP) (NEB) and gel extracted and purified as described in section **2.7.4**. The ligation reaction was subsequently used to transform competent DH5α *E. coli* as described in section **2.8.3.1**. Transformation mixtures were plated out onto LB agar (Appendix) plates containing 50µg/ml kanamycin and incubated for 16-20h at 37ºC. 2-8 colonies were selected for colony PCR (see section **2.7.2**) with the primers used to amplify the insert. Positive colonies were used to inoculate individual 5-10ml LB liquid (Appendix) cultures supplemented with 50µg/ml kanamycin, which were then incubated in an orbital incubator overnight at 37ºC (200rpm). Plasmid DNA was extracted as described in section **2.7.6** and screened for correct integration of the insert via diagnostic digests using NdeI and EcoRI. The Insert was then sequenced (Eurofins, Germany) from both ends using the universal primers *T7_F* and *M13_R* (see section **2.9.8** for primer sequences).

MYC-AtDOG1 was amplified from pGBKT7 in a PCR reaction using Phusion® High-Fidelity DNA polymerase (NEB) as per manufacturer's instructions with *XbaI-MYC_F* and *KpnI-AtDOG1_R* (see section **2.9.8** for primer sequences), using an annealing temperature of 55ºC, 3 minutes' extension time and 38 cycles. The PCR product was gel extracted and purified as described in section **2.7.4**, and directly digested using XbaI and KpnI for 2h at 37ºC. After being gel extracted and purified as described in section **2.7.4**, the digested PCR product was ligated with pBI121 that had been digested with XbaI and KpnI under the same conditions, dephosphorylated for an hour with 0.5U/µg Calf Intestinal Alkaline Phosphatase (CIP) (NEB) and gel extracted and purified as described in section **2.7.4**. The ligation reaction was

subsequently used to transform competent DH5α *E. coli* as described in section **2.8.3.1**. Transformation mixtures were plated out onto LB agar (Appendix) plates containing 50µg/ml kanamycin and incubated for 16-20h at 37ºC. 4 colonies were selected for colony PCR (see section **2**.**7.2**) using *p35S_F* and *KpnI-AtDOG1_R* with an annealing temperature of 55ºC, 3 minutes' extension time and 35 cycles. Positive colonies were used to inoculate individual 5-10ml LB liquid (Appendix) cultures supplemented with 50µg/ml kanamycin, which were then incubated in an orbital incubator overnight at 37ºC (200rpm). Plasmid DNA was extracted as described in section **2.7.6** and screened for correct integration of the insert via diagnostic digests using XbaI and KpnI. The insert was then sequenced (Eurofins, Germany) from both ends using *p35S_F* and *pBI121-Seq_R* (see section **2.9.8** for primer sequences).

2.9.6 Cloning of *PpPHY5B, PpPHOTA2* and *PpPHOTB1* in pHSP::MCS-GFP-108 for inducible overexpression in *P. patens*

PpPHY5B, PpPHOTA2 and *PpPHOTB1* cDNA (excluding the stop codons) was amplified using plasmid (pGBKT7) DNA as template in PCR reactions using Phusion® High-Fidelity DNA polymerase (NEB) as per manufacturer's instructions and *XhoI-PpPHY5B_F* with *SalI-PpPHY5B_R*, *SalI(ATG)-PpPHOTA2_F* with *SpeI-PpPHOTA2_R*, and *SpeI-PpPHOTB1_F* with *SpeI-PpPHOTB1_R* (see section **2.9.8** for primer sequences), using an annealing temperature of 55ºC, 4 minutes' extension time and 38 cycles. PCR products were gel extracted and purified as described in section **2.7.4**, and directly digested using either Sal and XhoI or SalI and SpeI or SpeI alone for 2h at 37ºC. The plasmid pHSP::MCS-GFP-108 was also digested using the same enzyme combinations for 2h at 37ºC and treated with 0.5U/µg Calf Intestinal

Alkaline Phosphatase (CIP) (NEB) for a further hour. Digested *PpPHY5B*, *PpPHOTA2* and *PpPHOTB1* were gel extracted and purified as described in section **2.7.4** and then ligated with digested pHSP::MCS-GFP-108 using T4 DNA ligase (NEB), as per manufacturer's instructions. Chemically competent DH5α *E. coli* were transformed with the ligation reactions as described in section **2.8.3.1**. Transformation mixtures were plated out onto LB agar plates containing 50µg/ml carbenicillin and incubated for 16-20h at 37^{o}C.

8-12 colonies were selected for colony PCR (see section **2.7.2**) using either *XhoI-PpPHY5B_F*, or *SalI(ATG)-PpPHOTA2_F* or *SpeI-PpPHOTB1_F* and *mGFP_R* (see section **2.9.8** for primer sequences). Positive colonies were used to inoculate individual 5-10ml LB liquid cultures supplemented with 50µg/ml carbenicillin, which were then incubated in an orbital incubator overnight at 37^{o}C (200rpm). Plasmid DNA was extracted as described in section **2.7.6** and sequenced (Eurofins, Germany) using a number of primers due to the large size of the inserted constructs. To confirm the presence of *PpPHY5B*, the following primers were used for sequencing: *pHSP_F*, *PpPHY5B-Seq_F, PpPHY5B-Seq2_F, PpPHY5B-Seq3_F* and *mGFP_R* (see section **2.9.8** for primer sequences). To confirm the presence of *PpPHOTA2* the following primers were used for sequencing: *pHSP_F*, *PpPHOTA2-Seq_F, PpPHOTA2-Seq2_F, PpPHOTA2-Seq3_F and mGFP_R* (see section **2.9.8** for primer sequences). Finally, to confirm the presence of *PpPHOTB1* the following primers were used for sequencing: *pHSP_F*, *PpPHOTB1-Seq_F, PpPHOTB1-Seq2_F, mGFP_R* (see section **2.9.8** for primer sequences).

2.9.7 Cloning of *PpDELLAs* in pEarleyGate-104 for transient overexpression in *N.benthamiana*

PpDELLAa and *PpDELLAb* CDS was amplified using plasmid DNA (*pHSP::PpDELLA-GFP-108-35SNPT,* see section **2.9.2**) as template in PCR reactions using Phusion® High-Fidelity DNA polymerase (NEB) as per manufacturer's instructions and *PpDELLAa_GW_F* with *PpDELLAa_GW_R* (see section **2.9.8** for primer sequences), using an annealing temperature of 60^{o}C, 3 minutes' extension time and 35 cycles. PCR products (containing *att*B sites) were gel extracted and purified as described in section **2.7.4** and then used in a BP clonase (ThermoFisher Scientific) reaction with Gateway^{TM} pDONR^{TM}/Zeo vector (ThermoFisher Scientific) as per manufacturer's instructions. BP reactions were incubated overnight at room temperature followed by treatment with Proteinase K (ThermoFisher Scientific) for 10 minutes at 37^{o}C. BP reactions were then used to transform chemically competent DH5α *E. coli* as described in section **2.8.3.1**. Transformation mixtures were plated out onto LB agar plates containing 50µg/ml zeocin and incubated for 16-20h at 37^{o}C. 1-4 colonies were selected for colony PCR (see section **2.7.2**) using *M13_F* and *SalI-PpDELLAa_pHSP-R* or *SalI-PpDELLAb_pHSP-R* (see section **2.9.8** for primer sequences). Positive colonies were used to inoculate individual 5-10ml LB liquid cultures supplemented with 50µg/ml zeocin, which were then incubated in an orbital incubator overnight at 37^{o}C (200rpm). Plasmid DNA was extracted as described in section **2.7.6** and sequenced (Eurofins, Germany) using *M13_F* and *M13_R* (see section **2.9.8** for primer sequences). The pDONR^{TM}/Zeo vectors containing *PpDELLAa* or *PpDELLAb* were used in LR clonase (ThermoFisher Scientific) reactions with pEarleyGate-104 (kindly provided by Prof. Miguel Blázquez, IBMCP, Spain) as per

manufacturer's instructions. 150ng of each plasmid (up to 4µl total volume) was mixed with 0.5µl LR clonase mix and incubated for 4 hours at 25ºC, followed by treatment with Proteinase K (ThermoFisher Scientific) for 10 minutes at 37ºC. LR reactions were then used to transform chemically competent DH5α *E. coli* as described in section **2.8.3.1**. Transformation mixtures were plated out onto LB agar plates containing 50µg/ml kanamycin and incubated for 16-20h at 37ºC. 1-5 colonies were selected for colony PCR (see section **2**.**7.2**) using *eYFP_F* and *SalI-PpDELLAa_pHSP-R* or *SalI-PpDELLAb_pHSP-R* (see section **2.9.8** for primer sequences). Positive colonies were used to inoculate individual 5-10ml LB liquid cultures supplemented with 50µg/ml kanamycin, which were then incubated in an orbital incubator overnight at 37ºC (200rpm). Plasmid DNA was extracted as described in section **2.7.6** and sequenced (Eurofins, Germany) using *eYFP_F* and *OCSter_R* (see section **2.9.8** for primer sequences).

2.9.8 Primer list

Primer Name	**Primer Sequence**
XhoI-PpDELLAa_pHSP-F	5'-AAACTCGAGATGGCGTATCAGTACTCTCCAG-3'
SalI-PpDELLAa_pHSP-R	5'-AAAGTCGACTGCACATTTCCATGCAGAAGC-3'
XhoI-PpDELLAb_pHSP-F	5'-AAACTCGAGATGGCATATCAGTACTATCCAGGT-3'
SalI-PpDELLAb_pHSP-R	5'-AAAGTCGACTGCACATTGCCATGCAGAGG-3'
BamHI-PpDELLAa_pGreen-F	5'-AAAGGATCCATGGCGTATCAGTACTCTCCAG-3'
NotI-PpDELLAa_pGreen-R	5'-AAAGCGGCCGCTGCACATTTCCATGCAGAAGC-3'
XbaI-PpDELLAb_pGreen-F	5'-AAATCTAGAATGGCATATCAGTACTATCCAGGT-3'
NotI-PpDELLAb_pGreen-R	5'-AAAGCGGCCGCTGCACATTGCCATGCAGAGG-3'

PpDELLAa_internal_F	5'-GGCTCCTCATAATGGCACG-3'
PpDELLAb_internal_F	5'-CGGAATCTATCCAGCGAGGG-3'
PpDELLAa_GW_F	5'-GGGGACAAGTTTGTACAAAAAAGCAGGCTTCATGG CGTATCAGTACTC-3'
PpDELLAa_GW_R	5'-GGGGACCACTTTGTACAAGAAAGCTGGGTCTCATG CACATTTCCATGC-3'
PpDELLAa_GW(NoStop)_R	5'-GGGGACCACTTTGTACAAGAAAGCTGGGTCTGCAC ATTTCCATGCAG-3'
PpDELLAb_GW_F	5'-GGGGACAAGTTTGTACAAAAAAGCAGGCTTCATGG CATATCAGTAC-3'
PpDELLAb_GW_R	5'-GGGGACCACTTTGTACAAGAAAGCTGGGTCTCATG CACATTGCCATGC-3'
PpDELLAb_GW(NoStop)_R	5'-GGGGACCACTTTGTACAAGAAAGCTGGGTCTGCAC ATTGCCATGCAG-3'
p35S-HygR-NOS_F	5'-AAAGATATCTCCACTGACGTAAGGGATG-3'
p35S-HygR-NOS_R	5'-AAAGATATCGATCTAGTAACATAGATGACACCG-3'
pHSP_F	5'-GTTCTAATATATTTACACAAGAC-3'
mGFP_R	5'-ATCTAATTCAACAAGAATTGGG-3'
35STer_R	5'-AGAGAGACTGGTGATTTCAG-3'
nptII_F	5'-AGACAATCGGCTGCTCTGAT-3'
108locus5'_R	5'-GGTGGAGGGATCAAACGTAAC-3'
M13_F	5'-GTAAAACGACGGCCAG-3'
M13_R	5'-CAGGAAACAGCTATGAC-3'
T7_F	5'-TAATACGACTCACTATAGGG-3'
NdeI-Pp3c13_11750_F	5'-AAACATATGGGGGATGCGGCGAGATTGACTCTC-3'
SalI-Pp3c13_11750_R	5'-AAAGTCGACTTAGCACGCAGAGCACTGATCTTC-3'

NdeI-Pp3c26_14620_F	5’-AAACATATGACGGCTTCTGTCCTCCTTGAGC-3’
SalI-Pp3c26_14620_R	5’-AAAGTCGACTCAACTCATTTTAGCATGTGGTC-3’
NdeI-Pp3c3_9650_F	5’-AAACATATGCGAGGGCCGGTGGTTCTGGATACGC-3’
SalI-Pp3c3_9650_R	5’-AAAGTCGACTCAGCACATGGACCATTGATCACC-3’
SalI- Pp3c13_11750_DOG_R	5’-AAAGTCGACAGAAGATCGTCCATTCGCATCTCC-3’
NdeI-Pp3c13_11750_ANK_F	5’-AAACATATGAGAGATTCTGGATCGAATGTCTGG-3’
SalI-Pp3c3_9650_DOG_R	5’-AAAGTCGACAGAAGACCGTGCATTCGCGTCTCC-3’
NdeI-Pp3c3_9650_ANK_F	5’-AAACATATGGGACATCCTGGAGTGAATATTTGG-3’
SalI-Pp3c26_14620V3.3_R	5’-AAAGTCGACTCATTTTAGCATGTGGTCCTCATG-3’
SalI-Pp3c26_14620_DOG_R	5’-AAAGTCGACGGAAGTCCGTGCATTCACATCTCC-3’
NdeI-Pp3c26_14620_ANK_F	5’-AAACATATGGATAATCCTGGTTTAAATATTTGGG-3’
SalI-Pp3c26_14620_SHR_R	5’-AAAGTCGACATAGACACGTACCAAAGGCGTC-3’
NdeI-AtDOG1_F	5’-AAACATATGGGATCTTCATCAAAGAACATCG-3’
EcoRI-AtDOG1_R	5’-AAAGAATTCTCAATTTCTCTCATTATTTGTCGTC-3’
SalI-PpPHOTA2_F	5’-AAAGTCGACTTGACGAATTTGGGAGAGTGAGTTCG-3’
NotI-PpPHOTA2_R	5’-AAAGCGGCCGCTCAAAAAGTATCATTGAACGTTGA GTC-3’
SalI(ATG)-PpPHOTA2_F	5’-AAAGTCGACATGGACGAATTTGGGAGAGTGAG-3’
SpeI-PpPHOTA2_R	5’-AAAACTAGTAAAAGTATCATTGAACGTTGAGTC-3’
PpPHOTA2-Seq_F	5’-CGGCAGGCTGTGAGGACTGG-3’
PpPHOTA2-Seq2_F	5’-GAGCACACTCGGAGGTGTCAG-3’
PpPHOTA2-Seq3_F	5’-GCAAGGCCAAGACACAGATC-3’
NdeI-PpPHY5B_F	5’-AAACATATGTCGTCCACTAAGTTGTCGTACTCG-3’
NotI-PpPHY5B_R	5’-AAAGCGGCCGCTCAGCAATTCAAAGGGCCCGAC-3’
XhoI-PpPHY5B_R	5’-AAACTCGAGTCAGCAATTCAAAGGGCCCGAC-3’

XhoI-PpPHY5B_F	5'-AAACTCGAGATGTCGTCCACTAAGTTGTCGTAC-3'
SalI-PpPHY5B_R	5'-AAAGTCGACGCAATTCAAAGGGCCCGACTGC-3'
PpPHY5B-Seq_F	5'-GGCCGTCATTGTGCATGATCAGG-3'
PpPHY5B-Seq2_F	5'-GGCAGCGAAAGCTGTTTCGCGG-3'
PpPHY5B-Seq3_F	5'-GCATGGACGAGCTTAGCACGG-3'
NdeI-PpPHOTB1_F	5'-AAACATATGGAGGAGCAGGATCCCGC-3'
NotI-PpPHOTB1_R	5'-AAAGCGGCCGCTCAGAATTCCTGAAATGTGG-3'
SpeI-PpPHOTB1_F	5'-AAAACTAGTATGGAGGAGCAGGATCCCGCCTC-3'
SpeI-PpPHOTB1_R	5'-AAAACTAGTGAATTCCTGAAATGTGGAAATAGG-3'
PpPHOTB1-Seq_F	5'-GCAAGGCGCTGGAACCGAC-3'
PpPHOTB1-Seq2_F	5'-GGTGTCGATGACGCTGCCTAC-3'
PpPHOTB1-Seq3_F	5'-CTCGTCTCCCAGACAATCCG-3'
XbaI-MYC_F	5'-AAATCTAGAATGGAGGAGCAGAAGCTGAT-3'
KpnI-MYC_F	5'-AAAGGTACCATGGAGGAGCAGAAGCTGATCTCAGAG-3'
p35S_F	5'-TTCGCAAGACCCTTCCTCTA-3'
pBI121-Seq_R	5'-CGACGTTGTAAAACGACGGCCAGTG-3'
KpnI-AtDOG1_R	5'-AAAGGTACCTCAATTTCTCTCATTATTTGTCGTC-3'
eYFP_F	5'-CGCCCTGAGCAAAGACCCCAACG-3'
OCSter_R	5'-GGATCTGAGCTACACATGCTCAGG-3'

2.10 Yeast two-hybrid assays

Yeast was transformed with the appropriate plasmids as described in section **2.8.3.2**. Samples from transformed colonies were picked up using sterile 10µl inoculation loops (Sigma-Aldrich) and diluted in 150µl nuclease free water. 5µl of diluted colony suspension was transferred on -AHLW Drop-Out (Appendix) and -LW

Drop-Out (Appendix) selection plates, which were incubated inverted at 30°C for up to 2-7 days. For testing DELLA and GID1 homologue interactions, selective media were left to cool down to 50°C and then GA_3, GA_9-ME, *ent*-kaurenoic acid or methanol (except for -LW media) were added to the media before pouring into 90mm petri dishes. For testing DELLA interactions with light receptor proteins, selective media were left to cool down to 50°C and then 1 or 2μM phycocyanobilin (PCB; purified from *Spirulina geitlerie*, kindly provided by Professor Jon Hughes (University of Giessen) or methanol (except for -LW media) were added to the media before pouring into 90mm petri dishes. Plates were incubated inverted at 30°C in the dark for 2-7 days. Plates supplemented with PCB (and solvent control plates) were incubated upright at 30°C in blue (5μmol$m^{-2}s^{-1}$) or red (5μmol$m^{-2}s^{-1}$), or far-red light (3μmol$m^{-2}s^{-1}$) or in the dark for 4 days. Plates were photographed using a Nikon D40 SLR camera.

2.11 Protein expression analysis

For protein expression analysis, 7-day old or 14-day old tissue of *P. patens* transformed with pHSP::PpDELLA-GFP-108-35SNPT or pHSP::GFP-108-35SNPT was incubated on BCDAT agar plates or in liquid BCDAT in 24-well plates for 1h at 37°C (heat shock to induce protein expression) or at 22±1°C (control treatments, no protein induction) and then transferred to 22±1°C for 6h or 18h. For experiments involving multiwell plates, half a plate of moss tissue was transferred to each well containing 1ml of liquid BCDAT supplemented with the relevant chemical. Incubation in multiwell plates at 22±1°C was accompanied by gentle agitation. Tissue was collected in 50ml Falcon tubes or 1.5ml Eppendorf tubes, flash frozen in liquid nitrogen and stored at -80°C.

For experiments testing proteasomal degradation, tissue in liquid BCDAT was pretreated with 100μM MG132 (Abcam, ab147047) before heat shock at 37°C, and collected 6h or 18h after completion of the heat shock. Similarly, for experiments testing the effect of hormones or other chemicals on protein expression, tissue was treated with MG132 before heat shock at 37°C, and collected 6h after completion of the heat shock. For experiments testing the effect of blocking protein translation on protein stability, tissue was treated with 100μM cycloheximide (CHX) (Sigma-Aldrich, 01810) for different durations, following the 6h-incubation at 22±1°C post heat shock. Solvent controls (methanol for hormones, ethanol or DMSO for CHX and MG132) were used in all experiments.

2.12 Protein extractions from plant cells

Frozen plant tissue was ground up using a mortar and a pestle (pretreated with 70% ethanol) in liquid nitrogen and left to reach room temperature before mixing with protein extraction buffer (50mM Tris/HCl pH 7.5 or HEPES pH 7.5, 150mM NaCl, 5% glycerol, 0.5% NP-40, cOmplete™ EDTA-free protease inhibitor tablets (Roche) - one per 10ml buffer). Grinding was continued for 30-60 seconds until a homogenous green suspension was formed and the lysate was then filtered through a single miracloth (Millipore) layer into 50ml falcon tubes and then into 1.5ml Eppendorf tubes or directly into 1.5ml Eppendorf tubes (depending on the lysate volume), and incubated on ice. The lysate was then centrifuged at 14000 g for 20-45 minutes at 4°C and the supernatant was transferred into clean tubes. Protein concentration was estimated as described in section **2.13**. A sample of the protein extract was diluted (4:1) in 5x

Laemmli buffer (Appendix), boiled for 10 minutes at 95°C and analysed by SDS-PAGE, and the remaining was flash frozen in liquid nitrogen and stored at -80°C.

2.13 Measurement of protein concentration

Protein concentration was estimated using a Bradford (AppliChem) assay. Protein extracts were diluted 5 times in water and 2-4µl of diluted sample was added to 250µl Bradford reagent in triplicates. Alternatively, 2µl of concentrated protein extract was directly added to 250µl Bradford reagent in triplicates. Absorbance was measured at 595nm using a spectrophotometer. Mean concentrations were calculated by comparing to a BSA standard curve.

2.14 Confocal microscopy for protein visualisation

Protonemata of *P. patens* transformed with *pHSP::PpDELLA-GFP-108-35SNPT* or *pHSP::GFP-108-35SNPT* were incubated in liquid BCDAT in 24-well plates and protein expression was induced as described in section **2.11**. Following incubation at 22±1°C post heat shock, tissue was mounted onto glass slides in dH_2O and confocal images or z-stacks of protein expression in protonemata were captured with the Zen 2012 software using the Zeiss LSM170 confocal microscope with a 20x objective. GFP expression was compared to wild-type protonema and protonema with uninduced GFP expression using identical laser power, gain and pinhole settings. Excitation and emission wavelengths for GFP fluorescence were 488nm and 530nm respectively, and for chloroplast autofluorescence 634nm and 696nm respectively.

2.15 Co-Immunoprecipitations (Co-IPs)

2.15.1 Co-IPs from a cell-free system

AtGID1c or *PpGLP1* in pGBKT7 (incorporating an N-terminal MYC tag) and *AtRGA1* or *PpDELLAa* or *PpDELLAb* in pGADT7 (incorporating an N-terminal HA tag) were translated *in vitro* using the TNT® T7 Coupled Reticulocyte Lysate System (Promega, Madison, WI, USA) as per manufacturer's instructions. For ribonuclease inhibition, 40U RNaseOut (Invitrogen) was added per 50ml reaction.

15µl protein-A sepharose magnetic beads (Amersham) for each Co-IP reaction were washed 3 times in 1-minute intervals with 1ml IP Buffer A (50mM HEPES pH 7.5, 150mM NaCl, 5% (v/v) glycerol, 0.1% Tween 20, cOmplete™ EDTA-free protease inhibitor tablets (Roche) - one per 10ml buffer) and incubated with 4µg α-MYC (Abcam, ab18185) and 250 µl IP Buffer A for 1h at room temperature on a turning wheel. Beads were then washed 3 times in 3-minute intervals with 1ml IP Buffer A. Beads were separated from the supernatant using a magnet.

Translated proteins (9µl each) and MYC-coupled beads were mixed in a total volume of 500µl IP buffer A supplemented with GA_3, GA_9-ME or methanol at 4°C for 3h on a turning wheel. Working in a cold room, the IP supernatant was collected and beads were washed 4 times in 3-minute intervals with 1ml IP Buffer B (50mM HEPES pH 7.5, 300mM NaCl, 5% (v/v) glycerol, 0.1% Tween 20, cOmplete™ EDTA-free protease inhibitor tablets (Roche) - one per 10ml buffer), followed by a 3-minute wash with 1ml IP Buffer A. Samples were then resuspended in 50µl 1x Laemmli buffer (Appendix), boiled for 10 minutes at 95°C and stored overnight at -20°C. Following overnight storage, samples were analysed by SDS-PAGE and western blotting.

2.15.2 Co-IPs from *N. benthamiana* leaves

Protein was extracted from *N. benthamiana* leaves infiltrated with *A. tumefaciens* as described in sections **2.5** and **2.12**. Normally, two halves from two different leaves infiltrated with the same Agrobacterium diluted culture were ground together to extract protein. Protein concentration was estimated using a Bradford assay as described in section **2.13**. Total protein was adjusted to 6.5mg (same for all samples) in a volume of 3.0-3.5ml of protein extraction buffer (same for all samples). 50µl from each protein extract were saved for western blotting (IP input). An equal volume (3-3.5ml) of dilution buffer (50mM Tris/HCl pH 7.5, 150mM NaCl, cOmplete™ EDTA-free protease inhibitor tablets (Roche) - one per 10ml buffer) was added to the protein extracts.

The Co-IP was performed using the GFP-trap® magnetic agarose kit (Chromotek, Germany, gtma-20) as per manufacturer's instructions with modifications. 10µl GFP-trap® magnetic agarose beads for each Co-IP reaction were washed 3 times with 1ml dilution buffer. Beads were separated from the supernatant using a magnet. After the last wash, the beads were resuspended in 1ml dilution buffer and divided equally into 15ml Falcon tubes containing the diluted protein extracts. Co-IP reactions were incubated at 4°C for 4h or overnight on a rotating wheel (half speed).

Following Co-IP, working in a cold room, the suspensions were divided into 1.5ml Eppendorf tubes and supernatants were separated from beads using a magnet. Beads were washed one time (lasting 5 minutes) with dilution buffer, followed by one wash (lasting 5 minutes) with high salt buffer (50mM Tris/HCl pH 7.5, 200mM NaCl, cOmplete™ EDTA-free protease inhibitor tablets (Roche) - one per 10ml buffer), and two more washes (lasting 5 minutes each) with dilution buffer. Beads were

resuspended in 100µl 2x Laemmli buffer (Appendix) and boiled at 95°C in 1.5ml Eppendorf tubes for 10 minutes to enable protein dissociation from beads and denaturation. Eluted proteins were separated from the beads using a magnet, stored at -20°C and analysed by SDS-PAGE (see section **2.18**).

2.16 Immunoprecipitations (IPs) for proteomic analysis

2.16.1 First attempt (Suboptimal)

Five plates of moss protonemata, which had been homogenised as described in section **2.1.2** and cultured on BCDAT for 15 days, containing either the *pHSP::PpDELLAa-GFP* or *pHSP::PpDELLAb-GFP or pHSP::GFP* construct, were incubated for 1h at 37°C to induce expression of the construct. Following heat shock, the plates were returned for 6h to 22±1°C with gentle agitation, after which time the tissue was flash frozen in 50ml Falcon tubes in liquid nitrogen and stored at -80°C. As a control, protonemata of the same age containing either the *pHSP::PpDELLAa-GFP* or the *pHSP::PpDELLAb-GFP* construct from 5 plates that were incubated continuously at 22±1°C were also flash frozen in liquid nitrogen and stored at -80°C.

Frozen tissue of the five treatments was ground up using a mortar and a pestle in liquid nitrogen and left to reach room temperature before mixing with 4ml protein extraction buffer (50mM HEPES pH 7.5, 5% glycerol, 150mM NaCl, 0.4% NP-40, cOmplete™ EDTA-free protease inhibitor tablets (Roche) - one per 10ml buffer). Grinding was continued for 30-60 seconds until a homogenous green suspension was formed, which was then filtered successively through a double and a single miracloth (Merck Millipore) layer into 50ml Falcon tubes. The suspensions were transferred into 2ml Eppendorf tubes and centrifuged at 12000 g for 30 minutes at 4°C. Supernatants

for each of the five protein extracts were collected into single 15ml Falcon tubes and total protein content was estimated using a Bradford assay as described in section **2.13**. Total protein was adjusted to 3.2mg and the total volume was made up to 6ml with protein extraction buffer. 40µl from each protein extract were saved for western blotting (IP input).

The GFP-trap® IP was performed using the GFP-trap® magnetic agarose kit (Chromotek, Germany, gtma-20) as per manufacturer's instructions with modifications. 125µl (25µl for each IP reaction) GFP-trap® magnetic agarose beads were washed 3 times with 1ml dilution buffer on a rotating wheel. Beads were separated from the supernatant using a magnet. After the last wash, the beads were resuspended in 1ml dilution buffer and divided into the 15ml Falcon tubes containing the five protein extracts (200µl bead suspension each): induced *Pp*DELLAa-GFP, uninduced *Pp*DELLAa-GFP, induced *Pp*DELLAb-GFP, uninduced *Pp*DELLAb-GFP and induced GFP. IP reactions were incubated at 4^{o}C for 2h on a rotating wheel (half speed).

Following IP, working in a cold room, the suspensions were divided into 1.5ml Eppendorf tubes and supernatants were separated from beads using a magnet. 80µl from the total supernatant from each of the five IP reactions was saved for western blotting and the remaining supernatant was discarded. Beads were collected into five single 1.5ml Eppendorf tubes (one for each IP) and washed twice (5 minutes each) with cold dilution buffer (kit's own), followed by one wash with high salt buffer (10mM Tris/HCl pH 7.5, 0.5mM EDTA, 175mM NaCl, cOmplete^{TM} EDTA-free protease inhibitor tablets (Roche) - one per 10ml buffer), one wash with dilution buffer (kit's own) and four washes with low salt buffer (10mM Tris/HCl pH 7.5, 0.5mM EDTA, 100mM NaCl, cOmplete^{TM} EDTA-free protease inhibitor tablets (Roche) - one per 10ml buffer).

Beads were resuspended in 50µl 2x Laemmli buffer (Appendix) and boiled at 95°C in 1.5ml Eppendorf tubes for 10 minutes to enable protein dissociation from beads and denaturation. Eluted proteins were separated from the beads using a magnet and stored at -20°C. 40µl of IP inputs and 80µl of IP supernatants collected for western blotting were mixed with 10µl and 20µl 5x Laemmli buffer respectively and boiled for 10 minutes at 95°C to induce protein denaturation.

2.16.2 Optimised protocol

Four plates of moss protonemata, which had been homogenised as described in section **2.1.2** and cultured on BCDAT for 17 days, containing either the *pHSP::PpDELLAa-GFP* or *pHSP::GFP* construct, were incubated for 1h at 37°C to induce expression of the construct. Following heat shock, the plates were returned for 6h to 22±1°C with gentle agitation, after which time the tissue was flash frozen in 50ml Falcon tubes in liquid nitrogen and stored at -80°C. As a control, protonemata of the same age containing the *pHSP::PpDELLAa-GFP* construct from 4 plates that were continuously incubated at 22±1°C was also flash frozen in liquid nitrogen and stored at -80°C.

Frozen tissue from the three treatments was ground up using a mortar and a pestle in liquid nitrogen and left to reach room temperature before mixing with 4ml protein extraction buffer (50mM Tris/HCl pH 7.5, 5% glycerol, 150mM NaCl, 0.2% triton X-100, cOmplete™ EDTA-free protease inhibitor tablets (Roche) - one per 10ml buffer). Grinding was continued for 30-60 seconds until a homogenous green suspension was formed, which was then filtered successively through a double and a single miracloth (Merck Millipore) layer into 50ml Falcon tubes. The suspensions were

transferred into 2ml Eppendorf tubes and centrifuged at 12000 g for 30 minutes at 4°C. Supernatants were transferred into new tubes and centrifugation was repeated. Supernatants for each of the three protein extracts were collected into single 15ml Falcon tubes and total protein content was estimated using a Bradford assay as described in section **2.12**. Total protein was adjusted to 4.8mg in 3.7ml protein extraction buffer and topped up to 7.4ml by adding an equal volume of dilution buffer (10mM Tris/HCl pH 7.5, 0.5mM EDTA, 150mM NaCl, cOmplete™ EDTA-free protease inhibitor tablets (Roche) - one per 10ml buffer). 80µl from each protein extract were saved for western blotting (IP input).

The GFP-trap® IP was performed using the GFP-trap® magnetic agarose kit (Chromotek, Germany) as per manufacturer's instructions with modifications. 120µl (40µl for each IP reaction) GFP-trap® magnetic agarose beads were washed 3 times with 1ml dilution buffer on a rotating wheel. Beads were separated from the supernatant using a magnet. After the last wash, the beads were resuspended in 900µl dilution buffer and divided into the 15ml falcon tubes containing the three protein extracts (300µl bead suspension each): induced *Pp*DELLAa-GFP, uninduced *Pp*DELLAa-GFP and induced GFP. IP reactions were incubated at 4°C for 90 minutes on a rotating wheel (half speed).

Following IP, working in a cold room, the suspensions were divided into 1.5ml Eppendorf tubes and supernatants were separated from beads using a magnet. 80µl from the total supernatant from each of the three IP reactions was saved for western blotting and the remaining supernatant was discarded. Beads were collected into three single 1.5ml Eppendorf tubes (one for each IP) and washed twice (5 minutes each) with a buffer with high salt concentration (10mM Tris/HCl pH 7.5, 0.5mM EDTA,

400mM NaCl, cOmplete™ EDTA-free protease inhibitor tablets (Roche) - one per 10ml buffer) to reduce non-specific protein binding, followed by two washes (5 minutes each) with dilution buffer. Beads were resuspended in 50µl 2x Laemmli buffer (Appendix) and boiled at 95°C in 1.5ml Eppendorf tubes for 10 minutes to enable protein dissociation from beads and denaturation. Eluted proteins were separated from the beads using a magnet and stored at -20°C. 80µl of IP inputs and supernatants collected for western blotting were mixed with 20µl 5x Laemmli buffer and boiled for 10 minutes at 95°C to induce protein denaturation.

2.17 Nuclear protein enrichment and IP for proteomic analysis

5g of 17-day old moss protonemata containing *pHSP::PpDELLAa-GFP* or *pHSP::PpDELLAb-GFP* construct was transferred into single wells (two wells per line) in a 6-well plate containing 6ml BCDAT supplemented with 100µM MG132 (Abcam, ab147047) and incubated for 1 h at 22±1°C with gentle agitation. The plate was then incubated at 37°C for 1h to induce the expression of *Pp*DELLA-GFP. Following the heat shock, the plate was returned for 6h into 22±1°C with gentle agitation, after which the tissue was flash frozen in 50ml Falcon tubes in liquid nitrogen and stored at -80°C.

Nuclear protein enrichment was carried out according to Xu and Copeland (2012) with some modifications. Frozen tissue (~5g) for each line was ground up to a fine powder using a mortar and a pestle in liquid nitrogen and left to reach room temperature. 10ml lysis buffer (20mM Tris/HCl pH 7.5, 25% glycerol, 250mM sucrose, 2mM EDTA, 2.5mM $MgCl_2$, 20mM KCl, 1M Hexylene glycol (Sigma-Aldrich), cOmplete™ EDTA-free protease inhibitor tablets (Roche) - one per 10ml buffer) was added to the lysate and grinding was continued for 30-60 seconds until a homogenous

green suspension was formed. Working on ice, the suspension was then filtered successively through a single and a double miracloth (Merck Millipore) layer into a 50ml Falcon tube. 160µl suspension (whole cell extract protein) was saved for analysis by western blotting. The remaining suspension was split into 2ml Eppendorf tubes and centrifuged at 1500 g for 20 minutes at 4^{o}C. Supernatants were collected in a 15ml Falcon tube and the suspension was centrifuged for at 1500 g for 10 minutes at 4^{o}C. 160µl supernatant (cytosolic fraction) was saved for analysis by western blotting and the rest was discarded. The pellet (nuclear fraction) was resuspended in 1ml wash buffer (20mM Tris/HCl pH 7.5, 25% glycerol, 2.5mM $MgCl_2$, 0.1% triton X-100, 0.5M Hexylene glycol and cOmplete^{TM} EDTA-free protease inhibitor tablets (Roche) – one per 10ml buffer) and split into three Eppendorf tubes for each line and centrifuged at 1500 g for 10 minutes at 4^{o}C. The pellet was washed with 1ml wash buffer and centrifuged again until the pellet was no longer green (3-4 times) and then flash frozen in liquid nitrogen and stored at -80^{o}C. All centrifugations were done with brakes off.

The pellets containing the nuclear fractions were lysed in 300µl RIPA buffer (from the GFP trap kit, Chromotek, Germany) and sonicated on ice for 15s at 3amps, with small stops in-between. The three tubes containing the lysed pellets for each line were merged into one tube. The GFP-trap® IP was performed using the GFP-trap® magnetic agarose kit as per manufacturer's instructions with small modifications. 44µl GFP-trap® magnetic agarose beads were washed 3 times with 500µl dilution buffer and after the last wash they were split into the two lysed nuclear fractions, one for *Pp*DELLAa-GFP and one for *Pp*DELLAb-GFP. The suspensions containing the beads and the lysed nuclear material were topped up to 10ml with dilution buffer (10mM Tris/HCl pH 7.5, 0.5mM EDTA, 150mM NaCl, cOmplete^{TM} EDTA-free protease

inhibitor tablets (Roche) – one per 10ml buffer) in 15ml Falcon tubes and incubated overnight on a rotating wheel at 4°C. Before incubation, 160µl of suspension (nuclear fraction) were saved for western blotting. Following overnight incubation, beads were separated from solution containing unbound material (IP supernatant) by means of a magnet and 160µl of the IP supernatant were saved for western blotting. The beads were washed twice with dilution buffer (kit's own), followed by two washes with high salt buffer (175mM NaCl, 0.5mM EDTA, 10mM Tris/HCl pH 7.5, cOmplete™ EDTA-free protease inhibitor tablets (Roche) – one per 10ml buffer) and four washes with low salt buffer (100mM NaCl, 0.5mM EDTA, 10mM Tris/HCl pH 7.5, cOmplete™ EDTA-free protease inhibitor tablets (Roche) – one per 10ml buffer). The beads were then incubated in 50µl 2x Laemmli buffer (Appendix) boiled for 10 minutes and separated from the eluted material by means of a magnet. The elution was stored at -20°C and proteins were subsequently analysed by SDS-PAGE (see section **2.18**).

2.18 SDS-PAGE

Proteins were analysed by SDS-PAGE using BioRad self-assembly kits. 10% resolving gel (4ml dH_2O, 3.3ml acrylamide (Protogel), 2.5ml 1.5M Tris pH8, 100µl 10% (w/v) SDS, 100µl 10% (w/v) ammonium persulfate (APS), 4µl N,N,N',N-tetramethylethylenediamine (TEMED) (Sigma-Aldrich)) was cast first. After pouring the resolving gel, ~300µl isopropanol was added to level the top of the gel. After the resolving gel had set, the isopropanol was poured off and the stacking gel (3.4ml dH_2O, 0.83ml acrylamide (Protogel), 0.63ml 1.0M Tris pH6.6, 50µl 10% (w/v) SDS, 50µl 10% (w/v) ammonium persulfate (APS), 5µl N,N,N',N-tetramethylethylenediamine (TEMED) (Sigma-Aldrich)) was cast on top of the resolving gel. A 10- or 15-well tooth comb was

inserted before the stacking gel had polymerised, which was removed after polymerisation. The gel was then assembled to the electrophoresis apparatus. Pre-boiled proteins were loaded and gels were run in 1x ELFO buffer (25mM Tris/HCl, 192mM glycine, 0.1% (v/v) SDS, pH8.3) at 60-100V for 1.5-3h.

In the case of SDS-PAGE for running immunoprecipitated proteins for proteomic analysis, a 10-well tooth comb was used and 20µl of eluted protein samples were loaded into the gel, so that they were separated from each other by one or two wells. Empty wells were filled up with 20µl of 2x Laemmli buffer (Appendix) to enable even running of the protein samples. 2µl protein ladder (PageRuler^{TM} prestained protein ladder, 10 to 180kDa) was loaded into the first well. The gel was run at 80V until proteins were 1/3-1/2 of the way into the resolving gel (about 1h). This was due to limitations assigned by the local Proteomics Facility on the acceptable size of excised gel.

2.19 Western blotting

2.19.1 Protein transfer

Proteins were resolved by SDS-PAGE and the stacking gel was removed. The gel was then transferred onto a foam pad overlaid with one sheet of Western blotting filter paper (ThermoScientific^{TM}) soaked in protein transfer buffer (25mM Tris, 190mM glycine, 20% methanol, pH8.0). PVDF transfer membrane (Hybond-P, Amersham) was cut to size, soaked in methanol and then in protein transfer buffer and placed over the gel. One more sheet of Western blotting filter paper (ThermoScientific^{TM}) overlaid with a foam pad was soaked in protein transfer buffer and placed on top of the membrane. The arrangement was then placed between two electroblotting pads

(BioRad) and inserted into an electroblotting tank (BioRad), which was filled with protein transfer buffer. BioRad power packs running at 16-20V overnight at 4°C were used to enable protein transfer onto the PVDF membrane. Alternatively the transfer was performed at 100V for 1h at room temperature. Following the transfer, the PVDF membrane was removed and placed in blocking solution (5% milk in TBS (50mM Tris, 150mM NaCl, pH 7.5 with 1M HCl)) for 1h on a rocker at room temperature or at 4°C overnight.

2.19.2 Antibody probing

The western blot was incubated with primary antibodies in 8-10 ml 5% (w/v) Marvel semi-skimmed milk in TBST (50mM Tris, 150mM NaCl, pH 7.5 with 1M HCl, 0.1% Tween 20). Mouse monoclonal α-HA (Abcam, ab130275) and α-MYC (Abcam, ab18185) were used at a 1:5000 or 1:2000 dilution and incubations were carried out for 3h and 1h respectively at room temperature or overnight at 4°C; rabbit polyclonal anti-GFP (Chromotek, Germany, PABG1) was used at 1:1000 or 1:500 dilution and incubations were carried out for either 3h at room temperature or overnight at 4°C (in most cases); α-H3 (Agrisera, AS10710) and α-UGPase (Agrisera, AS01008), nuclear and cytosolic markers respectively, were used at 1:4000 and incubations were carried out for 1h at room temperature.

Following incubation of primary antibody, the blot was washed 3 times (in 5-minute intervals) in TBST and then incubated with the appropriate horse radish peroxidase-conjugated secondary antibody. Goat anti-mouse immunoglobin (Abcam, ab6789) was used for α-HA and α-MYC at a 1:2000 or 1:5000 dilution in 5% (w/v) milk in TBST for 1.5h and goat anti-rabbit immunoglobin (Abcam, ab6721) was used for α-

GFP, α-H3 or α-UGPase at a 1:2000 dilution in 5% (w/v) milk in TBST for 1.5h. The blot was then washed was washed 3 times (in 5-minute intervals) in TBST.

2.19.3 Enhanced chemiluminescence (ECL) detection

ECL western blotting reagents (Amersham) were used to detect the secondary antibody. Reagent 1 and reagent 2 were mixed at a ratio of 1:1 and poured over the blot. The blot was incubated with the reagent mixture for 3 minutes at room temperature. Excess ECL reagent was removed and the blot was placed within two layers of transparent plastic film. Blots were exposed to X-ray film (GE Healthcare Amersham™ Hyperfilm™ ECL) in an intensifying screen cassette in a dark room and films were developed using an Xograph Compact X4 film processor. Films were photographed on a light box using a Nikon D40 SLR camera.

2.20 Staining of protein gels and membranes

2.20.1 Staining of PVDF transfer membranes

PVDF membranes were incubated in Coomassie stain (0.1% (w/v) Coomassie blue R-250, 45% (v/v) methanol, 10% (v/v) glacial acetic acid) for at least 30 minutes at room temperature with agitation and destained for at least 30 minutes in destain solution (30% (v/v) methanol, 10% (v/v) glacial acetic acid), before being dried overnight in a fume hood.

2.20.2 Staining of protein gels for proteomics

Gels were originally stained according to the Alphalyse silver staining protocol (www.alphalyse.com/wp-content/uploads/2015/09/silver-staining-protocol.pdf). Essentially, protein gels were incubated in Fixer for 1 hour at room temperature with

agitation and washed in dH_2O, with several changes, overnight. Gels were sensitised in 0.02% sodium thiosulfate for 1 minute, washed in dH_2O and incubated for 20 minutes in 0.1% silver nitrate solution (supplemented with 0.02% (v/v) formaldehyde just before use). Gels were then washed in dH_2O and developed in 3% sodium carbonate solution (supplemented with 0.05% (v/v) formaldehyde just before use). Following sufficient staining, gels were washed in dH_2O and staining was terminated by incubating in 5% acetic acid for 5 minutes. Gels were washed in water 3 times, each lasting 10 minutes, after which, stained gel bands were excised with sterile scalpels and submitted for LC/MS analysis in individual Eppendorf tubes.

After the IP/MS protocol was optimised, gels were stained using the ProteoSilver™ silver staining kit (Sigma-Aldrich) as per manufacturer's instructions. In summary, this involved fixing the gel, washing with ethanol, followed by washing with dH_2O, sensitising and washing again with dH_2O. The gel was then equilibrated with silver solution, washed with dH_2O and developed until the desired staining intensity was achieved (3 minutes). The gel was finally washed 3 times (15 minutes each) in dH_2O and then excised so that each of the three protein samples was split up into two pieces, an upper piece containing heavy proteins and a lower one containing light proteins. A strong band stained in the middle of all three protein samples was used as a reference for excising. All six gel pieces excised were submitted for trypsin digest and LC/MS analysis at the School of Biosciences Proteomics Facility, Birmingham.

2.21 Liquid Chromatography/Mass Spectrometry (LC/MS) analysis

Peptides were digested from silver stained excised gels using trypsin, and separated and analysed by LC/MS. The mass spectrometers used were the Orbitrap

Elite and Q-Exactive HF. Detected peptides were matched against the Uniprot database and presence of at least two unique peptides was used to identify proteins originally present in the samples. The cut-off protein false discovery rate (FDR) value was set to 1%.

CHAPTER 3: Flowering plant DELLA responses to diterpenes and stress signals are not conserved in *P. patens,* while roles in reproductive development appear to be conserved

3.1 Introduction

One of the main properties of DELLA proteins in vascular plants is GA-induced degradation via the 26S proteasome (Fu *et al.*, 2002). Exogenous treatment with GA_3 induces rapid degradation of DELLA proteins, while treatment with proteasome inhibitors, such as MG132, prevents DELLA degradation, and induces DELLA stabilisation in both the presence or absence of exogenously supplied GAs (Fu *et al*., 2002; Sasaki *et al*., 2003; Feng *et al*., 2008). This is also reflected at the plant phenotype level; for example leaf extension growth is promoted in the presence of GA_3, but prevented in the presence of MG132, which abolishes the effect of GA_3 (Fu *et al*., 2002). In addition, DELLA degradation is inhibited when the N-terminal DELLA domain is not present, highlighting the fact that this domain is necessary for proteasome-dependent GA-induced DELLA degradation (Feng *et al*., 2008). Although GA-induced DELLA degradation has been demonstrated in vascular plants, including ferns (Tanaka *et al.,* 2014) and lycophytes (Yasumura *et al*., 2007), it remains elusive whether bryophyte DELLA stability can be regulated by diterpenes or the 26S proteasome.

The evidence from one experiment so far suggests that GFP-*Pp*DELLAa remains stable in the presence of GA_3 when expressed in Arabidopsis cells (Yasumura *et al*., 2007). However, it has previously been shown that the diterpenes *ent*-kaurene and *ent*-kaurenoic acid, both of which are endogenously produced by *P. patens*, as well as the fern antheridiogen GA_9-ME, promote vegetative development and spore germination in *P. patens* (Hayashi *et al*., 2010; Vesty *et al*., 2016). Furthermore, recent data from the Coates lab have shown that *Pp*DELLA proteins repress spore germination (Vesty, unpublished), suggesting that a diterpene signalling mechanism

that may involve *Pp*DELLA proteins regulates spore germination in *P. patens*. Therefore, one of the aims of the work in this chapter was to investigate whether *Pp*DELLA proteins are regulated by diterpenes to deduce whether this is a conserved feature of DELLA proteins in comparison to vascular plants.

Another aim of the current project was to examine whether some of the most well-established functions of flowering plant DELLA proteins are conserved in *P. patens*. Of particular interest was the role of DELLAs in regulating stress responses, as *in silico* analyses have suggested that *Pp*DELLAs may be involved in stress response regulation (Briones-Moreno *et al*., 2017).

Flowering plant DELLA proteins are key regulators of abiotic stress responses (reviewed in Colebrook *et al.,* 2014), such as the response to salt stress. Achard *et al.* (2006) have shown that DELLA protein accumulation increases in response to salt stress and that the quadruple *Atdella* mutant is less sensitive to saline conditions compared to the wild type, displaying reduced growth inhibition. Similarly, under ABA treatment, DELLA protein levels are elevated and the quadruple *Atdella* mutant is impaired in the ABA-induced growth inhibition response (Achard *et al.,* 2006). Linking the two mechanisms together, Achard *et al.* (2006) have also shown that ABA mediates salt-induced growth restraint via ABA-INSENSITIVE1 (*At*ABI1)-dependent promotion of DELLA signalling, suggesting that DELLA proteins integrate environmental and endogenous signals to enable plant survival under stress conditions.

DELLA proteins have also been associated with responses to oxidative stress, which is induced by accumulation of reactive oxygen species (ROS) causing damage to proteins, lipids and nucleic acids and thus generating toxic reactive species (Apel

and Hirt, 2004). DELLAs inhibit the accumulation of ROS during biotic and abiotic stress, including salt stress, by upregulating the transcription of ROS-detoxification enzymes, such as superoxide dismutase (SOD) (Achard *et al*., 2008). For example, under saline conditions, in the *Atga1-3* (GA biosynthesis) mutant, where all *At*DELLAs are stabilised, there is no ROS accumulation, whereas in the quadruple *Atdella* mutant in an *Atga1-3* background, ROS accumulation is enhanced (Achard *et al.*, 2008). Furthermore, treatment of the *Atga1-3* mutant with exogenous hydrogen peroxide (a common type of reactive oxygen species) results in delayed senescence compared to the quadruple *Atdella* mutant an *Atga1-3* background, suggesting that DELLA proteins promote oxidative stress tolerance (Achard *et al.*, 2008). A recent study has also demonstrated that in *Marchantia polymorpha*, *Mp*DELLA, which is upregulated in response to ROS accumulation, promotes oxidative stress tolerance possibly via a mechanism involving upregulation of flavonoid biosynthesis and interaction with *Mp*PIF (Hernández-García *et al.*, 2021). This suggests that promotion of stress tolerance might be a conserved feature of DELLA proteins across land plant species.

Studies in tomato, Arabidopsis and *Brassica napus* have also shown that DELLA proteins promote tolerance under drought stress, a process known to involve ABA signalling (Nir *et al*., 2017; Wang *et al*., 2020; Wu *et al*., 2020). Arabidopsis plants overexpressing the non-degradable DELLA protein encoded by *Atgai-1* do not wilt after 3-week exposure to drought and are able to recover from the stress, while wild-type plants wilt and cannot recover (Wang *et al*., 2020). Similarly, tomato plants overexpressing non-degradable Arabidopsis DELLA protein (*AtrgaΔ17*) are more drought tolerant after a 10-day period of exposure to drought and are able to recover fully from the stress, while wild-type plants cannot (Nir *et al*., 2017). Furthermore, under

exogenous application of ABA, Arabidopsis and tomato plants overexpressing *AtrgaΔ17*, as well as *Brassica napus* plants overexpressing *bnaa6.rga-D* (non-degradable *B. napus* DELLA) display smaller stomatal aperture compared to the wild type, indicating increased drought tolerance (Nir *et al*., 2017; Wang *et al*., 2020; Wu *et al*., 2020).

The relationship between DELLA and ABA during drought stress has been further elucidated by the recent identification of the interaction between DELLA and the basic leucine zipper (bZIP) transcription factor ABA RESPONSIVE ELEMENT-BINDING FACTOR 2 (ABF2) in both Arabidopsis and *Brassica napus* (Wang *et al*., 2020; Wu *et al.*, 2020). The mechanism has been better-characterised in *B. napus*, where it has been shown that *Bna*A6.RGA and *Bna*A10.ABF2 are induced in response to drought stress and ABA treatment, and interact to co-activate the expression of drought tolerance-promoting genes, such as *RESPONSIVE TO ABA 18* (*BnaC9.RAB18*) (Wu *et al*., 2020).

Apart from the study linking *Mp*DELLA protein to oxidative stress tolerance (Hernández-García *et al.*, 2021), there is no other evidence as to whether DELLA proteins regulate stress responses in non-vascular plants. Therefore, work in this chapter aimed to examine this hypothesis further, by testing whether tolerance to stress conditions is promoted by DELLA proteins in *P. patens*.

Angiosperm DELLA proteins also have a key role in the regulation of reproductive development. While the global *della* mutant in a Landsberg (L*er*) background in Arabidopsis is partially fertile (Fuentes *et al*., 2012), loss of *AtRGA1* and *AtGAI1* in the Col-0 background results in complete male sterility due to defects in pollen development occurring following meiosis, with the phenotype being rescuable

by *At*RGA1 reintroduction (Plackett *et al*., 2014). Similarly, *della* loss of function mutants in barley and rice are sterile, with the *Hvslr1* mutant being pollenless (Lanahan and Ho, 1988; Ikeda *et al*., 2001). One mechanism by which male sterility is induced in Arabidopsis, at least by *At*RGA1 and *At*RGL2, has recently been described. Huang *et al*. (2020) have shown that *At*DELLAs interact with the MYB transcription factors *At*MYB21 and *At*MYB24 to repress filament-elongation-promoting transcription, required for normal stamen development (Huang *et al*., 2020). Numerous other *At*DELLA interactions with transcription factors regulating flowering have also been described, such as the interaction with SQUAMOSA PROMOTER BINDING PROTEIN-LIKE (*At*SLP) proteins (*At*SPL9 and *At*SPL15), which induce flowering via transactivation of *MADS-box* and other target genes (Yu *et al.*, 2012; Hyun *et al*., 2016). Whether additional interactions of DELLA proteins with other transcription factors are responsible for inhibiting pollen development remains unclear.

There is also evidence for a role of DELLA proteins in reproductive development outside flowering plants. In the fern *Lygodium japonicum*, young prothalli uptake GA_9-ME secreted by early-maturing prothalli, which is subsequently converted to GA_4, inducing DELLA degradation and promoting male sex organ (antheridium) development (Tanaka *et al*., 2014). This suggests that *Lj*DELLA promotes archegonium development, although this has not been shown experimentally, for example by examining the phenotype of an *Ljdella* mutant (Tanaka *et al*., 2014). In addition, in the lycophyte *Selaginella moellendorfii*, exogenous application of GA_4 induces an increase in outer exospore projection heights in microspores, suggesting that *Sm*DELLA proteins probably regulate the development of male reproductive

structures – although again, no *Smdella* mutant has been generated to confirm this (Aya *et al*., 2011).

There is currently very limited evidence as to whether DELLA proteins regulate reproductive development outside vascular plants. A recent study has shown that DELLA overexpression in *M. polymorpha* results in a delay in the formation of gametangiophores following treatment with far-red light (Hernández-García *et al*., 2021). Therefore, work in this chapter aimed at investigating whether DELLA-regulated reproductive development is also conserved in *P. patens*.

3.2 *Pp*DELLAs have divergent DELLA domains, but conserved GRAS domains compared to land plant orthologues

To investigate how similar *Pp*DELLA peptide sequences are to those from other land plant orthologues, an alignment was performed in SeaView software using full-length peptide sequences from well-characterised land plant DELLA proteins, as well as DELLA orthologues from recently sequenced hornwort and fern species, which have not been used in previously published alignments. Figure **3.1A** shows that out of the three motifs required for GID1 interaction, the DELLA and VHYNP motifs are highly divergent in mosses in general, while the LEQLE motif is more conserved. This is not the case for hornwort DELLAs, which show a high degree of conservation in the entire DELLA domain (Figure **3.1A**). In addition, the liverwort *Mp*DELLA has relatively conserved DELLA and VHYNP motifs, but a more divergent LEQLE motif (Figure **3.1A**). In the case of the LHR1 subdomain of the GRAS domain, required for DELLA protein-protein interactions with transcription factors, this is highly conserved among

land plant DELLAs (Figure **3.1B**), as is the case for the rest of the GRAS domain peptide sequence (Appendix).

A.

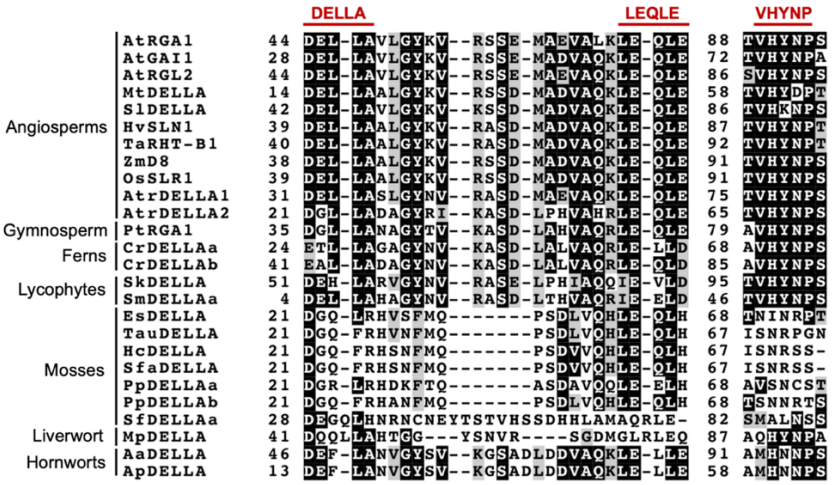

B.

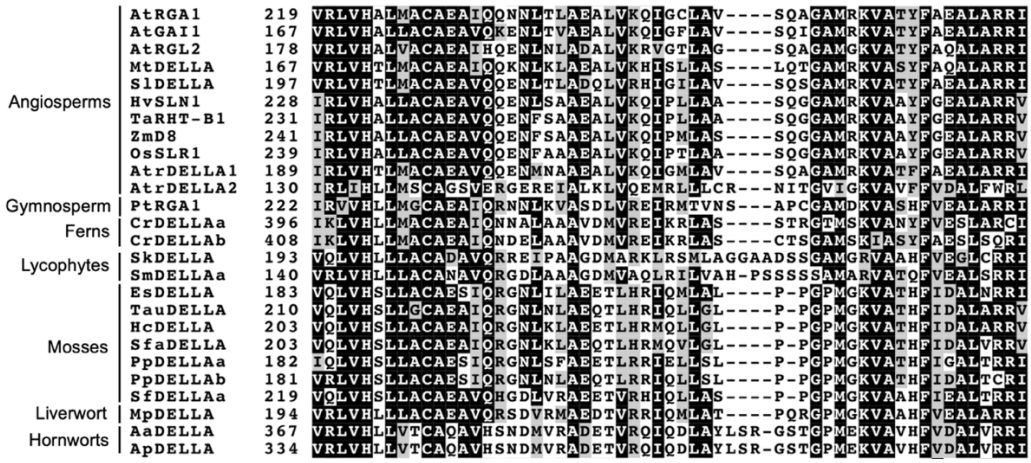

Figure 3.1. Alignment of DELLA peptide sequences from all major land plant groups. (A) Alignment of the DELLA domain containing the DELLA, LEQLE and VHYNP motifs, which are necessary for GID1 interaction. **(B)** Alignment of the LHR1 subdomain of the GRAS domain, which is required for DELLA interaction with various transcription factors. The LHR1 subdomain sequence was delimited according to Uniprot database (https://www.uniprot.org/). The alignment was created in SeaView software and presented using BoxShade. Black shading indicates that at least 50% of the aligned peptides in the same column are identical. Peptides that are similar to the column-consensus peptide are shaded grey. The DELLA peptide sequences used in the alignment are from the following species: *Arabidopsis thaliana, Medicago truncatula, Solanum lycopersicum, Hordeum vulgare, Triticum aestivum, Zea mays, Oryza sativa, Amborella trichopoda* (angiosperms), *Pinus tabuliformis* (gymnosperm), *Ceratopteris richardii* (fern), *Selaginella kraussiana, Selaginella moellendorfii* (lycophytes), *Encalypta streptocarpa, Timmia austriaca, Hedwigia ciliate, Schwetschkeopsis fabronia, Physcomitrium patens, Sphagnum fallax* (mosses), *Marchantia polymorpha* (liverwort), *Anthoceros agrestis* and *Anthoceros punctatus* (hornworts).

3.3 Phylogenetically, *Pp*DELLAs cluster within a monophyletic group with all bryophyte DELLAs

In order to further investigate the relationship between *Pp*DELLA protein sequences and land plant orthologous sequences, a phylogenetic tree of land plant DELLAs was constructed using full-length peptide sequences (Figure **3.2**). Two non-DELLA GRAS family proteins from Arabidopsis were included in the analysis to form an outgroup (*At*SCR and *At*SCL3). The phylogenetic tree was constructed using the maximum likelihood algorithm in SeaView.

Bryophyte DELLA proteins formed a monophyletic group, where *Pp*DELLAs form a sister group to the liverwort *Mp*DELLA protein, and moss and liverwort DELLAs collectively form a sister group to the hornworts (Figure **3.2**). Gymnosperm *Pt*RGA1 and angiosperm *Atr*DELLA2 (from *Amborella trichopoda*) cluster together, as they have the DGLLA sequence (Figure **3.1A**), which characterises DELLA3 clade proteins, while fern DELLAs from *Ceratopteris richardii* cluster on their own as a sister group to all other land plant DELLA proteins (Figure **3.2**), suggesting a large degree of divergence, which is also reflected in their relatively divergent DELLA motif sequence (Figure **3.1A**). Eudicot DELLA1 and DELLA2 clades can be distinguished, with *At*RGL2, *Sl*DELLA and *Mt*DELLA forming the DELLA2 clade, and *At*RGA1 and *At*GAI1 the DELLA1 clade, while monocot DELLAs from maize, rice, barley and wheat cluster together forming the monocot DELLA1/2 clade (Figure **3.2**). It is unclear from this tree which DELLA clade fern and lycophyte DELLAs can be assigned to, however it has previously been suggested that ferns only have DELLA3 clade proteins, while lycophytes have both DELLA3 and DELLA1/2 (Hernández-García *et al*., 2019).

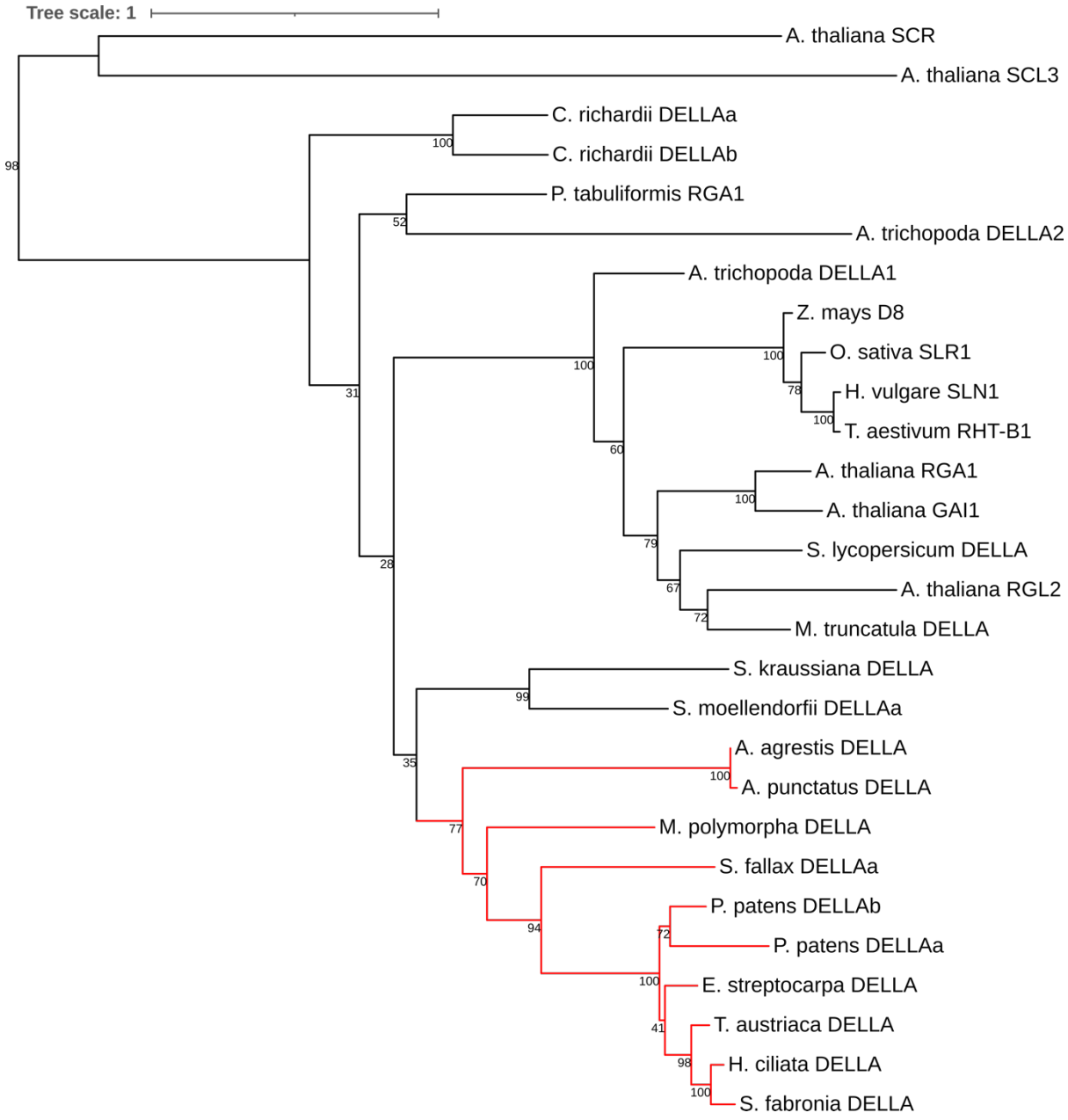

Figure 3.2. Maximum likelihood phylogenetic tree of peptide sequences of land plant DELLA orthologues. Peptide sequences and sequence annotations were obtained from Phytozome, NCBI or oneKP, depending on the availability of the species genome, by blasting with the peptide sequence of *At*RGA1. The tree was generated using the maximum likelihood algorithm in SeaView on default settings with 100 bootstrap replicates and the tree format was finalised using iTOL. Bootstrap values are indicated at the nodes. Scale bar indicates 0.1 substitutions per amino acid site. The bryophyte DELLA monophyletic group is highlighted in red.

3.4 Generation of *pHSP::PpDELLA-GFP* overexpression moss lines

In order to investigate the stability of *Pp*DELLA proteins under treatments with diterpenes, proteasome inhibitors, translation inhibitors and stress-inducing chemicals, stable moss lines were generated where *Pp*DELLAs, tagged with GFP on the carboxy-terminus, were overexpressed under a heat shock inducible promoter (*pHSP*) in wild-type *P. patens* (Figure **3.3**). An attempt had also been made to generate transformants with constitutive *Pp*DELLA-GFP overexpression using the maize ubiquitin promoter (*pUBI*), however no viable transformants could be obtained. *Pp*DELLAa or *Pp*DELLAb coding sequences (excluding the stop codon) were amplified and cloned into the moss transformation vector pHSP::MCS::GFP-108-35SNPT, which shares 1.9kb homology with the inert genomic locus of *P. patens*, allowing efficient integration into the moss genome via homologous recombination (Figure **3.3**). Control lines overexpressing *pHSP::GFP* were also generated by transforming *P. patens* with the empty vector.

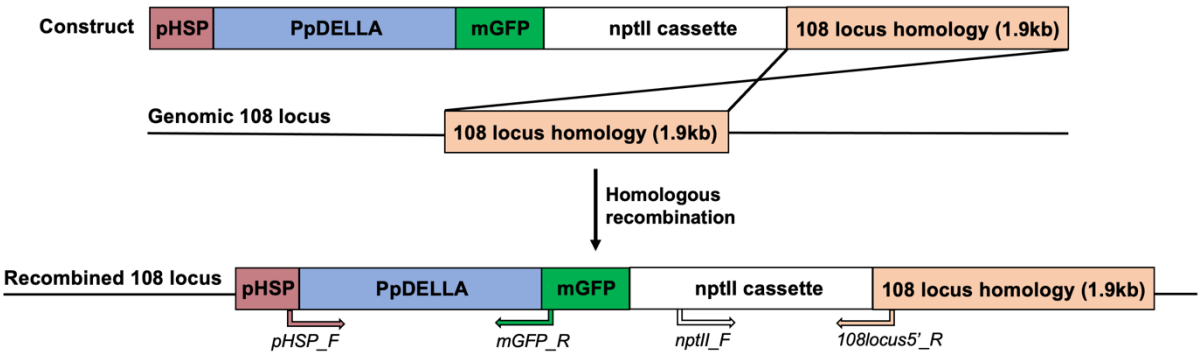

Figure 3.3. Cloning strategy for inducible overexpression of *Pp*DELLA-GFP proteins in *P. patens*. *PpDELLA*s were amplified by PCR from *P. patens* genomic DNA (as *PpDELLA*s are made up of one exon) and cloned in-frame with an *mGFP* gene in the pHSP::MCS::GFP-108-35SNPT moss transformation vector, which also contains a neomycin phosphotransferase (nptII) cassette for antibiotic selection in plant cells, and 1.9kb DNA sequence homology to the inert genomic 108 locus. The primers used for screening transformants for the presence of the construct are shown on the recombined 108 locus diagram (also see figures 3.4-3.6 and methods section 2.9.8 for primer sequences).

Transformants that survived two rounds of geneticin (G418) selection were screened for correct integration of the construct using PCR (Figures **3.4-3.6**). Multiple transformants of *pHSP::PpDELLAb-GFP* were genotyped using primers specific for *pHSP*, *mGFP*, *nptII* and 108 locus, and the PCR product containing *PpDELLAb* from one transformant (Plant1) was also sequenced (Figure **3.4**).

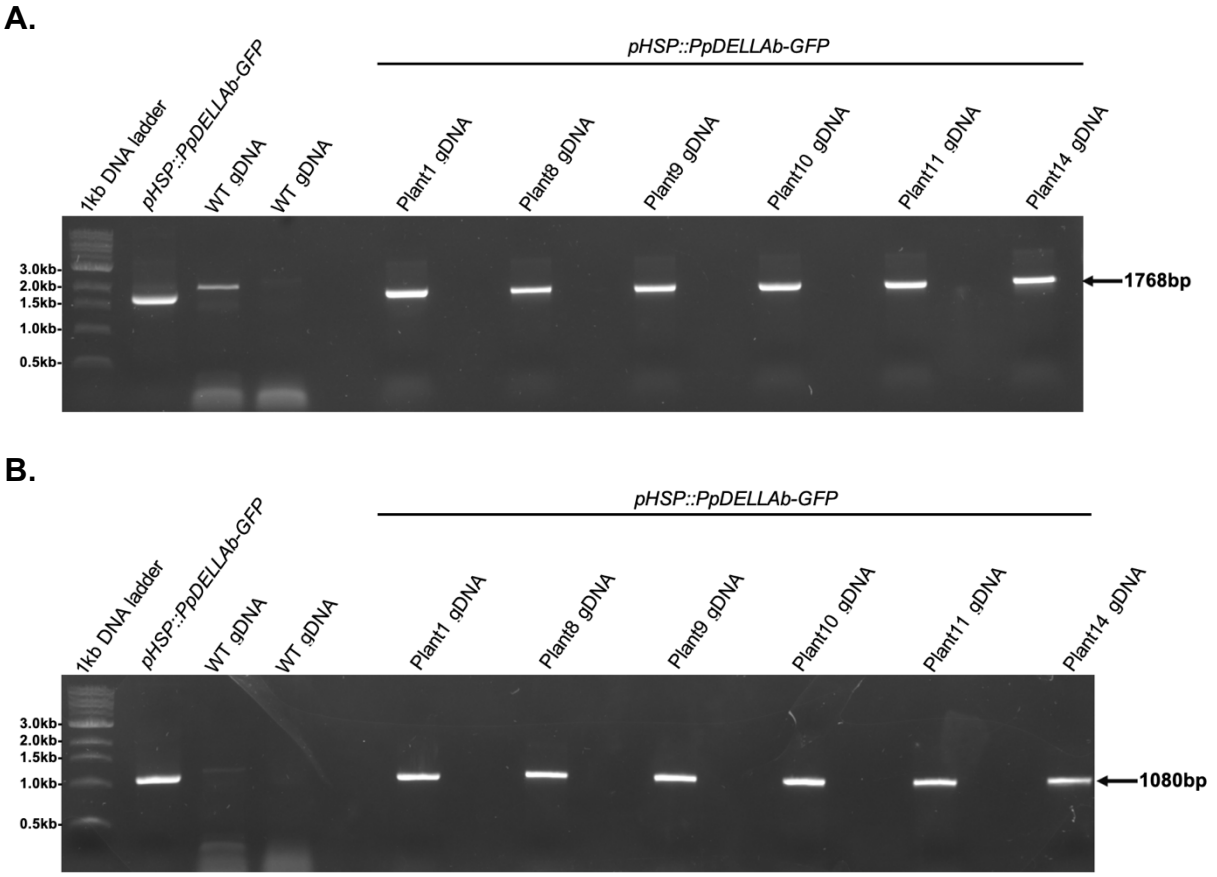

Figure 3.4. Genotyping *PpDELLAb* overexpression transformants by PCR to determine the presence of the *pHSP::DELLAb-GFP* construct in a *P. patens* wild-type (WT) background. (A) Integration of the *pHSP::DELLAb-GFP* construct into the genome was confirmed using the primers *pHSP_F* and *mGFP_R* (see section 2.9.8 for primer sequences) in 6 transformants that survived two rounds of geneticin (G418) selection. Genomic DNA (gDNA) from two wild-type plants was used as a negative control and the transformation vector was used as a positive control. Note the presence of a non-specific ~2kb amplification product in Wt gDNA **(B)** Integration of the *nptII* cassette into the *P. patens* genome was confirmed by PCR using the primers *nptII_F* and *108locus5'_R* (see section 2.9.8 for primer sequences) in 6 transformants that survived two rounds of G418 selection. Genomic DNA from two wild-type plants was used as a negative control and the transformation vector was used as a positive control. The PCR product from Plant1 in **(A)** was also sequenced using the PCR primers to further confirm the presence of the construct.

Regarding *pHSP::PpDELLAa-GFP*, only one transformant survived selection, despite multiple transformation attempts, which was genotyped in the same way as *pHSP::PpDELLAb-GFP* (Figure **3.5**). Due to the presence of a non-specific band of similar size to the *pHSP::PpDELLAa-GFP* band in the wild-type gDNA PCR (Figure **3.5A**), an additional PCR was performed using a *PpDELLAa*-specific forward primer (*XhoI-PpDELLAa_pHSP-F*) and *mGFP_R*, which indicated the presence of the construct in gDNA from the transformant and not in wild-type gDNA (Figure **3.5B**). Several transformants of *pHSP::GFP* to be used as controls were also genotyped using primers specific for *pHSP*, *mGFP*, *nptII* and 108 locus, as well as using PCR product sequencing (Figure **3.6**). It should be noted that the primers used in Figures **3.4B** and **3.5C** do not confirm integration into the 108 locus. It is possible that the construct was inserted at the *PpDELLAa* or *PpDELLAb* locus, as the lengths of homologous *PpDELLAa* and *PpDELLAb* sequences are nearly equivalent to that of the 108 sequence. A primer that is 108-specific and not represented in the construct itself, will need to be used in the future to confirm correct targeting to the 108 locus.

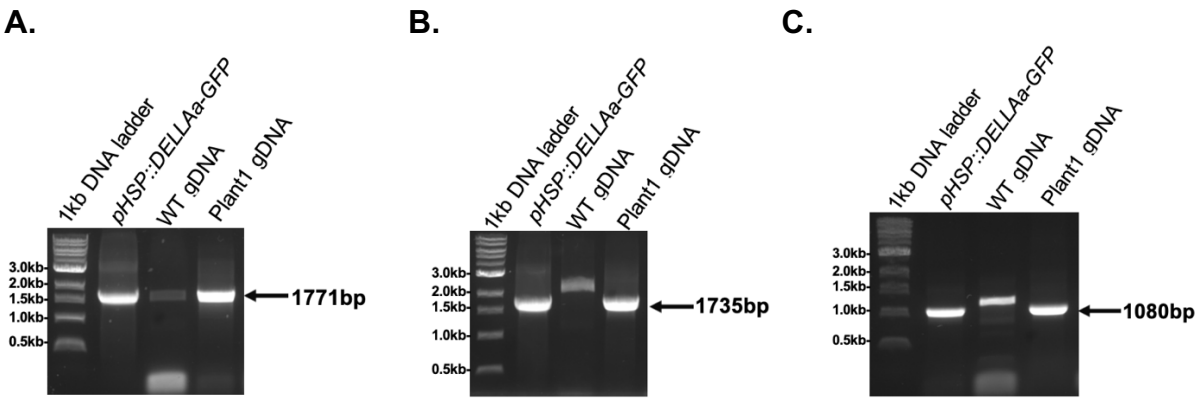

Figure 3.5. Genotyping *PpDELLAa* overexpression transformants by PCR to determine the presence of the *pHSP::DELLAa-GFP* construct in a *P. patens* wild-type (WT) background. Integration of the *pHSP::DELLAa-GFP* construct was confirmed by PCR using: **(A)** *pHSP_F* and *mGFP_R* primers and **(B)** *XhoI-PpDELLAa_pHSP_F* and *mGFP_R* primers in one plant that survived two rounds of geneticin (G418) selection (see section 2.9.8 for primer sequences). **(C)** Integration of the *nptII* cassette into the *P. patens* genome was confirmed by PCR using the primers *nptII_F* and *108locus5'_R* in one transformant that survived two rounds of G418 selection (see section 2.9.8 for primer sequences). In all cases, genomic DNA (gDNA) from a wild-type plant was used as a negative control and the transformation vector was used as a positive control. The PCR product from Plant1 in **(A)** was also sequenced using the PCR primers to further confirm the presence of the construct. Note the presence of non-specific amplification products in Wt gDNA in all three PCRs.

A.

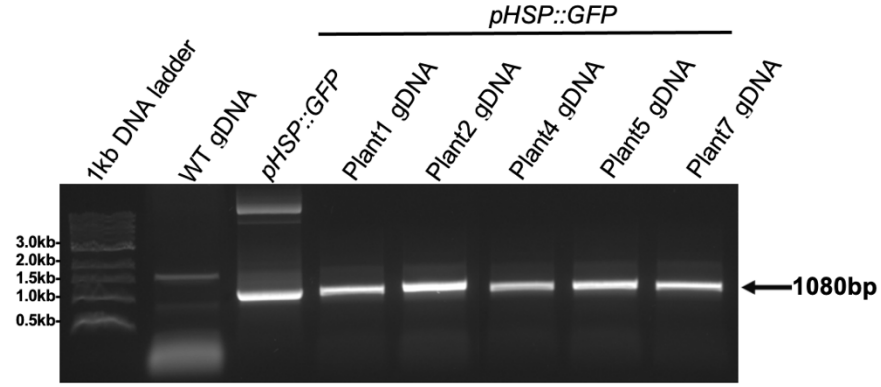

B.

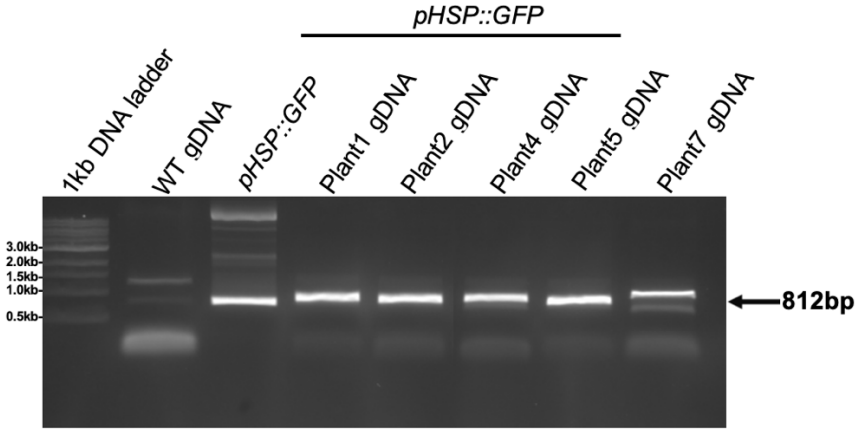

Figure 3.6. Genotyping *GFP* overexpression transformants by PCR to determine the presence of the *pHSP::GFP* construct in a *P. patens* wild-type (WT) background. (A) Integration of the *pHSP::GFP* construct into the genome was confirmed using the primers *pHSP_F* and *35STer_R* in 4 out of 5 transformants (Plants 1, 2, 4 and 5) that survived two rounds of geneticin (G418) selection (see section **2.9.8** for primer sequences). Genomic DNA (gDNA) from a wild-type plant was used as a negative control and the transformation vector was used as a positive control. **(B)** Integration of the construct into the *P. patens* genomic locus 108 was confirmed using the primers *nptII_F* and *108locus5'_R* in 5 transformants that survived two rounds of G418 selection (see section 2.9.8 for primer sequences). Genomic DNA from a wild-type plant was used as a negative control and the transformation vector was used as a positive control. The PCR products from Plants 1, 2 and 4 from **(A)** were also sequenced using the PCR primers to further confirm the presence of the construct.

3.5 *Pp*DELLA-GFP or GFP expressed under *pHSP* can be induced with 1-hour heat shock at 37ºC and be sustained for at least 26 hours

In order to confirm whether the moss transformants generated in section **3.4** could produce detectable *Pp*DELLA-GFP and GFP proteins, an anti-GFP western blot

was performed using protein extracts from transformants of *pHSP::PpDELLAa-GFP* (Plant1), *pHSP::PpDELLAb-GFP* (Plant1) and *pHSP::GFP* (Plant2), which had been incubated for 1 hour at 37°C, followed by incubation at 22°C for 6 or 26 hours (Figure **3.7**). Tissue from stable transformants that had not been incubated for 1 hour at 37°C did not produce detectable *Pp*DELLA-GFP or GFP proteins, while 1-hour heat shock induced *Pp*DELLA-GFP and GFP proteins, which could be detected both at 6 and 26 hours post induction (Figure **3.7**). It is worth noting that *Pp*DELLAa-GFP was always detected at lower levels compared to *Pp*DELLAb-GFP.

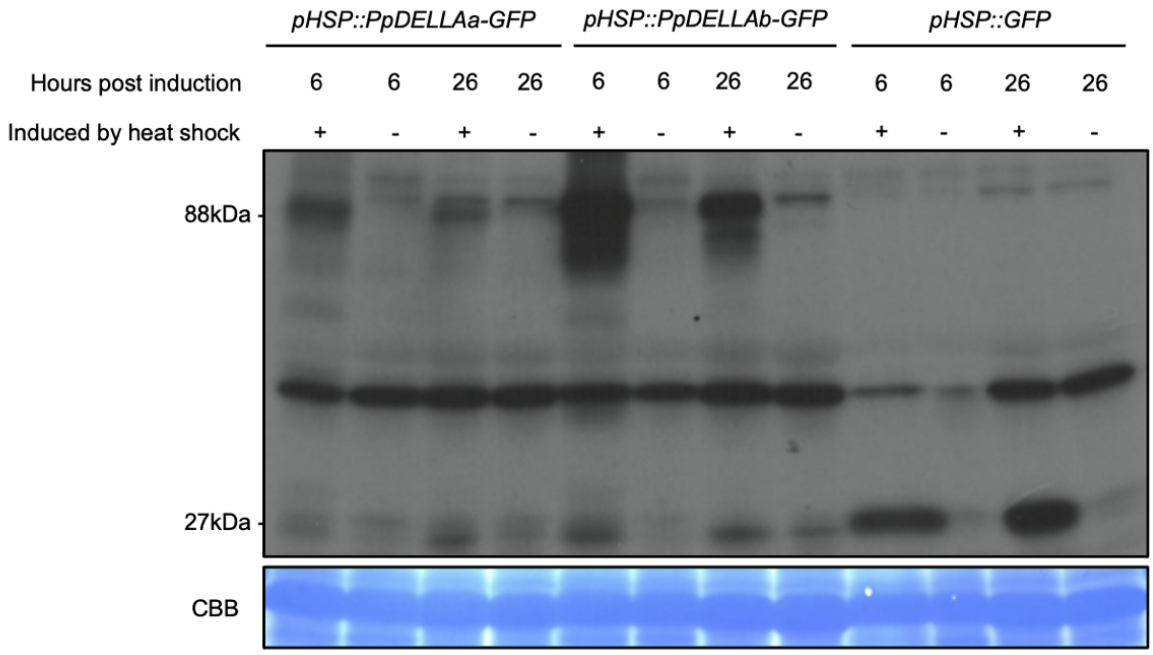

Figure 3.7. Overexpression of *Pp*DELLA-GFP and GFP proteins can be induced by heat shock and be sustained for at least 26 hours. *Pp*DELLAa-GFP (88kDa; Plant1), *Pp*DELLAb-GFP (88kDa; Plant1) and GFP (27kDa; Plant2) protein expression induced by one-hour's heat shock at 37°C detected by anti-GFP western blotting, 6 and 26 hours post induction. Protein was extracted from 10 day-old protonemata that had been incubated at 37°C in liquid BCDAT growth media for 1 hour followed by incubation at 22°C for 6 or 26 hours. CBB, Coomassie brilliant blue staining.

Expression of *Pp*DELLA-GFP proteins following induction by heat shock was also confirmed using confocal microscopy. Protonemata from *pHSP::PpDELLAa-GFP*

(Plant1) and *pHSP::PpDELLAb-GFP* (Plant1) transformants that had been incubated for 1 hour at 37ºC, followed by incubation at 22ºC for 6 or 21 hours accumulated *Pp*DELLA-GFP primarily in their nuclei, with *Pp*DELLAb-GFP always showing higher expression levels compared to *Pp*DELLAa-GFP (Figure **3.8**). When a heat shock was not applied to protonemata from the same moss lines cultured otherwise under the same conditions, no *Pp*DELLA-GFP expression could be detected, suggesting that the induction system is working (Figure **3.8**).

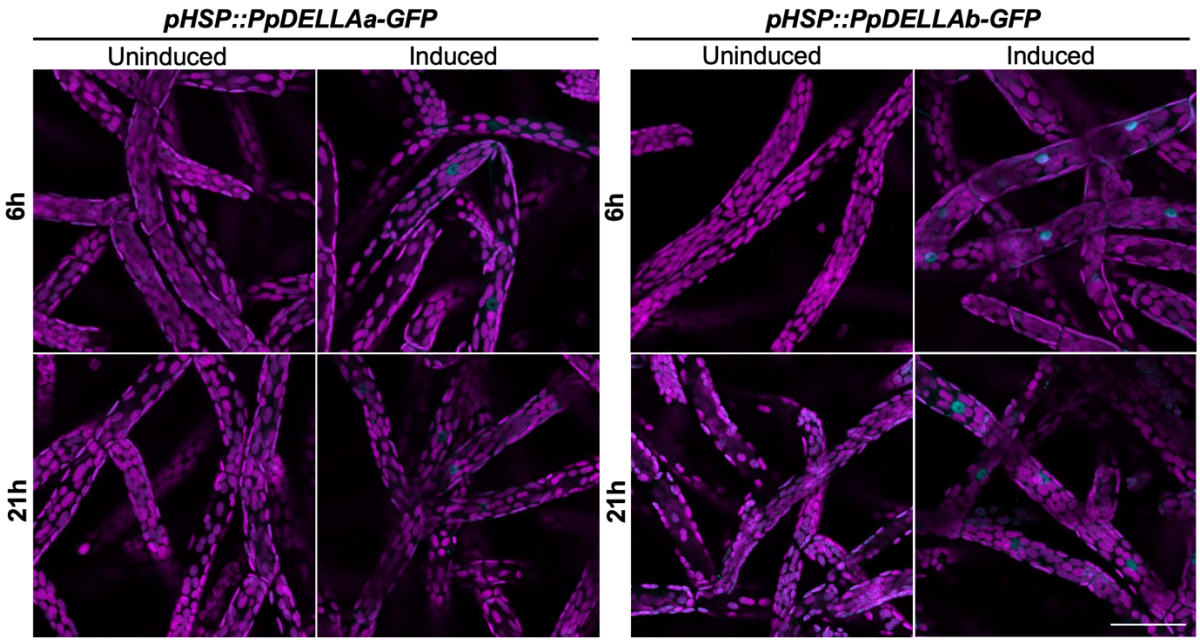

Figure 3.8. Induction of *Pp*DELLA-GFP expression by 1-hour heat shock at 37ºC. Confocal images showing *Pp*DELLAa-GFP (Plant1) and *Pp*DELLAb-GFP (Plant1) expression primarily in nuclei of 7-day old *P. patens* protonemata incubated in liquid BCDAT growth media for 1 hour at 37ºC followed by 6-hour or 21-hour incubation at 22ºC post heat shock (induced). When a heat shock was not applied to protonemata grown otherwise under the same conditions, no *Pp*DELLA-GFP expression could be observed (uninduced). Cyan: GFP signal; Magenta: chloroplast auto-fluorescent signal. (Scale bar, 50µm).

3.6 Diterpene-induced DELLA degradation does not occur in *P. patens*

In order to investigate whether *Pp*DELLA proteins can be degraded by diterpenes, the moss overexpression lines generated in section **3.4** and characterised in section **3.5** were used. 7-day old moss protonemata containing the *pHSP::PpDELLAa-GFP* or *pHSP::PpDELLAb-GFP* construct were incubated in liquid BCDAT medium at 37^{o}C for 1 hour followed by incubation at 22^{o}C for 6 hours to enable induction of *Pp*DELLA-GFP protein. Protonemata were then incubated for 2 hours in liquid BCDAT supplemented with either GA_3 or GA_9-ME (which is bioactive in moss) or methanol (the solvent of GAs). In addition, 7-day old Arabidopsis seedlings of the *pRGA::GFP-AtRGA1* line were incubated for 2 hours in liquid Murashige and Skoog (MS) medium supplemented with either GA_3 or GA_9-ME or methanol. DELLA stability was examined using *in vivo* confocal microscopy or western blotting.

As expected, treatment of *pRGA::GFP-AtRGA1* seedlings with GA_3 induced *At*RGA degradation, evident from both the loss of the nuclear fluorescent signal in Arabidopsis roots (Figure **3.9A**) as well the absence of a band corresponding to GFP-*At*RGA on an anti-GFP western blot (Figure **3.9B**), while treatment with GA_9-ME did not affect GFP-*At*RGA1 stability (Figures **3.9A-B**). In the case of *P. patens* protonemata, treatment with either GA_3 or GA_9-ME was not able to induce *Pp*DELLA-GFP degradation, suggesting that *Pp*DELLAs are not regulated by GAs as vascular plant DELLAs do (Figures **3.9A-B**).

7-day old protonemata from the *pHSP::PpDELLAa-GFP*, *pHSP::PpDELLAb-GFP* and *pHSP::GFP* overexpression lines were also incubated for 2 hours (following 6-hour incubation post heat shock) in liquid BCDAT supplemented with either the diterpene *ent*-kaurenoic acid or the GA biosynthesis inhibitors: uniconazole or

paclobutrazol (PAC), all of which affect moss development at least at the vegetative stage (Yasumura *et al.,* 2007; Hayashi *et al*., 2010) (Figure **3.9**). The stability of both *Pp*DELLAa-GFP or *Pp*DELLAb-GFP was not affected by either the GA biosynthesis inhibitors or *ent*-kaurenoic acid, suggesting that *Pp*DELLAs are not regulated by diterpenes and are most likely not involved in the *P. patens* diterpene signalling pathway (Figure **3.9**).

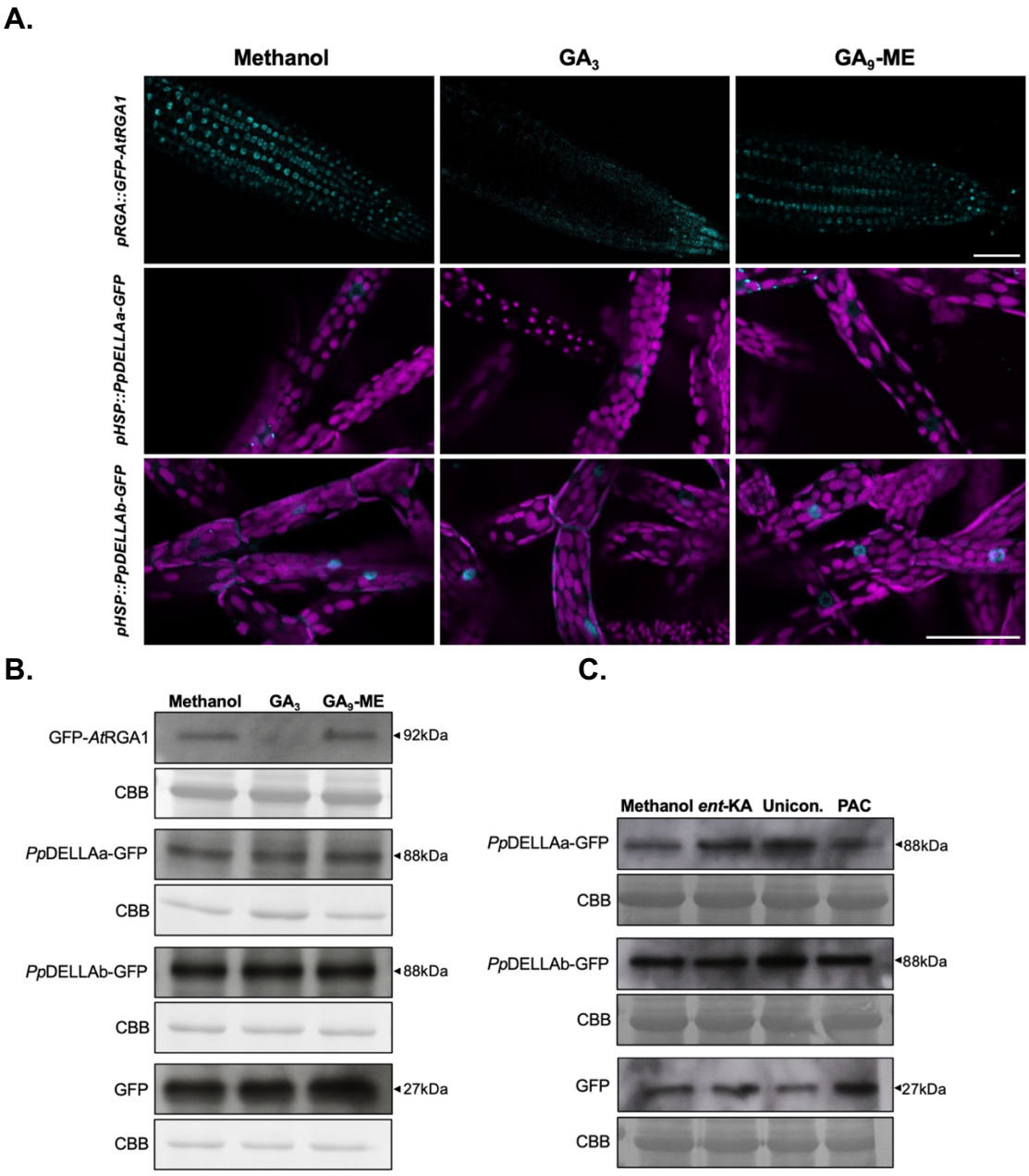

Figure 3.9. Diterpene-induced DELLA degradation does not occur in *P. patens*. (A) Confocal images showing GFP-*At*RGA1 degradation in 7-day old Arabidopsis (*pRGA::GFP-AtRGA1*) roots following 2-hour incubation with 10μM gibberellin A_3 (GA_3), and absence of *Pp*DELLA-GFP degradation in 7-day old *P. patens* protonemata following 2-hour incubation with either 10μM GA_3 or 10μM GA_9 methyl-ester (GA_9-ME). Cyan: GFP signal; Magenta: chloroplast auto-fluorescent signal. (Scale bars, 50μm). **(B)** Anti-GFP western blots showing GFP-*At*RGA1 degradation in 7-day old Arabidopsis (*pRGA::GFP-AtRGA1*) roots following 2-hour incubation with 10μM GA_3, and absence of *Pp*DELLA-GFP degradation in 7-day old *P. patens* protonema tissue following 2-hour incubation with either 10μM GA_3 or 10μM GA_9-ME. CBB, Coomassie brilliant blue staining. **(C)** Anti-GFP western blots showing no effect on the stability of *Pp*DELLA-GFP from 7-day old *P. patens* protonema tissue following 2-hour incubation with the diterpene *ent*-kaurenoic acid (ent-KA; 10μM) or the GA biosynthesis inhibitors: uniconazole (Unicon.; 10μM) or paclobutrazol (PAC; 10μM). CBB, Coomassie brilliant blue staining.

3.7 *Pp*DELLAs do not interact with *At*GID1c or its moss homologue *Pp*GLP1 in either a GA-dependent or a GA-independent manner

To examine whether *Pp*DELLAs can interact with GID1 homologues in a GA-dependent manner, a yeast two-hybrid assay was performed. *Pp*DELLAs and *At*RGA1 previously cloned in pGADT7 (Yasumura *et al*., 2007) were tested for interaction with *Pp*GLP1 or *At*GID1c, which were previously cloned in pGBKT7 (Yasumura *et al*., 2007). DELLA proteins were fused with the GAL4 activation domain (AD) and a HA tag, and GID1 homologues were fused with the GAL4 DNA-binding domain (DBD) and a MYC tag (Yasumura *et al*., 2007). While *At*RGA1 interacted with *At*GID1c in a GA_3-dependent manner, *Pp*DELLAs did not interact with *At*GID1c or *Pp*GLP1 in the presence of GA_3, GA_9-ME, *ent*-kaurenoic acid or methanol and neither did *At*RGA1 with *Pp*GLP1 (Figure **3.10A**). This suggests that GA-dependent interaction between DELLAs and GID1s is not present in *P. patens*. To confirm that the proteins tested were indeed expressed in yeast cells and thus any negative interactions were not simply due to lack of protein expression, anti-HA and anti-MYC western blots were performed, which confirmed that the proteins were expressed (Figure **3.10B**).

To complement these results, the proteins tested for interaction were also synthesised *in vitro* from the same vectors they were cloned in, using a cell free system, and a Co-IP was performed using anti-MYC-coupled beads. In the presence of GA_3, when MYC-*At*GID1c was pulled down, HA-*At*RGA1 could be detected in an anti-HA western blot, suggesting that the two proteins interacted in a GA-dependent manner (Figure **3.10C**). In contrast, when MYC-*Pp*GLP1 was pulled down in the presence of GA_9-ME, neither HA-*Pp*DELLAa nor HA-*Pp*DELLAb could be detected in an anti-HA western blot, suggesting no interaction (Figure **3.10C**).

A.

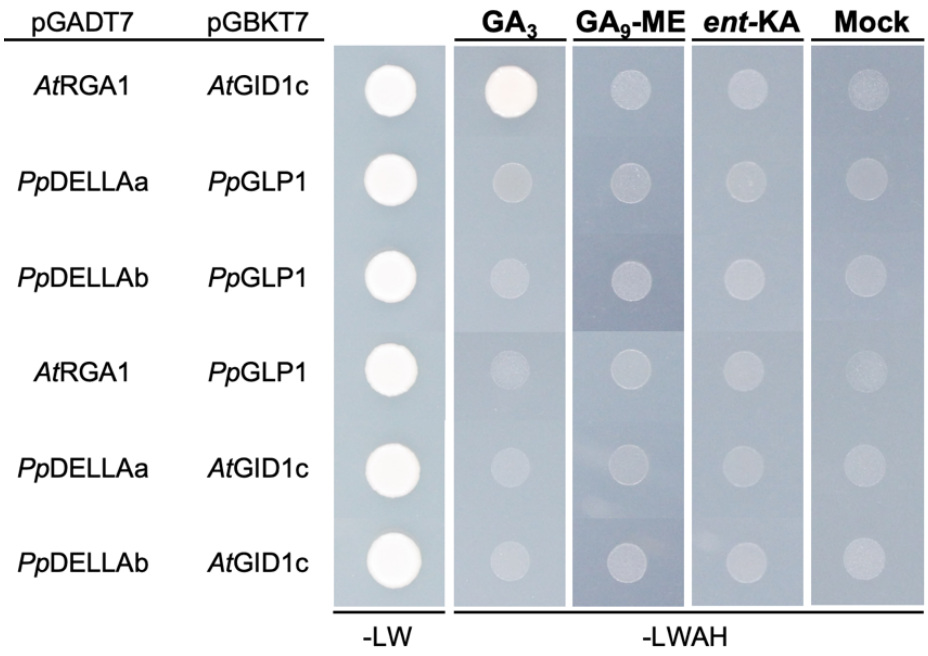
pGADT7
pGBKT7
GA3
GA9-ME
ent-KA
Mock
AtRGA1
AtGID1c
PpDELLAa
PpGLP1
PpDELLAb
PpGLP1
AtRGA1
PpGLP1
PpDELLAa
AtGID1c
PpDELLAb
AtGID1c
-LW
-LWAH

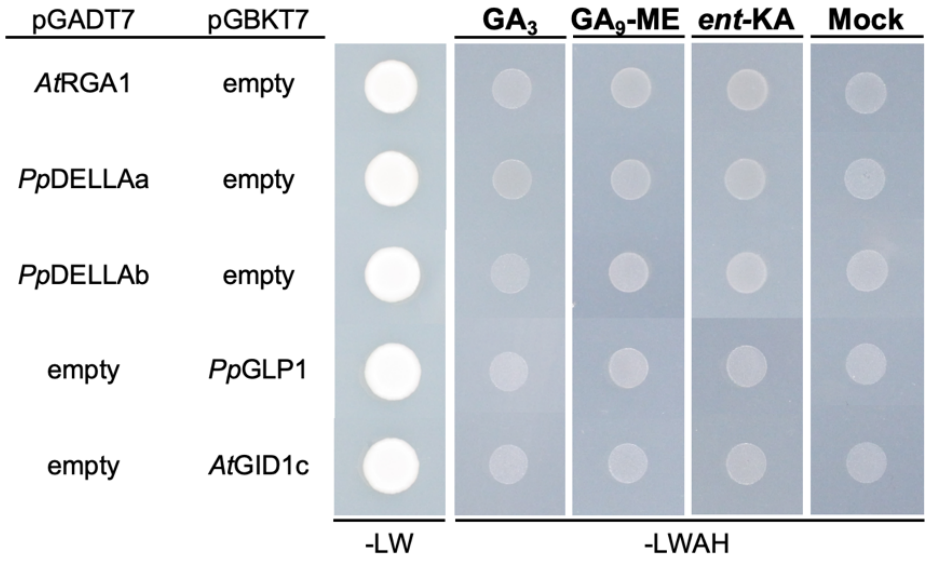
pGADT7
pGBKT7
GA3
GA9-ME
ent-KA
Mock
AtRGA1
empty
PpDELLAa
empty
PpDELLAb
empty
empty
PpGLP1
empty
AtGID1c
-LW
-LWAH

B.

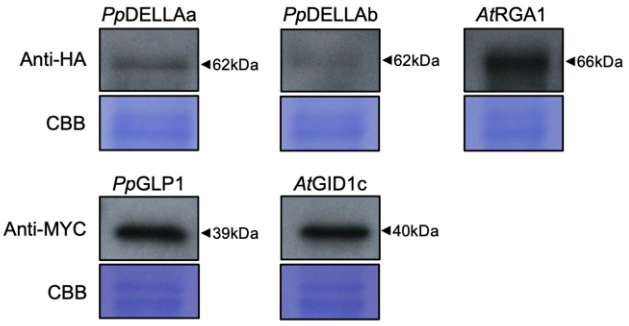
PpDELLAa
PpDELLAb
AtRGA1
Anti-HA
62kDa
62kDa
66kDa
CBB
PpGLP1
AtGID1c
Anti-MYC
39kDa
40kDa
CBB

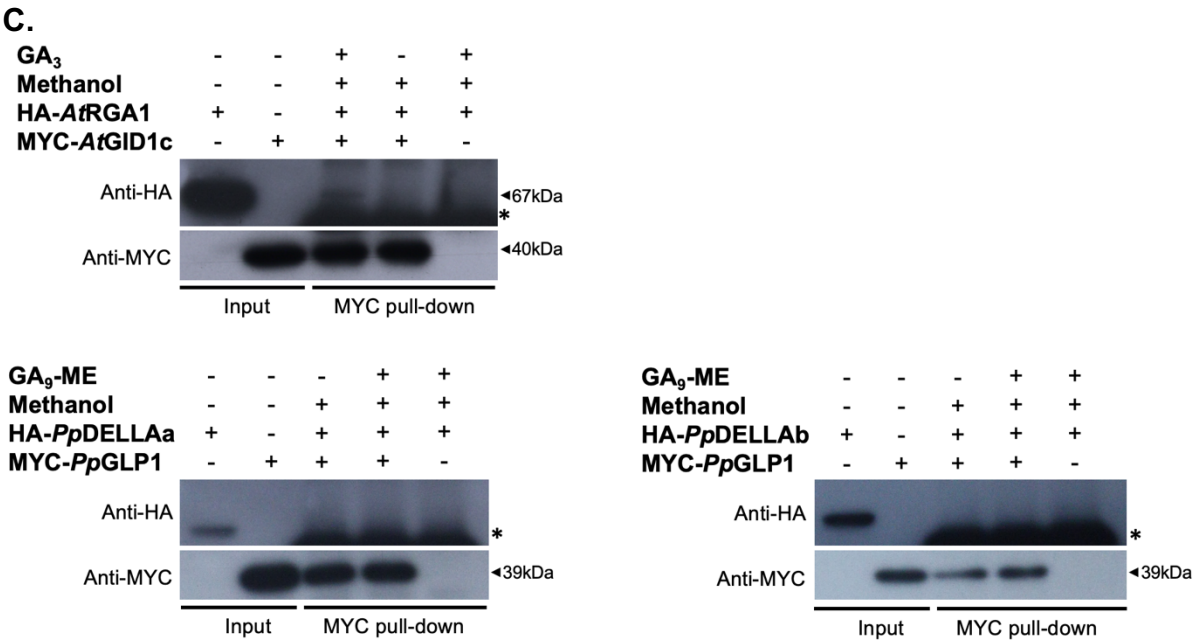

Figure 3.10. Gibberellin (GA)-dependent DELLA-GID1 interaction does not occur in *P. patens*. (A) Yeast two-hybrid assay between DELLA and GID1 homologues from *Arabidopsis* and *P. patens*. *At*RGA1 and *At*GID1c interact in a GA_3-dependent manner, while *Pp*DELLAs do not interact with *At*GID1c or its moss homologue *Pp*GLP1 in either a GA-dependent or a GA-independent manner (GA_9-ME: GA_9 methyl-ester; *ent*-KA: *ent*-kaurenoic acid; Mock: methanol). **(B)** Western blots showing that HA-tagged *Pp*DELLAs and *At*RGA1 and MYC-tagged *Pp*GLP1 and *At*GID1c are expressed in yeast cells. CBB, Coomassie brilliant blue staining. **(C)** Coimmunoprecipitation from a cell free system using α-MYC-coupled beads. HA-*At*RGA1 and MYC-*At*GID1c expressed *in vitro* interacted in a GA_3-dependent manner, while HA-*Pp*DELLAs and MYC-*Pp*GLP1 did not interact in a GA_9-ME-dependent or -independent manner (*, antibody heavy chain).

3.8 *PpdellaA* and *PpdellaB* mutant spores respond to GA_9-ME similarly to wild-type spores.

In order to assess whether GA_9-ME speeds up the rate of spore germination in a *Pp*DELLA-dependent manner, the germination rate of *Ppdella* mutant spores under treatment with GA_9-ME was examined. Due to very low production of sporophytes by the *PpdellaAB* mutant, the single mutants *PpdellaA* and *PpdellaB* were used instead. Treatment with 5μM GA_9-ME increased germination rate in wild-type and *PpdellaA* or *PpdellaB* mutant spores to a similar extent, especially 4, 5 and 7 days after spore plating, although differences were not always statistically significant with the Kruskal-

Wallis test (Figure **3.11**). The general trend of the data suggests that GA_9-ME speeds up spore germination in a *Pp*DELLA-independent manner, although the behaviour of the *PpdellaAB* mutant under treatment with GA_9-ME could not be assessed during the course of this project.

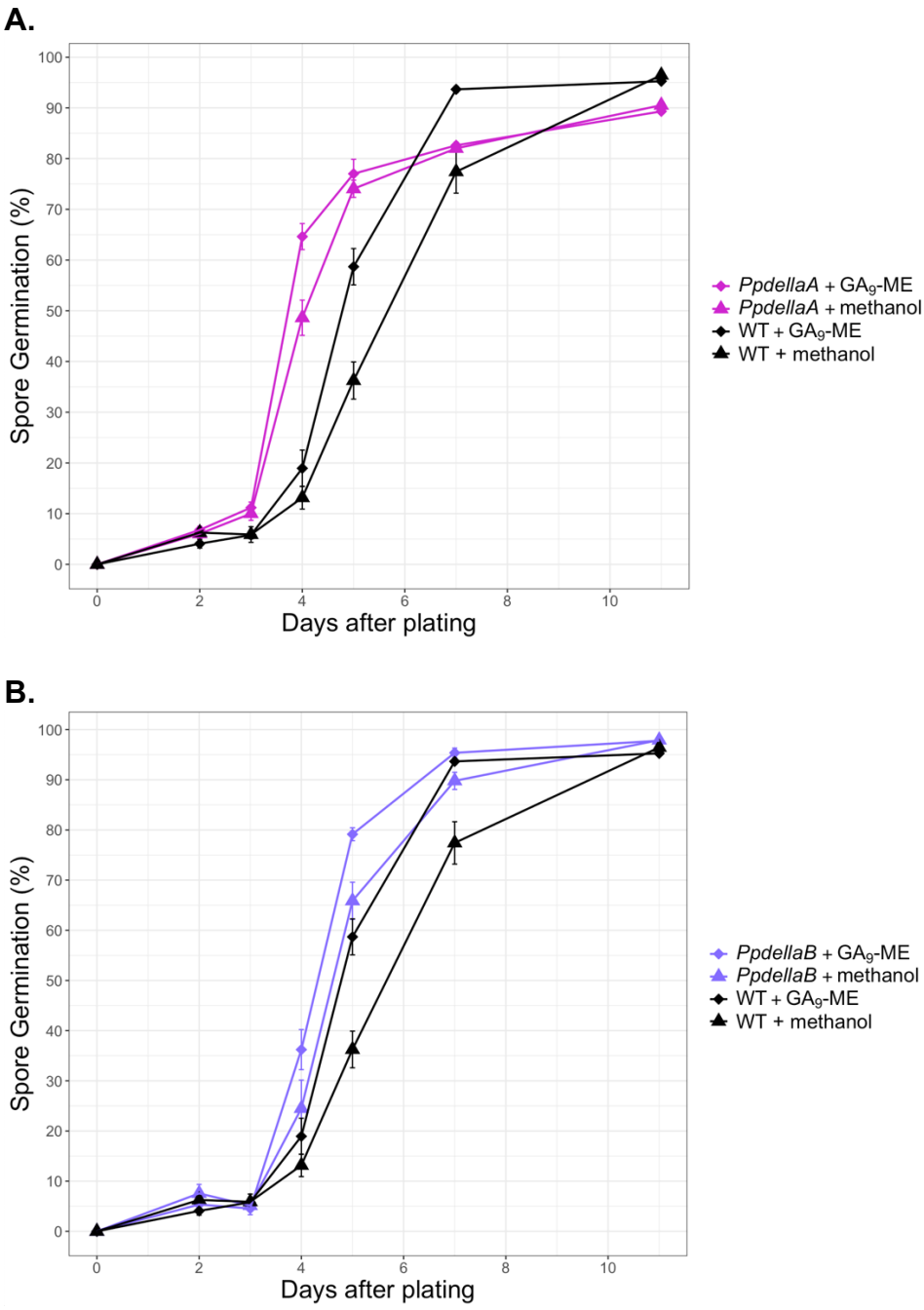

Figure 3.11. *Ppdella* mutant spores respond to GA_9 methyl-ester (GA_9-ME) similarly to wild-type spores. (A) Effect of 5μM GA_9-ME on wild-type (WT) and *PpdellaA* mutant spore germination. GA_9-ME increases spore germination rate of *PpdellaA* and Wt to a similar extent. A Kruskal-Wallis test indicates significant differences between *PpdellaA* + GA_9-ME and WT + methanol on days 4 and 5 ($p<0.01$), between *PpdellaA* + GA_9-ME and WT + GA_9-ME on day 4 ($p<0.05$), between *PpdellaA* + methanol and WT + methanol on day 5 ($p<0.05$), between WT + GA_9-ME and WT + methanol ($p<0.05$) on day 7, and between *PpdellaA* + methanol and WT + GA_9-ME on day 7 ($p<0.05$). Error bars, ± SEM. **(B)** Effect of 5μM GA_9-ME on wild-type (WT) and *PpdellaB* mutant spore germination. GA_9-ME increases spore germination rate of *PpdellaB* and WT to a similar extent. A Kruskal-Wallis test indicates significant differences between *PpdellaB* + GA_9-ME and WT + methanol on days 4, 5 and 7 ($p<0.05$). Error bars, ± SEM.

3.9 *Pp*DELLAs appear to be regulated indirectly by the 26S proteasome

To investigate whether *Pp*DELLAs are regulated by the 26S proteasome, *Pp*DELLA overexpression lines were treated with the 26S proteasome inhibitor MG132 for different durations and *Pp*DELLA protein levels were monitored. 7-day old protonemata from the *pHSP::PpDELLAa-GFP*, *pHSP::PpDELLAb-GFP* and *pHSP::GFP* overexpression lines underwent a 1-hour heat shock at 37°C in liquid BCDAT cultures supplemented with 100μM MG132 and were incubated for a further 6 hours in the same medium to induce *Pp*DELLA accumulation. Both *Pp*DELLAa-GFP and *Pp*DELLAb-GFP showed higher accumulation levels under treatment with MG132 compared to treatment with ethanol, suggesting that *Pp*DELLA proteins are regulated by the 26S proteasome (Figure **3.12**). This was not the case for GFP protein, which showed similar levels of accumulation with or without MG132 treatment (Figure **3.12**).

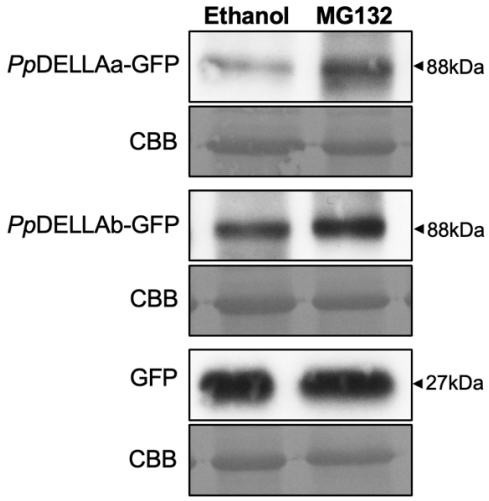

Figure 3.12. *Pp*DELLA proteins accumulate to higher levels under treatment with MG132. 7-day old protonemata from the *pHSP::PpDELLAa-GFP*, *pHSP::PpDELLAb-GFP* and *pHSP::GFP* overexpression lines underwent a one-hour heat shock at 37°C in liquid BCDAT cultures supplemented with 100μM MG132 or ethanol and were incubated for a further 6 hours in the same media to allow induction of the protein. *Pp*DELLAa-GFP and *Pp*DELLAb-GFP showed higher accumulation under treatment with MG132 compared to incubation in ethanol. GFP protein showed similar levels of accumulation with or without MG132 treatment. CBB, Coomassie brilliant blue staining.

The same experiment was repeated with the overexpression lines being incubated in 100μM MG132 for different periods of time: 0, 1.5, 3 or 18 hours post the 6-hour induction period following the heat shock, which is necessary for protein accumulation (Figure **3.13**). *Pp*DELLAb-GFP protein accumulated to much higher levels under treatment with MG132 compared to treatment with ethanol and this was observed at all incubation durations tested (Figure **3.13B**). *Pp*DELLAa-GFP showed higher accumulation in MG132 compared to ethanol at 3 hours post induction (Figure **3.13A**), while GFP accumulation levels were similar with or without MG132 incubation (Figure **3.13C**).

To examine if the effect of MG132 on *Pp*DELLA accumulation levels was direct, the same lines were treated with the translation inhibitor cycloheximide (CHX), for different amounts of time. It was hypothesised that if *Pp*DELLAs were degraded by the 26S proteasome, treatment with CHX would induce a decrease in *Pp*DELLA accumulation levels, as no more protein would be produced and the proteasome would degrade any protein that had already been synthesised. This was not the case for *Pp*DELLAa-GFP or *Pp*DELLAb-GFP, neither of which displayed lower levels of accumulation after 1.5, 3 or 18 hours of incubation with CHX and the same was observed for GFP protein too (Figure **3.13A-C**). The fact that CHX did not affect *Pp*DELLA accumulation levels suggests that *Pp*DELLAs are not regulated directly by the 26S proteasome. Instead, there may be other proteasome-regulated proteins that accumulate under MG132 treatment and regulate *Pp*DELLA accumulation levels, which suggests that *Pp*DELLAs may be regulated by the 26S proteasome indirectly.

A.

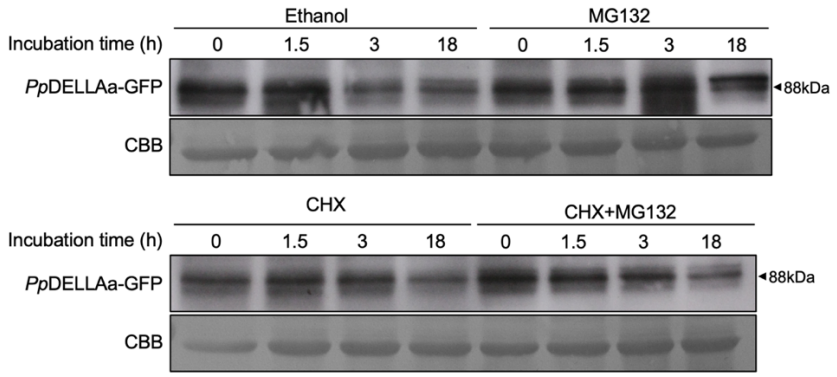

B.

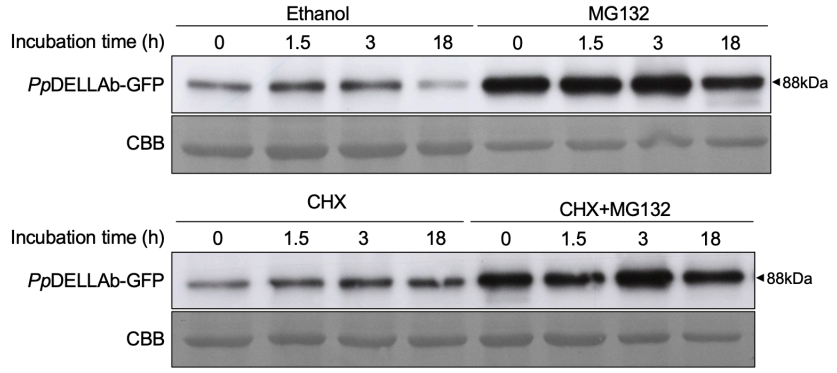

C.

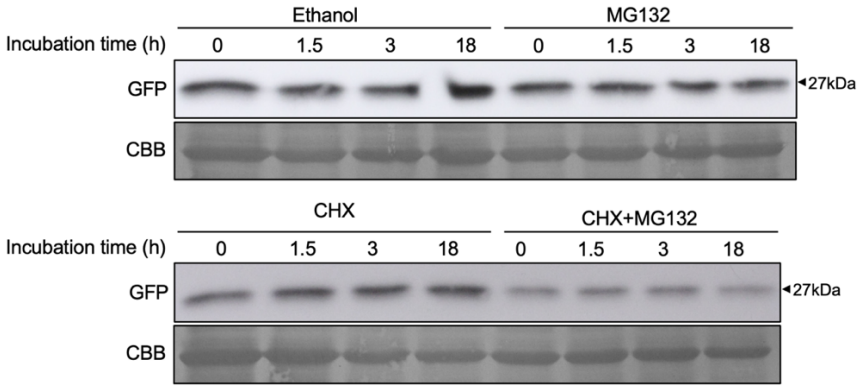

Figure 3.13. *Pp*DELLA proteins accumulate to higher levels under treatment with MG132, but remain stable under cycloheximide (CHX) treatment. 7-day old protonemata from the **(A)** *pHSP::PpDELLAa-GFP*, **(B)** *pHSP::PpDELLAb-GFP*, and **(C)** *pHSP::GFP* overexpression lines underwent a one-hour heat shock at 37°C in liquid BCDAT cultures supplemented with 100μM MG132 or ethanol and were incubated for a further 6 hours in the same media to allow induction of the protein (timepoint 0 = the end of the 6-hour induction period). Treatment with CHX following the induction period, did not affect the stability of *Pp*DELLA-GFP or GFP proteins. Treatment with MG132 induced consistently higher *Pp*DELLAb-GFP accumulation during all timepoints compared to ethanol treatment and higher *Pp*DELLAa-GFP accumulation at 3 hours post-induction. CBB, Coomassie brilliant blue staining.

3.10 Salt stress responses in *P. patens* are not DELLA-dependent

To investigate the hypothesis that *Pp*DELLA proteins are involved in the regulation of abiotic stress responses, the performance of the *PpdellaAB* mutant under varying levels of salt stress was examined at the vegetative stage. Under both 50mM and 100mM NaCl, the development of protonemata and gametophores was significantly suppressed, especially at 100mM, and the *PpdellaAB* responded to both concentrations of NaCl similarly to the wild type (Figure **3.14A**). Furthermore, *PpdellaAB* mutant and wild-type plants did not have significantly different plant area under treatment with 0mM, 50mM or 100mM NaCl (Figure **3.14B**), suggesting that *Pp*DELLA proteins may not be involved in the response to salt stress. In addition, there was no increase in the accumulation of *Pp*DELLAa-GFP or *Pp*DELLAb-GFP protein in response to NaCl treatment (Figure **3.15**), suggesting that salt stress responses in *P. patens* are not *Pp*DELLA-dependent.

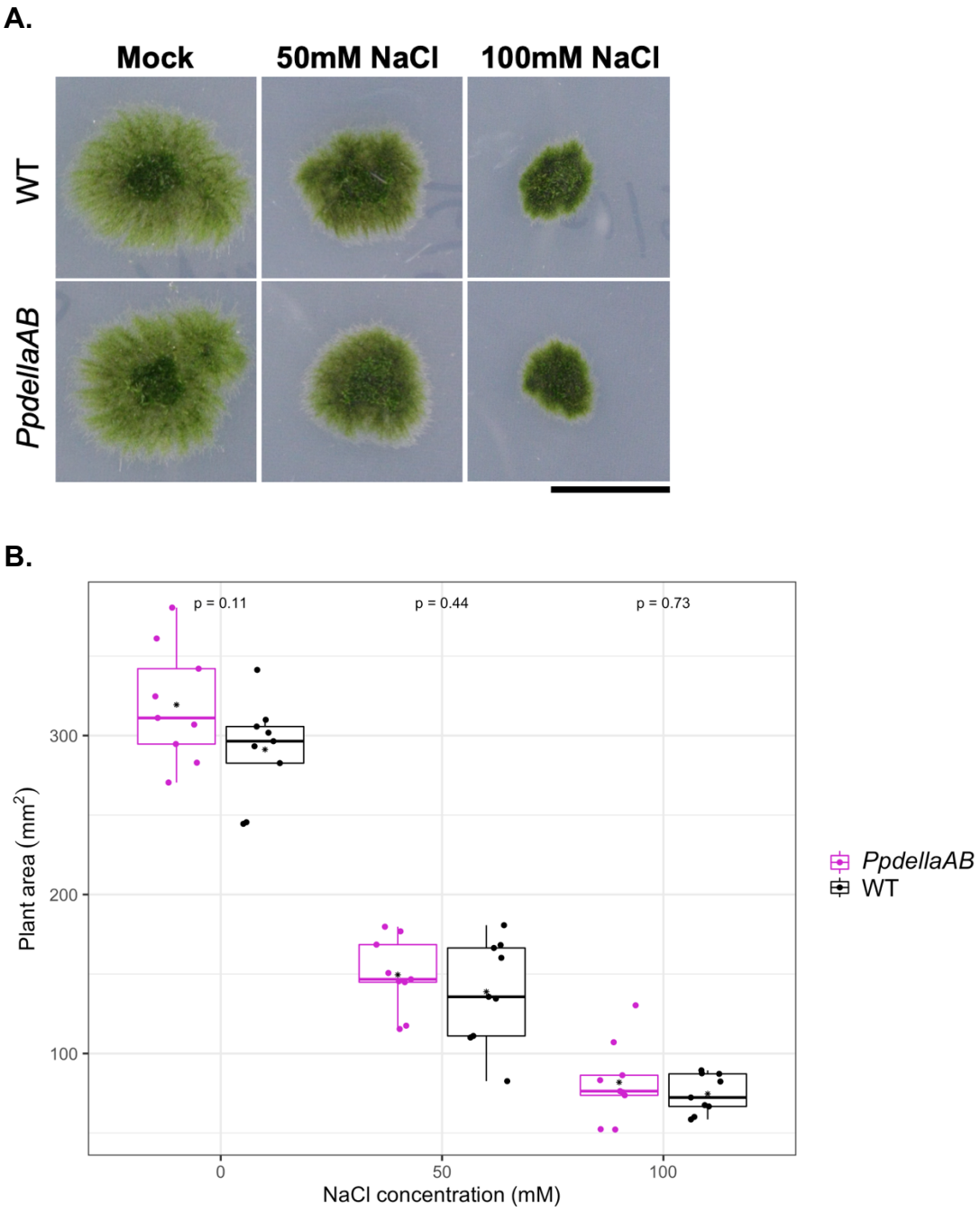

Figure 3.14. The *PpdellaAB* mutant responds to salt stress similarly to wild type (WT). *P. patens* protonemata grown for 15 days on BCDATG medium supplemented with different concentrations of salt (NaCl). **(A)** Treatment with NaCl causes defects in protonema and gametophore development. Scale bar, 10mm. **(B)** *PpdellaAB* and wild-type plants do not have significantly different plant area under treatment with 0mM, 50mM or 100mM NaCl (n=9 per genotype). Differences were tested for significance ($p<0.05$) using the Mann-Whitney U test and p-values are displayed above each treatment group. Black asterisks indicate the mean. To account for variability in plant area at the start of the experiment, this was subtracted from the plant area at the end of the experiment.

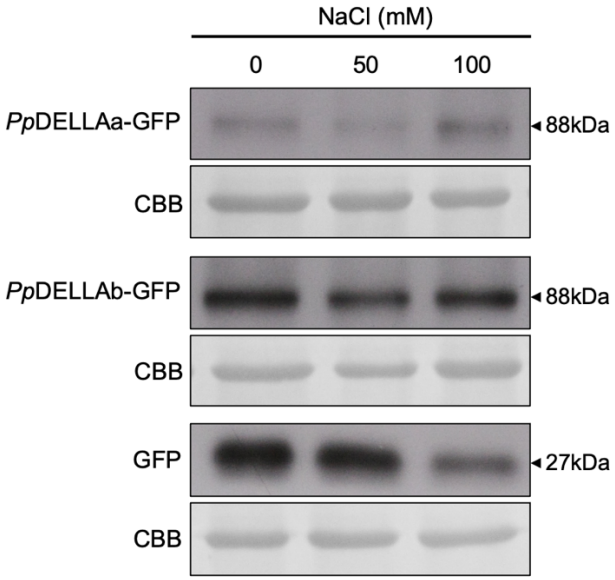

Figure 3.15. *Pp*DELLA protein accumulation is not affected by salt stress. 7-day old protonemata from the *pHSP::PpDELLAa-GFP*, *pHSP::PpDELLAb-GFP*, and *pHSP::GFP* overexpression lines underwent a one-hour heat shock at 37°C in liquid BCDAT cultures, were incubated for a further 6 hours in the same media and were then treated with 0, 50 or 100mM salt (NaCl) for 2 hours. Anti-GFP western blot shows that treatment with NaCl did not induce an increase in the accumulation of *Pp*DELLA-GFP proteins. CBB, Coomassie brilliant blue staining.

3.11 The *PpdellaAB* mutant responds to oxidative stress similarly to wild type

To further examine the putative involvement of *Pp*DELLAs in regulating abiotic stress responses, the behaviour of the *PpdellaAB* mutant under ROS overaccumulation, which is commonly induced in response to both biotic and abiotic stress in plants including *P. patens* (e.g. Inés Ponce de León, 2011; Chen *et al*., 2019), was studied. Protonemata of wild-type and *PpdellaAB* mutant plants were cultured onto cellophane-overlaid BCDATG plates supplemented with the herbicide methyl viologen (MV), known to stimulate O_2^- generation in chloroplasts (Kerchev *et al*., 2015). Wild-type and *PpdellaAB* mutant protonemata responded to different concentrations of MV in a similar manner (Figure **3.16**). Treatment with 1μM MV prevented gametophore differentiation and promoted protonema development in both lines, while

treatment with 10μM or 100μM MV resulted in growth arrest, again in both wild type and *PpdellaAB* mutant (Figure **3.16A**).

A.

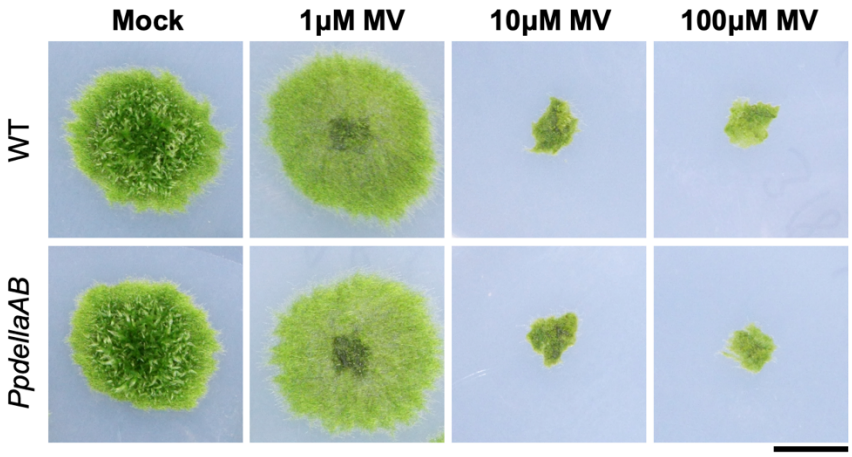

B.

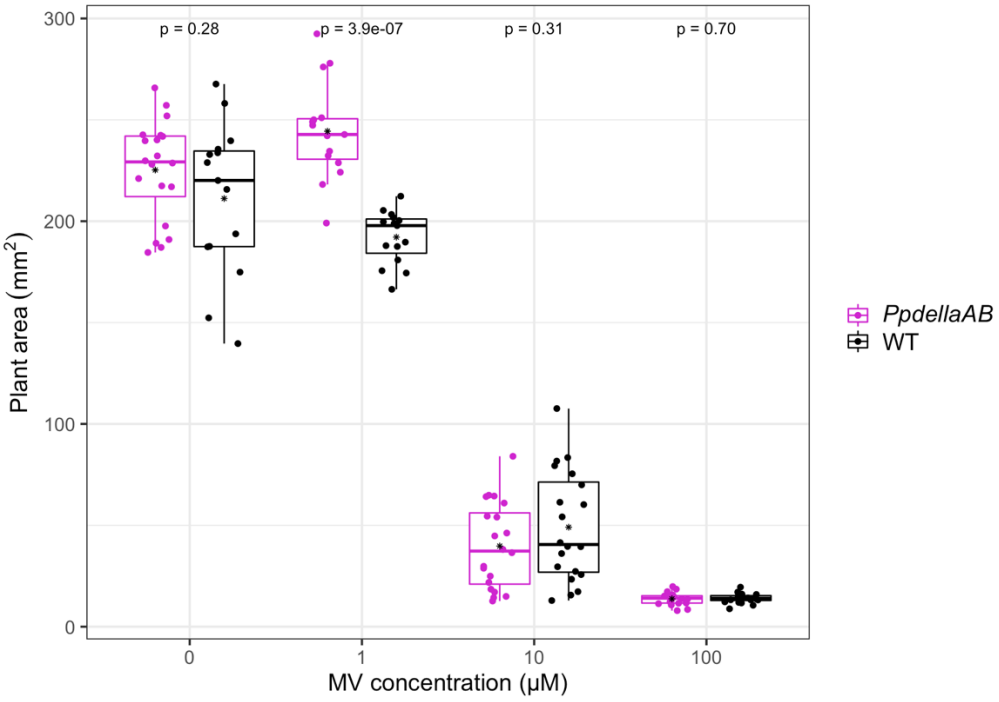

C.

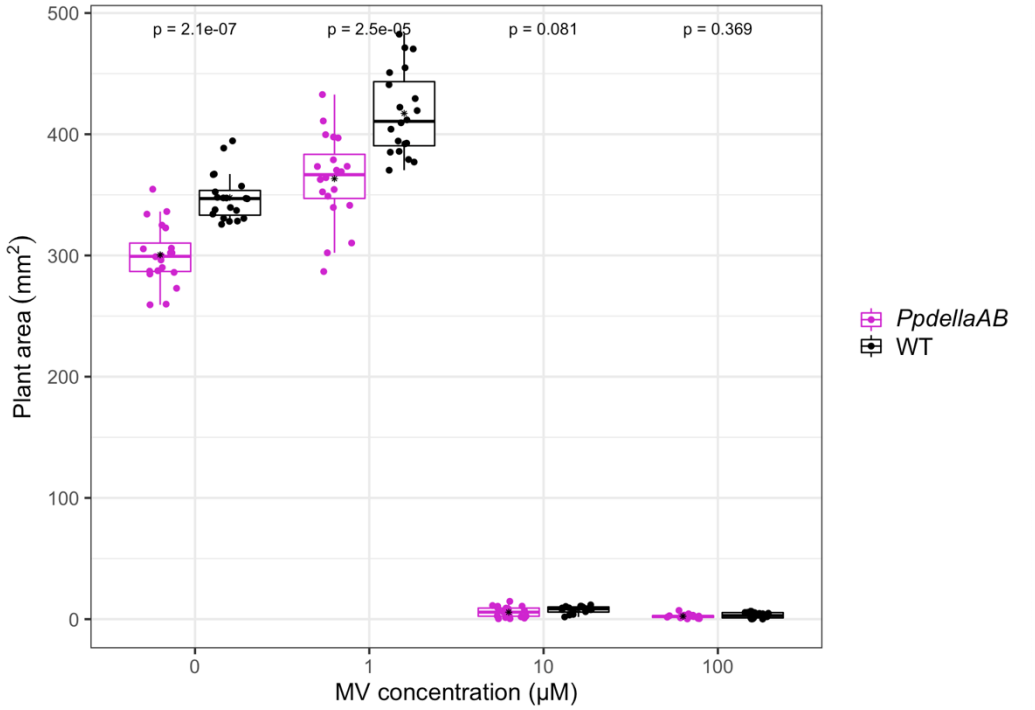

Figure 3.16. *PpdellaAB* mutant responds to oxidative stress similarly to wild type (WT). *P. patens* protonemata grown for 18 days on BCDATG medium supplemented with different concentrations of methyl viologen (MV), which induces generation of reactive oxygen species (ROS). **(A)** Treatment with 1μM MV prevents gametophore differentiation and promotes protonema development, while treatment with 10μM or 100μM MV results in growth arrest. *PpdellaAB* and wild type do not show obvious phenotypic differences at the conditions tested. Scale bar, 10mm. **(B)** *PpdellaAB* and wild-type plants do not have significantly different plant areas at 0μM, 10μM and 100μM MV, but they do at 1μM MV, where wild-type plants have smaller area (n=15-20 per genotype). Differences were tested for significance ($p<0.05$) using the Mann-Whitney U test and p-values are displayed above each treatment group. Black asterisks indicate the mean. To account for variability in plant area at the start of the experiment, this was subtracted from the plant area at the end of the experiment. **(C)** In a different biological replicate of the experiment, *PpdellaAB* and wild-type plants do not have significantly different plant areas at 10μM and 100μM MV, but they do at 0μM and 1μM MV, where wild-type plants have bigger area (n=20 per genotype). Differences were tested for significance ($p<0.05$) using the Mann-Whitney U test and p-values are displayed above each treatment group. Black asterisks indicate the mean. To account for variability in plant area at the start of the experiment, this was subtracted from the plant area at the end of the experiment.

In three biological replicates, *PpdellaAB* and wild-type plants did not have significantly different plant areas at 10μM or 100μM MV (Figure **3.16B-C**). However, in one replicate, *PpdellaAB* had bigger plant area at 1μM MV compared to the wild type (Figure **3.16B**), but in a second replicate, wild-type plants had bigger plant area at 1μM

MV compared to *PpdellaAB*, and this was the case for plant growth at 0μM MV as well (Figure **3.16C**). Therefore, while clearly *PpdellaAB* and wild-type responded similarly to high concentrations of MV, at 1μM MV there was some variation in the responses, which may be worth investigating further in the future. Overall, the results suggest that *Pp*DELLA proteins are not involved the response to oxidative stress induced by treatment with MV, at least at higher concentrations of the chemical.

3.12 The *PpdellaAB* mutant responds to desiccation stress similarly to wild type

To investigate the involvement of *Pp*DELLA proteins in regulating desiccation stress responses, the performance of the *PpdellaAB* mutant under desiccation conditions was assessed. Wild-type and *PpdellaAB* protonemata were cultured on BCDAT plates supplemented with either 10μM ABA, which is known to promote desiccation tolerance (Khandelwal *et al.*, 2010), or methanol, for 16 hours, and were then transferred onto fresh BCDAT plates for one week to recover from the stress. Both wild-type and *PpdellaAB* mutant protonemata that had not been pre-treated with ABA could not survive the recovery period, while treatment with ABA enabled both wild-type and *PpdellaAB* protonemata to continue growing normally (Figure **3.17**). This suggests that *Pp*DELLAs are not involved the regulation of desiccation stress responses in *P. patens*.

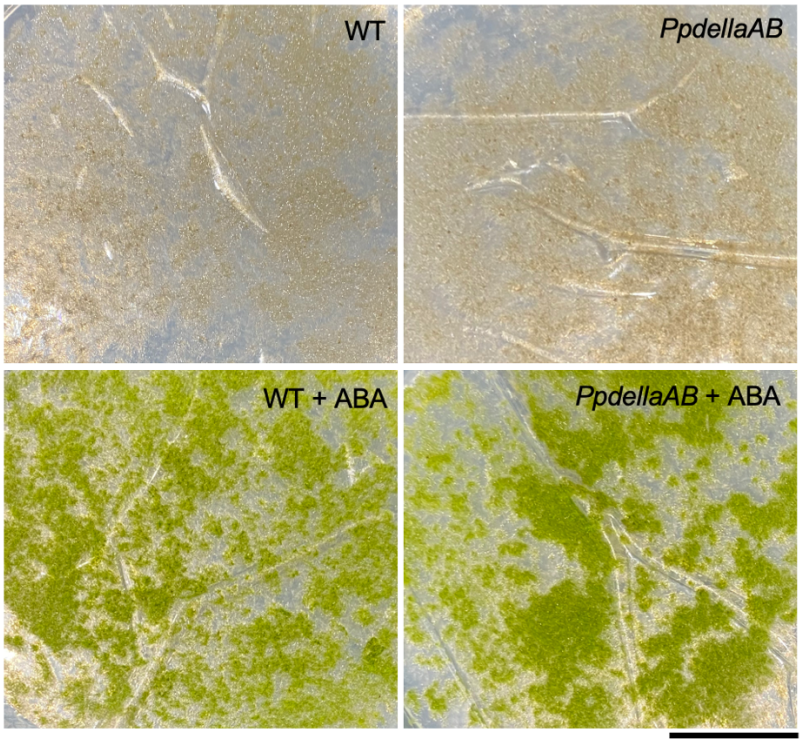

Figure 3.17. The *PpdellaAB* mutant responds to desiccation stress similarly to wild type (WT). *P. patens* protonemata were grown for 16 hours on cellophane-overlaid BCDAT plates supplemented with 10μM abscisic acid (ABA) or methanol, after which time cellophanes were transferred into empty petri dishes for 7 days (desiccation stress conditions). The images show the appearance of the tissue after a 7-day period of growth under normal conditions (recovery period) following the 7 days of incubation in drought stress conditions. Protonemata that had been pre-treated with 10μM ABA (bottom panels) displayed desiccation stress tolerance, whereas protonemata pre-treated with methanol (top panels) did not. Scale bar, 20mm.

3.13 ABA responses in *P. patens* are not *Pp*DELLA-dependent

As both salt and desiccation stress responses involve ABA signalling, the response of *Ppdella* mutant spores under ABA treatment was also investigated. *PpdellaB* and *PpdellaAB* mutant spore germination was inhibited by ABA to a similar extent compared to wild-type spore germination (Figure **3.18A-B**), suggesting that ABA-induced spore germination is not DELLA-dependent in *P. patens*. Furthermore, there was no increase in the accumulation of *Pp*DELLAa-GFP or *Pp*DELLAb-GFP protein in response to ABA treatment (Figure **3.19**), suggesting that ABA responses in *P. patens* are not *Pp*DELLA-dependent.

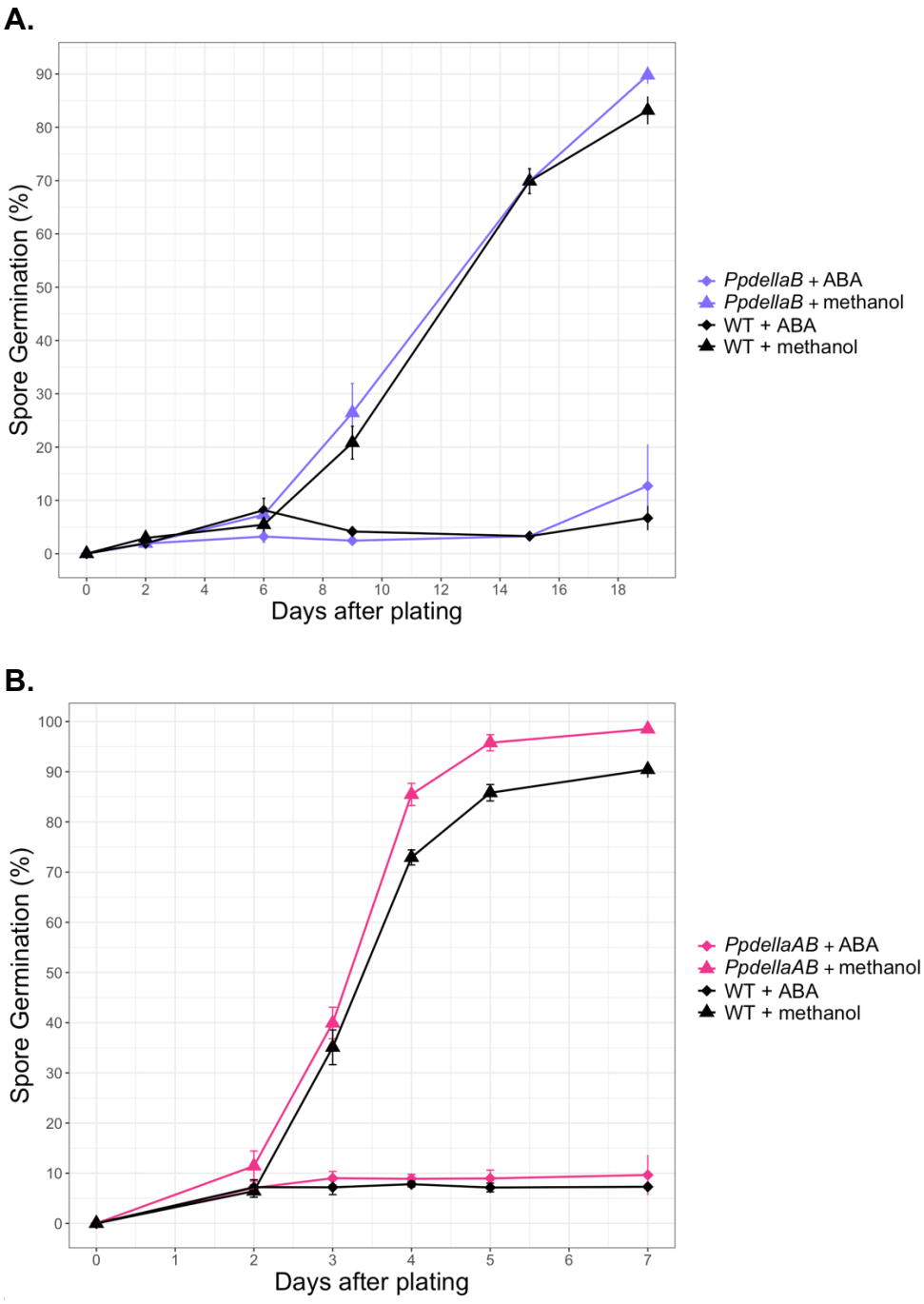

Figure 3.18. *Ppdella* mutant spores respond to abscisic acid (ABA) similarly to wild-type (WT) spores. (A) Effect of 10μM ABA on WT and *PpdellaB* mutant spore germination. ABA supresses spore germination rate of *PpdellaB* and WT to a similar extent. A Kruskal-Wallis test indicates significant differences between *PpdellaB* + ABA and WT + methanol on days 9 and 15, between *PpdellaB* + ABA and *PpdellaB* + methanol on days 9, 15 and 19, between *PpdellaB* + methanol and WT + ABA on days 15 and 19, and between WT + ABA and WT + methanol on day 15 ($p<0.05$). Error bars, ± SEM. **(B)** Effect of 10μM ABA on WT and *PpdellaAB* mutant spore germination. ABA supresses spore germination rate of *PpdellaAB* and WT to a similar extent. A Kruskal-Wallis test indicates significant differences between *PpdellaAB* + ABA and *PpdellaAB* + methanol on days 3, 4, 5 and 7, and between *PpdellaAB* + methanol and WT + ABA on 3, 4, 5 and 7 ($p<0.05$). Error bars, ± SEM.

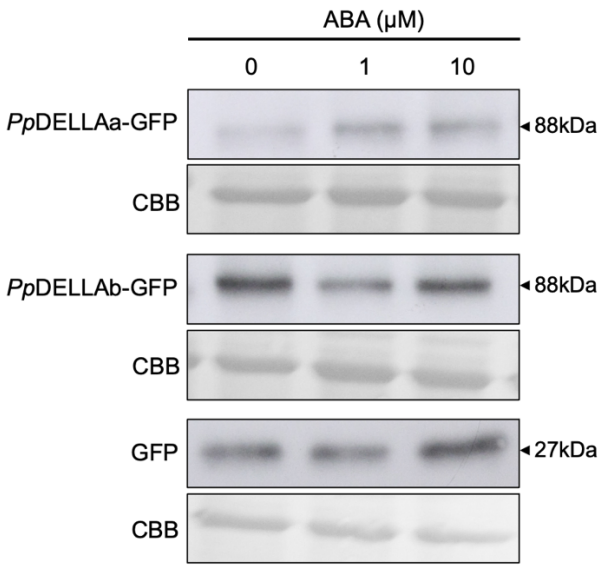

Figure 3.19. *Pp*DELLA protein accumulation is not affected by treatment with abscisic acid (ABA). 7-day old protonemata from the *pHSP::PpDELLAa-GFP*, *pHSP::PpDELLAb-GFP*, and *pHSP::GFP* overexpression lines underwent a one-hour heat shock at 37°C in liquid BCDAT cultures, were incubated for a further 6 hours in the same media and were then treated with 0, 1 or 10μM ABA for 2 hours. Anti-GFP western blot shows that treatment with ABA did not induce an increase in the accumulation of *Pp*DELLA-GFP proteins. CBB, Coomassie brilliant blue staining.

3.14 The *PpdellaAB* mutant has a defect in sporophyte development

To investigate whether *Pp*DELLA proteins are involved in reproductive development, the fertility of the *PpdellaAB* mutant was assessed in comparison with the wild type. Wild-type and *PpdellaAB* gametophores were incubated on minimal BCD agar medium at 15°C in short-day conditions to induce sex organ formation and subsequent fertilisation and sporophyte development. After 7 weeks of incubation under conditions promoting reproductive development, wild-type plants produced numerous sporophytes, while *PpdellaAB* plants did not produce any sporophytes (Figure **3.20**). This suggests that *Pp*DELLA proteins have a role in moss reproductive development.

This hypothesis was further explored by Dr Rabea Meyberg (University of Marburg), who showed that the *PpdellaAB* mutant has a male fertility defect that can

be rescued by crossing the *PpdellaAB* mutant with the *P. patens* Reute ecotype, which is male fertile (unpublished data). These findings suggest that the function of DELLA proteins in regulating reproductive development is conserved between *P. patens* and Arabidopsis.

A.

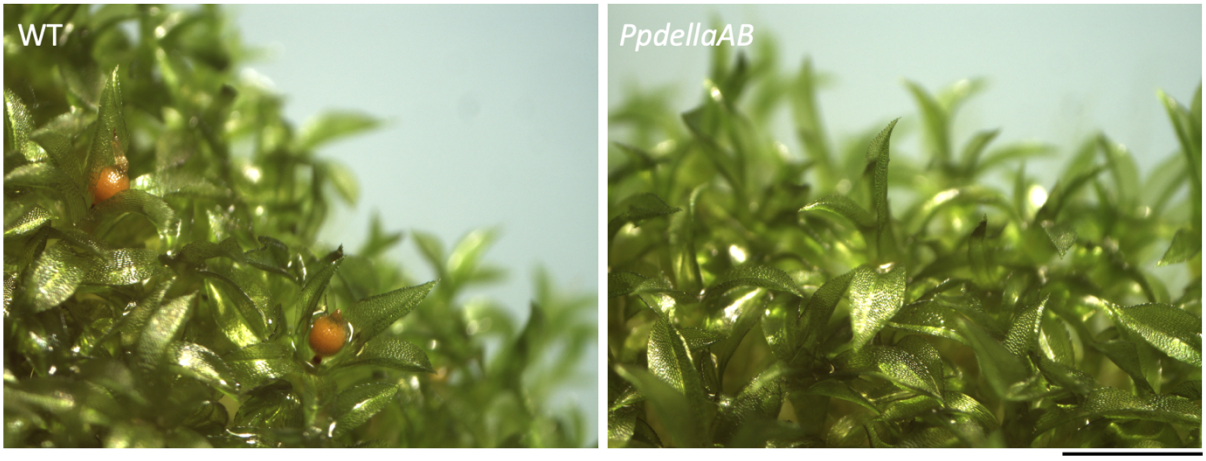

B.

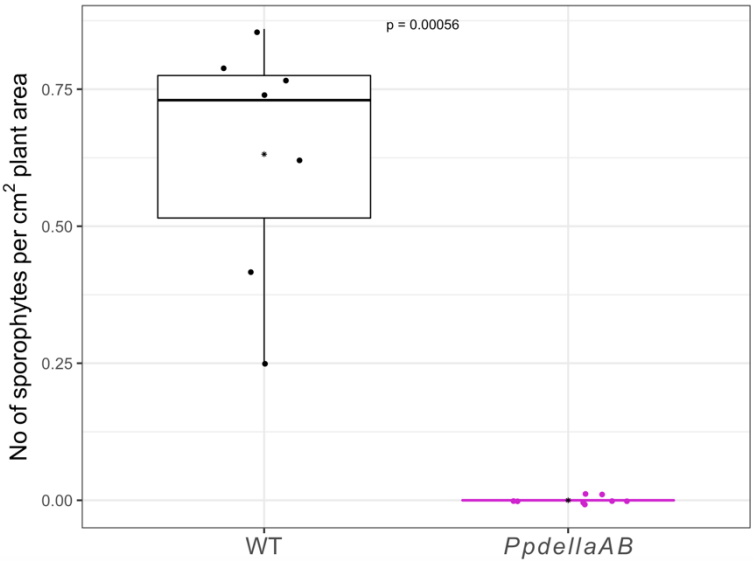

Figure 3.20. The *PpdellaAB* mutant has a defect in sporophyte development. *P. patens* wild-type (WT) and *PpdellaAB* gametophores were incubated on minimal BCD agar medium in magenta vessels at 15°C under an 8h light/16h darkness regime for 7 weeks to induce sex organ development and allow fertilisation and sporophyte development to take place. **(A)** *PpdellaAB* did not produce any sporophytes after 7 weeks at 15°C and short-day conditions, while WT plants produced numerous sporophytes. Scale bar, 2mm. **(B)** WT plants had a higher sporophyte density, expressed as number of sporophytes per cm^2 plant area, compared to *PpdellaAB* plants, which was statistically significant in a Mann-Whitney U test (n=7-8).

3.15 Discussion

3.15.1 Summary

In this chapter, the degree of conservation of some key functions and responses of DELLA proteins in *P. patens* has been studied. Although *Pp*DELLA proteins appear to respond differently to various hormone and stress signals tested in comparison to flowering plant DELLA proteins, some degree of functional conservation has been observed regarding reproductive development.

3.15.2 Flowering plant DELLA responses to diterpenes are not conserved in *P. patens*

Previous work from the Coates lab has shown that *Ppdella* mutant spores germinate faster compared to wild-type spores (Vesty, unpublished), suggesting that *Pp*DELLAs repress spore germination, analogous to their function in Arabidopsis, where *At*RGL2 represses seed germination (Lee *et al*., 2002). Furthermore, diterpene-less mutant spores in *P. patens* germinate slower compared to wild-type spores and the phenotype is rescued by exogenous application of diterpenes, including GA_9-ME, suggesting that diterpenes promote spore germination, analogous to the function of GAs in Arabidopsis (Vesty *et al*., 2016). The fact that a GA molecule (GA_9-ME) is bioactive in *P. patens* and that DELLAs and diterpenes show analogous functions in *P. patens* compared to Arabidopsis, stimulated the beginning of the present research.

Experiments involving western blotting and confocal microscopy showed that *Pp*DELLA degradation is not triggered by bioactive diterpenes, such as *ent*-KA or GA_9-ME. These observations are in line with Yasumura *et al*. (2007), where GA_3 did not stimulate *Pp*DELLA degradation in Arabidopsis cells. In addition, *Pp*DELLAs did not

interact with *At*GID1c or *Pp*GLP1 in a diterpene-dependent manner, again in line with Yasumura *et al*. (2007), where none of the diterpenes tested potentiated any kind of interaction between these proteins. It is worth noting that all interaction assays were only performed *in vitro*, therefore it is always possible that an interaction may be observed *in planta*. Furthermore, *Ppdella* mutant and wild-type spores respond similarly to exogenous application of GA_9-ME, suggesting that GA_9-ME-induced promotion of germination does not happen via *Pp*DELLA proteins. This is in agreement with the observation that wild-type and *PpdellaAB* protonema growth is equally suppressed under treatment with the GA biosynthesis inhibitor PAC (Yasumura *et al*., 2007), suggesting that PAC-induced growth inhibition is *Pp*DELLA-independent. Indeed, PAC treatment did not enhance *Pp*DELLA protein accumulation in the current work, supporting this hypothesis. Collectively the above observations suggest that canonical GA signalling is not present in *P. patens* and that diterpene signalling is uncoupled from *Pp*DELLA signalling.

This conclusion is further supported by the fact that no GID1 orthologues are encoded by the *P. patens* genome (Hernández-García *et al*., 2019), making it less likely that an analogous signalling pathway operates in moss. It is however possible that a different receptor is present in the *P. patens* genome that detects a different molecule triggering *Pp*DELLA degradation. One candidate for such a molecule is 3OH-KA, which is the final product in the *P. patens* diterpene biosynthesis pathway (Miyazaki *et al*., 2018). An attempt was made to get hold of this diterpene, however it was not available during the course of this project. In the future, it would be useful to test *Pp*DELLA stability under treatment with 3OH-KA in the presence or absence of

CHX, or test *Pp*DELLA and *Pp*GLP1 interaction in the presence of this diterpene, to test the possibility that it can regulate DELLA signalling in *P. patens*.

Furthermore, *Pp*DELLA proteins show increased levels of accumulation after treatment with the 26 proteasome inhibitor MG132, which mirrors the behaviour of *At*DELLA under treatment with MG132 in Arabidopsis (Feng *et al*., 2008). However, *Pp*DELLAs are not degraded by CHX treatment, even after 18 hours of incubation. This allows us to speculate that, unlike their angiosperm orthologues, *Pp*DELLAs are not directly regulated by the 26S proteasome, and that the effect seen by MG132 on *Pp*DELLA stability is probably indirect. This suggests that either proteasome-induced DELLA degradation evolved after the divergence of mosses or it was present in the earliest common ancestor of land plants and was then lost in mosses. Both hypotheses are supported by the fact that no *At*SLY1 orthologue is present in the *P. patens* genome (Hernández-García *et al*., 2019); although it is possible that a completely novel E3 ligase is responsible for *Pp*DELLA degradation in *P. patens*.

In order to provide more support for these conclusions in the future, it would be desirable to repeat the CHX assays using a *P. patens* line overexpressing *Pp*DELLAs under a native promoter, as well as a line overexpressing an *At*DELLA as a positive control or alternatively using a different chemical that can trigger *Pp*DELLA degradation in combination with CHX. The inducible overexpression system with the *pHSP* promoter was chosen here as a reliable method of protein overexpression in *P. patens*, due to the successful results it previously yielded using the PHYSCODILLO proteins (Moody *et al*., 2016). Indeed, this system enabled transient overexpression of *Pp*DELLA proteins, detectable by western blotting, confocal microscopy, immunoprecipitation and mass spectrometry (see Chapter 4), which may have not

been the case had a native promoter been used instead. However, it would be worth repeating the assays with a native promoter, to eliminate any unprecedented effect of the heat shock procedure on *Pp*DELLA stability. It would also be necessary to monitor *PpDELLA* mRNA levels under treatment with MG132, to ensure the increased *Pp*DELLA protein accumulation is a result of reduced protein degradation and not increased transcription.

Collectively, the results show that DELLA proteins in *P. patens* are regulated differently compared to angiosperm DELLA proteins: they are not degraded by diterpenes, they do not interact with GID1 homologues, they are not directly regulated by the 26S proteasome and they are uncoupled from *P. patens* diterpene signalling. Whether these observations are universal among bryophyte species remains elusive. DELLA degradation assays have not been performed in the liverwort *M. polymorpha* or in hornworts, and yeast two-hybrid assays have shown that among various bryophyte DELLA proteins, only DELLA protein from the hornwort *Nothoceros vincentianus* interacts with *At*GID1 in a GA-dependent manner (Yasumura *et al*., 2007; Hernández-García *et al*., 2019). If DELLA affinity for GID1 homologues is present in hornworts, this suggests that the ancestral land plant DELLA probably possessed GID1 affinity and it was later lost in mosses and liverworts. This is also reflected in the hornwort DELLA domain peptide sequence, as hornworts display a much more conserved DELLA domain – which is required for GID1 interaction – compared to liverworts and the majority of mosses (Hernández-García *et al*., 2019).

Studying how DELLA proteins are regulated in more bryophyte species and whether bryophyte diterpenes synthesised by those species are linked in any way with DELLA proteins, might provide more insights into how universal the present

observations are among bryophyte species and whether these features are representative of the biology of the most recent common ancestor of land plants.

3.15.3 Flowering plant DELLA responses to stress signals are not conserved in *P. patens*

In silico gene co-expression network analysis involving two flowering plant species, *P. patens* and a green alga identified 'response to stress' as a significantly enriched GO term among the three land plant species, suggesting that this may have been a role of the ancestral DELLA protein that was maintained during land plant evolution (Briones-Moreno *et al*., 2017). This finding led us to investigate whether *Pp*DELLA proteins are involved in the regulation of abiotic stress responses.

The *PpdellaAB* mutant responded to oxidative, saline and desiccation stress conditions similarly to wild-type plants at the vegetative stage, suggesting that responses to these types of stresses in *P. patens* are DELLA-independent. This is supported by Yasumura *et al*. (2007) who showed that *PpdellaAB* mutant protonemata respond to 75mM NaCl similarly to wild-type protonemata. In the present study, 50mM and 100mM were chosen to expand the range used by Yasumura *et al*. (2007), but similar responses were observed. In Arabidopsis, under 100mM NaCl treatment, quadruple *della* mutant seedlings display bigger roots, leaves and fresh weight compared to wild-type seedlings, suggesting that *At*DELLAs promote growth inhibition under salt stress conditions. Similar responses were not observed with the *PpdellaAB* mutant, demonstrating that the function of DELLAs in salt stress tolerance is not conserved in *P. patens*. This is supported by the observation that *Pp*DELLA proteins did not show increased accumulation following treatment with NaCl in the present

study, which is different to the DELLA response in Arabidopsis, where 1-hour treatment with 100mM NaCl promotes increased accumulation of *At*RGA1 (Achard *et al*., 2006).

In the case of oxidative stress, *PpdellaAB* mutant protonemata responded similarly to wild-type protonemata under higher concentrations with MV. This is not surprising as oxidative stress is frequently associated with salt stress (Achard *et al.*, 2008), and as the *PpdellaAB* mutant responded to salt stress similarly to the wild type, the same would be expected for its response to oxidative stress. This is different from *M. polymorpha*, where *Mp*DELLA overexpression enhances recovery from MV-induced oxidative stress conditions (Hernández-García *et al*., 2021). Recovery from MV stress was not assayed in *PpdellaAB*, however, given that all plants were tolerant to 100μM MV treatment, it is expected that they would have been able to recover fine. The above observations suggest that DELLA proteins act via different mechanisms in *P. patens* compared to angiosperms as well as the liverwort *M. polymorpha*. Nevertheless, as there was some variation in the responses of *PpdellaAB* to 1μM MV, it would be worth examining this further in the future, perhaps by including lower concentrations too in the assay, as *P. patens* seems quite sensitive even to 1μM MV.

Regarding desiccation stress, the *PpdellaAB* mutant responded similarly as with saline and oxidative stress. In Arabidopsis and other flowering plants, DELLA overexpression results in enhanced drought tolerance (Wang *et al*., 2020), similar to what has been observed with DELLA and oxidative stress in *M. polymorpha* (Hernández-García *et al*., 2021). The observations that the *PpdellaAB* mutant responds to ABA, which often accumulates in response to various forms of abiotic stress, similarly to wild type and that *Pp*DELLA is not upregulated in response to ABA

as *At*RGA does (Achard *et al.*, 2006), are in line with all other observations suggesting that responses to forms of abiotic stress in *P. patens* are not DELLA-dependent.

There are a number of considerations that should be made at this point. In the present study, the responses to abiotic stresses during vegetative growth were examined, as at this developmental stage, phenotypes are more easily detected. It is possible that during other developmental stages the *PpdellaAB* mutant would display different responses. Furthermore, recovery from stress was not assessed with all types of abiotic stresses, only with desiccation. Looking additionally at recovery from stress would have made the assays more comprehensive. It should also be noted that phenotyping was not exhaustive, as only plant area was measured. More parameters could have been quantified, such as cell size or cell division rate, which would have been more challenging. Despite these method limitations, all assays agree that *Pp*DELLAs are not involved in responses to abiotic stress responses, or if they do, other mechanisms are in place to compensate for DELLA loss of function in the *PpdellaAB* mutant.

In conclusion, the fact that both abiotic stress responses and diterpene responses seem to be DELLA-independent in *P. patens* suggests that *Pp*DELLAs are not functionally orthologous to flowering plant DELLAs, at least regarding these functions. Whether this is universal among bryophytes remains unclear. In *M. polymorpha*, DELLAs regulate oxidative stress responses (Hernández-García *et al*., 2021), which suggests that that either *M. polymorpha* or *P. patens* is not representative of all bryophytes, and that generalisations about functional conservation from studies using single species should be avoided. Studying similar responses in hornworts and other bryophyte species will help to elucidate whether the ancestral DELLA protein

possessed these features as well as how these have evolved in the different bryophyte groups.

3.15.4 Flowering plant DELLA roles in reproductory development appear to be conserved in *P. patens*

One of the most obvious phenotypes of the *PpdellaAB* mutant was its inability to produce big numbers of sporophytes under fertilisation-inducing conditions. In the majority of cases, the mutant did not produce any sporophytes at all, and in some cases it only produced very few that enabled some assays to be executed during the course of the present study. This was not the case for wild-type plants, which produced consistently big numbers of sporophytes, especially when grown on peat plugs. This led us to collaborate with the Rensing lab, who performed a more detailed characterisation of the *PpdellaAB* during reproductive development and concluded that the mutant suffers from a male sterility defect.

The above observation is in line with the roles of DELLA proteins in vascular plants. In Arabidopsis, loss of *AtRGA1* and *AtGAI1* in the Col-0 background induces male sterility due to defective pollen development (Plackett *et al*., 2014). In addition, in barley and rice, loss of DELLA induces male sterility, with barley being unable to produce pollen (Lanahan and Ho, 1988; Ikeda *et al*., 2001). In the fern *Lygodium japonicum*, *Lj*DELLA has been suggested to promote archegonium development (Tanaka *et al*., 2014) and in the lycophyte *Selaginella moellendorfii*, it has been proposed that *Sm*DELLA proteins regulate the development of male reproductive structures (Aya *et al*., 2011). Recently, a role for DELLA proteins in reproductive development has also been reported in non-vascular plants, as DELLA over-

expression in *M. polymorpha* delays the formation of gametangiophores (Hernández-García *et al*., 2021).

These findings propose that across the land plant phylogeny, DELLA proteins are involved in the regulation of reproductive development. This suggests that the ancestral DELLA protein may have had a role in the regulation of reproductive development too. In the future, it would be useful to characterise the molecular mechanism that leads to the induction of male fertility by *Pp*DELLAs in *P. patens*, which may involve interactions with transcription factors. Huang *et al*. (2020) have shown that *At*DELLA interactions with *At*MYB21 and *At*MYB24 is responsible for inhibiting filament elongation. Studying the *PpdellaAB* transcriptome during reproductive development stages would be a good starting point. In fact, analysis of the *PpdellaAB* mutant gametophore transcriptome in the current study has shown that the promoters of *Pp*DELLA-repressed targets have enriched binding sites for a MYB-family transcription factor, which is also a putative *Pp*DELLA interactor based on *Pp*DELLAa immunoprecipitation coupled to mass spectrometry (see Chapter 4). Therefore, studying further the involvement of this transcription factor in moss reproductive development and untangling its involvement in the *Pp*DELLA signalling pathway is important. In addition, examining *Pp*DELLA interactions with transcription factors with putative roles in *P. patens* male fertility regulation, such as *Pp*BELL1 or MADS-box proteins (Meyberg *et al*., 2020) would be sensible.

CHAPTER 4: Proteomics and transcriptomics reveal insights into DELLA protein-protein interactions

4.1 Introduction

As mentioned in Chapter 1 (section **1.5.4**), flowering plant DELLA proteins function as molecular 'hubs', regulating transcription via different mechanisms. Numerous studies have now been published that characterise DELLA interactions with transcription factors and transcriptional regulators in *Arabidopsis thaliana*, but very few studies have looked at DELLA interactions outside this species. Based on the information gathered from Arabidopsis and a few other flowering plants, such as *Medicago truncatula* and rice, the mechanisms by which DELLA protein-protein interactions regulate transcription can be divided into four categories. These are outlined in the sections below and illustrated in Figure **4.1**.

4.1.1 Sequestration of transcription factors and chromatin remodelling factors

The majority of DELLA protein-protein interactions characterised to date in flowering plants, involve the sequestration of transcription factors, often those that promote growth, thus preventing activation of their downstream target genes (Figure **4.1A**). The PHYTOCHROME-INTERACTING FACTORS (*At*PIFs) were the first transcription factors identified to be repressed via interaction with DELLA proteins, establishing a mechanism by which flowering plants are able to integrate light and GA signaling to regulate hypocotyl elongation (Feng *et al*., 2008; de Lucas *et al*., 2008). According to the characterised mechanism, light activates phytochrome photoreceptors (PHYs), which induce *At*PIF phosphorylation and subsequent degradation via the 26S proteasome, preventing *At*PIF-activated hypocotyl elongation (Park *et al*., 2004; Al-Sady *et al*., 2006). At the same time, light induces a reduction in GA levels that stabilises DELLA proteins (Achard *et al*., 2007) and allows them to

interact with the DNA-binding bHLH domain of *At*PIFs (an interaction that requires the LHR1 domain of DELLA), forming an inactive complex (Feng *et al*., 2008; de Lucas *et al*., 2008). Interaction with DELLA proteins prevents *At*PIFs from binding to G-box elements on promoters of target genes, such as *β-EXPANSIN* and *LIPID TRANSFER PROTEIN3* (*AtLTP3*), which promote GA-induced etiolation in the dark (skotomorphogenesis) (de Lucas *et al*., 2008).

In addition to transcription factors, DELLA proteins can also sequester chromatin remodelling factors to inhibit GA responses. Zhang *et al.* (2014) demonstrated that DELLAs interact with the chromatin remodelling factor PICKLE (*At*PKL) to prevent the latter from binding to transcription factors, such as *At*PIF3 and BRASSINAZOLE-RESISTANT 1 (*At*BZR1), and promoting histone H3 Lysine-27 trimethylation (H3K27me3) on promoters of target genes regulating GA- and brassinosteroid-induced hypocotyl elongation.

The transcription factor sequestration mechanism has also been observed in rice, another flowering plant, where the DELLA protein *Os*SLR1 interacts with NO APICAL MERISTEM 29 (*Os*NAC29) and *Os*NAC31 to prevent binding to *Os*NAC targets such as *OsMYB61*, which induces *CELLULOSE SYNTHASE (OsCESA)* genes that promote secondary wall cellulose synthesis required for internode development (Huang *et al.*, 2015). There is currently limited evidence as to whether the DELLA sequestration mechanism is present outside flowering plants. A recent study in *M. polymorpha* has shown that *Mp*DELLA interacts with *Mp*PIF and that *Mp*DELLA can inhibit the activation of *AtPIF3-LIKE1* (*AtPIL1*), which is an *AtPIF* target, by *MpPIF*, suggesting that the sequestration mechanism is present in *M. polymorpha* too (Hernández-García *et al.*, 2021). Whether the DELLA-PIF interaction and the

sequestration mechanism is also present in other bryophyte model species remains unclear.

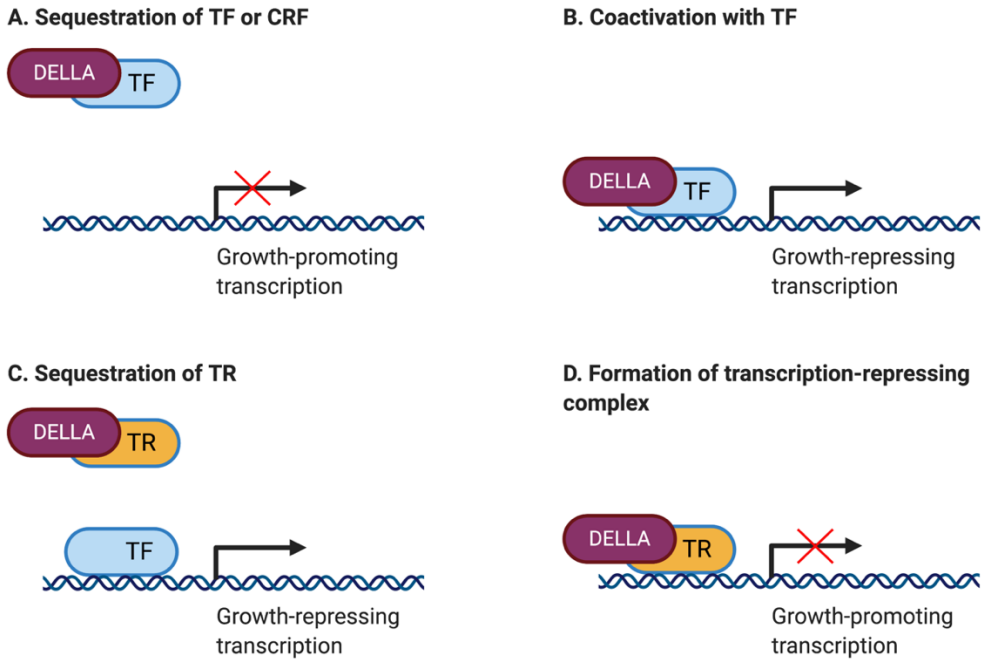

Figure 4.1. The four main mechanisms by which DELLA protein-protein interactions regulate transcription. (A) DELLA proteins sequester transcription factors (TF) or chromatin remodelling factors (CRF) to prevent activation of growth-promoting transcription. **(B)** DELLA proteins bind to transcription factors and coactivate growth-repressing transcription. **(C)** DELLA proteins sequester transcriptional regulators (TR) that repress transcription factors, thus promoting growth-repressing transcription. **(D)** DELLA proteins can form complexes with transcriptional regulators, which inhibit growth-promoting transcription (Figure created with BioRender.com).

4.1.2 Coactivation with transcription factors or regulators

A different mechanism by which DELLAs interact with other proteins is by acting as transcriptional coactivators, activating growth-repressing transcription (Figure **4.1B**). For example, DELLAs bind ABSCISIC ACID INSENSITIVE 3 (*At*ABI3) and *At*ABI5 and coactivate transcription of *SOMNUS* (*AtSOM*), which induces ABA biosynthesis and represses GA biosynthesis, forming a positive feedback loop to inhibit seed germination at high temperatures (Lim *et al*., 2013). DELLAs can also interact

with the transactivation domain of *At*ARR1, enhancing the transactivation of cytokinin-regulated *At*ARR1 targets, reducing the rate of cell division in the root meristem to maintain meristem identity (Marín-de la Rosa *et al*., 2015).

DELLA coactivation of gene expression has also been reported in *Medicago truncatula*, a eudicot flowering plant model species, which forms symbiotic relationships with the nitrogen-fixing bacteria of the genus *Rhizobium*. *Mt*DELLA proteins can interact with the transcription factors NODULATION SIGNALING PATHWAY2 (*Mt*NSP2) and *Mt*NF-YA1 to coactivate the expression of *ETHYLENE RESPONSIVE FACTOR REQUIRED FOR NODULATION1 (MtERN1),* which induces downstream gene expression required for the progression of rhizobial infections (Fonouni-Farde *et al*., 2016).

As the DELLA transactivation ability is conserved at least in members of lycophytes and all three bryophyte groups (Hernández-García *et al.*, 2019), this mechanism of interaction could have been a property of the ancestral DELLA protein. Investigating the transcriptome of bryophyte *della* mutants and looking at targets that are downregulated would be a good strategy to identify potential targets of DELLA transactivation and predicting putative interaction partners.

4.1.3 Sequestration of transcriptional regulators

A third mechanism by which DELLAs interact with other proteins is by sequestering transcriptional regulators to inhibit their repressive function on growth-repressing transcription (Figure **4.1C**). This was first demonstrated with the interaction between DELLA and JASMONATE-ZIM-DOMAIN PROTEIN 1 (*At*JAZ1), a negative regulator of jasmonate (JA) responses (Hou *et al*., 2010). Binding of DELLA to *At*JAZ1

prevents the latter from interacting with *At*MYC2 and repressing *At*MYC2-mediated JA-responsive gene expression regulating root development (Hou *et al*., 2010).

The DELLA-JAZ interaction has also been described in rice (Um *et al*., 2018), but it is unknown if it is conserved outside flowering plants. Given that bryophyte genomes, such as that of *M. polymorpha*, encode orthologs of *At*JAZ1 and *At*MYC2 (Bowman *et al*., 2017), investigating whether *Mp*DELLA interacts with *Mp*JAZ and whether this interaction regulates *MpMYC* transcription, would provide evidence on the presence or absence of the mechanism in bryophytes.

4.1.4 Repression on transcription by complex-formation

DELLA proteins are also able to repress transcriptional activation by acting as parts of transcriptional complexes that repress growth-promoting transcription (Figure **4.1D**). For example, DELLA requires the interaction and formation of a complex with the transcriptional regulator BOTRYTIS SUSCEPTIBLE1 INTERACTOR (*At*BOI), in order to inhibit GA responses such as germination, flowering and juvenile-to-adulthood phase transition via binding to promoters of GA-inducible genes such as *EXPANSIN 8* (*AtEXPA8)*, *PACLOBUTRAZOL RESISTANCE 1* (*AtPRE1)* and *AtPRE5* (Park *et al*., 2013). Regarding the regulation of flowering in particular, studies have shown that the *At*BOI-DELLA complex can delay flowering by targeting the *FLOWERING LOCUS T* (*AtFT)* promoter (Nguyen *et al*., 2015). Since *AtBOI* expression can be induced by *Botrytis cinerea* and *Pseudomonas syringae* pv tomato DC3000 (Luo *et al*., 2010), it is also likely that interaction with DELLA enables the regulation of various plant phase transitions during pathogen attack.

As bryophytes, such as *P. patens,* can be infected by *Botrytis cinerea* (Ponce de León *et al*., 2007; Reboledo *et al*., 2021) and the *P. patens* genome encodes *At*BOI homologs (Rensing *et al*., 2008), it would be interesting to test whether this mechanism and its relevance to pathogen attack is conserved in *P. patens* and other bryophytes.

4.2 Aims and objectives

Given that there is currently no information about DELLA protein-protein interactions in mosses, the aims of work described in this chapter were to identify *Pp*DELLA protein interaction partners and explore the biological significance of those protein-protein interactions using relevant experiments.

4.3 Optimisation of immunoprecipitation coupled to liquid chromatography/ mass spectrometry (IP-MS) protocol for identification of *Pp*DELLA protein-protein interaction partners

In order to identify *Pp*DELLA protein-protein interaction partners, IP-MS was chosen as a well-established *in vivo* method (Budayeva and Cristea, 2014). For this, the *pHSP::PpDELLAa-GFP, pHSP::PpDELLAb-GFP* and *pHSP::GFP* lines described in Chapter 3 were used. 15-day old *P. patens* plants from each of the three lines were heat shocked for 1 hour at 37^{o}C and protein was extracted following a 6-hour incubation period at 22^{o}C to allow protein induction. Tissue from the transgenic lines *pHSP::PpDELLAa-GFP* and *pHSP::PpDELLAb-GFP* that had not been incubated at 37^{o}C was used as a negative control. Following immunoprecipitations using anti-GFP-coupled beads, proteins with the expected size could be detected in the three samples

where expression had been induced by heat shock and not in the two protein extracts from plants with uninduced protein expression (Figure **4.2A**).

Protein extracts from the five samples were then run on two acrylamide gels, one for induced proteins and one for uninduced ones, silver stained, excised from gel and submitted for trypsin digest and liquid chromatography/mass spectrometry (LC/MS) analysis (Figure **4.2B**). Due to gel size restrictions imposed by the local proteomics facility, the acrylamide gels were only run for a short amount of time, until all proteins had entered into the running gel, as observed based on the protein marker.

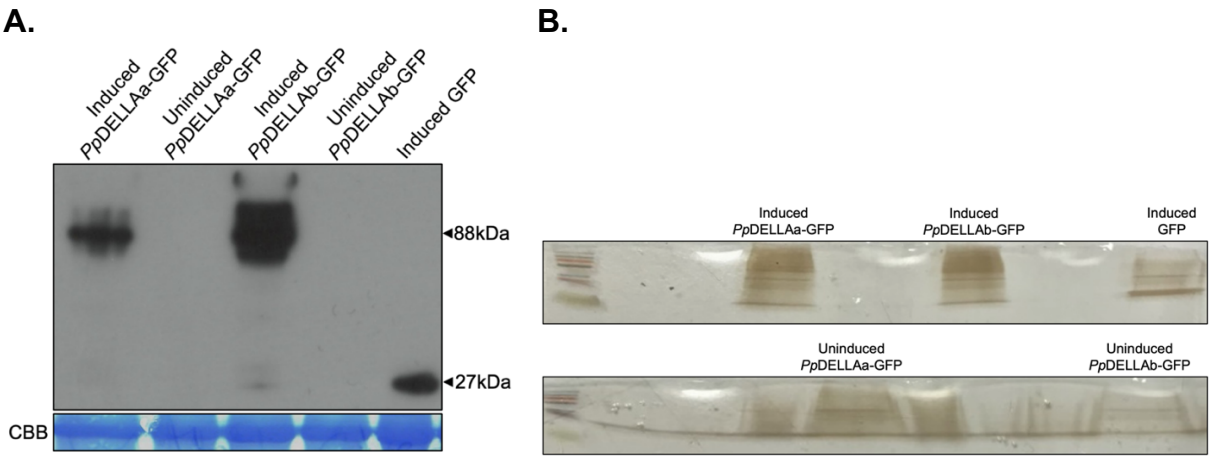

Figure 4.2. First attempt of immunoprecipitation coupled to liquid chromatography/ mass spectrometry (IP-MS) for *Pp*DELLAs using the GFP-trap kit. (A) Anti-GFP western blot showing pull-down of *Pp*DELLAa-GFP (88kDa), *Pp*DELLAb-GFP (88kDa) or GFP (27kDa) proteins induced by incubating for 1 hour at 37°C the transgenic moss lines *pHSP::PpDELLAa-GFP, pHSP::PpDELLAb-GFP* and *pHSP::GFP* (15-day old protonemata) respectively, followed by incubation at 22°C for 6 hours. No protein could pulled down when heat shock was not applied to the moss tissue that was used as a negative control (uninduced expression). 5µl out of 50µl elution was loaded in each well. CBB, Coomassie brilliant blue staining of IP inputs **(B)** Silver stained acrylamide gels with the five protein samples submitted for liquid chromatography/mass spectrometry analysis, before excision from the gel. The five samples contain all the proteins that could be pulled down with the anti-GFP trap from each protein extract. 20µl out of 50µl elution was loaded in each well.

The results of the LC/MS analysis for four out of the five samples are shown in Table **4.1**. One of the five samples (uninduced *Pp*DELLAa-GFP) gave no proteins, perhaps due to suboptimal processing from the proteomics facility, as visible protein bands were present on the silver-stained gel that was submitted for trypsin digestion. The table displays the proteins that were highly abundant in either *Pp*DELLAa-GFP or *Pp*DELLAb-GFP overexpression samples or in both. *Pp*DELLAb was present in all samples, suggesting the occurrence of sample cross-contamination. Due to the fact that contamination was present and a very small number of proteins could be identified by the mass spectrometer in each sample, the experiment was repeated after certain adjustments to the method were made, to enable identification of more putative interactors (see section **4.4**).

Table 4.1. List of putative *Pp*DELLA interaction partners based on first attempt of IP-MS. The table displays putative *Pp*DELLA interaction partners that were found to be abundant in samples where *Pp*DELLAa-GFP and *Pp*DELLAb-GFP were induced and absent in samples where they were not induced or where only GFP protein were induced. Proteins are ranked based on peptide score matches (PSMs), i.e. the number of identified peptide matches. The sample corresponding to uninduced *Pp*DELLAa-GFP could not be analysed by the proteomics facility, despite the presence of visible protein bands on the gel before trypsin digest.

Protein name/description	Accession	Protein Abundance			
		pHSP:: PpDELLAa-GFP (induced)	***pHSP:: PpDELLAb-GFP (induced)***	***pHSP::GFP (induced)***	***pHSP:: PpDELLAb-GFP (uninduced)***
*Pp*DELLAb	A7U4T7	High	High	High	High
*Pp*DELLAa	A7U4T6	High	Not Found	Not Found	Not Found
Predicted protein PHYPA_006565	A9TRK2	High	Not Found	Not Found	Not Found
Chlorophyll a-b binding protein, chloroplastic PHYPA_022864	A9RNP2	High	High	Not Found	Not Found
Chlorophyll a-b binding protein, chloroplastic PHYPA_006353	A9RJS3	High	Not Found	Not Found	Not Found
Predicted protein PHYPA_013696	A9SUK7	High	High	Not Found	Not Found
Photosystem II protein D1 (psbA)	Q6YXN7	High	High	Not Found	Not Found
ATP synthase subunit b, chloroplastic (atpF)	A0A2R2WV43	High	High	Not Found	Not Found
Uncharacterised protein PHYPA_008710	A0A2K1KEX8	Not Found	High	Not Found	Not Found
Predicted protein PHYPA_021401	A9REG3	High	High	Not Found	Not Found
Carbonic anhydrase PHYPA_000833	A9S2F9	Not Found	High	Not Found	Not Found
Eukaryotic translation initiation factor 5A PHYPA_017435	A9T3D3	Not Found	High	Not Found	Not Found
ATP synthase subunit alpha (atp1)	Q1XGA4	Not Found	High	Not Found	Not Found
Uncharacterized protein PHYPA_025076	A0A2K1IV25	Not Found	High	Not Found	Not Found
Non-symbiotic hemoglobin 0 (GLB0)	Q9M630	Not Found	High	Not Found	Not Found
Uncharacterized protein PHYPA_005731	A0A2K1KM28	Not Found	High	Not Found	Not Found
Predicted protein PHYPA_023596	A9SRQ5	Not Found	High	Not Found	Not Found
Photosystem I P700 chlorophyll a apoprotein A2 (psaB)	A0A2R2WW76	Not Found	High	Not Found	Not Found
Photosystem II 22kDa chloroplast protein (PSBS)	A9TJ15	Not Found	High	Not Found	Not Found
Phi class glutathione S-transferase (GSTF1)	A9SCV0	Not Found	High	Not Found	Not Found

Key

*Pp*DELLAs | Pulled down with *Pp*DELLAa only | Pulled down with *Pp*DELLAb only | Pulled down with both

4.4 IP-MS results from optimised protocol show that *Pp*DELLA proteins interact with photoreceptors *in vivo*

To improve the IP-MS protocol, various adjustments to the method were tested. In order to reduce the presence of highly abundant chloroplastic and cytosolic proteins and identify interactors that localise to the nucleus, nuclear fractionation was attempted before carrying out the IP (Figure **4.3**). Despite successful fractionation, evident from western blots using anti-histone-3 antibody (a nuclear marker), *Pp*DELLA-GFP proteins were not enriched in the nuclear fraction, but were more abundant in the cytosolic fraction, probably due to the fact that DELLA proteins do not directly bind chromatin and are therefore easily leaking out of nuclei during fractionation (Figure **4.3**). This suggested that nuclear fractionation could not help to improve the IP-MS protocol.

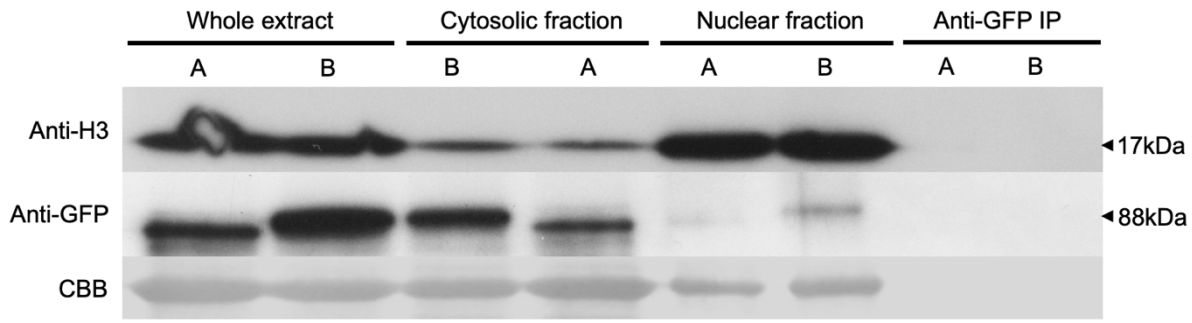

Figure 4.3. Nuclear fractionation and immunoprecipitation (IP) of *Pp*DELLA-GFP for LC/MS analysis. Anti-histone-3 (Anti-H3) shows that nuclear proteins have been enriched in the nuclear fraction, while anti-GFP western blot shows that *Pp*DELLA-GFP is not abundant in the nuclear fraction nor it is enriched after IP. A, *Pp*DELLAa-GFP, B, *Pp*DELLAb-GFP. CBB, Coomassie brilliant blue staining.

In order to improve the elimination of non-specific protein binding that may have been masking true interactors in the first IP-MS attempt, two main amendments were made to the protocol for analysis of whole cell extracts. First, following

immunoprecipitation, the pulled-down proteins were washed with high salt concentration (400mM) buffers. In addition, the samples were run for a longer time period on the acrylamide gel and each sample was excised into two pieces, which were both submitted separately for LC/MS analysis (Figure **4.4**). This time, *Pp*DELLAb-GFP samples were not used to avoid potential cross-contamination of samples. Instead, induced and uninduced *Pp*DELLAa-GFP samples were used, as well as induced GFP (Figure **4.4**). Two gel pieces were submitted for trypsin digest and LC/MS for each sample and all 6 samples were analysed separately.

A.

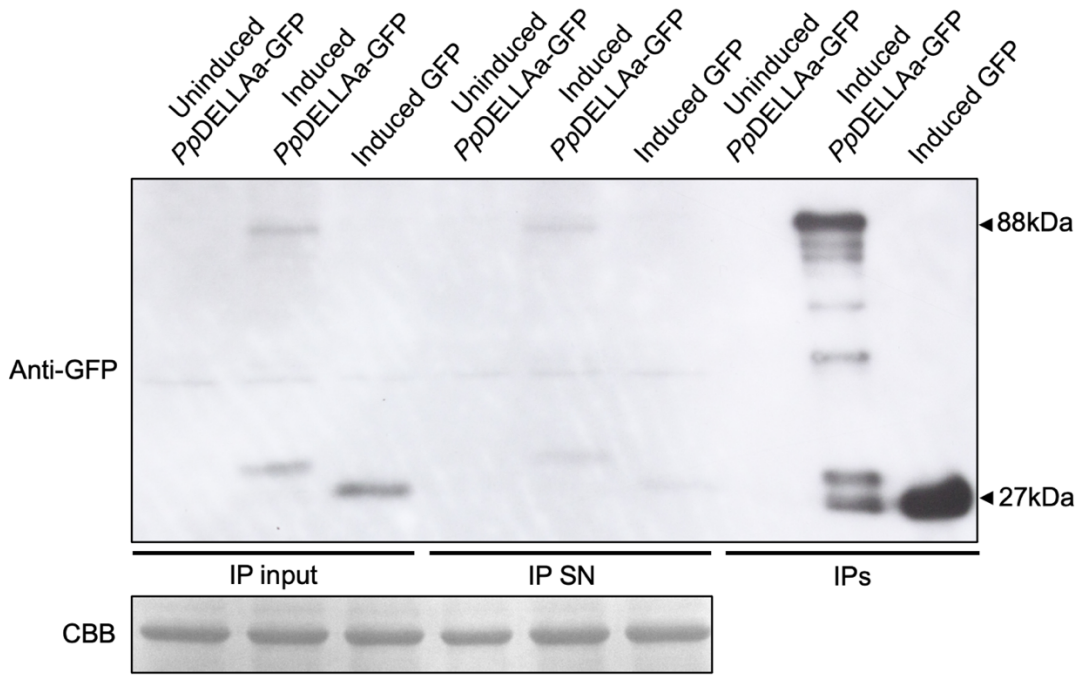

B.

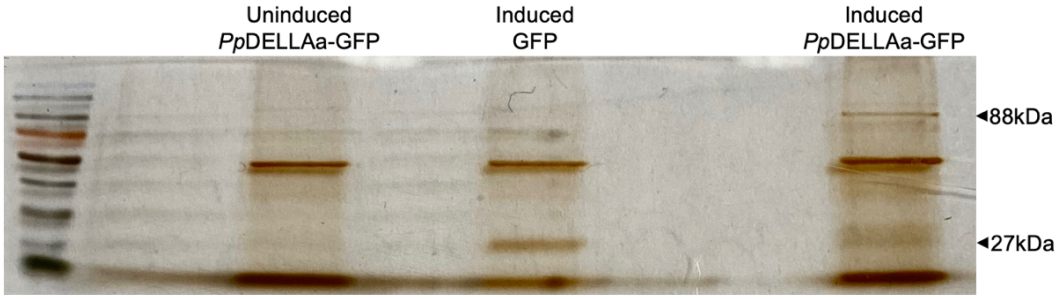

Figure 4.4. Immunoprecipitation coupled to liquid chromatography/mass spectrometry (IP-MS) for identification of *Pp*DELLA protein-protein interaction partners using the GFP-trap kit. (A) Anti-GFP western blot showing pull-down of induced *Pp*DELLAa-GFP (88kDa), uninduced *Pp*DELLAa-GFP, and induced GFP (27kDa) proteins. Induction was achieved by incubating for 1 hour at 37°C the transgenic moss lines *pHSP::PpDELLAa-GFP* and *pHSP::GFP* (17-day old protonemata), followed by incubation at 22°C for 6 hours. No protein could pulled down when heat shock was not applied to the moss line *pHSP::PpDELLAa-GFP* that was used as a negative control (uninduced expression). IP SN, IP supernatant. CBB, Coomassie brilliant blue staining of IP inputs and supernatants. **(B)** Silver stained acrylamide gel showing immunoprecipitation of induced or uninduced *Pp*DELLAa-GFP and induced GFP protein using anti-GFP-coupled beads. The bands for *Pp*DELLAa-GFP (88kDa) and GFP (27kDa) are marked with arrows. Each sample was excised into two pieces; the non-specific band present in the middle of all three samples was used as a reference for splitting the samples into a top and a bottom part.

Analysis of the induced *Pp*DELLAa-GFP immunoprecipitation identified 1013 proteins with a protein False Discovery Rate (FDR) of ≤1% as putative *Pp*DELLAa-GFP interactors. To isolate *Pp*DELLAa-specific putative interactors from the analysed datasets, the proteins identified in the uninduced *Pp*DELLAa-GFP and induced GFP sample that were present in the induced *Pp*DELLAa-GFP sample dataset (total of 605) were removed (Figure **4.5A**). This left 408 unique proteins identified as putative *Pp*DELLAa interactors. For those 408 proteins, GO term enrichment was performed using the Gene Ontology AmiGO database (Figures **4.5B**). Among the GO terms for biological process with the highest fold enrichment was 'chromophore-protein linkage', which was of particular interest, as *At*DELLAs interact with *At*PIFs to regulate responses to light (Figure **4.5B**) (Feng *et al*., 2008; de Lucas *et al*., 2008). Response to abiotic stimulus, which is a key biological function of flowering plant DELLAs, was also enriched, however, this was expected due to the nature of the overexpression protocol, which involved application of a heat shock. The most enriched GO term was 'tRNA aminoacylation for protein translation'.

In addition, GO terms for cellular component did not include the nucleus (Figure **4.5B**), even though the majority of DELLA functions characterised to date involve regulation of transcription. This is probably attributed to the fact that transcription factors are not very abundant in the cell and are therefore less likely to be detected by the mass spectrometer due to masking by the more highly abundant proteins (Smaczniak *et al.*, 2012). Instead, GO terms for membrane coat were enriched, while GO terms for molecular function pointed towards roles in primary metabolism and ligase activity (Figure **4.5B**).

As mentioned earlier, due to the involvement of flowering plant DELLAs in light signalling, the GO terms for ‘chromophore-protein linkage’ were explored further. The ‘chromophore-protein linkage’ dataset included two blue light photoreceptors: PHOTOTROPIN A2 (*Pp*PHOTA2) and *Pp*PHOTB1 and a red/far-red light photoreceptor: PHYTOCHROME 5B (*Pp*PHY5B) (Figure **4.5C**). This was very interesting because (i) photoreceptors are transcriptional regulators and (ii) flowering plant DELLA proteins and PHYs are known to interact with PIFs, however no DELLA-PHY interaction has previously been described.

A.

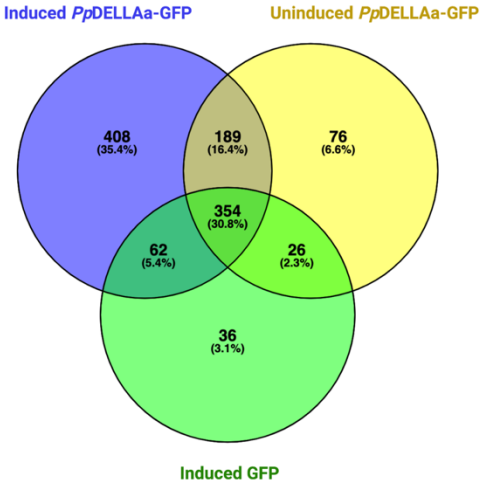
Induced PpDELLAa-GFP
Uninduced PpDELLAa-GFP
Induced GFP
408
(35.4%)
189
(16.4%)
76
(6.6%)
354
(30.8%)
62
(5.4%)
26
(2.3%)
36
(3.1%)

B.

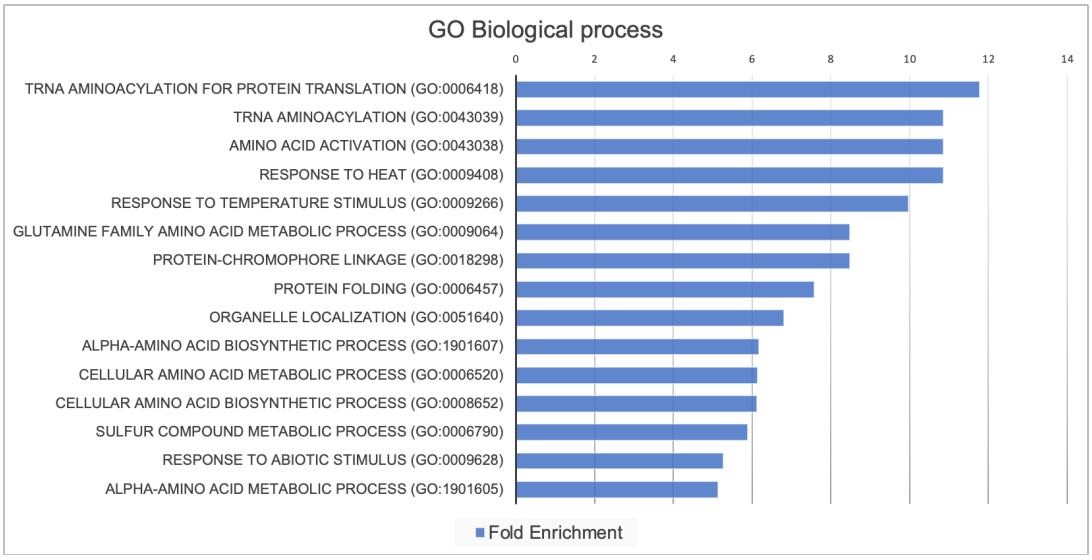
GO Biological process
0
2
4
6
8
10
12
14
TRNA AMINOACYLATION FOR PROTEIN TRANSLATION (GO:0006418)
TRNA AMINOACYLATION (GO:0043039)
AMINO ACID ACTIVATION (GO:0043038)
RESPONSE TO HEAT (GO:0009408)
RESPONSE TO TEMPERATURE STIMULUS (GO:0009266)
GLUTAMINE FAMILY AMINO ACID METABOLIC PROCESS (GO:0009064)
PROTEIN-CHROMOPHORE LINKAGE (GO:0018298)
PROTEIN FOLDING (GO:0006457)
ORGANELLE LOCALIZATION (GO:0051640)
ALPHA-AMINO ACID BIOSYNTHETIC PROCESS (GO:1901607)
CELLULAR AMINO ACID METABOLIC PROCESS (GO:0006520)
CELLULAR AMINO ACID BIOSYNTHETIC PROCESS (GO:0008652)
SULFUR COMPOUND METABOLIC PROCESS (GO:0006790)
RESPONSE TO ABIOTIC STIMULUS (GO:0009628)
ALPHA-AMINO ACID METABOLIC PROCESS (GO:1901605)
Fold Enrichment

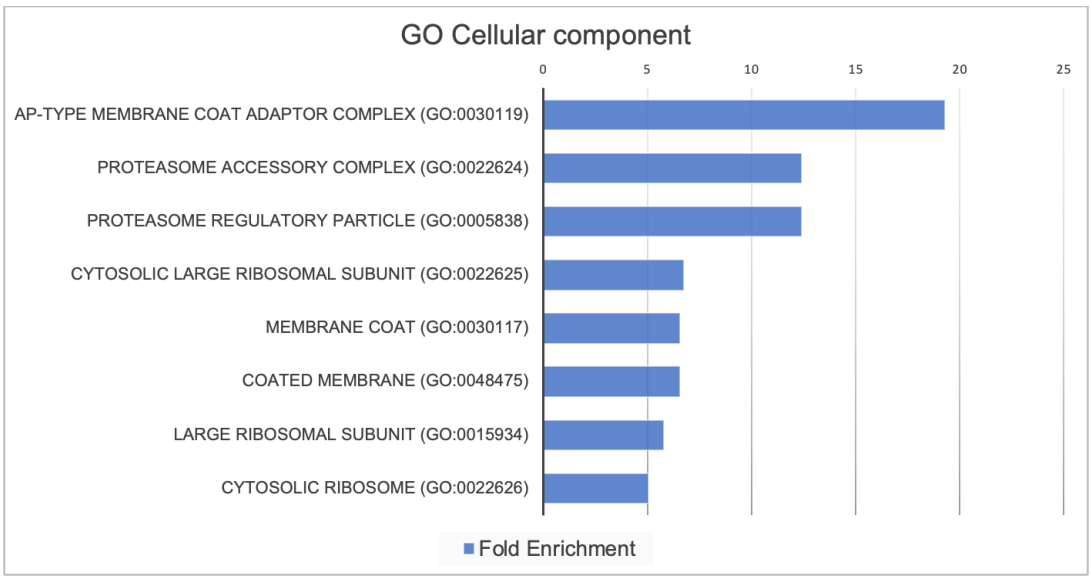
GO Cellular component
0
5
10
15
20
25
AP-TYPE MEMBRANE COAT ADAPTOR COMPLEX (GO:0030119)
PROTEASOME ACCESSORY COMPLEX (GO:0022624)
PROTEASOME REGULATORY PARTICLE (GO:0005838)
CYTOSOLIC LARGE RIBOSOMAL SUBUNIT (GO:0022625)
MEMBRANE COAT (GO:0030117)
COATED MEMBRANE (GO:0048475)
LARGE RIBOSOMAL SUBUNIT (GO:0015934)
CYTOSOLIC RIBOSOME (GO:0022626)
Fold Enrichment

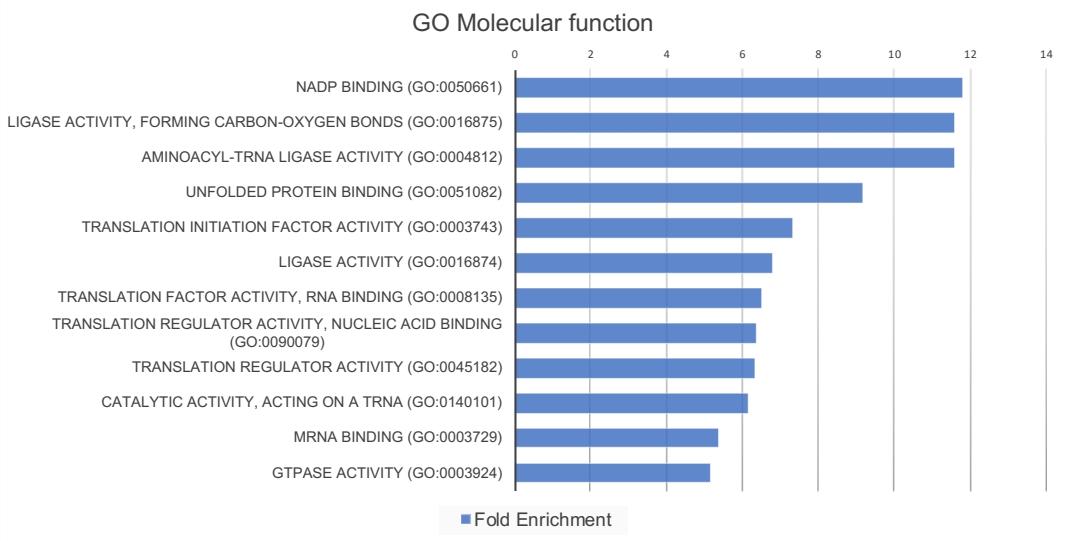

C.

	Uniprot Accession	Phytozome Accession	Gene name	PANTHER family/subfamily
1	A0A2K1IB10	Pp3c27_7010	Chlorophyll a-b binding protein, chloroplastic	PHOTOSYSTEM I CHLOROPHYLL A/B-BINDING PROTEIN 3-1, CHLOROPLASTIC (PTHR21649:SF14)
2	Q6BCU0	Pp3c21_21410	Phototropin A2 blue light photoreceptor	FLIPPASE KINASE 1-RELATED (PTHR45637:SF22)
3	A0A2K1K0D5	Pp3c10_25371	Chlorophyll a-b binding protein, chloroplastic	PHOTOSYSTEM I CHLOROPHYLL A/B-BINDING PROTEIN 2, CHLOROPLASTIC (PTHR21649:SF80)
4	Q6YXM8	Pp3c21_5650	Photosystem II CP47 reaction center protein	PHOTOSYSTEM II CP43 REACTION CENTER PROTEIN (PTHR33180:SF7)
5	A9SLL8	Pp3c12_9240	Phytochrome 5B	PHYTOCHROME B-RELATED (PTHR43719:SF12)
6	Q6BCT8	Pp3c2_10380	Phototropin B1 blue light photoreceptor	FLIPPASE KINASE 1-RELATED (PTHR45637:SF22)
7	A0A2K1IQV9	Pp3c21_5650	CYTB_NTER domain-containing protein	CYTOCHROME B (PTHR19271:SF16)
8	A0A2K1IZ77	Pp3c19_20900	Chlorophyll a-b binding protein, chloroplastic	CHLOROPHYLL A-B BINDING PROTEIN 3, CHLOROPLASTIC (PTHR21649:SF7)

Figure 4.5. IP-MS results for *Pp*DELLAa-GFP reveal putative interactions with photoreceptors. (A) Venn diagram showing the number and percentage of common and unique proteins identified in each of the three immunoprecipitated samples: induced *Pp*DELLAa-GFP, uninduced *Pp*DELLAa-GFP or induced GFP (Figure created with Venny [Oliveros, 2007-2015] and edited with BioRender.com). **(B)** GO term enrichment analysis (with ≥5-fold enrichment) for biological process, cellular component and molecular function, performed in the Gene Ontology AmiGO database using the PANTHER overrepresentation test. The Fisher's exact test was used with Bonferroni correction. **(C)** GO biological function 'chromophore-protein linkage' (GO:0018298) proteins immunoprecipitated with *Pp*DELLAa contain three photoreceptors.

4.5 *Pp*DELLAs interact directly with photoreceptors in yeast cells in a chromophore- and light-independent manner

To complement the IP-MS results, *Pp*DELLA interactions with photoreceptors were also tested using the yeast two-hybrid system. *Pp*DELLAa and *Pp*DELLAb previously cloned in pGADT7, fused with the GAL4 activation domain (AD) and a HA

tag (Yasumura *et al*., 2007), were tested for interaction with *Pp*PHOTA2, *Pp*PHOTB1 or *Pp*PHY5B, which were cloned during the course of this project in pGBKT7, fused with the GAL4 DNA-binding domain (DBD) and a MYC tag. Both *Pp*DELLAa and *Pp*DELLAb interacted directly with *Pp*PHY5B in yeast cells and *Pp*DELLAb also interacted with *Pp*PHOTA2 (Figure **4.6A**). No interaction between *Pp*DELLAs and *Pp*PHOTB1 was detected, however this was most likely due to the fact that *Pp*PHOTB1 could not be expressed in yeast cells, evident by the absence of a visible band on an anti-MYC western blot (Figure **4.6B**).

A.

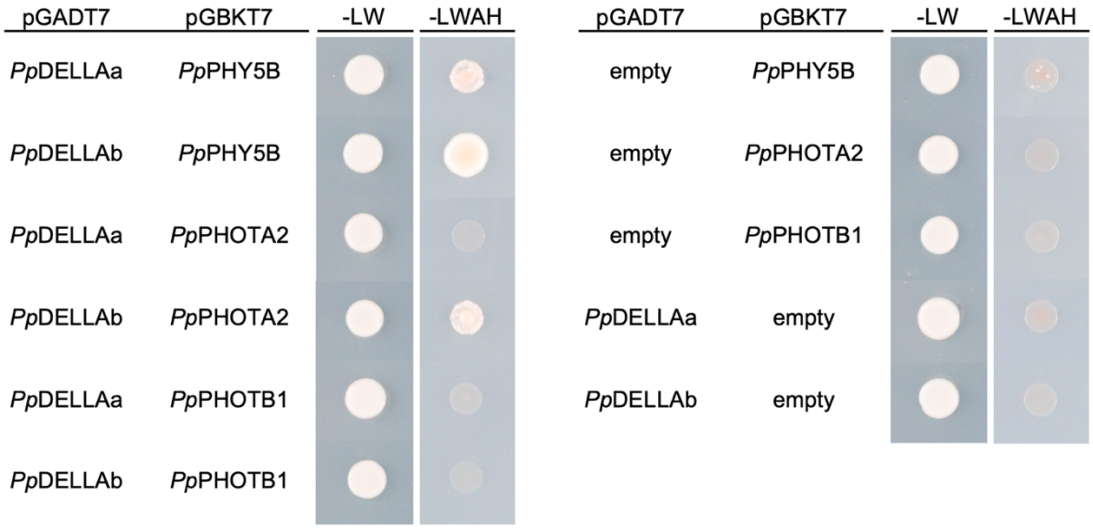

B.

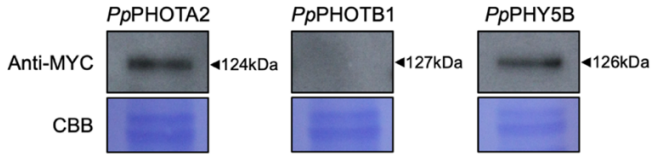

Figure 4.6. *Pp*DELLA proteins interact with photoreceptors in yeast cells. (A) Yeast two-hybrid assay between *Pp*DELLAs fused with the GAL4 activation domain (AD) in pGADT7 and the photoreceptors: *Pp*PHOTA2, *Pp*PHOTB1 and *Pp*PHY5B, fused with the DNA-binding (DBD) domain in pGBKT7. *Pp*DELLAa interacted with *Pp*PHY5B, and *Pp*DELLAb interacted with both *Pp*PHY5B and *Pp*PHOTA2. **(B)** Anti-MYC western blot showing that MYC-tagged *Pp*PHOTA2 (124kDa) and *Pp*PHY5B (126kDa) are expressed in yeast cells, while *Pp*PHOTB1 (127kDa) is not. CBB, Coomassie brilliant blue staining.

To investigate whether *Pp*DELLA interactions with photoreceptors are affected by different light wavelengths, the yeast two-hybrid assays were also performed under red, blue or far-red illumination, or in the dark. Yeast selective media were supplemented with 1μM phycocyanobilin (PCB), the chromophore required for light-induced activation of photoreceptors.

*Pp*DELLAb, which interacted with both *Pp*PHY5B and *Pp*PHOTA2 in the earlier assays, was still able to interact with these photoreceptors in a chromophore- and light-independent manner (Figure **4.7**). As in the earlier assays too, *Pp*DELLAa did not to interact with *Pp*PHOTA2, suggesting that this interaction cannot be potentiated by light, while *Pp*DELLAb did not interact with *Pp*PHOTB1, as expected due to the inability of *Pp*PHOTB1 to be expressed in yeast cells (Figure **4.6B**). These data suggest that *Pp*DELLA interactions with *Pp*PHY5B *or Pp*PHOTA2 may not be relevant to the light-dependent activity of the photoreceptors.

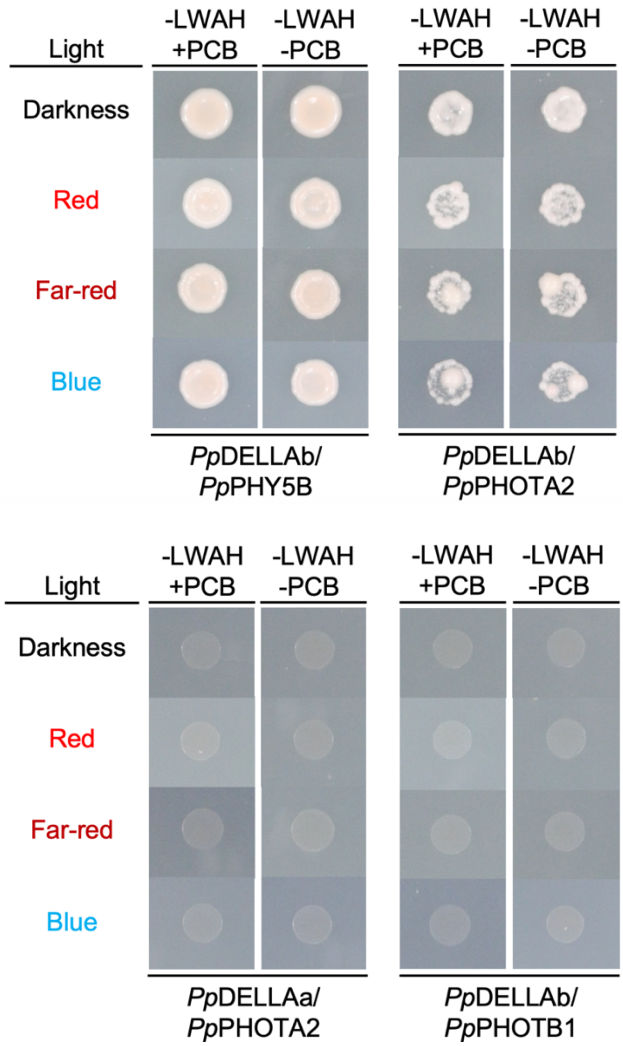

Figure 4.7. *Pp*DELLA proteins interact with photoreceptors in yeast cells in a light- and chromophore-independent manner. Yeast two-hybrid assay between *Pp*DELLAs fused with the GAL4 activation domain (AD) in pGADT7 and the photoreceptors: *Pp*PHOTA2, *Pp*PHOTB1 and *Pp*PHY5B, fused with the DNA-binding (DBD) domain in pGBKT7, under illumination with different light wavelengths in the presence or absence of chromophore (phycocyanobilin, PCB; 1µM). *Pp*DELLAb interacted with both *Pp*PHY5B and *Pp*PHOTA2 in a light- and chromophore-independent manner (top panel), while *Pp*DELLAa-*Pp*PHOTA2 and *Pp*DELLAb/*Pp*PHOTB1 did not interact under any light wavelength and in neither the presence nor the absence of the chromophore (bottom panel). Red, 640-695nM, 5µmol$m^{-2}s^{-1}$; Far-red, 730nM, 3µmol$m^{-2}s^{-1}$; Blue, 445-490nM, 5µmol$m^{-2}s^{-1}$.

4.6 The *PpdellaAB* mutant responds to different light wavelengths similarly to wild type

To investigate further whether *Pp*DELLAs are involved in light responses in *P. patens*, *PpdellaAB* mutant and wild-type protonemata were grown under continuous

illumination from above with red, far-red, blue or white light. The *PpdellaAB* mutant responded to the different light wavelengths tested similarly to wild type (Figure **4.8**). Under red light, protonema development was suppressed, and under far-red light, protonema development was inhibited and gametophores displayed etiolated growth, growing towards the light source (Figure **4.8**). Under blue light, protonema development was promoted at the expense of gametophore development (Figure **4.8**). These observations suggest that in *P. patens*, responses to red, blue and far-red light during vegetative growth are *Pp*DELLA-independent.

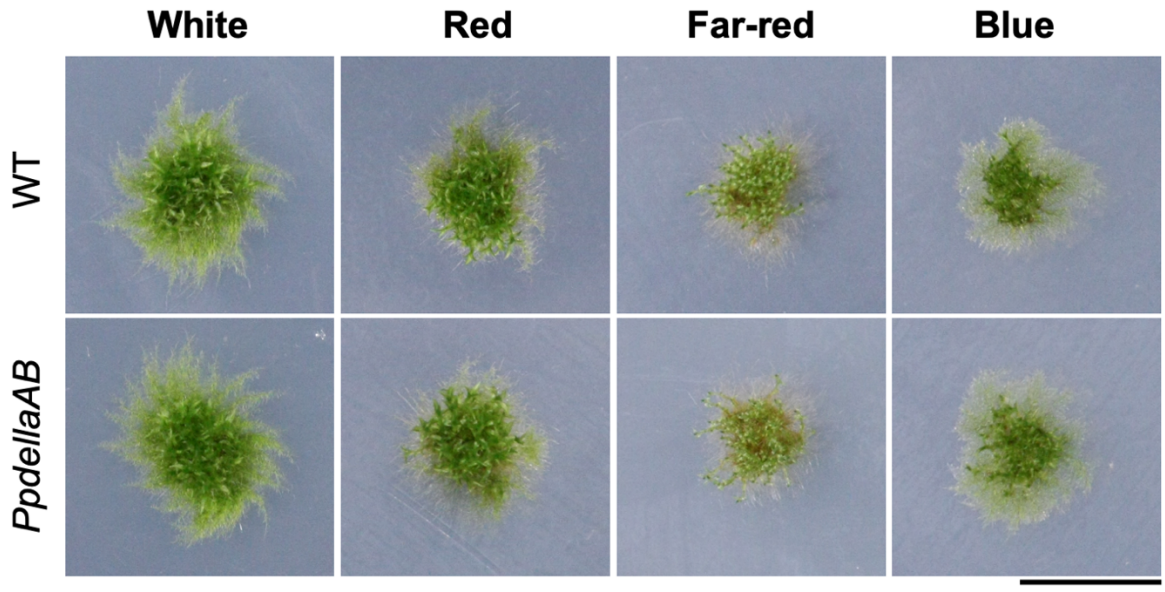

Figure 4.8. The *PpdellaAB* mutant responds to different light wavelengths similarly to the wild type (WT) during vegetative growth. Moss protonemata after 11 days of incubation at 22°C under continuous illumination from above with white light (63μmolm^{-2}s^{-1}), red light (640-695nM; 26μmolm^{-2}s^{-1} intensity), blue light (445-490nM; 16μmolm^{-2}s^{-1} intensity) or far-red light (730nM; 16μmolm^{-2}s^{-1} intensity). Red and far-red light inhibit protonema development, while blue light promotes it at the expense of gametophore development. Far-red light induces etiolated growth in gametophores, which display a 'slender' phenotype, growing towards the light source. Scale bar, 10mm.

The responses of the *PpdellaAB* mutant to red and blue light were also examined at the spore germination stage. It has already been established that blue

light inhibits spore germination in *P. patens*, while red light speeds up the rate of germination compared to white light (Cove *et al*., 1978). Blue light completely inhibited germination in both *PpdellaAB* mutant and wild-type spores, while red light increased the rate of spore germination in the *PpdellaAB* mutant and wild type to a similar extent (Figure **4.9**). These observations suggest that, in *P. patens*, spore responses to red and blue light during germination are *Pp*DELLA-independent.

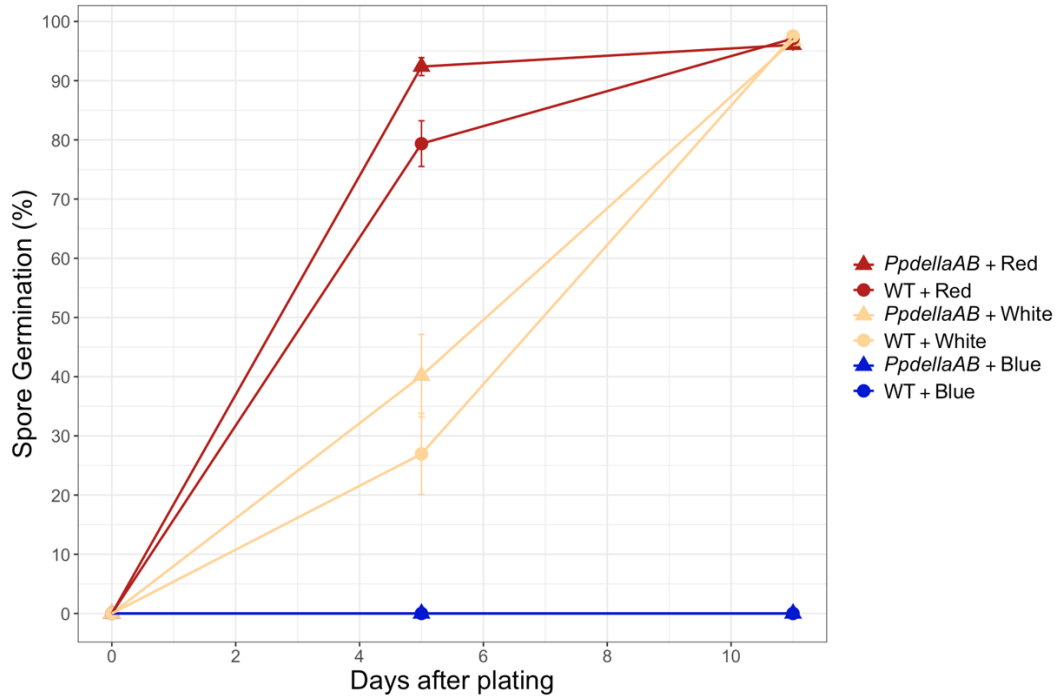

Figure 4.9. *PpdellaAB* mutant spores respond to different light wavelengths similarly to wild-type (WT) spores. Spore germination rate under continuous illumination with white light (63µmolm^{-2}s^{-1}), red light (640-695nM; 26µmolm^{-2}s^{-1} intensity) or blue light (445-490nM; 16µmolm^{-2}s^{-1} intensity) at 22°C. Red light increased the rate of spore germination compared to white light, and blue light inhibited germination. A Kruskal-Wallis test indicates significant differences between *PpdellaAB* + blue light and *PpdellaAB* + red light on day 5 ($p<0.01$), between *PpdellaAB* + blue light and WT + red light on days 5 and 11 ($p<0.05$), between WT + blue light and *PpdellaAB* + red light on day 5 ($p<0.01$), between WT + blue light and WT + red light on days 5 and 11 ($p<0.05$), between WT + blue light and WT + white light on day 11 ($p<0.05$), and between *PpdellaAB* + blue light and WT + white light on day 11 ($p<0.05$). Error bars, ± SEM.

4.7 *PpdellaAB* mutant spores respond to thermoinhibition similarly to wild-type spores

A well-characterised role of phytochromes in Arabidopsis is to function as temperature sensors, with warmer temperatures inducing their conversion into the inactive form (Legris *et al*., 2016). DELLAs are also implemented in high temperature responses: *Atrgl2* mutant seeds show resistance to germination inhibition under high temperatures (thermoinhibition) (Toh *et al*., 2008). At the molecular level, *At*DELLAs coactivate transcription of *At*SOM with *At*ABI3 and *At*ABI5, to induce ABA biosynthesis and inhibit seed germination at high temperatures (Lim *et al*., 2013). Therefore, we sought to investigate whether the *Pp*DELLA-*Pp*PHY5B interaction plays any role in high temperature responses in *P. patens*, using thermoinhibition assays.

PpdellaAB mutant and wild-type spores were incubated at 35°C for 7 days, as it has been shown that spore germination is inhibited by incubation at 35°C (Vesty *et al*., 2016). *PpdellaAB* and wild-type spores were equally thermoinhibited by incubation at 35°C, while spores from the same batch that had been incubated at 22°C for 7 days germinated almost fully (Figure **4.10**). When the thermoinhibited spores were subsequently transferred to 22°C for another 7 days, both *PpdellaAB* and wild-type spores germinated fully (Figure **4.10**). This suggests that spore responses to thermoinhibition in *P. patens* are not *Pp*DELLA-dependent.

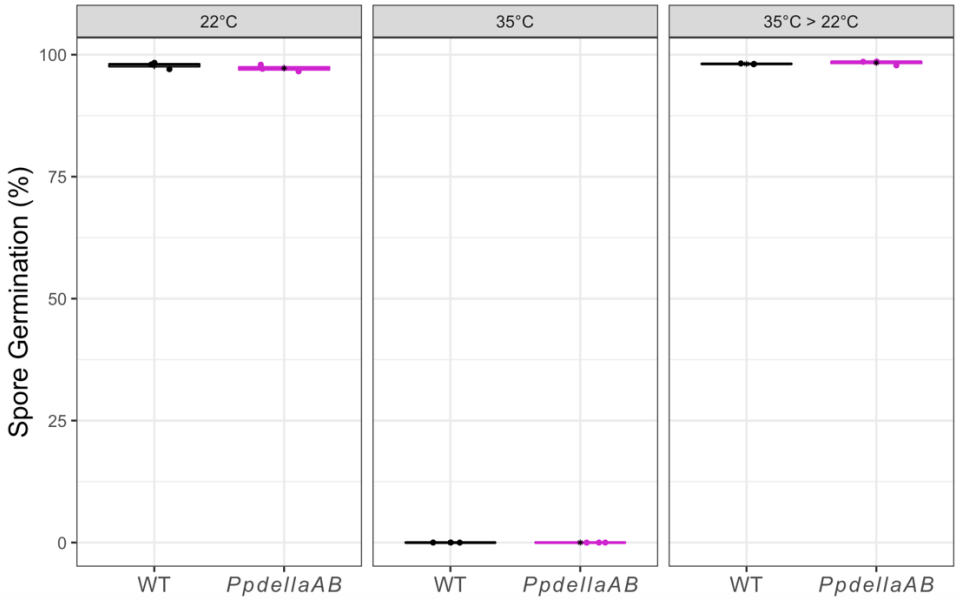

Figure 4.10. *PpdellaAB* mutant spores respond to thermoinhibition similarly to wild-type spores (WT). Spores were incubated at either normal growth conditions (22°C) or thermoinhibitory conditions (35°C) for 7 days. *PpdellaAB* or WT spores at 22°C germinated fully, whereas spores at 35°C did not germinate. Spores at 35°C were then transferred to 22°C for a further 7-day period (35°C > 22°C). *PpdellaAB* or WT spores were able to germinate fully upon transfer to 22°C. Black asterisks indicate the mean.

4.8 Generation of constructs for inducible overexpression of *Pp*PHOTA2 and *Pp*PHOTB1 in *PpdellaAB* protoplasts

In order to examine their localisation in wild-type and *PpdellaAB* mutant protoplasts, *Pp*PHOTA2 and *Pp*PHOTB1 were cloned in the moss transformation vector pHSP::MCS-GFP-108. Due to time limitations, transformation could not be completed, but the vectors can be used in the future to co-transform *P. patens* protoplasts with *pHSP::PpPHOT-GFP* and *pHSP::NLS-mCherry* in order to compare *Pp*PHOT-GFP localisation in wild-type and *PpdellaAB* mutant protoplasts. This will provide information on whether *Pp*DELLAs regulate the localisation of photoreceptors. *Pp*PHY5B could not be ligated with the digested vector during the course of this work despite multiple attempts.

4.9 *PpdellaAB* mutant transcriptomics suggest *Pp*DELLAs function as transcriptional regulators and interact with transcription factors belonging to the same families as angiosperm DELLA interactors

In order to assess whether *Pp*DELLAs function as molecular 'hubs' that regulate transcription, the transcriptome of *PpdellaAB* gametophores was analysed alongside that of wild-type gametophores. This was done in collaboration with the Blázquez lab in the Institute for Plant Molecular and Cell Biology (IBMCP, Valencia). Three biological replicates of age-matched *PpdellaAB* and wild-type sporophytes were isolated and sent to the Blázquez lab, who germinated, cultured them, and extracted RNA from gametophores for sequencing. RNA-sequencing analysis with a cutoff of p-adj<0.01 from the Blázquez lab showed that 783 genes were downregulated in the *PpdellaAB* mutant compared to wild type, suggesting that *Pp*DELLA activity is responsible for inducing them, while 906 genes were upregulated, suggesting that they are repressed by *Pp*DELLAs. Among the most significant enriched GO terms for biological process were 'oxidation-reduction process', 'cell wall organisation and biogenesis' as well as 'single-organism biosynthetic or metabolic process' (Figure **4.11A**). Consequently, 'catalytic activity', 'oxidoreductase activity' and 'monoxygenase activity' were among the most significant enriched GO terms for molecular function (Figure **4.11B**), while 'plastid' and 'chloroplast' were the most significant enriched GO terms for cellular component (Figure **4.11C**).

A. GO Biological process

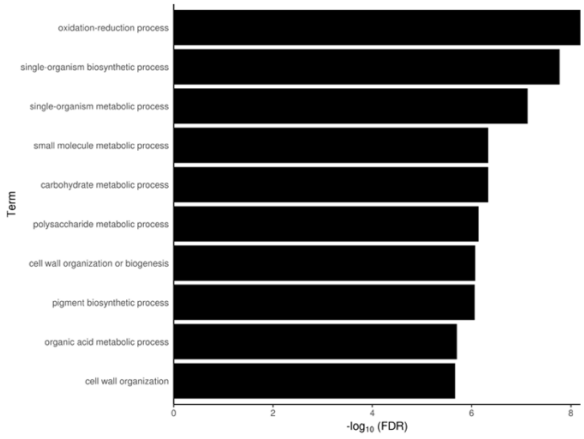

B. GO Molecular function

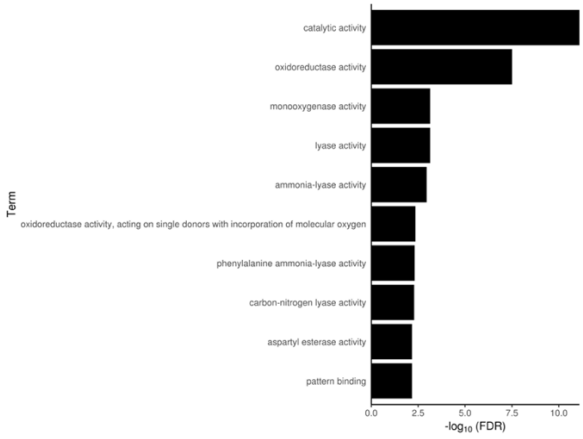

C. GO Cellular component

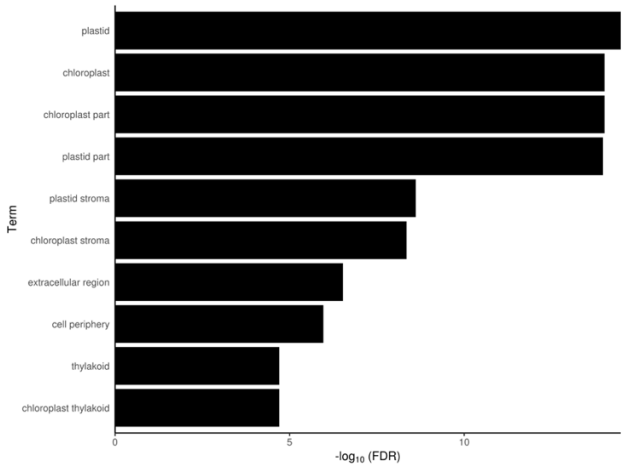

Figure 4.11. GO term enrichment analysis for *PpdellaAB* mutant transcriptome. The ten most over-represented GO terms for biological process **(A)**, molecular function **(B)** and cellular component **(C)**. Analysis was performed in the PlantRegMap website using the topGO package and Fisher's exact test (p≤0.01).

In order to predict possible *Pp*DELLA interactions with transcription factors, a transcription factor enrichment analysis was performed in PlantRegMap, first using only the induced genes and then only the repressed ones. This tested if there was an enrichment in certain transcription factor binding sites among the promoters of the induced or repressed genes. Analysis of the genes induced by *Pp*DELLAs, identified 21 transcription factors with enriched binding sites, which can be considered putative *Pp*DELLA interactors (Table **4.2**). These belonged to the following families: C2H2,

DOF, LBD, bZIP, ERF, C3H, bHLH, SBP, WRKY, G2-like and Trihelix. Analysis of the genes repressed by *Pp*DELLAs, identified 41 transcription factors with enriched binding sites, which can be also considered putative *Pp*DELLA interactors (Table **4.3**). These belonged to the same families as the induced ones: LBD, ERF, bZIP, WRKY, bHLH, C2H2, as well as additional ones: CAMTA, MYB, TCP, NAC, HSF, AP2 and BES1. These results suggest that *Pp*DELLAs, like angiosperm DELLAs, probably function as transcriptional 'hubs' too, regulating transcription via interactions with transcription factors belonging to similar families.

Table 4.2. Transcription factors (TF) with enriched binding sites among promoters of *Pp*DELLA-induced gene targets. Also displayed are Fisher's exact test results, the family that each TF is predicted to belong to and the TF's closest homologue in *Arabidopsis thaliana*.

TF	p_value	q_value	TF Family	Best hit in Arabidopsis
Pp3c11_480	2.54E-07	2.87E-05	C2H2	AT1G72050
Pp3c3_26370	2.83E-04	1.60E-02	DOF	AT3G47500
Pp3c22_5950	1.22E-03	4.61E-02	LBD	AT5G63090
Pp3c21_5710	3.44E-03	8.59E-02	bZIP	AT1G32150
Pp3c5_22280	3.87E-03	8.59E-02	ERF	AT2G40340
Pp3c1_22180	5.32E-03	8.59E-02	C3H	AT3G12130
Pp3c1_22185	5.32E-03	8.59E-02	C3H	AT3G12130
Pp3c11_17710	6.17E-03	8.72E-02	bZIP	AT5G11260
Pp3c10_7030	9.34E-03	1.07E-01	ERF	AT5G25190
Pp3c18_19240	9.51E-03	1.07E-01	bZIP	AT2G35530
Pp3c15_5820	1.11E-02	1.14E-01	bZIP	AT2G18160
Pp3c13_15030	1.21E-02	1.14E-01	bZIP	AT3G10800
Pp3c17_21890	1.63E-02	1.42E-01	bHLH	AT1G09530
Pp3c2_33310	2.33E-02	1.88E-01	ERF	AT5G47220
Pp3c3_31330	3.14E-02	2.16E-01	SBP	AT5G18830
Pp3c3_31350	3.14E-02	2.16E-01	SBP	AT5G18830
Pp3c9_6350	3.25E-02	2.16E-01	bZIP	AT5G28770
Pp3c13_10830	3.73E-02	2.34E-01	WRKY	AT2G44745
Pp3c8_16910	4.43E-02	2.51E-01	G2-like	AT1G32240
Pp3c21_18550	4.44E-02	2.51E-01	Trihelix	AT1G76880
Pp3c15_4480	4.92E-02	2.65E-01	G2-like	AT2G03500

Table 4.3. Transcription factors (TF) with enriched binding sites among promoters of *Pp*DELLA-repressed gene targets. Also displayed are Fisher's exact test results, the family that each TF is predicted to belong to and the TF's closest homologue in *Arabidopsis thaliana*. The TF also present in the *Pp*DELLAa IP-MS dataset is highlighted in yellow.

TF	p_value	q_value	TF Family	Best hit in Arabidopsis
Pp3c8_2690	5.39E-10	6.15E-08	CAMTA	AT2G22300.2
Pp3c23_14630	6.70E-06	3.82E-04	LBD	AT2G30340.1
Pp3c5_880	3.50E-05	9.97E-04	ERF	AT2G33710.1
Pp3c6_28370	3.50E-05	9.97E-04	ERF	AT5G13330.1
Pp3c22_5950	1.20E-04	2.74E-03	LBD	AT5G63090.2
Pp3c19_15700	1.99E-04	3.24E-03	bZIP	AT1G06070.1
Pp3c19_15710	1.99E-04	3.24E-03	bZIP	AT1G06070.1
Pp3c10_7030	3.19E-04	4.54E-03	ERF	AT5G25190.1
Pp3c3_17580	3.82E-04	4.84E-03	MYB	AT1G09770.1
Pp3c3_21440	5.01E-04	5.71E-03	WRKY	AT4G04450.1
Pp3c13_15010	5.66E-04	5.86E-03	bZIP	AT1G75390.1
Pp3c5_22280	7.68E-04	7.13E-03	ERF	AT1G75490.1
Pp3c14_15890	8.13E-04	7.13E-03	bHLH	AT2G24260.1
Pp3c3_24450	1.00E-03	8.18E-03	TCP	AT1G69690.1
Pp3c21_5710	1.15E-03	8.40E-03	bZIP	AT1G32150.1
Pp3c13_10830	1.18E-03	8.40E-03	WRKY	AT2G44745.1
Pp3c13_23600	1.31E-03	8.80E-03	C2H2	AT1G34370.3
Pp3c8_6080	1.58E-03	9.88E-03	NAC	AT5G04410.1
Pp3c18_19240	1.65E-03	9.88E-03	bZIP	AT2G35530.1
Pp3c11_15370	2.06E-03	1.15E-02	bHLH	AT1G32640.1
Pp3c1_32480	2.12E-03	1.15E-02	HSF	AT5G16820.2
Pp3c15_1990	3.80E-03	1.89E-02	ERF	AT5G44210.1
Pp3c17_10170	3.80E-03	1.89E-02	ERF	AT5G44210.1
Pp3c23_21930	4.28E-03	1.93E-02	BES1	AT1G78700.1
Pp3c15_5820	4.34E-03	1.93E-02	bZIP	AT2G18160.1
Pp3c11_17710	4.40E-03	1.93E-02	bZIP	AT5G11260.1
Pp3c6_9520	4.74E-03	2.00E-02	bHLH	AT3G07340.1
Pp3c2_33310	7.46E-03	3.04E-02	ERF	AT5G47220.1
Pp3c17_21890	7.80E-03	3.07E-02	bHLH	AT1G09530.2
Pp3c3_32860	9.00E-03	3.42E-02	WRKY	AT1G69310.2
Pp3c22_1800	1.20E-02	4.40E-02	ERF	AT3G57600.1
Pp3c9_6350	1.23E-02	4.40E-02	bZIP	AT5G28770.1
Pp3c19_20750	1.68E-02	5.80E-02	MYB	AT5G14340.1
Pp3c9_15970	1.84E-02	5.98E-02	MYB	AT5G16600.1
Pp3c9_15975	1.84E-02	5.98E-02	MYB	AT5G16600.1
Pp3c18_9360	2.95E-02	9.35E-02	HSF	AT1G46264.1
Pp3c5_8580	3.08E-02	9.48E-02	ERF	AT5G19790.1
Pp3c7_5230	3.63E-02	1.06E-01	Unknown	N/A
Pp3c1_27710	3.63E-02	1.06E-01	ERF	AT2G33710.1
Pp3c15_4400	3.97E-02	1.13E-01	AP2	AT5G60120.1
Pp3c1_5010	4.44E-02	1.23E-01	ERF	AT4G31060.1

Comparison between all 62 transcription factors with significantly enriched binding sites and the *Pp*DELLAa IP-MS dataset showed that one transcription factor, *Pp*3c3_17580, was present in both datasets. This is predicted to be a MYB-family

transcription factor and is described as a pre-mRNA splicing factor. So, *Pp*3c3_17580 putatively interacts with *Pp*DELLAa *in vivo* and has enriched binding sites among the promoters of *Pp*DELLA-repressed downstream targets. The targets with promoter binding sites for *Pp*3c3_17580 are listed in Table **4.4**. *Pp*3c3_17580 binds targets that are among the *Pp*DELLA-repressed genes in the transcriptomics dataset, which suggests a possible mechanism of sequestration by *Pp*DELLAs to repress downstream gene expression. The putative targets of a possible *Pp*DELLA-*Pp*3c3_17580 interaction are those in table **4.4**, and they need to be studied further to elucidate the mechanism and the biological significance of this interaction.

Table 4.4. *Pp*DELLA gene targets whose promoters have enriched binding sites for the putative MYB-family transcription factor *Pp*3c3_17580. These targets are repressed by *Pp*DELLAs. Log2FoldChange refers to their levels of expression in wild-type gametophores relative to their expression levels in *PpdellaAB* gametophores.

PpDELLA targets	Protein description	log2FoldChange
Pp3c1_19610	Peroxidase	-6.316125993
Pp3c17_20210	B3 DNA binding domain	-5.869181017
Pp3c9_2960	Uncharacterised nodulin-like protein	-3.65088784
Pp3c1_470	Uncharacterised protein	-2.218516654
Pp3c8_1800	Glycosyltransferase family 92 protein	-1.496582354
Pp3c23_1430	Cupin domain	-1.28483673
Pp3c23_1420	Cupin domain	-1.238185168
Pp3c3_36450	Invertase/Pectin methylesterase inhibitor	-1.18335154
Pp3c17_7570	Uncharacterised protein	-0.987471126
Pp3c25_14500	Zinc finger protein-like protein	-0.970154957
Pp3c14_3630	Glutaredoxin-3	-0.948491933
Pp3c26_3030	Exostosin heparan sulfate glycosyltransferase-related	-0.837456529
Pp3c9_15130	L-aspartate oxidase	-0.789275148
Pp3c21_180	Acyl-CoA 11-(Z)-desaturase / Z/E11-desaturase	-0.783784953
Pp3c9_570	Alpha/Beta hydrolase fold-containing protein	-0.738941193
Pp3c1_42420	Uncharacterised protein	-0.705851855
Pp3c11_25530	Elongation factor 2	-0.678398578
Pp3c12_19290	Peroxidase 1-related	-0.671253297
Pp3c20_1460	VQ motif	-0.599942642
Pp3c14_15640	S-type anion channel SLAH2-related	-0.585400533
Pp3c15_5630	Zinc transport protein	-0.58532166
Pp3c10_2210	Sterol 3beta-glucosyltransferase / Glc b1-3 sterol	-0.451676107
Pp3c1_38950	Uncharacterised protein	-0.430710994
Pp3c20_20510	Heat shock 70kDa protein 4	-0.425690711

4.10 Discussion

4.10.1 Summary

In this chapter, a protocol for IP-MS from *P. patens* tissue overexpressing *Pp*DELLAa protein was optimised. Using this protocol, a number of putative *Pp*DELLAa protein-protein interactors were identified, among which some blue or red/far-red light receptors. Yeast two-hybrid assays confirmed the interactions and showed that they are chromophore- and light-independent. In line with this observation, the *PpdellaAB* mutant responded to different light wavelengths similarly to wild-type under different developmental stages. In addition, *PpdellaAB* mutant transcriptomics suggested that *Pp*DELLAs regulate the expression of hundreds of genes and that the promoters of those genes have enriched binding sites for transcription factors belonging to similar families as those of DELLA interactors in Arabidopsis and rice. Interestingly, a MYB-family transcription factor, *Pp*3c3_17580, was identified in both the IP-MS and the RNA-sequencing dataset as a putative *Pp*DELLAa interactor, which makes it an attractive target for future characterisation.

4.10.2 IP-MS is a reliable *in vivo* method for identification of protein-protein interactions in *P. patens*

In this work, IP-MS was chosen as a suitable method for identification of *Pp*DELLA protein-protein interactions. Among the biggest advantages of IP-MS is that it is an *in vivo* method, therefore there is a good chance that the interactions identified are real and not false positives. In addition, it is a non-targeted method that can identify a big number of interactions in a single experiment, and can help to identify multipartite interactions, which is important, as some proteins may only work as part of protein

complexes (Smaczniak *et al*., 2012). On the other hand, IP-MS has several disadvantages that may lead to the identification of false positive interactions. Many of these disadvantages have been addressed in the method design, while others could not be addressed.

A common problem of immunoprecipitations, especially those where polyclonal antibodies are used, is non-specific protein binding (Budayeva and Cristea, 2014). In order to eliminate non-specific binding, high stringency washes were performed following the immunoprecipitation. Furthermore, two negative controls were used: one to control for non-specific binding to the anti-GFP-coupled beads (uninduced *Pp*DELLAa-GFP) and another one to control for non-specific binding to the GFP tag (induced GFP). Another common problem in IP-MS experiments is masking of low-abundance proteins, such as transcription factors, by the more abundant proteins in the protein sample (Smaczniak *et al*., 2012). In order to reduce the masking of the low-abundance proteins, each immunoprecipitated protein sample was split into two parts, which were analysed separately by the mass spectrometer. This provided higher resolution compared to the previous analysis where samples were not split up, and increased the chances of detecting proteins with lower abundance. Furthermore, an attempt was made to improve the identification of low-abundance nuclear proteins using nuclear fractionation; however, this was not suitable for *Pp*DELLAs, as they do not bind chromatin directly and leak out of the nuclear fraction during fractionation.

Some disadvantages of the method that could not be addressed were the fact that the bait protein was expressed ectopically and at very high levels, as a non-native promoter was used, and the protein was tagged with a GFP tag and therefore certain interactions may have been blocked due to the different conformation of the protein

(Guard *et al.*, 2019). An alternative would be to tag the endogenous *Pp*DELLAs with a GFP tag or overexpress *Pp*DELLA-GFP under a native promoter. Both alternatives though risk *Pp*DELLAs not being enriched enough to enable identification of interactors. In addition, due to the high cost of the mass spectrometry analysis, only one replicate per sample was analysed, so the confidence of the results would have been greater had more replicates been used.

Despite these disadvantages, 408 proteins were identified as putative *Pp*DELLAa interactors. Some of the those, *Pp*PHY5B and *Pp*PHOTA2, could be validated using an independent method in a different biological system, where *Pp*DELLAs were tagged on a different terminus (N-terminus) and with a different epitope (HA). Absence of nuclear enrichment did not prevent the identification of one transcription factor predicted to belong to the MYB family, as well as a C2H2-type domain-containing protein, which, however, could not be assigned to a transcription factor family based on its peptide sequence. An alternative method suitable for detection of transcription factor interactions would have been to use yeast two-hybrid screening of a *P. patens* cDNA library, however, this was not available. Furthermore, the option of protein-protein or protein-DNA crosslinking, which allows more transient interactions to be maintained, was avoided in this case, as it could have also led to the identification of more false positive interactions (Smaczniak *et al*., 2012).

Overall, the method was optimised to the best possible level under the circumstances and the output appears to be reliable. To the best of our knowledge, this is the first time that this method has been used efficiently to identify protein-protein interactions in *P. patens*.

4.10.3 *Pp*DELLA interactions with photoreceptors are chromophore- and light-independent

Among the most enriched GO terms in the IP-MS dataset was 'chromophore-protein linkage', which included three photoreceptors. This attracted our attention as the involvement of DELLA proteins in light signalling regulation has been well-characterised in Arabidopsis. In light conditions, DELLA proteins are stabilised due to a reduction in GA biosynthesis and an increase in GA catabolism (Achard *et al*., 2007), which allows them to sequester *At*PIFs and repress *At*PIF-induced downstream activation that promotes GA-induced etiolation in darkness (Feng *et al*., 2008; de Lucas *et al*., 2008) or induce 26S-proteasome-mediated *At*PIF degradation (Li *et al.*, 2016). In addition, light activates phytochromes (*At*PHYs) – red light activates *At*PHYB and continuous far-red or red light activates *At*PHYA (Quail *et al*., 1995) – which induce *At*PIF phosphorylation and degradation mediated by the 26S proteasome, thus inhibiting etiolation (Park *et al*., 2004; Al-Sady *et al*., 2006). *At*PIFs interact with both DELLAs and *At*PHYs, but DELLAs do not interact with *At*PHYs (de Lucas *et al*., 2008), nor does their abundance affect the *At*PIF-*At*PHY interaction (Feng *et al.,* 2008). Moreover, DELLA-promoted *At*PIF degradation does not require *At*PHYB, and *At*PHYB-induced *At*PIF degradation does not require DELLAs, suggesting that DELLAs and PHYs regulate PIFs independently (Li *et al.*, 2016). Consequently, a direct interaction between *Pp*DELLAs and *Pp*PHY5B observed in yeast two-hybrid assays was a novel observation in land plants.

The fact that *Pp*DELLAa appears to interact with *Pp*PHY5B *in vivo*, as shown by IP-MS, suggests that the phytochrome is light-activated during the interaction, as plants in the experiment were grown in light conditions. It is intriguing that *Pp*DELLAs

were able to interact with *Pp*PHY5B even in the absence of a chromophore, in yeast cells, where the photoreceptor is inactive. There are a few hypotheses that could explain this observation. The first hypothesis is that *Pp*DELLAs are always bound to *Pp*PHY5B, both in the dark and in the light, but under one of the two conditions, other plant proteins, which are not found in yeast cells, are recruited to the complex to repress its function, for example by inactivating the complex, or abolishing the *Pp*DELLA-*Pp*PHY5B interaction, for instance via the involvement of a ubiquitin E3 ligase. An alternative hypothesis is that the *Pp*PHY5B-*Pp*DELLA interaction regulates light-independent functions in *P. patens*, which is supported by our experiments showing that different light wavelengths affect the *PpdellaAB* mutant similarly to wild type. One possibility was that this interaction is involved in the regulation of thermoinhibition, however, the results suggest that this response is *Pp*DELLA-independent.

A study in tomato has previously suggested that *Sl*PHYA regulates carbon flux in the dark by repressing primary metabolic pathways, including the tricarboxylic acid (TCA) cycle, β-oxidation and glycolysis (Carlson *et al*., 2019). This is in line with a study in Arabidopsis, which shows that *At*PHYs are implemented in the regulation of carbon flux (Yang *et al*., 2016). Carlson *et al*. (2019) propose that *Sl*PHYA, perhaps in its inactive state, regulates sugar and lipid breakdown in the dark to conserve energy resources while conditions for photosynthesis are unfavourable. It is possible that in *P. patens*, inactive *Pp*PHY5B promotes a similar response in the dark, forming a complex with *Pp*DELLAs that is chromophore-independent and activates an energy-saving mechanism. This is in line with some of the most enriched GO terms in the *PpdellaAB* mutant transcriptome, which include ‘single organism metabolic process’,

‘carbohydrate metabolic process’, ‘polysaccharide metabolic process’ and ‘small molecule metabolic process’, as well as enriched GO terms in the *Pp*DELLAa IP-MS, such as ‘α-amino acid metabolic process’, ‘cellular amino acid metabolic process’ and ‘glutamine family amino acid metabolic process’, pointing towards the regulation of metabolism by *Pp*DELLAs.

Whether the *Pp*DELLA-*Pp*PHY5B interaction occurs in the cytoplasm or nucleus remains unclear. If the interaction is nuclear, it probably involves interaction with *Pp*PIF proteins too, as *Pp*PIFs have been shown to interact with other *Pp*PHYs (*Pp*PHY1-4) (Possart *et al*., 2017), and *At*PIFs regulate sucrose-dependent growth in Arabidopsis (Stewart *et al*., 2011). In addition, *Mp*DELLA interacts with *Mp*PIF in *M. polymorpha*, suggesting that the interaction might be present in other bryophytes too (Hernández-García *et al.*, 2021). Despite the fact that inactive *At*PHYs localise in the cytosol, localisation studies in *P. patens* suggest that a different phytochrome, *Pp*PHY4, localises in the nucleus even in the dark or under far-red illumination, when the protein is supposed to be in the inactive state (Jaedicke *et al.*, 2012). In addition, *Pp*PHY4 interacts with *Pp*PHOTs *in vivo* in *N. benthamiana* following pre-treatment with far-red light and incubation in the dark (Jaedicke *et al.*, 2012), conditions under which *Pp*PHY4 is inactive, suggesting that inactive PHYs may have physiological roles not yet elucidated. It is also possible that the *Pp*DELLA-*Pp*PHY5B complex is inactive in the dark and only has a physiological role in the light, mediated by interactions with other proteins.

In the future, testing the *Pp*DELLA-*Pp*PHY5B interaction *in vivo* under different light treatments would help elucidate more the biological significance of this interaction. Although this was attempted in the yeast two-hybrid system too, there was no positive

control in the experiment, such as *At*PHYA and FAR-RED ELONGATED HYPOCOTYL1 (*At*FHY1), which interact in red light but not in far-red light, and therefore it is unclear if *Pp*PHY5B was indeed photoactivated by red light in the yeast two-hybrid assay. Also, identifying which *Pp*PHY5B protein domain is necessary for the interaction as well as visualising the localisation of the interaction *in vivo* would provide useful insights into how the biological significance of the interaction. As there are currently no published data on the localisation, or any of the biological roles of *Pp*PHY5B, studying the phenotypes of a *Ppphy5B* mutant would be critical. Phylogenetic studies also suggest that *Pp*PHYs arose by convergent evolution (Li *et al.*, 2015) and it is thus likely that subfunctionalisation has led to the evolution of a novel, very specific function for each one of them. For example, this could be a specific role in reproductive development, in which we have shown that *Pp*DELLAs are involved. Until a *Ppphy5B* mutant is generated, testing whether *Pp*DELLAs interact with any other *Pp*PHYs, for which a lot more is known, could provide more insights into the role of *Pp*DELLA-*Pp*PHY interactions. In addition, investigating a potential *Pp*DELLA-*Pp*PIF interaction is also an important experiment that should be performed in the future.

The observation that *Pp*DELLAs interact directly with *Pp*PHOTA2 and *Pp*PHOTB1 was also a novel finding in land plants. *Pp*PHOTs are involved in chloroplast translocation in response to both red and blue light in *P. patens*: mediating avoidance under high fluence rates, and accumulation under low fluence rates (Kasahara *et al.*, 2004). *Pp*PHOTs (especially *Pp*PHOTA2) also regulate polarotropism and phototropism in red light and not blue light (Jaedicke *et al.*, 2012).

Although they are not red light receptors, *Pp*PHOTs respond to red light possibly downstream of *Pp*PHYs (Kasahara *et al*., 2004).

It has previously been demonstrated that in *P. patens, Pp*PHOTs interact with *Pp*PHY4 at the plasma membrane to regulate the *Pp*PHOT-mediated responses mentioned earlier (Jaedicke *et al.*, 2012). As *Pp*DELLAs interact with both *Pp*PHOTs and a *Pp*PHY, it is possible that *Pp*DELLAs form part of a *Pp*PHY5B-*Pp*PHOT-*Pp*DELLA complex that regulates chloroplast translocation in response to red or blue light, or phototropism and polarotropism in response to red light. As DELLA proteins in Arabidopsis are involved in microtubule organisation via their interaction with PREFOLDIN5 (*At*PFD5) (Locascio *et al.*, 2013), it is possible that *Pp*DELLAs are involved in the above light responses by interacting with proteins regulating components of the cytosketeton. Due to lack of relevant specialised equipment for correct experimental setup, phototropic or polarotropic responses or chloroplast translocation could not be tested in the *PpdellaAB* mutant, but it would be useful to test them in a lab that specialises in light signalling. In the future, it would also be useful to test if the *PpdellaAB* mutant or a *Ppphy5B* mutant shows defects in these light responses under blue or red illumination to provide more support for this hypothesis. In addition, testing the interaction between *Pp*DELLA and *Pp*PHOTA2 or *Pp*PHOTB1 or *Pp*PHY5B using live imaging would provide information about the localisation of the complex and whether localisation is affected by light.

Regarding thermoinhibition, this response in seeds is regulated hormonally via increased ABA biosynthesis and reduced GA biosynthesis (Toh *et al*., 2008). Seed thermoinhibition can be rescued by exogenous application of GA or by ABA biosynthesis inhibition (Toh *et al*., 2012), whereas spore thermoinhibition cannot (Vesty

et al., 2016). Our results demonstrate that apart from diterpenes (Vesty *et al*., 2016), thermoinhibition is also not regulated by *Pp*DELLA proteins, suggesting that in *P. patens,* it is subject to a completely different regulatory mechanism compared to seed plants. These findings do not provide support for any involvement of the *Pp*DELLA-*Pp*PHY5B interaction in spore thermoinhibition regulation.

4.10.4 *Pp*DELLAs most likely act as molecular 'hubs' regulating transcription

In order to assess whether *Pp*DELLAs function as molecular 'hubs' that regulate transcription, the transcriptome of the *PpdellaAB* was analysed in collaboration with the Blázquez lab. Transcription factor (TF) enrichment and TF family prediction suggested that *Pp*DELLA proteins possibly interact with TFs belonging to similar families to those of DELLA interactors in angiosperms to regulate downstream transcription. For example, DELLA proteins in Arabidopsis interact with TFs belonging to the bZIP family to transactivate downstream targets. One such TF is *At*ABI5, which activates seed-germination-repressing transcription at high temperatures (Lim *et al*., 2013). Similarly, TF enrichment suggests that *Pp*DELLAs interact with TFs belonging to the bZIP and other families to induce target genes whose promoters have respective TF binding sites. Regarding the sequestration mechanism, DELLAs in Arabidopsis interact with TFs belonging to the bHLH family for example, such as *At*PIFs, to repress transcription promoting hypocotyl elongation, or TFs belonging to the ERF family, such as ETHYLENE INSENSITIVE3 (*At*EIN3) and EIN3-LIKE1 (*At*EIL1), to prevent transactivation of *HOOKLESS1 (AtHLS1)*, which promotes asymmetric auxin accumulation giving rise to the apical hook (An *et al*., 2012). Similarly, *Pp*DELLAs are predicted to interact with TFs belonging to the bHLH, ERF or other families to repress

downstream expression. Importantly, one of the TFs predicted to interact with *Pp*DELLAs by the TF enrichment analysis, *Pp*3c3_17580, has already been identified as a putative interactor by the *Pp*DELLAa IP-MS experiment, and is predicted to belong to the MYB family.

Several MYB TFs have already been characterised as DELLA interactors in Arabidopsis and rice. For example, *Os*SLR1 interacts with *Os*MYB103-like (*Os*MYB103L) encoded by *CULM EASILY FRAGILE (OsCEF)*, and represses activation of its downstream targets, such as *CELLULOSE SYNTHASE (OsCESA)* genes and *BRITTLE CULM 1 (OsBC1),* which mediate secondary wall cellulose synthesis (Ye *et al*., 2015). *At*DELLAs interact with GLABRA3 (AtGL3), ENHANCER OF GLABRA3 (AtEGL3), and the MYB-family TF GLABRA1 (AtGL1), proteins that form part of the WD-repeat/bHLH/MYB complex to sequester targets responsible for promoting GA- and jasmonate (JA)-induced trichome initiation (Qi *et al*., 2014). In addition, *At*DELLAs interact with *At*MYB21 and *At*MYB24 to repress JA- and GA-induced transcription that promotes filament elongation, thus repressing male reproductory organ (stamen) development (Huang *et al*., 2020). Interestingly, we have observed a male fertility defect in the *PpdellaAB*, which suggests that *Pp*DELLAs may be sequestering *Pp*3c3_17580 to inhibit activation of *Pp*3c3_17580-induced gene expression that promotes male infertility in *P. patens* (Figure **4.12**). Under this hypothetical scenario, loss of *Pp*DELLAs in the *PpdellaAB* mutant allows *Pp*3c3_17580 to induce transcription promoting male infertility, rendering the *PpdellaAB* mutant male infertile.

In the future, it would be useful to confirm that *Pp*DELLAs indeed interact with *Pp*3c3_17580 using more methods, such as yeast two-hybrid or bimolecular

fluorescence complementation (BiFC), and then use ChIP or yeast one-hybrid to test whether *Pp*3c3_17580 can bind promoters of *Pp*DELLA-repressed targets (some of which are actually TFs) that have binding sites for *Pp*3c3_17580. Also, generating a *Pp3c3_17580* mutant and checking for a reduced male fertility phenotype would provide more support for the hypothesis that *Pp*DELLA promotes male fertility via interaction with *Pp*3c3_17580.

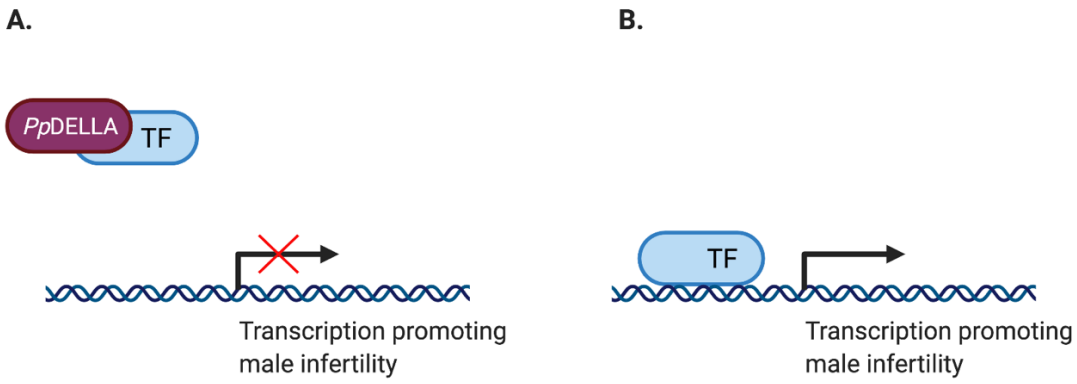

Figure 4.12. Hypothetical model for the interaction of *Pp*DELLA with the putative MYB-family transcription factor *Pp*3c3_17580 (TF). (A) *Pp*DELLA sequesters *Pp*3c3_17580 to prevent the activation of downstream gene expression responsible for male infertility induction. **(B)** In the absence of *Pp*DELLA, *Pp*3c3_17580 activates downstream gene expression promoting male infertility (Figure created with BioRender.com).

Overall, the results from the transcriptomic analysis suggest that *Pp*DELLAs are functioning as transcriptional 'hubs' regulating the expression of hundreds of genes via interactions with transcription factors. Unpublished results from the Blázquez lab using transcriptomic analysis of DELLA-deficient or DELLA-overexpressing plants belonging to different land plant groups, including angiosperms, liverworts and lycophytes, support the hypothesis that the function of DELLAs as transcriptional 'hubs' is universal among land plants. This supports the hypothesis that GA signalling appeared with the evolution of vascular plants, exploiting the transactivation domain of DELLA proteins

to enable DELLA interaction with the GA-GID1 complex, and the pre-existing DELLA-regulated signalling mechanisms to control growth-regulating transcription (Hernández-García *et al.*, 2019).

CHAPTER 5: *Pp*DELLAs and *Pp*DOG1s interact and regulate spore germination

5.1 Introduction

Being the only developmental stage enabling motility, dispersal is an important stage in the life cycle of land plants, ensuring transition to the next generation and survival. In bryophytes, lycophytes and ferns, dispersal is achieved by means of unicellular, haploid spores, whereas in gymnosperms and angiosperms, it is achieved via multicellular, diploid seeds (Linkies *et al*., 2011).

Both dispersal units show similar responses to certain environmental and hormonal stimuli; for example their germination is inhibited by far-red light (Cove, 1978; Seo *et al.*, 2006; Possart and Hiltbrunner, 2013) or high temperature (thermoinhibition) (Toh *et al.*, 2008; Vesty *et al.*, 2016), and both responses are reversible. In addition, ABA can inhibit both spore and seed germination, although much higher concentrations are required for complete inhibition of spore germination (Finkelstein, 1994; Moody *et al*., 2016). Despite some basic similarities, seeds and spores bear big differences, both structurally and physiologically. For example, although GAs are absolutely required for seed germination in flowering plants (Koornneef and van der Veen, 1980), diterpenes promote spore germination in *P. patens*, but are not absolutely required for it, as diterpene-less mutants can germinate fully (Vesty *et al.*, 2016). In addition, seeds show primary dormancy, requiring a period of after-ripening to break it, while spores do not (Vesty *et al*., 2016).

DELLA proteins are among the key transcriptional regulators of seed germination. Lee *et al*. (2002) have shown that the *Atrgl2* mutant is insensitive to PAC-induced inhibition of germination, suggesting that GA-induced *At*RGL2 degradation promotes germination. In line with this observation, loss of *At*RGL2 rescues the repressed seed germination phenotype of the *Atga1-3* (GA biosynthesis) mutant (Lee

et al., 2002). In addition, it has been shown that *At*RGL2 acts by maintaining high levels of ABA in the endosperm (Lee *et al*., 2010), the layer surrounding the seed embryo, and repressing the expression of cell wall remodelling genes, such as *ALPHA EXPANSIN 3 (AtEXPA3)* and *AtEXPA8* (Stamm *et al*., 2012). Consequently, *At*RGL2 inhibits endosperm weakening and embryonic cell elongation, processes regulated by GAs, which are required for seed germination (Weitbrecht *et al*., 2011; Stamm *et al*., 2012). A more recent study has also demonstrated that *At*RGL2 sequesters NAC-family transcription factors, thus repressing the expression of *At*EXPA2, which is involved in GA-induced endosperm cell expansion (Sánchez-Montesino *et al*., 2019). In addition, *At*DELLA proteins interact with ABSCISIC ACID INSENSITIVE 3 (*At*ABI3) and *At*ABI5 to coactivate transcription of *SOMNUS* (*AtSOM*), inducing ABA biosynthesis and repressing GA biosynthesis, to prevent seed germination at high temperatures (Lim *et al*., 2013).

DELLA proteins appear to have a conserved role in germination of dispersal units. Work in the Coates lab has shown that *Ppdella* mutant spores germinate faster than wild-type spores, suggesting that *Pp*DELLAs repress spore germination (Vesty, unpublished). In line with this observation, *Pp*DELLA mRNA levels are high in dry spores, but fall in imbibed spores incubated in growth conditions that favour spore germination, suggesting that during imbibition, *Pp*DELLA-induced germination repression is lifted (Vesty, unpublished). This is similar to the expression pattern of *At*RGL2 in seeds. *At*RGL2 is highly expressed in imbibed seeds incubated at 4^{o}C, an unfavourable temperature for germination, but its expression sharply declines upon transfer to 23^{o}C, an optimal temperature for seed germination (Lee *et al*., 2002).

Apart from DELLA proteins, other key regulators of seed germination related to GA signalling have also been identified in angiosperms. Of particular importance is the quantitative trait locus *DELAY OF GERMINATION-1* (*AtDOG1*), a master regulator of primary dormancy (Bentsink *et al*., 2006). Mutations in *At*DOG1 produce seeds which are non-dormant and therefore do not require after-ripening to break primary dormancy (Bentsink *et al*., 2006). *At*DOG1 inhibits germination at suboptimal temperatures by repressing GA-induced cell wall remodelling proteins participating in endosperm weakening, such as *At*EXPA2 and *At*EXPA9 (Graeber *et al.*, 2014). This suggests that *At*DELLA and *At*DOG1 signalling converge on similar targets. In addition, *At*DOG1 overexpression regulates the expression of *AtGA20ox* in a temperature-dependent manner, decreasing GA biosynthesis and increasing the GA requirement for germination at warmer temperatures (Graeber *et al*., 2014).

*At*DOG1 also interacts with the negative regulators of ABA signalling, ABA-HYPERSENSITIVE GERMINATION 1 (*At*AHG1) and *At*AHG3, inhibiting activation of downstream targets that promote germination (Née *et al*., 2017; Nishimura *et al*., 2018 cite). Although they appear to function in largely independent molecular pathways (Nakabayashi *et al.,* 2012), both ABA and *At*DOG1 are necessary for the induction and maintenance of primary dormancy (Bentsink *et al*., 2006).

Similar to DELLA proteins, DOG1 appears to have a conserved role in regulating the germination of dispersal units. Our collaborators in the Rensing lab (University of Marburg) have identified three DOG1 homologues in *P. patens*, which contain an N-terminal DOG1 domain, regulating dormancy in Arabidopsis, and a C-terminal domain containing ankyrin repeats (Ank), which are known to mediate protein-protein interactions (Vo *et al.*, 2015). One of the three *PpDOG1s* is alternatively

spliced, producing a shorter protein that lacks Ank domains (unpublished data) and resembles *At*DOG1, which also lacks Ank domains. Interestingly, phylogenetic analysis from the Rensing lab has suggested that Ank domains were gradually lost during land plant evolution, as angiosperm DOG1 homologues do not have them, whereas both Ank-domain-bearing and non-bearing DOG1s are found in bryophytes, lycophytes and ferns (unpublished data). In addition, under the conditions tested in the Rensing lab, spores from all three *Ppdog1* single mutants generated displayed faster germination rates compared to wild-type spores of the Reute ecotype (unpublished data). This phenotype is very similar to that observed in the Coates lab with the *Ppdella* mutants.

The facts that (i) *Ppdella* and *Ppdog1* mutants display similar spore germination phenotypes, (ii) *Pp*DOG1s have Ank domains known to mediate protein-protein interactions, and (iii) DELLA proteins are known to function via protein-protein interactions, led us to investigate the possibility that the two proteins regulate spore germination via protein-protein interaction. Therefore, the aims of the work in this chapter were to (i) confirm that *Ppdog1* spores indeed display the same phenotype as *Ppdella* mutants under the Coates lab conditions, (ii) investigate whether *Pp*DOG1 proteins interact with *Pp*DELLA proteins, (iii) test whether the putative interaction is mediated by *Pp*DOG1 Ank domains.

5.2 *Ppdog1* mutant spores germinate faster than wild-type spores

In order to test whether *Pp*DOG1 proteins regulate spore germination, the rate of spore germination of the three *Ppdog1* single mutants generated by the Rensing lab was compared to that of age-matched wild-type spores of the Reute ecotype. Spores

of all three *Ppdog1* mutants germinated significantly faster than wild-type spores at least on days 3-5 post plating (Figure **5.1**). This was very similar to the spore germination phenotype observed with the *Ppdella* mutant spores in the Coates lab, suggesting that *Pp*DELLAs and *Pp*DOG1s may be regulating spore germination via the same pathway.

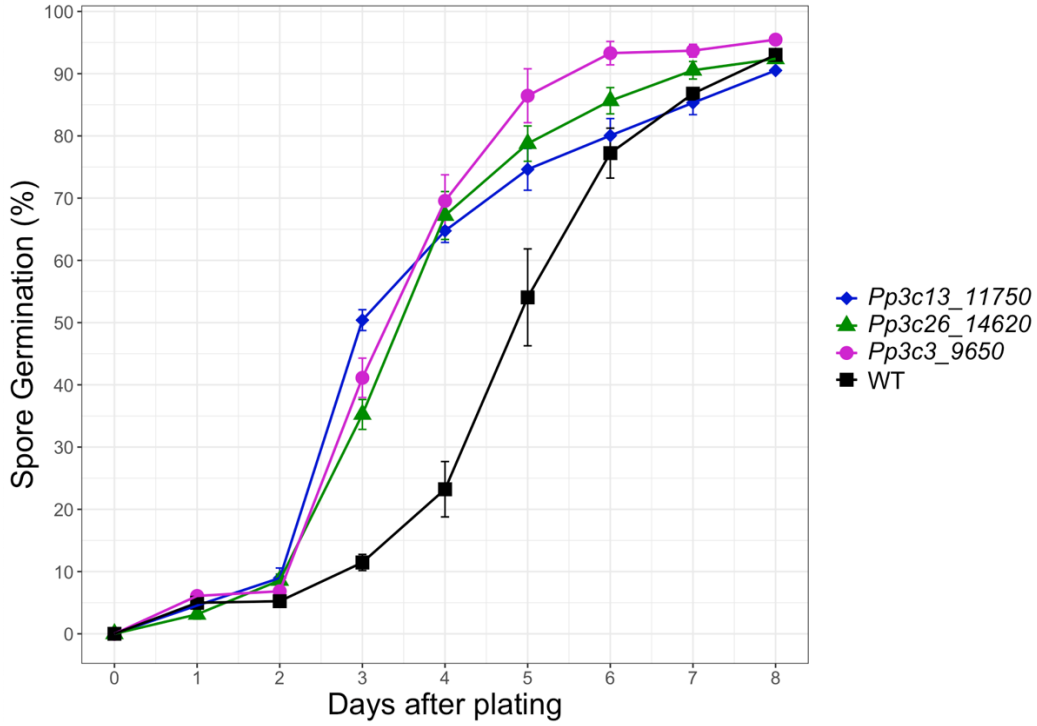

Figure 5.1. Spore germination rate in *Ppdog1* mutants. Single mutant *Ppdog1* spores germinate faster compared to wild-type spores (WT) of the Reute ecotype. Z-tests indicated significant differences in spore germination between *Pp3c26_14620* and WT on days 3-6 ($p<0.00001$), between *Pp3c3_9650* and WT on days 3-7 ($p<0.00001$), and between *Pp3c13_11750* and WT on days 3-5 ($p<0.00001$). Error bars, ± SEM.

5.3 *Pp*DOG1 proteins interact with *Pp*DELLAs in yeast cells

To examine whether *Pp*DOG1s can interact with *Pp*DELLAs, a yeast two-hybrid assay was performed. *Pp*DELLAa and *Pp*DELLAb previously cloned in pGADT7 (Yasumura *et al*., 2007), fused with the GAL4 activation domain (AD) and a HA tag, were tested for interaction with the three *Pp*DOG1s, which were cloned during the

course of this project in pGBKT7, fused with the GAL4 DNA-binding domain (DBD) and a MYC tag. In yeast cells, both *Pp*DELLAa and *Pp*DELLAb interacted with *Pp*3c26_14620 and *Pp*3c3_9650, but not with *Pp*3c13_11750 (Figure **5.2A**). Anti-MYC western blots showed that all three *Pp*DOG1 proteins could be expressed in yeast cells, suggesting that the absence of growth on quadruple selection of yeast co-transformed with *Pp*3c13_11750 and *Pp*DELLAa or *Pp*DELLAb was due to absence of protein-protein interaction and not due to absence of protein expression (Figure **5.2B**). Some autoactivation was observed with *Pp*3c26_14620 in pGBKT7 (Figure **5.2A**), however yeast always grew much more when *Pp*DELLAa or *Pp*DELLAb were co-expressed with *Pp*3c26_14620. These results demonstrate that *Pp*DELLAs interact with *Pp*DOG1 proteins in yeast cells, which provides evidence for them working in the same pathway, possibly to regulate spore germination.

The fact that *Pp*3c13_11750 did not interact with *Pp*DELLAs suggested that it may be missing a domain required for *Pp*DELLA interaction. To investigate this possibility, conserved domain searches for the three *Pp*DOG1 proteins were performed using the Pfam database (v33.1) via the NCBI website with default settings. Pfam search showed that the Ank domains of *Pp*3c13_11750 were different from those of the other two *Pp*DOG1 proteins, containing an Ank_4 superfamily domain instead of a second Ank_2 domain (Figure **5.2C**). This suggested that the Ank domains of *Pp*DOG1 proteins may be determining whether *Pp*DOG1s can interact with *Pp*DELLA proteins.

An attempt was also made to confirm these findings using a Co-IP from *N. benthamiana* leaf protein extracts. *Pp*DOG1 proteins, including the short splicing variant of *Pp*3c26_14620, and *At*DOG1 were cloned with an N-terminal MYC tag in the

binary vector pBI121 for overexpression in *N. benthamiana*, and *Pp*DELLAs were cloned with an N-terminal YFP tag in pEG104. *N. benthamiana* leaves were infiltrated with *A. tumefaciens* overexpressing *Pp*DELLAs and DOG1 proteins, and protein was extracted 3 days after the infiltration. Co-IPs were performed, which showed that YFP-*Pp*DELLA proteins could not be immunoprecipitated due to protein cleavage, evident from multiple bands, including a strong YFP band, on an anti-GFP western blot (Figure **5.3**). This suggested that a different method should be chosen to confirm the interactions *in planta*.

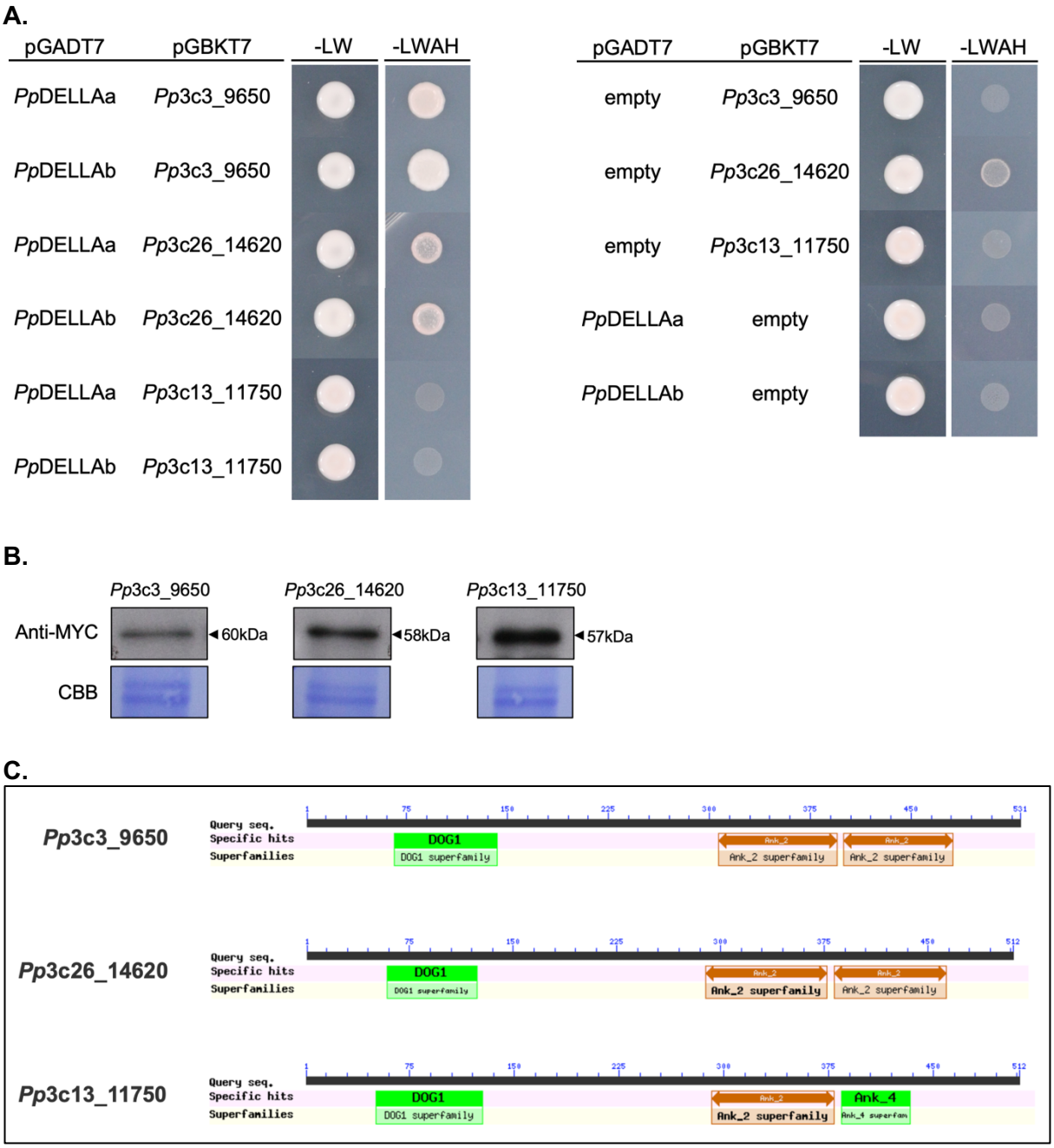

Figure 5.2. *Pp*DOG1 proteins interact with *Pp*DELLA proteins in yeast cells. (A) Yeast two-hybrid assay between *Pp*DELLAs fused with the GAL4 activation domain (AD) in pGADT7 and *Pp*DOG1 proteins: *Pp*3c3_9650, *Pp*3c26_14620 and *Pp*3c13_11750, fused with the DNA-binding (DBD) domain in pGBKT7. *Pp*DELLAs interacted with *Pp*3c3_9650 and *Pp*3c26_14620, and not with *Pp*3c13_11750. **(B)** Anti-MYC western blot showing that MYC-tagged *Pp*3c3_9650 (60kDa) *Pp*3c26_14620 (58kDa) and *Pp*3c13_11750 (57kDa) are expressed in yeast cells. CBB, Coomassie brilliant blue staining. **(C)** Conserved domain search for the three *Pp*DOG1 proteins performed using the Pfam database (v33.1) via the NCBI website with default settings. Pfam search shows that all three *Pp*DOG1 proteins contain the conserved DOG1 domain and ankyrin repeats (Ank) domains, with *Pp*3c13_11750 having an Ank_4 superfamily domain instead of a second Ank_2 superfamily domain. Domain diagrams were taken directly from the NCBI website.

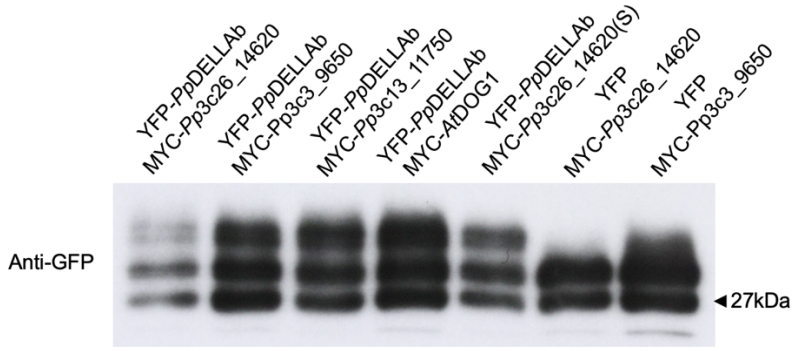

Figure 5.3. GFP immunoprecipitation from protein extracted from *N. benthamiana* infiltrated with *A. tumefaciens* overexpressing *p35S::YFP-PpDELLAb* or *p35S::YFP* and *p35S::MYC-PpDOG1* or *p35S::MYC-AtDOG1*. The three *Pp*DOG1 proteins encoded by *Pp3c3_9650*, *Pp3c26_14620* and *Pp3c13_11750* were used, as well a short splicing variant encoded by *Pp3c26_14620* [*Pp*3c26_14620(S)]. YFP-*Pp*DELLA could not be precipitated due to protein cleavage, evident from multiple bands including a YFP band, on the anti-GFP western blot.

5.4 DELLAs from *P. patens* and *A. thaliana* interact with *Pp*DOG1s but not with *At*DOG1 in yeast cells

To examine whether DOG1 and DELLA proteins from Arabidopsis interact with each other or with the respective *P. patens* homologues, *At*DOG1 was also cloned in pGBKT7, fused with the GAL4 DBD and a MYC tag. *At*RGA1 had previously been cloned in pGADT7 (Yasumura *et al*., 2007), fused with the GAL4 AD and a HA tag. *At*RGA1 did not interact with *At*DOG1 in yeast cells, and neither did *Pp*DELLA proteins, suggesting that the Arabidopsis DOG1 cannot interact with DELLA proteins from across land plant groups (Figure **5.4A**). The expression of MYC-*At*DOG1 in yeast cells was confirmed by western blotting (Figure **5.4B**). Interestingly, *At*RGA1 interacted with both *Pp*3c26_14620 and *Pp*3c3_9650, but not with *Pp*3c13_11750, exactly like DELLA proteins from *P. patens* (Figure **5.4A**). This suggests that despite differences in peptide sequence between *Pp*DELLAs and *At*RGA1, they still share the regions necessary for interaction with *Pp*DOG1s. This does not seem to be the case for *At*DOG1s and *Pp*DOG1s, which appear to have peptide sequence differences that affect their ability

to interact with DELLA proteins. The fact that *At*DOG1, which lacks any kind of Ank domains did not interact with DELLA proteins, provided more support for the hypothesis that Ank domains might be necessary for interaction with DELLA proteins.

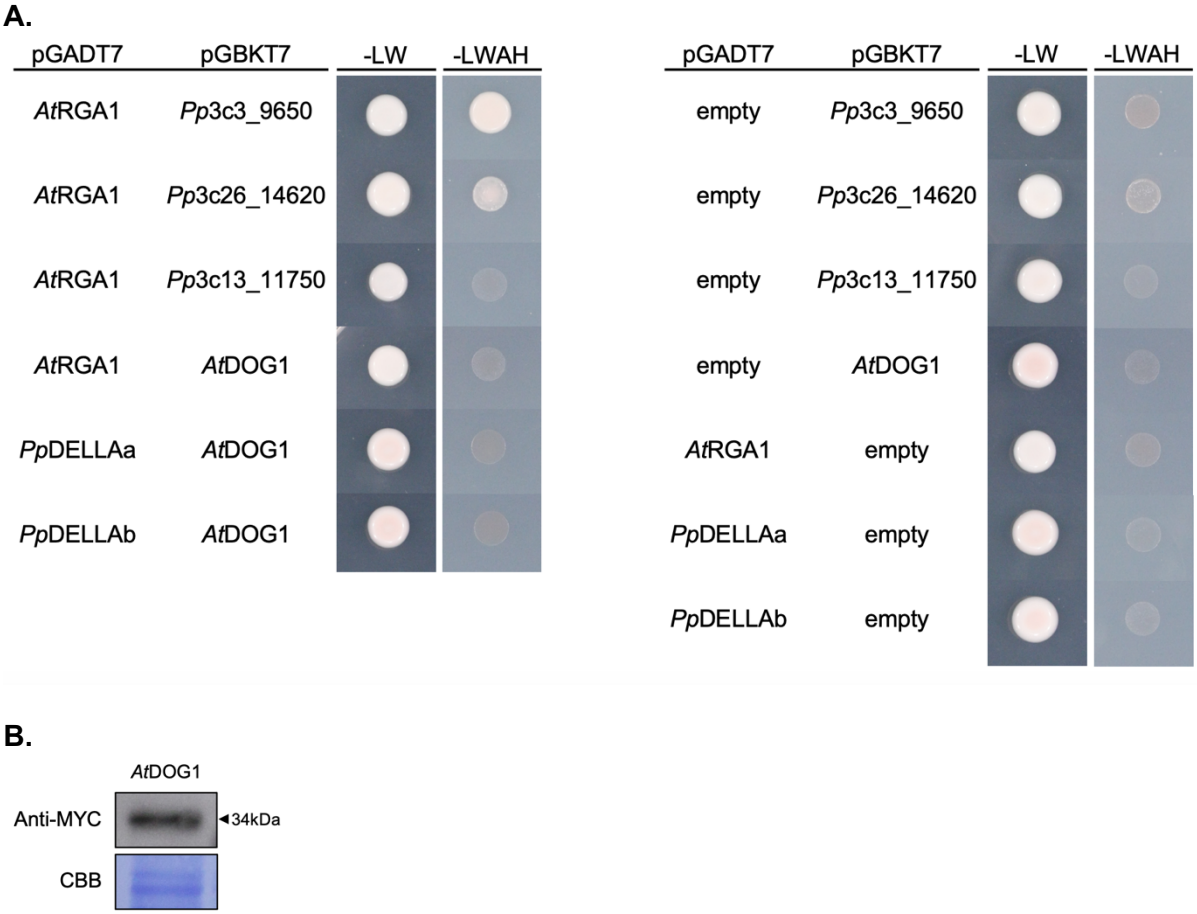

Figure 5.4. Cross-species interaction assay between DELLA and DOG1 proteins. (A) Yeast two-hybrid assay between *At*RGA1or *Pp*DELLAs fused with the GAL4 activation domain (AD) in pGADT7 and *At*DOG1 or *Pp*DOG1 proteins: *Pp*3c3_9650, *Pp*3c26_14620 and *Pp*3c13_11750, fused with the DNA-binding (DBD) domain in pGBKT7. *At*RGA1 interacted with *Pp*3c3_9650 and *Pp*3c26_14620, and not with *Pp*3c13_11750 or *At*DOG1. **(B)** Anti-MYC western blot showing that MYC-tagged *At*DOG1 (34kDa) is expressed in yeast cells. CBB, Coomassie brilliant blue staining.

5.5 The DOG1 domain is necessary and sufficient for interaction with DELLA proteins in yeast cells

To determine whether Ank domains are necessary for DOG1 interaction with DELLA proteins, each of the two *Pp*DOG1s that showed interaction with DELLAs (*Pp*3c26_14620 and *Pp*3c3_9650), were truncated into two parts, to separate the DOG1 domain from the Ank domains (Figure **5.5A**). Uniprot, Pfam, NCBI and SMART databases were all used to predict where each domain is located on the protein and the truncations were designed in regions clearly not defined as DOG1 or Ank by any of the databases, roughly in the middle of the protein (Figure **5.5A**). *Pp*DOG1 truncations were cloned in pGBKT7, fused with the GAL4 DBD and a MYC tag, for yeast two-hybrid assays. Western blotting confirmed that all four MYC-tagged truncations were expressed in yeast cells (Figure **5.5B**).

To our surprise, *Pp*DELLAa and *Pp*DELLAb interacted with the N-terminal truncation containing the DOG1 domain and not with the C-terminal truncation containing the Ank domains (Figure **5.5C**). More specifically, *Pp*DELLAb interacted with the DOG1 domain from both *Pp*3c26_14620 and *Pp*3c3_9650 and *Pp*DELLAa interacted with the DOG1 domain from *Pp*3c26_14620 and not from *Pp*3c3_9650 (Figure **5.5C**). This demonstrates that the DOG1 domain is necessary and sufficient for interaction with *Pp*DELLA proteins. In the case of *At*RGA1, the protein did not interact specifically with any of the two truncations from either *Pp*3c26_14620 or *Pp*3c3_9650, suggesting that neither truncation is sufficient and both are necessary for interaction with *At*RGA1 (Figure **5.5C**).

A.

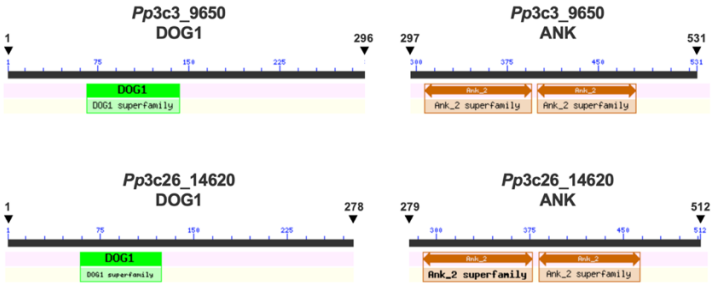

B.

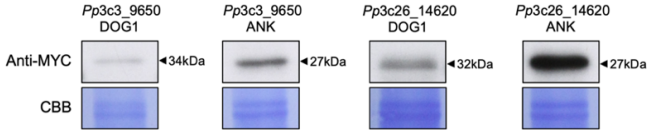

C.

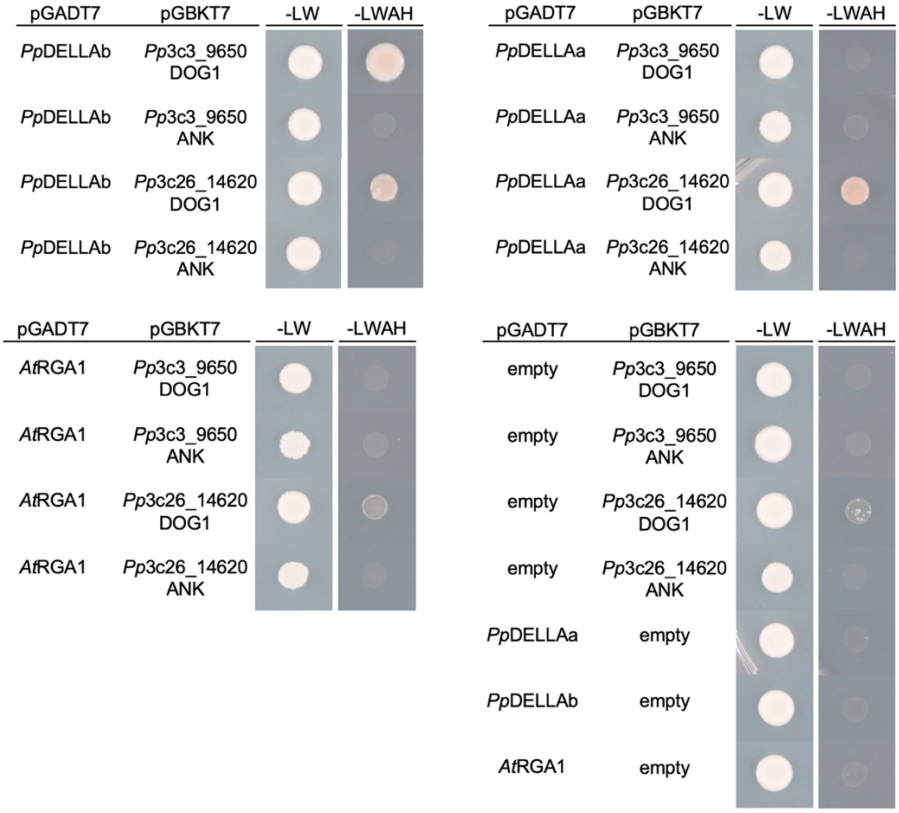

Figure 5.5. The DOG1 domain is necessary and sufficient for interaction with *Pp*DELLAs, but not with *At*RGA1. (A) Diagram showing the truncated versions of *Pp*DOG1s used in the yeast two-hybrid assay. Protein domain diagrams were taken from the NCBI website and modified. **(B)** Anti-MYC western blot showing that MYC-tagged truncated versions of the *Pp*DOG1 proteins encoded by *Pp3c3_9650* and *Pp3c26_14620*. CBB, Coomassie brilliant blue staining. **(C)** Yeast two-hybrid assay between *Pp*DELLAs or *At*RGA1 fused with the GAL4 activation domain (AD) in pGADT7 and truncated *Pp*DOG1 proteins: *Pp*3c3_9650 and *Pp*3c26_14620, fused with the DNA-binding (DBD) domain in pGBKT7. The DOG1 domain is necessary and sufficient for interaction with *Pp*DELLAs, but not with *At*RGA1. DOG1, DOG1 domain; ANK, ankyrin repeats domain.

Alignment of the N-terminal domains of the three *Pp*DOG1 proteins shows that the DOG1 domain is highly conserved, whereas alignment with *At*DOG1 shows that the Arabidopsis DOG1 domain is more divergent (Figure **5.6**). Targeting the residues which are not shared between the DOG1 proteins that show interaction with DELLAs (*Pp*3c26_14620 and *Pp*3c3_9650) and those that do not (*Pp*3c13_11750 and *At*DOG1), could be a good strategy to identify amino acid residues responsible for disrupting the interaction between DOG1s and DELLA proteins.

5.6 Complementation of *At*DOG1 function in *Atdog1-2* mutant by *Pp*DOG1s

To investigate whether *Pp*DOG1 proteins can complement the function of *At*DOG1 in the *Atdog1-2* mutant (Nakabayashi *et al.*, 2012), the CDS of *Pp*DOG1s, including the shorter splicing variant of *Pp*3c26_14620 (where the first twelve bases from the third intron are translated and added to the first three exons), or gDNA from *At*DOG1 were cloned in pBI121 with an N-terminal MYC tag. Col-0 and *Atdog1-2* mutant plants were transformed with pBI121 containing the above constructs or the empty vector. The T1 generation was harvested but due to time limitations could not be screened for presence of the construct by kanamycin selection. These lines will be useful in showing whether *Pp*DOG1 proteins can induce dormancy in Arabidopsis, imposing a requirement of after-ripening in order for germination to proceed.

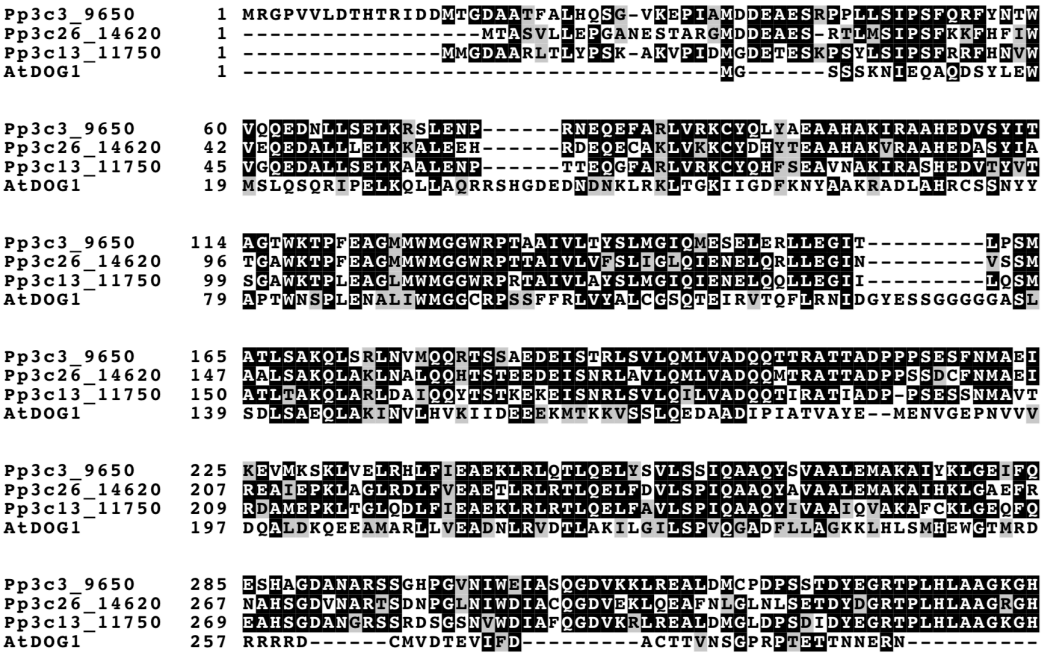

Figure 5.6. Alignment of *At*DOG1 protein with the N-terminal domain of *Pp*DOG1 proteins containing the DOG1 domain. The N-terminal domain is highly conserved among the three *Pp*DOG1 proteins but *At*DOG1 is more divergent.

5.7 Discussion

5.7.1 Summary

In this chapter, it was confirmed that *Ppdog1* mutant spores germinate faster than wild-type spores, similar to the phenotype of *Ppdella* mutant spores. In addition, it was shown that *Pp*DELLA proteins interact with *Pp*DOG1 proteins in yeast cells and that the DOG1 domain is necessary and sufficient for interaction with *Pp*DELLAs. *Pp*DOG1s also interacted with *At*RGA1, however *At*DOG1 did not show interaction with any DELLA protein, suggesting that the DELLA-DOG1 interaction may have been lost during land plant evolution due to DOG1 divergence.

5.7.2 *Pp*DELLA and *Pp*DOG1 proteins interact and regulate spore germination

Yeast two-hybrid assays have shown that *Pp*DELLAs can interact with *Pp*DOG1. As both proteins can regulate spore germination negatively, this suggests that their interaction may be mediating their inhibitory function on spore germination. A similar relationship is observed in Arabidopsis between *At*DELLAs and *At*ABI3 or *At*ABI5, where the two proteins interact to coactivate transcription of *AtSOM* and repress seed germination at high temperatures (Lim *et al*., 2013). Therefore, it is possible that *Pp*DELLAs and *Pp*DOG1s coactivate expression of downstream genes that repress spore germination (Figure **5.7A**). Unlike *At*ABI3 and *At*ABI5, there is no evidence that *At*DOG1 functions as a transcription factor in Arabidopsis, although *At*DOG1 and *At*DOG1-like proteins do share peptide sequence similarity with TGACG motif-binding transcription factors (Sall *et al.*, 2019). Instead, it has been suggested that DOG1 family proteins may be able to regulate transcription by binding to the iron-binding protoporphyrin IX molecule heme, which controls signal transduction among other biological processes (Nishimura *et al*., 2018). Similarly with *At*DOG1, it is unclear

if *Pp*DOG1s can bind DNA directly. Therefore, the *Pp*DELLA-*Pp*DOG1 interaction may involve the formation of a tripartite complex with a transcription factor, which activates spore-germination-repressing transcription (Figure **5.7A**).

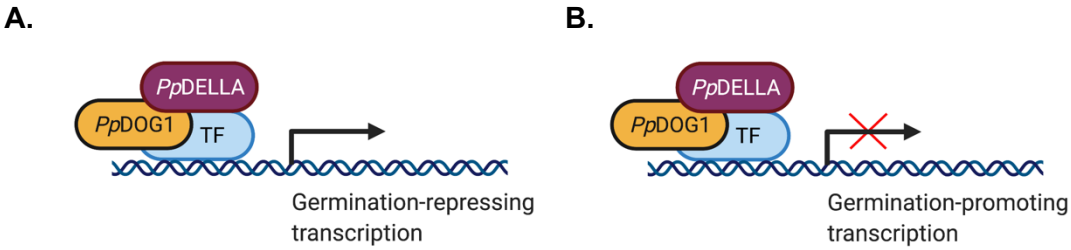

Figure 5.7. Hypothetical models for the putative interaction between *Pp*DELLA and *Pp*DOG1 proteins. (A) *Pp*DELLAs and *Pp*DOG1s form a complex with a transcription factor to coactivate transcription that represses spore germination. **(B)** *Pp*DELLAs and *Pp*DOG1s form a complex with a transcription factor and repress transcription that promotes spore germination (Figure created with BioRender.com).

An alternative model of interaction would be one where *Pp*DELLAs and *Pp*DOG1s form a transcription-repressing complex that binds on promoters of spore-germination-promoting genes to inhibit their activation (Figure **5.7B**). This mechanism of DELLA interaction has been demonstrated in Arabidopsis, where *At*DELLAs form a transcription-repressing complex with BOTRYTIS SUSCEPTIBLE1 INTERACTOR (*At*BOI), inhibiting germination, flowering and juvenile-to-adulthood phase transition by binding to promoters of GA-inducible genes (Park *et al.*, 2013). In the future, it would be useful to study the transcriptome of the triple *Ppdog1* mutant and compare it with that of *PpdellaAB* to identify genes that are either repressed or induced in both datasets. These common genes would be potential targets of co-repression or co-activation by the two proteins. In Arabidopsis, *At*DOG1 represses GA-induced cell wall remodelling proteins regulating endosperm weakening, such as *At*EXPA2 and *At*EXPA9 (Graeber *et al.*, 2014). Interestingly, one of the most enriched GO terms for

biological function in the *PpdellaAB* transcriptome was cell wall organisation and biogenesis (see Chapter 4, figure **4.11**), suggesting that *Pp*DELLAs may be regulating spore germination by inhibiting cell wall remodelling in the spore coat, and that this function might be shared with *Pp*DOG1s. The fact that *PpdellaAB* mutant spores respond to ABA similarly to wild-type spores (see Chapter 3, figure **3.18**), suggests that *Pp*DELLA regulation on germination might be ABA-independent. It is currently, unknown whether *Pp*DOG1s function in an ABA-dependent manner, and this is an area that should be enlightened in the future. In addition, crossing the *PpdellaAB* mutant with a triple *Ppdog1* mutant and looking at the spore germination phenotype could provide more insights into whether the two protein groups function in the same pathway. Furthermore, it would be necessary to confirm the *Pp*DOG1-*Pp*DELLA interaction by an *in vivo* method too, perhaps by Bimolecular Fluorescence Complementation (BiFC) or via Co-IP from tobacco leaf protein, after optimising the protocol to prevent YFP-*Pp*DELLA protein cleavage that was observed during the course of this work.

The fact that the DOG1 domain of *Pp*DOG1s was sufficient for interaction with *Pp*DELLAs suggests that it may be the domain responsible for repression on spore germination. This is analogous to the case in Arabidopsis, where DOG1 is defined as the domain regulating seed dormancy. The fact that DOG1 proteins in *P. patens* and other land plants possess Ank domains, suggests that these proteins may have an additional layer of regulation that possibly involves protein-protein interactions that other DOG1 proteins do not share. Screening the *Pp*DOG1 Ank truncations for interaction with a cDNA library from *P. patens*, could elucidate this additional layer of

*Pp*DOG1 regulation, or suggest novel roles for DOG1 proteins, which could even be unrelated to spore germination.

Regarding cross-species interaction assays, *At*DOG1 did not interact with any DELLA proteins in yeast cells, whereas *At*RGA1 interacted with *Pp*DOG1s. This suggests that the DELLA-DOG1 interaction may have been lost during land plant evolution due to DOG1 divergence. It would be interesting to test whether this interaction takes place in other land plant groups, such as lycophytes or ferns, or whether *At*RGA1 can interact *in vivo* with *Pp*DOG1s overexpressed in Arabidopsis. In addition, examining whether *Pp*DOG1s can complement the function of AtDOG1 in the *Atdog1-2* mutant can provide insights into whether the Arabidopsis molecular machinery can respond to *Pp*DOG1s.

CHAPTER 6: Discussion

6.1 Using *P. patens* to answer evolutionary biology questions

In the previous decades, *P. patens* had been the only bryophyte with a sequenced genome and for this reason it attracted the attention of evolutionary biologists studying the evolution of land plants. For many years, there was a view that *P. patens* and other bryophytes have not changed much since they first diverged and thus can be considered 'living fossils' or 'basal' land plants. This view has lately been challenged and it is now acknowledged that bryophytes have most probably been evolving for more generations than angiosperms and therefore the terms 'basal' or 'early-diverging' are inaccurate (McDaniel, 2021). Nevertheless, comparative studies remain one of the key tools we have in order to generate evolutionary biology hypotheses, as long as we interpret their results with caution.

In this work, DELLA functions in *P. patens* were characterised, in order to infer what properties of DELLA proteins may be common in different land plant groups and what properties might be unique to moss DELLA proteins. Such comparisons allow us to infer what features of the proteins may have always been under selection and what features may have been lost or gained at different timepoints during land plant evolution. In addition, identification of universal properties of DELLA proteins can enable us to reconstruct the biochemical profile of the ancestral DELLA protein and suggest possible reasons why DELLA proteins evolved in the most recent common ancestor of land plants.

6.2 Divergent roles of *Pp*DELLAs in *P. patens*

Among the key properties of DELLA proteins in angiosperms are GA-induced degradation (Fu *et al.*, 2002), germination and growth repression (Lee *et al.,* 2002;

Peng *et al*., 1997), and regulation of stress responses (Colebrook *et al.,* 2014). In this work, we have shown that DELLA proteins in *P. patens* cannot be degraded by diterpenes, neither can they interact with *At*GID1 homologues in a diterpene-dependent or independent manner, at least *in vitro*. Furthermore, PAC treatment did not induce *Pp*DELLA-GFP accumulation in *P. patens*, and spore germination assays suggested that GA_9-ME-induced promotion of spore germination is *Pp*DELLA-independent. The above observations, along with the fact that *PpdellaAB* mutants respond to PAC-induced growth inhibition similarly to the wild-type (Yasumura *et al*., 2007), provide no evidence that diterpene signalling in *P. patens* is related to *Pp*DELLA signalling. Although the fern antheridiogen GA_9-ME can promote growth responses in *P. patens*, it most likely acts independently of *Pp*DELLAs, perhaps by being perceived by *P. patens* as one of its endogenous diterpenes. This supports the hypothesis that GA signalling evolved with the appearance of bioactive GAs in the ancestor of vascular plants and not earlier (Yasumura *et al.*, 2007; Hernández-García *et al.*, 2019).

Although *Pp*DELLAs are orthologous to angiosperm DELLA proteins, work from the present study and Yasumura *et al.* (2007) agree that *Pp*DELLAs do not regulate vegetative growth, at least under the conditions tested. Furthermore, *Pp*DELLAs do not regulate responses to stresses, such as oxidative, salt or desiccation stress, which is not in agreement with *in silico* analyses by Briones-Moreno *et al.* (2017) proposing that *Pp*DELLAs function in stress response regulation. This is different from what has been observed in Arabidopsis (Colebrook *et al.,* 2014) or even in *M. polymorpha*, where *Mp*DELLA overexpression enhances recovery from oxidative stress (Hernández-García *et al*., 2021). Therefore, although it can be hypothesised that DELLA proteins evolved in the most recent common ancestor of land plants because

they conferred resistance under conditions of oxidative or other forms of stress, the current work from *P. patens* does not provide support for this hypothesis. Nevertheless, it does not disprove the hypothesis that DELLA proteins may have contributed to the transition to land by promoting stress resilience. As mentioned earlier, it is not wise to generalise from observations from only one or two bryophyte species. The fact *Mp*DELLA and *Pp*DELLAs may not be regulating similar responses highlights that DELLAs in each bryophyte species have been under different forms of selection during million years of evolution and may have developed different characteristics that are not universal among other bryophytes or even the most recent common ancestor of land plants. It is for this reason that studying a wider variety of bryophyte species, including representatives from the hornwort family, will allow for more robust hypotheses to be generated regarding the evolution of DELLA proteins within the land plant lineage.

In addition, a novel interaction for DELLA proteins has been identified in this study: the direct interaction with photoreceptors of the phytochrome and phototropin families. Given that this type of interaction has not been observed in Arabidopsis or other angiosperms, and that phytochromes and phototropins have emerged by convergent evolution in the different land plant groups (Li *et al.*, 2015), it is likely that these interactions are unique to *P. patens* and perhaps other mosses too. The biological significance of these interactions could not be elucidated in the present study, however, more suggestions could be made with the future generation of a *Ppphy5B* mutant. Given the results of our experiments, it is likely that this interaction regulates light-independent functions.

6.3 Conserved roles of *Pp*DELLAs in *P. patens*

Despite the divergent roles of *Pp*DELLA proteins identified in this work, a number of conserved roles have also been observed both in the current report and in previous studies from the Coates lab. These include the involvement of *Pp*DELLA proteins in the regulation of germination and reproductive development.

Regarding the regulation of germination, evidence has been gathered that this may be achieved via interaction with *Pp*DOG1s, which also regulate spore germination negatively. *Pp*DELLAs may be forming a transcription-repressing complex or a transactivation complex with *Pp*DOG1s to regulate germination, as their orthologues do with other transcriptional regulators in angiosperms. The data so far suggest that the role of *Pp*DELLAs in spore germination is independent from hormones that have been shown to regulate spore germination, such as diterpenes or ABA, but it is unclear if the same applies to *Pp*DOG1s.

Another plant hormone, ethylene, has also been implicated in the regulation of spore germination. Exogenous application of the ethylene precursor 1-aminocyclopropane-1-carboxylic acid (ACC), repressed spore germination in *P. patens* (Vesty *et al*., 2016). Interestingly, in the transcriptome of the *PpdellaAB* mutant, among the promoters of differentially expressed genes there was an enrichment in ETHYLENE RESPONSE FACTOR (ERF)-binding sites, suggesting that *Pp*DELLAs might be involved in ethylene-induced spore germination repression. In addition, in Arabidopsis, *At*DOG1 is involved in ethylene signalling, as its expression is directly regulated by *At*ERF12 (Li *et al.*, 2019). Therefore, exploring whether the *Pp*DELLA-*Pp*DOG1 interaction is related to ethylene signalling during spore germination might be a good strategy.

More evidence from other non-seed plants would be necessary to deduce whether the involvement of DELLA proteins in dispersal unit germination is universal across the land plant lineage and whether it may have been a property of the ancestral DELLA that aided establishment on land. The fact that it is a conserved feature between a bryophyte and an angiosperm, suggests that it might have been. In addition, as *At*RGA1 has been shown to interact with *Pp*DOG1s, the potential of engineering Arabidopsis or crops to overexpress *Pp*DOG1s and how this might benefit angiosperms should be explored further.

Regulation of reproductive development by DELLAs appears to be widespread in land plants. Loss of DELLA proteins in different angiosperms, including crops, induces male sterility due to defects in pollen development (Lanahan and Ho, 1988; Ikeda *et al*., 2001; Plackett *et al*., 2014). There is also evidence that DELLA proteins are implicated in the regulation of reproductive development in lycophytes and ferns as well (Tanaka *et al*., 2014; Aya *et al*., 2011), and DELLA overexpression in *M. polymorpha* delays gametangiophores formation (Hernández-García *et al*., 2021). In *P. patens*, we have shown that loss of *Pp*DELLA proteins results in male sterility, although the precise aspect of reproductive development that is affected remains elusive. These observations suggest that the regulation of reproductive development might have been a property of the ancestral DELLA protein that was maintained due to selection pressure in the different land plant groups. In Arabidopsis, *At*DELLAs interact with *At*MYB21 and *At*MYB24 to repress stamen development (Huang *et al*., 2020), and in this study *Pp*DELLAa interacted with a predicted MYB-family transcription factor (*Pp*3c3_17580) in the IP-MS screen. We have proposed that *Pp*DELLAs may be inhibiting activation of *Pp*3c3_17580-induced gene expression that

promotes male infertility in *P. patens*, however more evidence to support this hypothesis is needed.

In addition, transcriptomic analysis of the *PpdellaAB* mutant suggests that *Pp*DELLA proteins are probably acting as molecular 'hubs', regulating transcription by interacting with other proteins. A number of those interactors have been predicted by transcription factor enrichment analysis, among which a putative MYB-family transcription factor mentioned earlier. This finding along with the observations that *Pp*DELLA signalling is most likely uncoupled from diterpene signalling in *P. patens*, support the hypothesis that GA signalling evolved by exploiting the already established DELLA signalling mechanisms in order to control growth-regulating transcription (Hernández-García *et al.*, 2019).

Molecular exploitation appears to be a common mechanism driving the evolution of hormone signalling across kingdoms. A very well-known example of this phenomenon is the evolution of steroid hormone receptors in vertebrates (Eick and Thornton, 2011). The biosynthetic pathway of estrogens (female sex steroid hormones) involves the production of testosterone and progesterone as precursors (Hanukoglu, 1992). Interestingly, nuclear receptors specific for estrogens evolved first, and receptors with affinities for testosterone and progesterone diverged later, exploiting steroid precursors that were already present (Thornton, 2001).

In addition, it has been shown that the mineralocorticoid receptor (MR) of the steroid hormone aldosterone, regulating electrolyte homeostasis, evolved affinity for the hormone before aldosterone had actually emerged (Bridgham *et al*., 2006). In fact, the ancestral receptor had affinity for structurally similar steroids that appeared early in vertebrate evolution, and this affinity was later exploited by aldosterone, which

emerged more recently in the ancestor of tetrapods, establishing a tetrapod-specific MR-aldosterone partnership with a novel function (Bridgham *et al*., 2006). Similarly, in vascular plants, the DELLA N-terminal domain regulating transactivation was exploited by the GA-GID1 complex for interaction, recruiting DELLA signalling into GA signalling (Hernández-García *et al*., 2019). These examples demonstrate that across kingdoms, novel interactions can evolve when newly emerged small molecules or proteins are co-opted to interact with pre-existing modules. This enables development of novel functions and adds to the complexity of signalling pathways (Bridgham *et al*., 2006).

6.4 Future perspectives

The fact that there is no evidence for a relationship between diterpene and *Pp*DELLA signalling in *P. patens* suggests that future research should concentrate on other, novel properties of *Pp*DELLA proteins elucidated in this study. Given that *Pp*DOG1s and *Pp*DELLAs share the same function in *P. patens* and interact in yeast cells, unravelling this molecular mechanism would be a priority in the study of *Pp*DELLA proteins. Looking at the transcriptome of a triple *Ppdog1* mutant and identifying common sets of genes with the transcriptome of the double *Ppdella* mutant and then testing those via ChIP or similar would be a good strategy. Also, confirming the *Pp*DOG1-*Pp*DELLA interaction *in planta* by BiFC or a similar method would be necessary to provide more firm conclusions. Crossing the *PpdellaAB* mutant with the *Ppdog1* triple mutant would also be useful to study any combined effects on spore germination or study its transcriptome and compare it with those of the individual mutants.

Establishing how exactly *Pp*DELLAs impose male sterility in *P. patens* would be another priority. Unpublished work from the Rensing lab so far suggests that this is not related to the morphology of male reproductory structures, so other possibilities, such as defects in sperm motility are currently being under investigation.

Another priority would be to further characterise the interaction between *Pp*DELLAs and the predicted MYB-family transcription factor *Pp*3c3_17580, which (i) interacted with *Pp*DELLAa in IP-MS and (ii) has enriched binding sites among the promoters of DELLA-repressed genes. At first, the interaction must be confirmed by another method, such as yeast two-hybrid and/or BiFC and then it must be confirmed that the putative targets of *Pp*3c3_17580 identified in the *PpdellaAB* transcriptome are true targets, for example using ChIP. Similarly, testing the putative interactions between *Pp*DELLA proteins and the remaining 61 transcription factors with enriched binding sites among the promoters of *Pp*DELLA-regulated genes via yeast two-hybrid would provide useful data for future research.

Establishing the molecular mechanisms by which DELLA proteins function in *P. patens* can provide more insights into how DELLA proteins have evolved in the different land plant lineages. However, unless DELLA proteins from more model species belonging to underrepresented land plant groups, such as ferns, lycophytes and bryophytes, are studied, DELLA signalling evolution cannot be fully characterised. Understanding how DELLA signalling mechanisms have evolved and how DELLAs respond to environmental signals could enable us to engineer better crops, in order to contribute to mitigating the effects of global warming and achieving global food security. As DELLA proteins function via protein-protein interactions, targeting their interaction capacity by either identifying novel *DELLA* alleles or by manipulating some

of the DELLA interaction partners could be a potential avenue for enabling production or breeding of a new generation of resilient land plants.

CHAPTER 7: List of references

Achard, P., Cheng, H., De Grauwe, L., Decat, J., Schoutteten, H., Moritz, T., Van Der Straeten, D., Peng, J., & Harberd, N. P. (2006). Integration of plant responses to environmentally activated phytohormonal signals. *Science*, *311*(5757), 91–94. https://doi.org/10.1126/science.1118642

Achard, P., Liao, L., Jiang, C., Desnos, T., Bartlett, J., Fu, X., & Harberd, N. P. (2007). DELLAs contribute to plant photomorphogenesis. *Plant Physiology*, *143*, 1163–1172. https://doi.org/10.1104/pp.106.092254

Achard, P., Renou, J.-P., Berthomé, R., Harberd, N. P., & Genschik, P. (2008). Plant DELLAs restrain growth and promote survival of adversity by reducing the levels of reactive oxygen species. *Current Biology*, *18*(9), 656–660. https://doi.org/10.1016/j.cub.2008.04.034

Al-Sady, B., Ni, W., Kircher, S., Schäfer, E., & Quail, P. H. (2006). Photoactivated phytochrome induces rapid PIF3 phosphorylation prior to proteasome-mediated degradation. *Molecular Cell*, *23*, 439–446. https://doi.org/10.1016/j.molcel.2006.06.011

Alexa A. and Rahnenfuhrer J. (2020). *topGO: Enrichment Analysis for Gene Ontology*. R package version 2.42.0. DOI: 10.18129/B9.bioc.topGO

An, F., Zhang, X., Zhu, Z., Ji, Y., He, W., Jiang, Z., Li, M., & Guo, H. (2012). Coordinated regulation of apical hook development by gibberellins and ethylene in etiolated Arabidopsis seedlings. *Cell Research*, *22*, 915–927. https://doi.org/10.1038/cr.2012.29

Apel, K., & Hirt, H. (2004). REACTIVE OXYGEN SPECIES: Metabolism, oxidative stress, and signal transduction. *Annual Review of Plant Biology*, *55*(1), 373–399. https://doi.org/10.1146/annurev.arplant.55.031903.141701

Arana, M. V., Marín-de la Rosa, N., Maloof, J. N., Blázquez, M. A., & Alabadí, D. (2011). Circadian oscillation of gibberellin signaling in *Arabidopsis*. *Proceedings of the National Academy of Sciences of the United States of America*, *108*, 9292–9297. https://doi.org/10.1073/pnas.1101050108

Arif, M. A., Hiss, M., Tomek, M., Busch, H., Meyberg, R., Tintelnot, S., Reski, R., Rensing, S. A., & Frank, W. (2019). ABA-induced vegetative diaspore formation in *Physcomitrella patens*. *Frontiers in Plant Science*, *10*. https://doi.org/10.3389/fpls.2019.00315

Ariizumi, T., Murase, K., Sun, T., & Steber, C. M. (2008). Proteolysis-independent downregulation of DELLA repression in *Arabidopsis* by the gibberellin receptor GIBBERELLIN INSENSITIVE DWARF1. *The Plant Cell*, *20*, 2447–2459. https://doi.org/10.1105/tpc.108.058487

Aya, K., Hiwatashi, Y., Kojima, M., Sakakibara, H., Ueguchi-Tanaka, M., Hasebe, M., & Matsuoka, M. (2011). The gibberellin perception system evolved to regulate a pre-existing GAMYB-mediated system during land plant evolution. *Nature Communications*, *2*, 544. https://doi.org/10.1038/ncomms1552

Bai, M.-Y., Shang, J.-X., Oh, E., Fan, M., Bai, Y., Zentella, R., Sun, T., & Wang, Z.-Y. (2012). Brassinosteroid, gibberellin and phytochrome impinge on a common transcription module in *Arabidopsis*. *Nature Cell Biology*, *14*, 810–817. https://doi.org/10.1038/ncb2546

Bailey, M., Ivanauskaite, A., Grimmer, J., Akintewe, O., Payne, A. C., Osborne, R., Labandera, A.-M., Etherington, R. D., Rantala, M., Baginsky, S., Mulo, P., & Gibbs, D. J. (2021). The Arabidopsis NOT4A E3 ligase promotes PGR3

expression and regulates chloroplast translation. *Nature Communications*, *12*(1), 251. https://doi.org/10.1038/s41467-020-20506-4

Bassel, G. W., Mullen, R. T., & Bewley, J. D. (2008). *procera* is a putative DELLA mutant in tomato (*Solanum lycopersicum*): Effects on the seed and vegetative plant. *Journal of Experimental Botany*, *59*, 585–593. https://doi.org/10.1093/jxb/erm354

Bentsink, L., Jowett, J., Hanhart, C. J., & Koornneef, M. (2006). Cloning of DOG1, a quantitative trait locus controlling seed dormancy in Arabidopsis. *Proceedings of the National Academy of Sciences*, *103*(45), 17042–17047. https://doi.org/10.1073/pnas.0607877103

Blanco-Touriñán, N., Legris, M., Minguet, E. G., Costigliolo-Rojas, C., Nohales, M. A., Iniesto, E., García-León, M., Pacín, M., Heucken, N., Blomeier, T., Locascio, A., Černý, M., Esteve-Bruna, D., Díez-Díaz, M., Brzobohatý, B., Frerigmann, H., Zurbriggen, M. D., Kay, S. A., Rubio, V., … Alabadí, D. (2020a). COP1 destabilizes DELLA proteins in *Arabidopsis*. *Proceedings of the National Academy of Sciences*, *117*, 13792–13799. https://doi.org/10.1073/pnas.1907969117

Blanco-Touriñán, N., Serrano-Mislata, A., & Alabadí, D. (2020b). Regulation of DELLA Proteins by Post-translational Modifications. *Plant and Cell Physiology*, *61*, 1891-1901. https://doi.org/10.1093/pcp/pcaa113

Blázquez, M. A., Nelson, D. C., & Weijers, D. (2020). Evolution of Plant Hormone Response Pathways. *Annual Review of Plant Biology*, *71*, 327–353. https://doi.org/10.1146/annurev-arplant-050718-100309

Bowman, J. L., Kohchi, T., Yamato, K. T., Jenkins, J., Shu, S., Ishizaki, K., Yamaoka, S., Nishihama, R., Nakamura, Y., Berger, F., Adam, C., Aki, S. S., Althoff, F., Araki, T., Arteaga-Vazquez, M. A., Balasubrmanian, S., Barry, K., Bauer, D., Boehm, C. R., … Schmutz, J. (2017). Insights into land plant evolution garnered from the *Marchantia polymorpha* genome. *Cell*, *171*, 287-304. https://doi.org/10.1016/j.cell.2017.09.030

Bridgham, J. T., Carroll, S. M., & Thornton, J. W. (2006). Evolution of hormone-receptor complexity by molecular exploitation. *Science*, *312*, 97–101. https://doi.org/10.1126/science.1123348

Briones-Moreno, A., Hernández-García, J., Vargas-Chávez, C., Romero-Campero, F. J., Romero, J. M., Valverde, F., & Blázquez, M. A. (2017). Evolutionary analysis of DELLA-associated transcriptional networks. *Frontiers in Plant Science*, *8*. https://doi.org/10.3389/fpls.2017.00626

Budayeva, H. G., & Cristea, I. M. (2014). A mass spectrometry view of stable and transient protein interactions. *Advances in Experimental Medicine and Biology*, *806*, 263–282. https://doi.org/10.1007/978-3-319-06068-2_11

Cao, D., Cheng, H., Wu, W., Soo, H. M., & Peng, J. (2006). Gibberellin mobilizes distinct DELLA-dependent transcriptomes to regulate seed germination and floral development in *Arabidopsis*. *Plant Physiology*, *142*, 509–525. https://doi.org/10.1104/pp.106.082289

Carbon, S., Ireland, A., Mungall, C. J., Shu, S., Marshall, B., & Lewis, S. (2009). AmiGO: Online access to ontology and annotation data. *Bioinformatics*, *25*(2), 288–289. https://doi.org/10.1093/bioinformatics/btn615

Carlson, K. D., Bhogale, S., Anderson, D., Tomanek, L., & Madlung, A. (2019). Phytochrome A regulates carbon flux in dark grown tomato seedlings. *Frontiers in Plant Science*, *10*. https://doi.org/10.3389/fpls.2019.00152

Chen, L., Bao, F., Tang, S., Zuo, E., Lv, Q., Zhang, D., Hu, Y., Wang, X., & He, Y. (2019). *Pp*AKR1A, a novel aldo-keto reductase from *Physcomitrella patens*, plays a positive role in salt stress. *International Journal of Molecular Sciences*, *20*(22). https://doi.org/10.3390/ijms20225723

Claeys, H., De Bodt, S., & Inzé, D. (2014). Gibberellins and DELLAs: Central nodes in growth regulatory networks. *Trends in Plant Science*, *19*(4), 231–239. https://doi.org/10.1016/j.tplants.2013.10.001

Clough, S. J., & Bent, A. F. (1998). Floral dip: A simplified method for Agrobacterium-mediated transformation of *Arabidopsis thaliana*. *The Plant Journal: For Cell and Molecular Biology*, *16*(6), 735–743. https://doi.org/10.1046/j.1365-313x.1998.00343.x

Colebrook, E. H., Thomas, S. G., Phillips, A. L., & Hedden, P. (2014). The role of gibberellin signalling in plant responses to abiotic stress. *Journal of Experimental Biology*, *217*(1), 67–75. https://doi.org/10.1242/jeb.089938

Conti, L., Nelis, S., Zhang, C., Woodcock, A., Swarup, R., Galbiati, M., Tonelli, C., Napier, R., Hedden, P., Bennett, M., & Sadanandom, A. (2014). Small ubiquitin-like modifier protein SUMO enables plants to control growth independently of the phytohormone gibberellin. *Developmental Cell*, *28*, 102–110. https://doi.org/10.1016/j.devcel.2013.12.004

Cove, D. J., Schild, A., Ashton, N. W., & Hartmann, E. (1978). Genetic and physiological studies of the effect of light on the development of the moss, *Physcomitrella patens*. *Photochemistry and Photobiology*, *27*(2), 249–254. https://doi.org/10.1111/j.1751-1097.1978.tb07596.x

Dai, C., & Xue, H.-W. (2010). Rice early flowering1, a CKI, phosphorylates DELLA protein SLR1 to negatively regulate gibberellin signalling. *The EMBO Journal*, *29*, 1916–1927. https://doi.org/10.1038/emboj.2010.75

de Lucas, M., Davière, J.-M., Rodríguez-Falcón, M., Pontin, M., Iglesias-Pedraz, J. M., Lorrain, S., Fankhauser, C., Blázquez, M. A., Titarenko, E., & Prat, S. (2008). A molecular framework for light and gibberellin control of cell elongation. *Nature*, *451*, 480–484. https://doi.org/10.1038/nature06520

Dill, A., & Sun, T. (2001). Synergistic derepression of gibberellin signaling by removing RGA and GAI function in *Arabidopsis thaliana*. *Genetics*, *159*, 777–785.

Dill, A., Jung, H.-S., & Sun, T. (2001). The DELLA motif is essential for gibberellin-induced degradation of RGA. *Proceedings of the National Academy of Sciences of the United States of America*, *98*, 14162–14167. https://doi.org/10.1073/pnas.251534098

Dill, A., Thomas, S. G., Hu, J., Steber, C. M., & Sun, T.-P. (2004). The *Arabidopsis* F-box protein SLEEPY1 targets gibberellin signaling repressors for gibberellin-induced degradation. *The Plant Cell*, *16*, 1392–1405. https://doi.org/10.1105/tpc.020958

Earley, K. W., Haag, J. R., Pontes, O., Opper, K., Juehne, T., Song, K., & Pikaard, C. S. (2006). Gateway-compatible vectors for plant functional genomics and proteomics. *The Plant Journal*, *45*(4), 616–629. https://doi.org/10.1111/j.1365-313X.2005.02617.x

Eick, G. N., & Thornton, J. W. (2011). Evolution of steroid receptors from an estrogen-sensitive ancestral receptor. *Molecular and Cellular Endocrinology*, *334*, 31–38. https://doi.org/10.1016/j.mce.2010.09.003

Evenson, R. E., & Gollin, D. (2003). Assessing the impact of the Green Revolution, 1960 to 2000. *Science*, *300*, 758–762. https://doi.org/10.1126/science.1078710

Feng, S., Martinez, C., Gusmaroli, G., Wang, Y., Zhou, J., Wang, F., Chen, L., Yu, L., Iglesias-Pedraz, J. M., Kircher, S., Schäfer, E., Fu, X., Fan, L.-M., & Deng, X. W. (2008). Coordinated regulation of *Arabidopsis thaliana* development by light and gibberellins. *Nature*, *451*, 475–479. https://doi.org/10.1038/nature06448

Finkelstein, R. R. (1994). Maternal effects govern variable dominance of two abscisic acid response mutations in *Arabidopsis thaliana*. *Plant Physiology*, *105*(4), 1203–1208. https://doi.org/10.1104/pp.105.4.1203

Fonouni-Farde, C., Tan, S., Baudin, M., Brault, M., Wen, J., Mysore, K. S., Niebel, A., Frugier, F., & Diet, A. (2016). DELLA-mediated gibberellin signaling regulates Nod factor signaling and rhizobial infection. *Nature Communications*, *7*. https://doi.org/10.1038/ncomms12636

Fu, X., Richards, D. E., Ait-ali, T., Hynes, L. W., Ougham, H., Peng, J., & Harberd, N. P. (2002). Gibberellin-mediated proteasome-dependent degradation of the barley DELLA protein SLN1 repressor. *The Plant Cell*, *14*, 3191–3200. https://doi.org/10.1105/tpc.006197

Fuentes, S., Ljung, K., Sorefan, K., Alvey, E., Harberd, N. P., & Østergaard, L. (2012). Fruit growth in Arabidopsis occurs via DELLA-dependent and DELLA-independent gibberellin responses. *The Plant Cell*, *24*(10), 3982–3996. https://doi.org/10.1105/tpc.112.103192

Gale, M. D., & Youssefian, S. (1985). Chapter 1—Dwarfing genes in wheat. In G. E. Russell (Ed.), *Progress in Plant Breeding–1* (pp. 1–35). Butterworth-Heinemann. https://doi.org/10.1016/B978-0-407-00780-2.50005-9

Gallego-Bartolomé, J., Minguet, E. G., Marín, J. A., Prat, S., Blázquez, M. A., & Alabadí, D. (2010). Transcriptional diversification and functional conservation between DELLA proteins in *Arabidopsis*. *Molecular Biology and Evolution*, *27*, 1247–1256. https://doi.org/10.1093/molbev/msq012

Gallego-Bartolomé, J., Alabadí, D., & Blázquez, M. A. (2011). DELLA-induced early transcriptional changes during etiolated development in *Arabidopsis thaliana*. *PLoS ONE*, *6*, e23918. https://doi.org/10.1371/journal.pone.0023918

Gomi, K., Sasaki, A., Itoh, H., Ueguchi-Tanaka, M., Ashikari, M., Kitano, H., & Matsuoka, M. (2004). GID2, an F-box subunit of the SCF E3 complex, specifically interacts with phosphorylated SLR1 protein and regulates the gibberellin-dependent degradation of SLR1 in rice. *The Plant Journal: For Cell and Molecular Biology*, *37*, 626–634. https://doi.org/10.1111/j.1365-313x.2003.01990.x

Graeber, K., Linkies, A., Steinbrecher, T., Mummenhoff, K., Tarkowská, D., Turečková, V., Ignatz, M., Sperber, K., Voegele, A., Jong, H. de, Urbanová, T., Strnad, M., & Leubner-Metzger, G. (2014). *DELAY OF GERMINATION 1* mediates a conserved coat-dormancy mechanism for the temperature- and gibberellin-dependent control of seed germination. *Proceedings of the*

National Academy of Sciences, *111*(34), E3571–E3580. https://doi.org/10.1073/pnas.1403851111
Guard, S. E., Ebmeier, C. C., & Old, W. M. (2019). Label-free immunoprecipitation mass spectrometry workflow for large-scale nuclear interactome profiling. *Journal of Visualized Experiments: JoVE*, *153*. https://doi.org/10.3791/60432
Gubler, F., Chandler, P. M., White, R. G., Llewellyn, D. J., & Jacobsen, J. V. (2002). Gibberellin signaling in barley aleurone cells. Control of SLN1 and GAMYB expression. *Plant Physiology*, *129*, 191–200. https://doi.org/10.1104/pp.010918
Hanukoglu, I. (1992). Steroidogenic enzymes: Structure, function, and role in regulation of steroid hormone biosynthesis. *The Journal of Steroid Biochemistry and Molecular Biology*, *43*, 779–804. https://doi.org/10.1016/0960-0760(92)90307-5
Hayashi, K., Kawaide, H., Notomi, M., Sakigi, Y., Matsuo, A., & Nozaki, H. (2006). Identification and functional analysis of bifunctional *ent*-kaurene synthase from the moss *Physcomitrella patens*. *FEBS Letters*, *580*, 6175–6181. https://doi.org/10.1016/j.febslet.2006.10.018
Hayashi, K., Horie, K., Hiwatashi, Y., Kawaide, H., Yamaguchi, S., Hanada, A., Nakashima, T., Nakajima, M., Mander, L. N., Yamane, H., Hasebe, M., & Nozaki, H. (2010). Endogenous diterpenes derived from *ent*-kaurene, a common gibberellin precursor, regulate protonema differentiation of the moss *Physcomitrella patens*. *Plant Physiology*, *153*, 1085–1097. https://doi.org/10.1104/pp.110.157909
Hedden, P. (2003). The genes of the Green Revolution. *Trends in Genetics: TIG*, *19*, 5–9. https://doi.org/10.1016/s0168-9525(02)00009-4
Hernández-García, J., Briones-Moreno, A., Dumas, R., & Blázquez, M. A. (2019). Origin of gibberellin-dependent transcriptional regulation by molecular exploitation of a transactivation domain in DELLA proteins. *Molecular Biology and Evolution*, *36*, 908–918. https://doi.org/10.1093/molbev/msz009
Hernández-García, J., Briones-Moreno, A., & Blázquez, M. A. (2020). Origin and evolution of gibberellin signaling and metabolism in plants. *Seminars in Cell & Developmental Biology*. https://doi.org/10.1016/j.semcdb.2020.04.009
Hernández-García, J., Sun, R., Serrano-Mislata, A., Inoue, K., Vargas-Chávez, C., Esteve-Bruna, D., Arbona, V., Yamaoka, S., Nishihama, R., Kohchi, T., & Blázquez, M. A. (2021). Coordination between growth and stress responses by DELLA in the liverwort *Marchantia polymorpha*. *BioRxiv*, 2021.02.11.430820. https://doi.org/10.1101/2021.02.11.430820
Hirano, K., Asano, K., Tsuji, H., Kawamura, M., Mori, H., Kitano, H., Ueguchi-Tanaka, M., & Matsuoka, M. (2010). Characterization of the molecular mechanism underlying gibberellin perception complex formation in rice. *The Plant Cell*, *22*, 2680–2696. https://doi.org/10.1105/tpc.110.075549
Hirano, K., Nakajima, M., Asano, K., Nishiyama, T., Sakakibara, H., Kojima, M., Katoh, E., Xiang, H., Tanahashi, T., Hasebe, M., Banks, J. A., Ashikari, M., Kitano, H., Ueguchi-Tanaka, M., & Matsuoka, M. (2007). The GID1-mediated gibberellin perception mechanism is conserved in the lycophyte *Selaginella moellendorffii* but not in the bryophyte *Physcomitrella patens*. *The Plant Cell*, *19*, 3058–3079. https://doi.org/10.1105/tpc.107.051524

Hirano, K., Kouketu, E., Katoh, H., Aya, K., Ueguchi-Tanaka, M., & Matsuoka, M. (2012). The suppressive function of the rice DELLA protein SLR1 is dependent on its transcriptional activation activity. *The Plant Journal: For Cell and Molecular Biology*, *71*, 443–453. https://doi.org/10.1111/j.1365-313X.2012.05000.x

Hou, X., Lee, L. Y. C., Xia, K., Yan, Y., & Yu, H. (2010). DELLAs modulate jasmonate signaling via competitive binding to JAZs. *Developmental Cell*, *19*, 884–894. https://doi.org/10.1016/j.devcel.2010.10.024

Huang, D., Wang, S., Zhang, B., Shang-Guan, K., Shi, Y., Zhang, D., Liu, X., Wu, K., Xu, Z., Fu, X., & Zhou, Y. (2015). A gibberellin-mediated DELLA-NAC signaling cascade regulates cellulose synthesis in rice. *The Plant Cell*, *27*, 1681–1696. https://doi.org/10.1105/tpc.15.00015

Huang, H., Gong, Y., Liu, B., Wu, D., Zhang, M., Xie, D., & Song, S. (2020). The DELLA proteins interact with MYB21 and MYB24 to regulate filament elongation in Arabidopsis. *BMC Plant Biology*, *20*(1), 64. https://doi.org/10.1186/s12870-020-2274-0

Hussain, A., Cao, D., Cheng, H., Wen, Z., & Peng, J. (2005). Identification of the conserved serine/threonine residues important for gibberellin-sensitivity of *Arabidopsis* RGL2 protein. *The Plant Journal: For Cell and Molecular Biology*, *44*, 88–99. https://doi.org/10.1111/j.1365-313X.2005.02512.x

Hyun, Y., Richter, R., Vincent, C., Martinez-Gallegos, R., Porri, A., & Coupland, G. (2016). Multi-layered regulation of SPL15 and cooperation with SOC1 integrate endogenous flowering pathways at the Arabidopsis shoot meristem. *Developmental Cell*, *37*(3), 254–266. https://doi.org/10.1016/j.devcel.2016.04.001

Ikeda, A., Ueguchi-Tanaka, M., Sonoda, Y., Kitano, H., Koshioka, M., Futsuhara, Y., Matsuoka, M., & Yamaguchi, J. (2001). Slender rice, a constitutive gibberellin response mutant, is caused by a null mutation of the SLR1 gene, an ortholog of the height-regulating gene GAI/RGA/RHT/D8. *The Plant Cell*, *13*(5), 999–1010. https://doi.org/10.1105/tpc.13.5.999

Itoh, H., Ueguchi-Tanaka, M., Sato, Y., Ashikari, M., & Matsuoka, M. (2002). The gibberellin signaling pathway is regulated by the appearance and disappearance of SLENDER RICE1 in nuclei. *The Plant Cell*, *14*, 57–70. https://doi.org/10.1105/tpc.010319

Itoh, H., Sasaki, A., Ueguchi-Tanaka, M., Ishiyama, K., Kobayashi, M., Hasegawa, Y., Minami, E., Ashikari, M., & Matsuoka, M. (2005a). Dissection of the phosphorylation of rice DELLA protein, SLENDER RICE1. *Plant & Cell Physiology*, *46*, 1392–1399. https://doi.org/10.1093/pcp/pci152

Itoh, H., Shimada, A., Ueguchi-Tanaka, M., Kamiya, N., Hasegawa, Y., Ashikari, M., & Matsuoka, M. (2005b). Overexpression of a GRAS protein lacking the DELLA domain confers altered gibberellin responses in rice. *The Plant Journal*, *44*, 669–679. https://doi.org/10.1111/j.1365-313X.2005.02562.x

Jaedicke, K., Lichtenthäler, A. L., Meyberg, R., Zeidler, M., & Hughes, J. (2012). A phytochrome-phototropin light signaling complex at the plasma membrane. *Proceedings of the National Academy of Sciences of the United States of America*, *109*(30), 12231–12236. https://doi.org/10.1073/pnas.1120203109

Jasinski, S., Tattersall, A., Piazza, P., Hay, A., Martinez-Garcia, J. F., Schmitz, G., Theres, K., McCormick, S., & Tsiantis, M. (2008). PROCERA encodes a

DELLA protein that mediates control of dissected leaf form in tomato. *The Plant Journal*, *56*, 603–612. https://doi.org/10.1111/j.1365-313X.2008.03628.x
Kasahara, M., Kagawa, T., Sato, Y., Kiyosue, T., & Wada, M. (2004). Phototropins mediate blue and red light-induced chloroplast movements in *Physcomitrella patens*. *Plant Physiology*, *135*(3), 1388–1397. https://doi.org/10.1104/pp.104.042705
Kerchev, P., De Smet, B., Waszczak, C., Messens, J., & Van Breusegem, F. (2015). Redox strategies for crop improvement. *Antioxidants & Redox Signaling*, *23*(14), 1186–1205. https://doi.org/10.1089/ars.2014.6033
Khandelwal, A., Cho, S. H., Marella, H., Sakata, Y., Perroud, P.-F., Pan, A., & Quatrano, R. S. (2010). Role of ABA and ABI3 in desiccation tolerance. *Science*, *327*(5965), 546–546. https://doi.org/10.1126/science.1183672
Komatsu, K., Nishikawa, Y., Ohtsuka, T., Taji, T., Quatrano, R. S., Tanaka, S., & Sakata, Y. (2009). Functional analyses of the ABI1-related protein phosphatase type 2C reveal evolutionarily conserved regulation of abscisic acid signaling between Arabidopsis and the moss *Physcomitrella patens*. *Plant Molecular Biology*, *70*, 327–340. https://doi.org/10.1007/s11103-009-9476-z
Koornneef, M., & van der Veen, J. H. (1980). Induction and analysis of gibberellin sensitive mutants in Arabidopsis thaliana (L.) heynh. *Theoretical and Applied Genetics*, *58*(6), 257–263. https://doi.org/10.1007/BF00265176
Lanahan, M. B., & Ho, T.-H. D. (1988). Slender barley: A constitutive gibberellin-response mutant. *Planta*, *175*(1), 107–114. https://doi.org/10.1007/BF00402887
Lantzouni, O., Alkofer, A., Falter-Braun, P., & Schwechheimer, C. (2020). GROWTH-REGULATING FACTORS interact with DELLAs and regulate growth in cold stress. *The Plant Cell*, *32*, 1018–1034. https://doi.org/10.1105/tpc.19.00784
Lee, S., Cheng, H., King, K. E., Wang, W., He, Y., Hussain, A., Lo, J., Harberd, N. P., & Peng, J. (2002). Gibberellin regulates Arabidopsis seed germination via RGL2, a GAI/RGA-like gene whose expression is up-regulated following imbibition. *Genes & Development*, *16*(5), 646–658. https://doi.org/10.1101/gad.969002
Lee, K. P., Piskurewicz, U., Turecková, V., Strnad, M., & Lopez-Molina, L. (2010). A seed coat bedding assay shows that RGL2-dependent release of abscisic acid by the endosperm controls embryo growth in Arabidopsis dormant seeds. *Proceedings of the National Academy of Sciences of the United States of America*, *107*(44), 19108–19113. https://doi.org/10.1073/pnas.1012896107
Leebens-Mack, J. H., Barker, M. S., Carpenter, E. J., Deyholos, M. K., Gitzendanner, M. A., Graham, S. W., Grosse, I., Li, Z., Melkonian, M., Mirarab, S., Porsch, M., Quint, M., Rensing, S. A., Soltis, D. E., Soltis, P. S., Stevenson, D. W., Ullrich, K. K., Wickett, N. J., DeGironimo, L., … One Thousand Plant Transcriptomes Initiative. (2019). One thousand plant transcriptomes and the phylogenomics of green plants. *Nature*, *574*(7780), 679–685. https://doi.org/10.1038/s41586-019-1693-2
Legris, M., Klose, C., Burgie, E. S., Rojas, C. C. R., Neme, M., Hiltbrunner, A., Wigge, P. A., Schäfer, E., Vierstra, R. D., & Casal, J. J. (2016). Phytochrome B integrates light and temperature signals in *Arabidopsis*. *Science*, *354*(6314), 897–900. https://doi.org/10.1126/science.aaf5656

Lenton, T. M., Crouch, M., Johnson, M., Pires, N., & Dolan, L. (2012). First plants cooled the Ordovician. *Nature Geoscience*, *5*, 86–89. https://doi.org/10.1038/ngeo1390

Lenton, T. M., Dahl, T. W., Daines, S. J., Mills, B. J. W., Ozaki, K., Saltzman, M. R., & Porada, P. (2016). Earliest land plants created modern levels of atmospheric oxygen. *Proceedings of the National Academy of Sciences*, *113*, 9704–9709. https://doi.org/10.1073/pnas.1604787113

Li, F.-W., Melkonian, M., Rothfels, C. J., Villarreal, J. C., Stevenson, D. W., Graham, S. W., Wong, G. K.-S., Pryer, K. M., & Mathews, S. (2015). Phytochrome diversity in green plants and the origin of canonical plant phytochromes. *Nature Communications*, *6*(1), 7852. https://doi.org/10.1038/ncomms8852

Li, Y., Deng, H., Miao, M., Li, H., Huang, S., Wang, S., & Liu, Y. (2016). Tomato MBD5, a methyl CpG binding domain protein, physically interacting with UV-damaged DNA binding protein-1, functions in multiple processes. *New Phytologist*, *210*(1), 208–226. https://doi.org/10.1111/nph.13745

Li, X., Chen, T., Li, Y., Wang, Z., Cao, H., Chen, F., Li, Y., Soppe, W. J. J., Li, W., & Liu, Y. (2019). ETR1/RDO3 regulates seed dormancy by relieving the inhibitory effect of the ERF12-TPL complex on DELAY OF GERMINATION1 expression. *The Plant Cell*, *31*(4), 832–847. https://doi.org/10.1105/tpc.18.00449

Li, F.-W., Nishiyama, T., Waller, M., Frangedakis, E., Keller, J., Li, Z., Fernandez-Pozo, N., Barker, M. S., Bennett, T., Blázquez, M. A., Cheng, S., Cuming, A. C., de Vries, J., de Vries, S., Delaux, P.-M., Diop, I. S., Harrison, C. J., Hauser, D., Hernández-García, J., … Szövényi, P. (2020). *Anthoceros* genomes illuminate the origin of land plants and the unique biology of hornworts. *Nature Plants*, *6*(3), 259–272. https://doi.org/10.1038/s41477-020-0618-2

Lim, S., Park, J., Lee, N., Jeong, J., Toh, S., Watanabe, A., Kim, J., Kang, H., Kim, D. H., Kawakami, N., & Choi, G. (2013). ABA-INSENSITIVE3, ABA-INSENSITIVE5, and DELLAs interact to activate the expression of SOMNUS and other high-temperature-inducible genes in imbibed seeds in Arabidopsis. *The Plant Cell*, *25*, 4863–4878. https://doi.org/10.1105/tpc.113.118604

Linkies, A., Graeber, K., Knight, C., & Leubner-Metzger, G. (2010). The evolution of seeds. *New Phytologist*, *186*(4), 817–831. https://doi.org/10.1111/j.1469-8137.2010.03249.x

Locascio, A., Blázquez, M. A., & Alabadí, D. (2013a). Dynamic regulation of cortical microtubule organization through prefoldin-DELLA interaction. *Current Biology*, *23*, 804–809. https://doi.org/10.1016/j.cub.2013.03.053

Locascio, A., Blázquez, M. A., & Alabadí, D. (2013b). Genomic analysis of DELLA protein activity. *Plant and Cell Physiology*, *54*, 1229–1237. https://doi.org/10.1093/pcp/pct082

Luo, H., Laluk, K., Lai, Z., Veronese, P., Song, F., & Mengiste, T. (2010). The Arabidopsis Botrytis Susceptible1 Interactor defines a subclass of RING E3 ligases that regulate pathogen and stress responses. *Plant Physiology*, *154*, 1766–1782. https://doi.org/10.1104/pp.110.163915

MacMillan, J. (2001). Occurrence of gibberellins in vascular plants, fungi, and bacteria. *Journal of Plant Growth Regulation*, *20*, 387–442. https://doi.org/10.1007/s003440010038

Marchant, D. B., Sessa, E. B., Wolf, P. G., Heo, K., Barbazuk, W. B., Soltis, P. S., & Soltis, D. E. (2019). The C-Fern (*Ceratopteris richardii*) genome: Insights into plant genome evolution with the first partial homosporous fern genome assembly. *Scientific Reports*, *9*(1), 18181. https://doi.org/10.1038/s41598-019-53968-8

Marín-de la Rosa, N., Sotillo, B., Miskolczi, P., Gibbs, D. J., Vicente, J., Carbonero, P., Oñate-Sánchez, L., Holdsworth, M. J., Bhalerao, R., Alabadí, D., & Blázquez, M. A. (2014). Large-scale identification of gibberellin-related transcription factors defines Group VII ETHYLENE RESPONSE FACTORS as functional DELLA partners. *Plant Physiology*, *166*, 1022–1032. https://doi.org/10.1104/pp.114.244723

Marín-de la Rosa, N., Pfeiffer, A., Hill, K., Locascio, A., Bhalerao, R. P., Miskolczi, P., Grønlund, A. L., Wanchoo-Kohli, A., Thomas, S. G., Bennett, M. J., Lohmann, J. U., Blázquez, M. A., & Alabadí, D. (2015). Genome wide binding site analysis reveals transcriptional coactivation of cytokinin-responsive genes by DELLA proteins. *PLoS Genetics*, *11*, e1005337. https://doi.org/10.1371/journal.pgen.1005337

McGinnis, K. M., Thomas, S. G., Soule, J. D., Strader, L. C., Zale, J. M., Sun, T., & Steber, C. M. (2003). The *Arabidopsis* SLEEPY1 gene encodes a putative F-box subunit of an SCF E3 ubiquitin ligase. *The Plant Cell*, *15*, 1120–1130. https://doi.org/10.1105/tpc.010827

Meyberg, R., Perroud, P.-F., Haas, F. B., Schneider, L., Heimerl, T., Renzaglia, K. S., & Rensing, S. A. (2020). Characterisation of evolutionarily conserved key players affecting eukaryotic flagellar motility and fertility using a moss model. *New Phytologist*, *227*(2), 440–454. https://doi.org/10.1111/nph.16486

Miura, K., Lee, J., Jin, J. B., Yoo, C. Y., Miura, T., & Hasegawa, P. M. (2009). Sumoylation of ABI5 by the *Arabidopsis* SUMO E3 ligase SIZ1 negatively regulates abscisic acid signaling. *Proceedings of the National Academy of Sciences*, *106*, 5418–5423. https://doi.org/10.1073/pnas.0811088106

Miyazaki, S., Hara, M., Ito, S., Tanaka, K., Asami, T., Hayashi, K.-I., Kawaide, H., & Nakajima, M. (2018). An ancestral gibberellin in a moss *Physcomitrella patens*. *Molecular Plant*, *11*(8), 1097–1100. https://doi.org/10.1016/j.molp.2018.03.010

Moody, L. A., Saidi, Y., Smiles, E. J., Bradshaw, S. J., Meddings, M., Winn, P. J., & Coates, J. C. (2012). ARABIDILLO gene homologues in basal land plants: Species-specific gene duplication and likely functional redundancy. *Planta*, *236*(6), 1927–1941.

Moody, L. A., Saidi, Y., Gibbs, D. J., Choudhary, A., Holloway, D., Vesty, E. F., Bansal, K. K., Bradshaw, S. J., & Coates, J. C. (2016). An ancient and conserved function for Armadillo-related proteins in the control of spore and seed germination by abscisic acid. *The New Phytologist*, *211*(3), 940–951. https://doi.org/10.1111/nph.13938

Moody, L. A., Kelly, S., Rabbinowitsch, E., & Langdale, J. A. (2018). Genetic Regulation of the 2D to 3D Growth Transition in the Moss *Physcomitrella patens*. *Current Biology: CB*, *28*(3), 473-478.e5. https://doi.org/10.1016/j.cub.2017.12.052

Morris, J. L., Puttick, M. N., Clark, J. W., Edwards, D., Kenrick, P., Pressel, S., Wellman, C. H., Yang, Z., Schneider, H., & Donoghue, P. C. J. (2018). The

timescale of early land plant evolution. *Proceedings of the National Academy of Sciences of the United States of America*, *115*, E2274–E2283. https://doi.org/10.1073/pnas.1719588115

Muangprom, A., Thomas, S. G., Sun, T.-P., & Osborn, T. C. (2005). A novel dwarfing mutation in a Green Revolution gene from *Brassica rapa*. *Plant Physiology*, *137*, 931–938. https://doi.org/10.1104/pp.104.057646

Murase, K., Hirano, Y., Sun, T., & Hakoshima, T. (2008). Gibberellin-induced DELLA recognition by the gibberellin receptor GID1. *Nature*, *456*, 459–463. https://doi.org/10.1038/nature07519

Nakabayashi, K., Bartsch, M., Xiang, Y., Miatton, E., Pellengahr, S., Yano, R., Seo, M., & Soppe, W. J. J. (2012). The time required for dormancy release in arabidopsis is determined by DELAY OF GERMINATION1 protein levels in freshly harvested seeds. *The Plant Cell*, *24*(7), 2826–2838. https://doi.org/10.1105/tpc.112.100214

Née, G., Kramer, K., Nakabayashi, K., Yuan, B., Xiang, Y., Miatton, E., Finkemeier, I., & Soppe, W. J. J. (2017). DELAY OF GERMINATION1 requires PP2C phosphatases of the ABA signalling pathway to control seed dormancy. *Nature Communications*, *8*(1), 72. https://doi.org/10.1038/s41467-017-00113-6

Nguyen, K. T., Park, J., Park, E., Lee, I., & Choi, G. (2015). The Arabidopsis RING domain protein BOI inhibits flowering via CO-dependent and CO-independent mechanisms. *Molecular Plant*, *8*, 1725–1736. https://doi.org/10.1016/j.molp.2015.08.005

Nir, I., Shohat, H., Panizel, I., Olszewski, N., Aharoni, A., & Weiss, D. (2017). The tomato DELLA protein PROCERA acts in guard cells to promote stomatal closure. *The Plant Cell*, *29*(12), 3186–3197. https://doi.org/10.1105/tpc.17.00542

Nishihama, R., Ishizaki, K., Hosaka, M., Matsuda, Y., Kubota, A., & Kohchi, T. (2015). Phytochrome-mediated regulation of cell division and growth during regeneration and sporeling development in the liverwort *Marchantia polymorpha*. *Journal of Plant Research*, *128*, 407–421. https://doi.org/10.1007/s10265-015-0724-9

Nishimura, N., Tsuchiya, W., Moresco, J. J., Hayashi, Y., Satoh, K., Kaiwa, N., Irisa, T., Kinoshita, T., Schroeder, J. I., Yates, J. R., Hirayama, T., & Yamazaki, T. (2018). Control of seed dormancy and germination by DOG1-AHG1 PP2C phosphatase complex via binding to heme. *Nature Communications*, *9*(1), 2132. https://doi.org/10.1038/s41467-018-04437-9

Nohales, M. A., & Kay, S. A. (2019). GIGANTEA gates gibberellin signaling through stabilization of the DELLA proteins in *Arabidopsis*. *Proceedings of the National Academy of Sciences*, *116*, 21893–21899. https://doi.org/10.1073/pnas.1913532116

Oliveros, J.C. (2007-2015) Venny. An interactive tool for comparing lists with Venn's diagrams. https:://bioinfogp.cnb.csic.es/tools/venny/index.html

Olszewski, N., Sun, T., & Gubler, F. (2002). Gibberellin signaling: biosynthesis, catabolism, and response pathways. *The Plant Cell*, *14*(suppl 1), S61–S80. https://doi.org/10.1105/tpc.010476

Pan, X.-W., Han, L., Zhang, Y.-H., Chen, D.-F., & Simonsen, H. T. (2015). Sclareol production in the moss *Physcomitrella patens* and observations on growth and

terpenoid biosynthesis. *Plant Biotechnology Reports*, *9*(3), 149–159. https://doi.org/10.1007/s11816-015-0353-8

Park, E., Kim, J., Lee, Y., Shin, J., Oh, E., Chung, W.-I., Liu, J. R., & Choi, G. (2004). Degradation of phytochrome interacting factor 3 in phytochrome-mediated light signaling. *Plant & Cell Physiology*, *45*, 968–975. https://doi.org/10.1093/pcp/pch125

Park, J., Nguyen, K. T., Park, E., Jeon, J.-S., & Choi, G. (2013). DELLA proteins and their interacting RING finger proteins repress gibberellin responses by binding to the promoters of a subset of gibberellin-responsive genes in Arabidopsis. *The Plant Cell*, *25*, 927–943. https://doi.org/10.1105/tpc.112.108951

Peng, J., & Harberd, N. P. (1993). Derivative alleles of the *Arabidopsis* gibberellin-insensitive (gai) mutation confer a wild-type phenotype. *The Plant Cell*, *5*, 351–360. https://doi.org/10.1105/tpc.5.3.351

Peng, Jinrong, Carol, P., Richards, D. E., King, K. E., Cowling, R. J., Murphy, G. P., & Harberd, N. P. (1997). The *Arabidopsis* GAI gene defines a signaling pathway that negatively regulates gibberellin responses. *Genes & Development*, *11*, 3194–3205.

Peng, Jinrong, Richards, D. E., Hartley, N. M., Murphy, G. P., Devos, K. M., Flintham, J. E., Beales, J., Fish, L. J., Worland, A. J., Pelica, F., Sudhakar, D., Christou, P., Snape, J. W., Gale, M. D., & Harberd, N. P. (1999). 'Green revolution' genes encode mutant gibberellin response modulators. *Nature*, *400*, 256–261. https://doi.org/10.1038/22307

Plackett, A. R. G., Ferguson, A. C., Powers, S. J., Wanchoo-Kohli, A., Phillips, A. L., Wilson, Z. A., Hedden, P., & Thomas, S. G. (2014). DELLA activity is required for successful pollen development in the Columbia ecotype of Arabidopsis. *New Phytologist*, *201*(3), 825–836. https://doi.org/10.1111/nph.12571

Ponce de León, I., Oliver, J. P., Castro, A., Gaggero, C., Bentancor, M., & Vidal, S. (2007). *Erwinia carotovora* elicitors and *Botrytis cinerea* activate defense responses in *Physcomitrella patens*. *BMC Plant Biology*, *7*, 52. https://doi.org/10.1186/1471-2229-7-52

Ponce de León, I. (2011). The moss *Physcomitrella patens* as a model system to study interactions between plants and phytopathogenic fungi and oomycetes. *Journal of Pathogens*; Hindawi. https://doi.org/10.4061/2011/719873

Possart, A., & Hiltbrunner, A. (2013). An evolutionarily conserved signaling mechanism mediates far-red light responses in land plants. *The Plant Cell*, *25*(1), 102–114. https://doi.org/10.1105/tpc.112.104331

Possart, A., Xu, T., Paik, I., Hanke, S., Keim, S., Hermann, H.-M., Wolf, L., Hiß, M., Becker, C., Huq, E., Rensing, S. A., & Hiltbrunner, A. (2017). Characterization of phytochrome interacting factors from the moss *Physcomitrella patens* illustrates conservation of phytochrome signaling modules in land plants. *The Plant Cell*, *29*(2), 310–330. https://doi.org/10.1105/tpc.16.00388

Prigge, M. J., Lavy, M., Ashton, N. W., & Estelle, M. (2010). *Physcomitrella patens* auxin-resistant mutants affect conserved elements of an auxin-signaling pathway. *Current Biology: CB*, *20*, 1907–1912. https://doi.org/10.1016/j.cub.2010.08.050

Pysh, L. D., Wysocka-Diller, J. W., Camilleri, C., Bouchez, D., & Benfey, P. N. (1999). The GRAS gene family in *Arabidopsis*: Sequence characterization and basic expression analysis of the SCARECROW-LIKE genes. *The Plant*

Journal: For Cell and Molecular Biology, *18*, 111–119. https://doi.org/10.1046/j.1365-313x.1999.00431.x
Qaim, M., & Kouser, S. (2013). Genetically modified crops and food security. *PLOS ONE*, *8*, e64879. https://doi.org/10.1371/journal.pone.0064879
Qi, T., Huang, H., Wu, D., Yan, J., Qi, Y., Song, S., & Xie, D. (2014). *Arabidopsis* DELLA and JAZ proteins bind the WD-Repeat/bHLH/MYB complex to modulate gibberellin and jasmonate signaling synergy. *The Plant Cell*, *26*, 1118–1133. https://doi.org/10.1105/tpc.113.121731
Quail, P. H., Boylan, M. T., Parks, B. M., Short, T. W., Xu, Y., & Wagner, D. (1995). *Phytochromes: photosensory perception and signal transduction*. *268*, 7.
Ranjan, A., Dickopf, S., Ullrich, K. K., Rensing, S. A., & Hoecker, U. (2014). Functional analysis of COP1 and SPA orthologs from *Physcomitrella* and rice during photomorphogenesis of transgenic *Arabidopsis* reveals distinct evolutionary conservation. *BMC Plant Biology*, *14*, 178. https://doi.org/10.1186/1471-2229-14-178
Ravindran, P., Verma, V., Stamm, P., & Kumar, P. P. (2017). A Novel RGL2–DOF6 complex contributes to primary seed dormancy in *Arabidopsis thaliana* by regulating a GATA transcription factor. *Molecular Plant*, *10*, 1307–1320. https://doi.org/10.1016/j.molp.2017.09.004
Reboledo, G., Agorio, A.d., Vignale, L., Batista-García, R.A., Ponce de León, I (2021). Transcriptional profiling reveals conserved and species-specific plant defense responses during the interaction of *Physcomitrium patens* with *Botrytis cinerea*. *Plant Mol Biol*. https://doi.org/10.1007/s11103-021-01116-0
Rensing, S. A., Lang, D., Zimmer, A. D., Terry, A., Salamov, A., Shapiro, H., Nishiyama, T., Perroud, P.-F., Lindquist, E. A., Kamisugi, Y., Tanahashi, T., Sakakibara, K., Fujita, T., Oishi, K., Shin-I, T., Kuroki, Y., Toyoda, A., Suzuki, Y., Hashimoto, S., … Boore, J. L. (2008). The *Physcomitrella* genome reveals evolutionary insights into the conquest of land by plants. *Science*, *319*, 64–69. https://doi.org/10.1126/science.1150646
Rensing, S. A., Goffinet, B., Meyberg, R., Wu, S.-Z., & Bezanilla, M. (2020). The moss *Physcomitrium* (*Physcomitrella*) *patens*: A model organism for non-seed plants. *The Plant Cell*, *32*, 1361–1376. https://doi.org/10.1105/tpc.19.00828
Ribeiro, D. M., Araújo, W. L., Fernie, A. R., Schippers, J. H. M., & Mueller-Roeber, B. (2012). Action of gibberellins on growth and metabolism of Arabidopsis plants associated with high concentration of carbon dioxide. *Plant Physiology*, *160*, 1781–1794. https://doi.org/10.1104/pp.112.204842
Sall, K., Dekkers, B. J. W., Nonogaki, M., Katsuragawa, Y., Koyari, R., Hendrix, D., Willems, L. A. J., Bentsink, L., & Nonogaki, H. (2019). DELAY OF GERMINATION 1-LIKE 4 acts as an inducer of seed reserve accumulation. *The Plant Journal*, *100*(1), 7–19. https://doi.org/10.1111/tpj.14485
Sánchez-Fernández, R., Ardiles-Díaz, W., Montagu, M. V., Inzé, D., & May, M. J. (1998). Cloning of a novel *Arabidopsis thaliana* RGA-like gene, a putative member of the VHIID-domain transcription factor family. *Journal of Experimental Botany*, *49*, 1609–1610. https://doi.org/10.1093/jxb/49.326.1609
Sánchez-Montesino, R., Bouza-Morcillo, L., Marquez, J., Ghita, M., Duran-Nebreda, S., Gómez, L., Holdsworth, M. J., Bassel, G., & Oñate-Sánchez, L. (2019). A regulatory module controlling GA-mediated endosperm cell expansion is

critical for seed germination in Arabidopsis. *Molecular Plant*, *12*(1), 71–85. https://doi.org/10.1016/j.molp.2018.10.009
Sasaki, A., Itoh, H., Gomi, K., Ueguchi-Tanaka, M., Ishiyama, K., Kobayashi, M., Jeong, D.-H., An, G., Kitano, H., Ashikari, M., & Matsuoka, M. (2003). Accumulation of phosphorylated repressor for gibberellin signaling in an F-box mutant. *Science*, *299*, 1896–1898. https://doi.org/10.1126/science.1081077
Schaefer, D., Zryd, J.-P., Knight, C. D., & Cove, D. J. (1991). Stable transformation of the moss *Physcomitrella patens*. *Molecular and General Genetics MGG*, *226*(3), 418–424. https://doi.org/10.1007/BF00260654
Schaefer, D. G. (2002). A new moss genetics: Targeted mutagenesis in Physcomitrella patens. *Annual Review of Plant Biology*, *53*, 477–501. https://doi.org/10.1146/annurev.arplant.53.100301.135202
Seo, M., Hanada, A., Kuwahara, A., Endo, A., Okamoto, M., Yamauchi, Y., North, H., Marion-Poll, A., Sun, T., Koshiba, T., Kamiya, Y., Yamaguchi, S., & Nambara, E. (2006). Regulation of hormone metabolism in Arabidopsis seeds: phytochrome regulation of abscisic acid metabolism and abscisic acid regulation of gibberellin metabolism. *The Plant Journal*, *48*(3), 354–366. https://doi.org/10.1111/j.1365-313X.2006.02881.x
Shibaya, T., & Sugawara, Y. (2007). Involvement of arabinogalactan proteins in the regeneration process of cultured protoplasts of *Marchantia polymorpha*. *Physiologia Plantarum*, *130*, 271–279. https://doi.org/10.1111/j.1399-3054.2007.00905.x
Shimada, A., Ueguchi-Tanaka, M., Nakatsu, T., Nakajima, M., Naoe, Y., Ohmiya, H., Kato, H., & Matsuoka, M. (2008). Structural basis for gibberellin recognition by its receptor GID1. *Nature*, *456*, 520–523. https://doi.org/10.1038/nature07546
Silverstone, A. L., Mak, P. Y., Martínez, E. C., & Sun, T. P. (1997). The new RGA locus encodes a negative regulator of gibberellin response in *Arabidopsis thaliana*. *Genetics*, *146*, 1087–1099.
Silverstone, A. L., Ciampaglio, C. N., & Sun, T. (1998). The *Arabidopsis* RGA gene encodes a transcriptional regulator repressing the gibberellin signal transduction pathway. *The Plant Cell*, *10*, 155–169. https://doi.org/10.1105/tpc.10.2.155
Smaczniak, C., Li, N., Boeren, S., America, T., van Dongen, W., Goerdayal, S. S., de Vries, S., Angenent, G. C., & Kaufmann, K. (2012). Proteomics-based identification of low-abundance signaling and regulatory protein complexes in native plant tissues. *Nature Protocols*, *7*(12), 2144–2158. https://doi.org/10.1038/nprot.2012.129
Smith, P., & Gregory, P. J. (2013). Climate change and sustainable food production. *Proceedings of the Nutrition Society*, *72*, 21–28. https://doi.org/10.1017/S0029665112002832
Sparkes, I. A., Runions, J., Kearns, A., & Hawes, C. (2006). Rapid, transient expression of fluorescent fusion proteins in tobacco plants and generation of stably transformed plants. *Nature Protocols*, *1*(4), 2019–2025. https://doi.org/10.1038/nprot.2006.286
Stamm, P., Ravindran, P., Mohanty, B., Tan, E. L., Yu, H., & Kumar, P. P. (2012). Insights into the molecular mechanism of RGL2-mediated inhibition of seed germination in *Arabidopsis thaliana*. *BMC Plant Biology*, *12*(1), 179. https://doi.org/10.1186/1471-2229-12-179

Stewart, J. L., Maloof, J. N., & Nemhauser, J. L. (2011). PIF genes mediate the effect of sucrose on seedling growth dynamics. *PLOS ONE*, *6*(5), e19894. https://doi.org/10.1371/journal.pone.0019894

Tanaka, J., Yano, K., Aya, K., Hirano, K., Takehara, S., Koketsu, E., Ordonio, R. L., Park, S.-H., Nakajima, M., Ueguchi-Tanaka, M., & Matsuoka, M. (2014). Antheridiogen determines sex in ferns via a spatiotemporally split gibberellin synthesis pathway. *Science*, *346*, 469–473. https://doi.org/10.1126/science.1259923

Tao, S., & Estelle, M. (2018). Mutational studies of the Aux/IAA proteins in *Physcomitrella* reveal novel insights into their function. *The New Phytologist*, *218*, 1534–1542. https://doi.org/10.1111/nph.15039

The Royal Society (London). (2009). *Reaping the benefits science and the sustainable intensification of global agriculture*. The Royal Society.

Thornton, J. W. (2001). Evolution of vertebrate steroid receptors from an ancestral estrogen receptor by ligand exploitation and serial genome expansions. *Proceedings of the National Academy of Sciences*, *98*, 5671–5676. https://doi.org/10.1073/pnas.091553298

Tian, F., Yang, D.C., Meng, Y.Q., Jin, J. and Gao, G. (2020). PlantRegMap: charting functional regulatory maps in plants. *Nucleic Acids Res*, *48*, D1104-D1113.

Toh, S., Imamura, A., Watanabe, A., Nakabayashi, K., Okamoto, M., Jikumaru, Y., Hanada, A., Aso, Y., Ishiyama, K., Tamura, N., Iuchi, S., Kobayashi, M., Yamaguchi, S., Kamiya, Y., Nambara, E., & Kawakami, N. (2008). High temperature-induced abscisic acid biosynthesis and its role in the inhibition of gibberellin action in Arabidopsis seeds. *Plant Physiology*, *146*(3), 1368–1385. https://doi.org/10.1104/pp.107.113738

Toh, S., Kamiya, Y., Kawakami, N., Nambara, E., McCourt, P., & Tsuchiya, Y. (2012). Thermoinhibition uncovers a role for strigolactones in Arabidopsis seed germination. *Plant and Cell Physiology*, *53*(1), 107–117. https://doi.org/10.1093/pcp/pcr176

Ueguchi-Tanaka, M., Ashikari, M., Nakajima, M., Itoh, H., Katoh, E., Kobayashi, M., Chow, T., Hsing, Y. C., Kitano, H., Yamaguchi, I., & Matsuoka, M. (2005). GIBBERELLIN INSENSITIVE DWARF1 encodes a soluble receptor for gibberellin. *Nature*, *437*, 693–698. https://doi.org/10.1038/nature04028

Ueguchi-Tanaka, M., Nakajima, M., Katoh, E., Ohmiya, H., Asano, K., Saji, S., Hongyu, X., Ashikari, M., Kitano, H., Yamaguchi, I., & Matsuoka, M. (2007). Molecular interactions of a soluble gibberellin receptor, GID1, with a rice DELLA protein, SLR1, and gibberellin. *The Plant Cell*, *19*, 2140–2155. https://doi.org/10.1105/tpc.106.043729

Van De Velde, K., Ruelens, P., Geuten, K., Rohde, A., & Van Der Straeten, D. (2017). Exploiting DELLA signaling in cereals. *Trends in Plant Science*, *22*, 880–893. https://doi.org/10.1016/j.tplants.2017.07.010

Van De Velde, K., Thomas, S. G., Heyse, F., Kaspar, R., Van Der Straeten, D., & Rohde, A. (2021). N-terminal truncated RHT-1 proteins generated by translational reinitiation cause semi-dwarfing of wheat Green Revolution alleles. *Molecular Plant*. https://doi.org/10.1016/j.molp.2021.01.002

Vesty, E. F., Saidi, Y., Moody, L. A., Holloway, D., Whitbread, A., Needs, S., Choudhary, A., Burns, B., McLeod, D., Bradshaw, S. J., Bae, H., King, B. C., Bassel, G. W., Simonsen, H. T., & Coates, J. C. (2016). The decision to

germinate is regulated by divergent molecular networks in spores and seeds. *New Phytologist*, *211*(3), 952–966. https://doi.org/10.1111/nph.14018

Vo, K. T. X., Kim, C.-Y., Chandran, A. K. N., Jung, K.-H., An, G., & Jeon, J.-S. (2015). Molecular insights into the function of ankyrin proteins in plants. *Journal of Plant Biology*, *58*(5), 271–284. https://doi.org/10.1007/s12374-015-0228-0

Wang, F., Zhu, D., Huang, X., Li, S., Gong, Y., Yao, Q., Fu, X., Fan, L.-M., & Deng, X. W. (2009). Biochemical insights on degradation of *Arabidopsis* DELLA proteins gained from a cell-free assay system. *The Plant Cell*, *21*, 2378–2390. https://doi.org/10.1105/tpc.108.065433

Wang, W., Zhang, J., Qin, Q., Yue, J., Huang, B., Xu, X., Yan, L., & Hou, S. (2014). The six conserved serine/threonine sites of REPRESSOR OF ga1-3 protein are important for its functionality and stability in gibberellin signaling in *Arabidopsis*. *Planta*, *240*, 763–779. https://doi.org/10.1007/s00425-014-2113-3

Wang, Z., Liu, L., Cheng, C., Ren, Z., Xu, S., & Li, X. (2020). GAI functions in the plant response to dehydration stress in *Arabidopsis thaliana*. *International Journal of Molecular Sciences*, *21*(3). https://doi.org/10.3390/ijms21030819

Weitbrecht, K., Müller, K., & Leubner-Metzger, G. (2011). First off the mark: Early seed germination. *Journal of Experimental Botany*, *62*(10), 3289–3309. https://doi.org/10.1093/jxb/err030

Wen, C.-K., & Chang, C. (2002). *Arabidopsis* RGL1 encodes a negative regulator of gibberellin responses. *The Plant Cell*, *14*, 87–100. https://doi.org/10.1105/tpc.010325

Wu, J., Yan, G., Duan, Z., Wang, Z., Kang, C., Guo, L., Liu, K., Tu, J., Shen, J., Yi, B., Fu, T., Li, X., Ma, C., & Dai, C. (2020). Roles of the *Brassica napus* DELLA protein BnaA6.RGA, in modulating drought tolerance by interacting with the ABA signaling component BnaA10.ABF2. *Frontiers in Plant Science*, *11*. https://doi.org/10.3389/fpls.2020.00577

Xu, F., & Copeland, C. (2012). Nuclear extraction from *Arabidopsis thaliana*. *Bio-Protocol*, *2*(24), e306–e306.

Yan, J., Li, X., Zeng, B., Zhong, M., Yang, J., Yang, P., Li, X., He, C., Lin, J., Liu, X., & Zhao, X. (2020). FKF1 F-box protein promotes flowering in part by negatively regulating DELLA protein stability under long-day photoperiod in *Arabidopsis*. *Journal of Integrative Plant Biology*. https://doi.org/10.1111/jipb.12971

Yang, D., Seaton, D. D., Krahmer, J., & Halliday, K. J. (2016). Photoreceptor effects on plant biomass, resource allocation, and metabolic state. *Proceedings of the National Academy of Sciences*, *113*(27), 7667–7672. https://doi.org/10.1073/pnas.1601309113

Yasumura, Y., Moylan, E. C., & Langdale, J. A. (2005). A conserved transcription factor mediates nuclear control of organelle biogenesis in anciently diverged land plants. *The Plant Cell*, *17*(7), 1894–1907. https://doi.org/10.1105/tpc.105.033191

Yasumura, Y., Crumpton-Taylor, M., Fuentes, S., & Harberd, N. P. (2007). Step-by-step acquisition of the gibberellin-DELLA growth-regulatory mechanism during land-plant evolution. *Current Biology*, *17*, 1225–1230. https://doi.org/10.1016/j.cub.2007.06.037

Ye, Y., Liu, B., Zhao, M., Wu, K., Cheng, W., Chen, X., Liu, Q., Liu, Z., Fu, X., & Wu, Y. (2015). CEF1/OsMYB103L is involved in GA-mediated regulation of secondary wall biosynthesis in rice. *Plant Molecular Biology*, *89*(4), 385–401. https://doi.org/10.1007/s11103-015-0376-0

Yoshida, H., Tanimoto, E., Hirai, T., Miyanoiri, Y., Mitani, R., Kawamura, M., Takeda, M., Takehara, S., Hirano, K., Kainosho, M., Akagi, T., Matsuoka, M., & Ueguchi-Tanaka, M. (2018). Evolution and diversification of the plant gibberellin receptor GID1. *Proceedings of the National Academy of Sciences*, *115*, E7844–E7853. https://doi.org/10.1073/pnas.1806040115

Yu, S., Galvão, V. C., Zhang, Y.-C., Horrer, D., Zhang, T.-Q., Hao, Y.-H., Feng, Y.-Q., Wang, S., Schmid, M., & Wang, J.-W. (2012). Gibberellin regulates the *Arabidopsis* floral transition through miR156-targeted SQUAMOSA PROMOTER BINDING–LIKE transcription factors. *The Plant Cell*, *24*, 3320–3332. https://doi.org/10.1105/tpc.112.101014

Zentella, R., Zhang, Z.-L., Park, M., Thomas, S. G., Endo, A., Murase, K., Fleet, C. M., Jikumaru, Y., Nambara, E., Kamiya, Y., & Sun, T.-P. (2007). Global analysis of DELLA direct targets in early gibberellin signaling in *Arabidopsis*. *The Plant Cell*, *19*, 3037–3057. https://doi.org/10.1105/tpc.107.054999

Zentella, R., Hu, J., Hsieh, W.-P., Matsumoto, P. A., Dawdy, A., Barnhill, B., Oldenhof, H., Hartweck, L. M., Maitra, S., Thomas, S. G., Cockrell, S., Boyce, M., Shabanowitz, J., Hunt, D. F., Olszewski, N. E., & Sun, T. (2016). O-GlcNAcylation of master growth repressor DELLA by SECRET AGENT modulates multiple signaling pathways in *Arabidopsis*. *Genes & Development*, *30*, 164–176. https://doi.org/10.1101/gad.270587.115

Zentella, R., Sui, N., Barnhill, B., Hsieh, W.-P., Hu, J., Shabanowitz, J., Boyce, M., Olszewski, N. E., Zhou, P., Hunt, D. F., & Sun, T. (2017). The *Arabidopsis* O-fucosyltransferase SPINDLY activates nuclear growth repressor DELLA. *Nature Chemical Biology*, *13*, 479–485. https://doi.org/10.1038/nchembio.2320

Zhang, D., Jing, Y., Jiang, Z., & Lin, R. (2014). The chromatin-remodeling factor PICKLE integrates brassinosteroid and gibberellin signaling during skotomorphogenic growth in Arabidopsis. *The Plant Cell*, *26*, 2472–2485. https://doi.org/10.1105/tpc.113.121848

CHAPTER 8: Appendix

Recipes for growth media and buffers

BCD minimal growth medium (per 1L)

250mg $MgSO_4$-$7H_2O$

250mg KH_2PO_4 (pH 6.5)

1.010g KNO_3

12.5mg $FeSO_4$-$7H_2O$

0.001% Trace Element Solution

0.8% plant agar (only for solid medium)

Trace Element Solution (per 1L; 1000x)

0.614mg H_3BO_3

0.055mg $AlK(SO_4)_2$-$12H_2O$

0.055mg $CuSO_4$-$5H_2O$

0.028mg KBr

0.028mg LiCl

0.389mg $MnCl_2$-$4H_2O$

0.055mg $CoCl_2$-$6H_2O$

0.055mg $ZnSO_4$-$7H_2O$

0.028mg KI

0.028mg $SnCl_2$-$2H_2O$

LB liquid

10g bacto-tryptone

5g bacto-yeast extract

10g NaCl

to 1L dH_2O

LB agar

10g bacto-tryptone

5g bacto-yeast extract

10g NaCl

15g bacto-agar

to 1L dH_2O

Low salt LB liquid

10g bacto-tryptone

5g bacto-yeast extract

5g NaCl

to 1L dH_2O

Low salt LB agar

10g bacto-tryptone

5g bacto-yeast extract

5g NaCl

15g bacto-agar

to 1L dH_2O

Yeast Drop-Out -LW medium

1.54g/L Drop-Out (–Leu-Trp) (Formedium™)

6.7g/L Yeast Nitrogen Base without amino acids

Agar 2% (only for solid medium)

After autoclaving, supplement with filter sterilised glucose (10g/L)

Yeast Drop-Out -HLW medium

1.47g/L Drop-Out (-His-Leu-Trp) (Formedium™)

6.7g/L Yeast Nitrogen Base without amino acids

Agar 2%

After autoclaving, supplement with filter sterilised glucose (10g/L)

Yeast Drop-Out -AHLW

1.452g/L Drop-Out (-Ade-His-Leu-Trp) (Formedium™)

6.7g/L Yeast Nitrogen Base without amino acids

Agar 2%

After autoclaving, supplement with filter sterilised glucose (10g/L)

Laemmli buffer (5x)

67.5% (v/v) Tris-HCl (2M, pH6.8)

10% (w/v) SDS

50% (w/v) glycerol

5% β-mercaptoethanol

0.005% (w/v) bromophenol blue

Alignment of land plant DELLA proteins

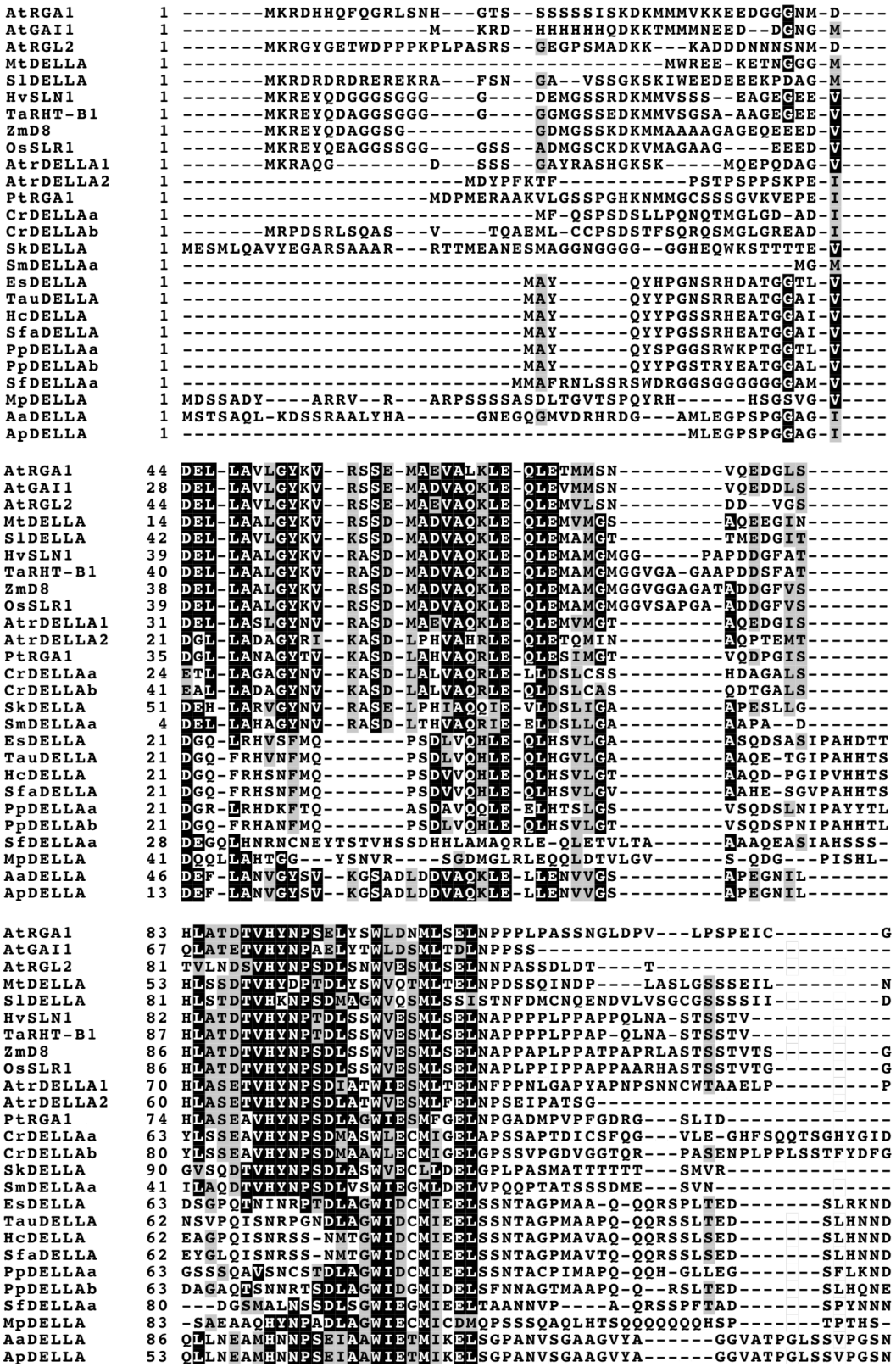

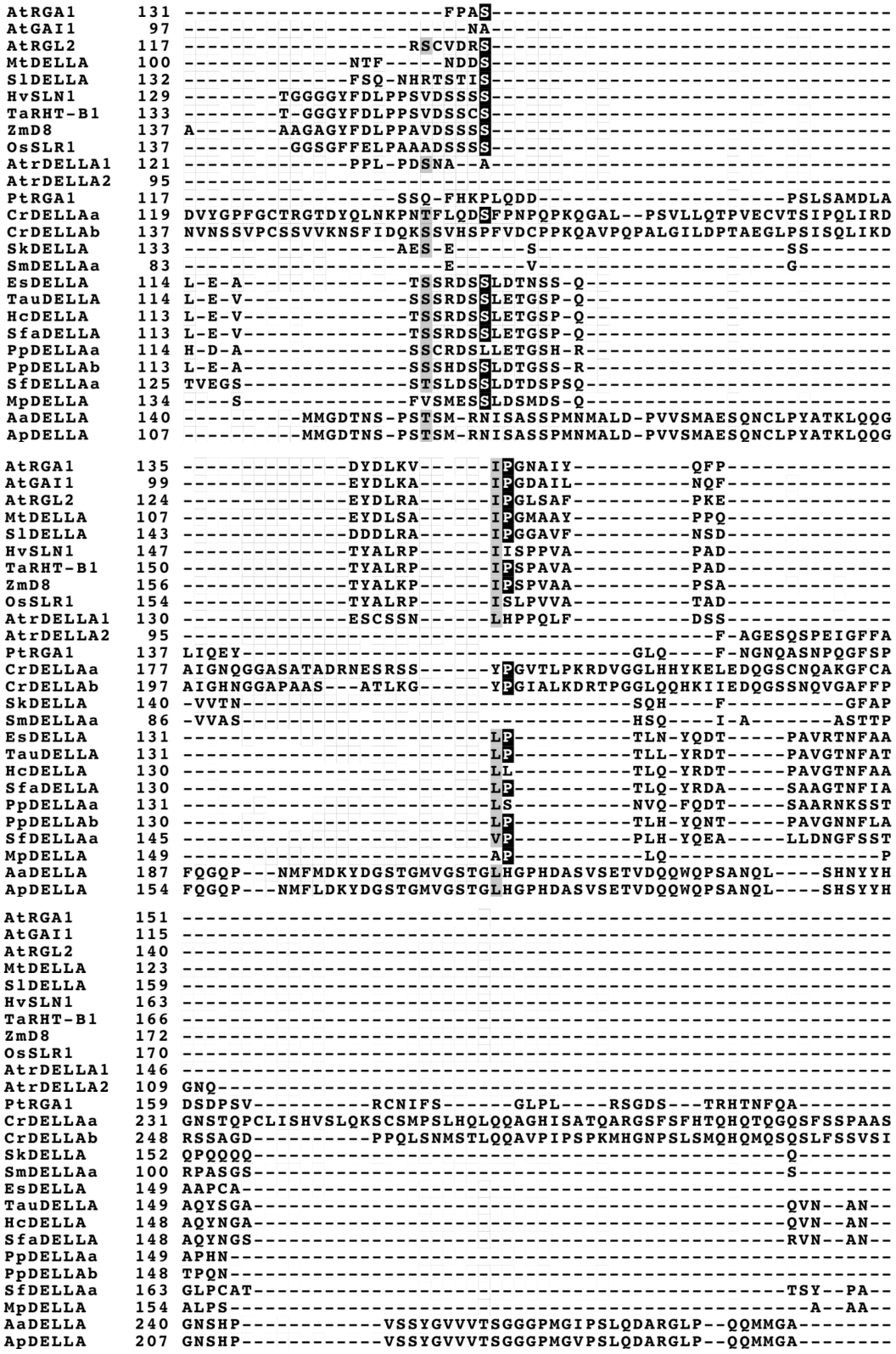
AtRGA1 131 ----------FPAS----------
AtGAI1 97 ----------NA----------
AtRGL2 117 ----------RSCVDRS----------
MtDELLA 100 ----------NTF-----NDDS----------
SlDELLA 132 ----------FSQ-NHRTSTIS----------
HvSLN1 129 --------TGGGGYFDLPPSVDSSSS----------
TaRHT-B1 133 --------T-GGGYFDLPPSVDSSCS----------
ZmD8 137 A--------AAGAGYFDLPPAVDSSSS----------
OsSLR1 137 ----------GGSGFFELPAAADSSSS----------
AtrDELLA1 121 ----------PPL-PDSNA--A----------
AtrDELLA2 95 ----------
PtRGA1 117 ----------SSQ-FHKPLQDD----------PSLSAMDLA
CrDELLAa 119 DVYGPFGCTRGTDYQLNKPNTFLQDSFPNPQPKQGAL--PSVLLQTPVECVTSIPQLIRD
CrDELLAb 137 NVNSSVPCSSVVKNSFIDQKSSVHSPFVDCPPKQAVPQPALGILDPTAEGLPSISQLIKD
SkDELLA 133 ----------AES-E------S----------SS-------
SmDELLAa 83 ----------E------V----------G--------
EsDELLA 114 L-E-A----------TSSRDSSLDTNSS-Q----------
TauDELLA 114 L-E-V----------SSSRDSSLETGSP-Q----------
HcDELLA 113 L-E-V----------TSSRDSSLETGSP-Q----------
SfaDELLA 113 L-E-V----------TSSRDSSLETGSP-Q----------
PpDELLAa 114 H-D-A----------SSCRDSLLETGSH-R----------
PpDELLAb 113 L-E-A----------SSSHDSSLDTGSS-R----------
SfDELLAa 125 TVEGS----------STSLDSSLDTDSPSQ----------
MpDELLA 134 ----S----------FVSMESSLDSMDS-Q----------
AaDELLA 140 ----------MMGDTNS-PSTSM-RNISASSPMNMALD-PVVSMAESQNCLPYATKLQQG
ApDELLA 107 ----------MMGDTNS-PSTSM-RNISASSPMNMALD-PVVSMAESQNCLPYATKLQQG
AtRGA1 135 ----------DYDLKV------IPGNAIY----------QFP----------
AtGAI1 99 ----------EYDLKA------IPGDAIL----------NQF----------
AtRGL2 124 ----------EYDLRA------IPGLSAF----------PKE----------
MtDELLA 107 ----------EYDLSA------IPGMAAY----------PPQ----------
SlDELLA 143 ----------DDDLRA------IPGGAVF----------NSD----------
HvSLN1 147 ----------TYALRP------IISPPVA----------PAD----------
TaRHT-B1 150 ----------TYALRP------IPSPAVA----------PAD----------
ZmD8 156 ----------TYALKP------IPSPVAA----------PSA----------
OsSLR1 154 ----------TYALRP------ISLPVVA----------TAD----------
AtrDELLA1 130 ----------ESCSSN------LHPPQLF----------DSS----------
AtrDELLA2 95 ----------F-AGESQSPEIGFFA
PtRGA1 137 LIQEY----------GLQ----F-NGNQASNPQGFSP
CrDELLAa 177 AIGNQGGASATADRNESRSS------YPGVTLPKRDVGGLHHYKELEDQGSCNQAKGFCA
CrDELLAb 197 AIGHNGGAPAAS---ATLKG------YPGIALKDRTPGGLQQHKIIEDQGSSNQVGAFFP
SkDELLA 140 -VVTN----------SQH----F----------GFAP
SmDELLAa 86 -VVAS----------HSQ----I-A-------ASTTP
EsDELLA 131 ----------LP----------TLN-YQDT-----PAVRTNFAA
TauDELLA 131 ----------LP----------TLL-YRDT-----PAVGTNFAT
HcDELLA 130 ----------LL----------TLQ-YRDT-----PAVGTNFAA
SfaDELLA 130 ----------LP----------TLQ-YRDA-----SAAGTNFIA
PpDELLAa 131 ----------LS----------NVQ-FQDT-----SAARNKSST
PpDELLAb 130 ----------LP----------TLH-YQNT-----PAVGNNFLA
SfDELLAa 145 ----------VP----------PLH-YQEA-----LLDNGFSST
MpDELLA 149 ----------AP----------LQ----------P
AaDELLA 187 FQGQP---NMFMDKYDGSTGMVGSTGLHGPHDASVSETVDQQWQPSANQL----SHNYYH
ApDELLA 154 FQGQP---NMFLDKYDGSTGMVGSTGLHGPHDASVSETVDQQWQPSANQL----SHSYYH
AtRGA1 151 ----------
AtGAI1 115 ----------
AtRGL2 140 ----------
MtDELLA 123 ----------
SlDELLA 159 ----------
HvSLN1 163 ----------
TaRHT-B1 166 ----------
ZmD8 172 ----------
OsSLR1 170 ----------
AtrDELLA1 146 ----------
AtrDELLA2 109 GNQ----------
PtRGA1 159 DSDPSV----------RCNIFS------GLPL----RSGDS---TRHTNFQA---------
CrDELLAa 231 GNSTQPCLISHVSLQKSCSMPSLHQLQQAGHISATQARGSFSFHTQHQTQGQSFSSPAAS
CrDELLAb 248 RSSAGD----------PPQLSNMSTLQQAVPIPSPKMHGNPSLSMQHQMQSQSLFSSVSI
SkDELLA 152 QPQQQQ----------Q---------
SmDELLAa 100 RPASGS----------S---------
EsDELLA 149 AAPCA----------
TauDELLA 149 AQYSGA----------QVN--AN--
HcDELLA 148 AQYNGA----------QVN--AN--
SfaDELLA 148 AQYNGS----------RVN--AN--
PpDELLAa 149 APHN----------
PpDELLAb 148 TPQN----------
SfDELLAa 163 GLPCAT----------TSY--PA--
MpDELLA 154 ALPS----------A--AA--
AaDELLA 240 GNSHP----------VSSYGVVVTSGGGPMGIPSLQDARGLP--QQMMGA---------
ApDELLA 207 GNSHP----------VSSYGVVVTSGGGPMGVPSLQDARGLP--QQMMGA---------

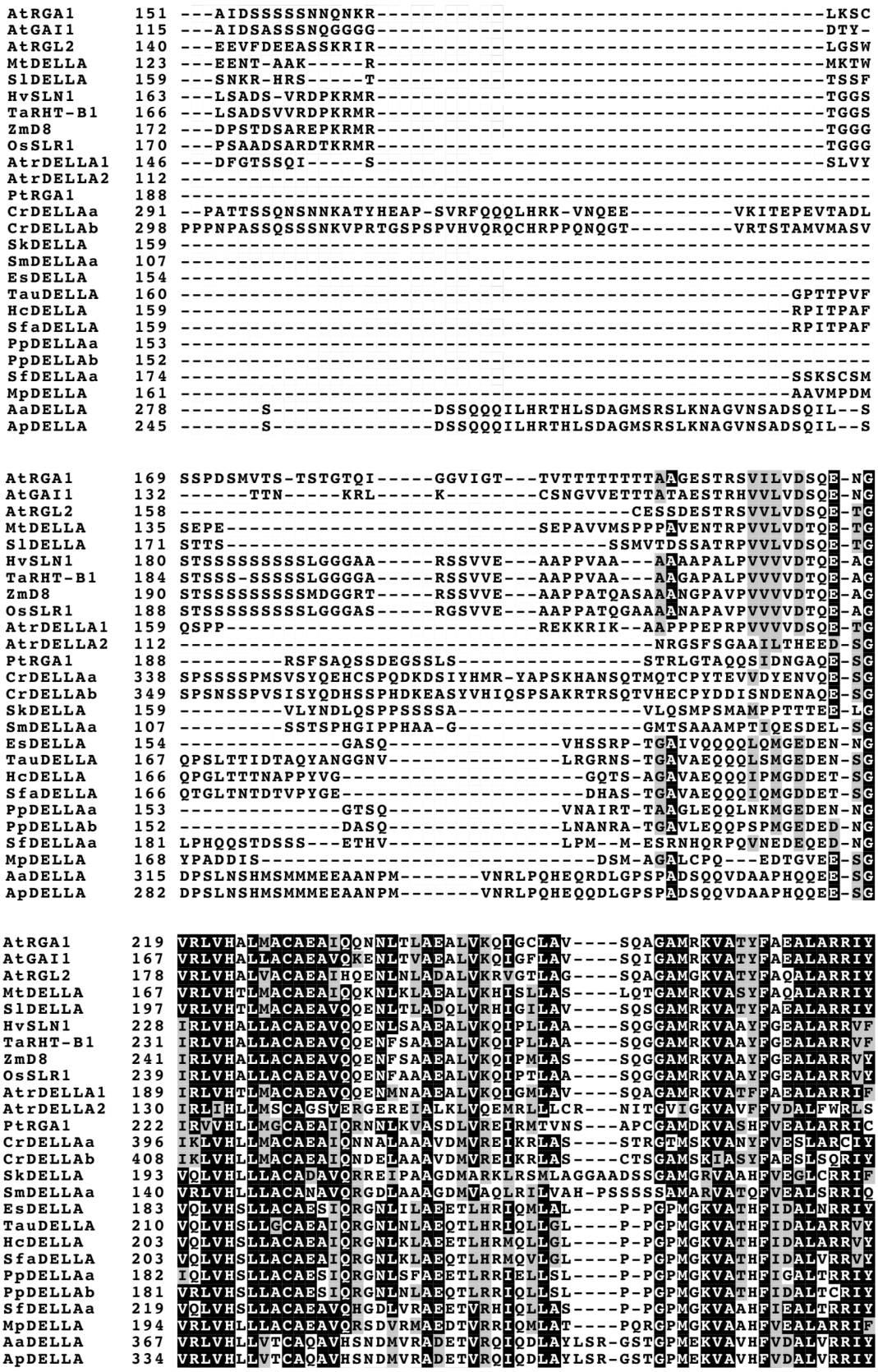
AtRGA1 151 ---AIDSSSSSNNQNKR----------LKSC
AtGAI1 115 ---AIDSASSSNQGGGG----------DTY-
AtRGL2 140 ---EEVFDEEASSKRIR----------LGSW
MtDELLA 123 ---EENT-AAK-----R----------MKTW
SlDELLA 159 ---SNKR-HRS-----T----------TSSF
HvSLN1 163 ---LSADS-VRDPKRMR----------TGGS
TaRHT-B1 166 ---LSADSVVRDPKRMR----------TGGS
ZmD8 172 ---DPSTDSAREPKRMR----------TGGG
OsSLR1 170 ---PSAADSARDTKRMR----------TGGG
AtrDELLA1 146 ---DFGTSSQI-----S----------SLVY
AtrDELLA2 112 ----------
PtRGA1 188 ----------
CrDELLAa 291 --PATTSSQNSNNKATYHEAP-SVRFQQQLHRK-VNQEE---------VKITEPEVTADL
CrDELLAb 298 PPPNPASSQSSSNKVPRTGSPSPVHVQRQCHRPPQNQGT---------VRTSTAMVMASV
SkDELLA 159 ----------
SmDELLAa 107 ----------
EsDELLA 154 ----------
TauDELLA 160 ----------GPTTPVF
HcDELLA 159 ----------RPITPAF
SfaDELLA 159 ----------RPITPAF
PpDELLAa 153 ----------
PpDELLAb 152 ----------
SfDELLAa 174 ----------SSKSCSM
MpDELLA 161 ----------AAVMPDM
AaDELLA 278 -------S--------------DSSQQQILHRTHLSDAGMSRSLKNAGVNSADSQIL--S
ApDELLA 245 -------S--------------DSSQQQILHRTHLSDAGMSRSLKNAGVNSADSQIL--S
AtRGA1 169 SSPDSMVTS-TSTGTQI-----GGVIGT---TVTTTTTTTTAAGESTRSVILVDSQE-NG
AtGAI1 132 ------TTN-----KRL-----K--------CSNGVVETTTATAESTRHVVLVDSQE-NG
AtRGL2 158 ----------CESSDESTRSVVLVDSQE-TG
MtDELLA 135 SEPE----------SEPAVVMSPPPAVENTRPVVLVDTQE-TG
SlDELLA 171 STTS----------SSMVTDSSATRPVVLVDSQE-TG
HvSLN1 180 STSSSSSSSSSLGGGAA-----RSSVVE---AAPPVAA---AAAAPALPVVVVDTQE-AG
TaRHT-B1 184 STSSS-SSSSSLGGGGA-----RSSVVE---AAPPVAA---AAGAPALPVVVVDTQE-AG
ZmD8 190 STSSSSSSSSSMDGGRT-----RSSVVE---AAPPATQASAAANGPAVPVVVVDTQE-AG
OsSLR1 188 STSSSSSSSSSLGGGAS-----RGSVVE---AAPPATQGAAAANAPAVPVVVVDTQE-AG
AtrDELLA1 159 QSPP----------REKKRIK--AAPPPEPRPVVVVDSQE-TG
AtrDELLA2 112 ----------NRGSFSGAAILTHEED-SG
PtRGA1 188 ---------RSFSAQSSDEGSSLS----------STRLGTAQQSIDNGAQE-SG
CrDELLAa 338 SPSSSSPMSVSYQEHCSPQDKDSIYHMR-YAPSKHANSQTMQTCPYTEVVDYENVQE-SG
CrDELLAb 349 SPSNSSPVSISYQDHSSPHDKEASYVHIQSPSAKRTRSQTVHECPYDDISNDENAQE-SG
SkDELLA 159 ---------VLYNDLQSPPSSSSA----------VLQSMPSMAMPPTTTEE-LG
SmDELLAa 107 ---------SSTSPHGIPPHAA-G----------GMTSAAAMPTIQESDEL-SG
EsDELLA 154 ----------GASQ----------VHSSRP-TGAIVQQQQLQMGEDEN-NG
TauDELLA 167 QPSLTTIDTAQYANGGNV----------LRGRNS-TGAVAEQQQLSMGEDEN-SG
HcDELLA 166 QPGLTTTNAPPYVG----------GQTS-AGAVAEQQQIPMGDDET-SG
SfaDELLA 166 QTGLTNTDTVPYGE----------DHAS-TGAVAEQQQIQMGDDET-SG
PpDELLAa 153 ----------GTSQ----------VNAIRT-TAAGLEQQLNKMGEDEN-NG
PpDELLAb 152 ----------DASQ----------LNANRA-TGAVLEQQPSPMGEDED-NG
SfDELLAa 181 LPHQQSTDSSS---ETHV----------LPM--M-ESRNHQRPQVNEDEQED-NG
MpDELLA 168 YPADDIS----------DSM-AGALCPQ---EDTGVEE-SG
AaDELLA 315 DPSLNSHMSMMMEEAANPM-------VNRLPQHEQRDLGPSPADSQQVDAAPHQQEE-SG
ApDELLA 282 DPSLNSHMSMMMEEAANPM-------VNRLPQHEQQDLGPSPADSQQVDAAPHQQEE-SG
AtRGA1 219 VRLVHALMACAEAIQQNNLTLAEALVKQIGCLAV----SQAGAMRKVATYFAEALARRIY
AtGAI1 167 VRLVHALLACAEAVQKENLTVAEALVKQIGFLAV----SQIGAMRKVATYFAEALARRIY
AtRGL2 178 VRLVHALVACAEAIHQENLNLADALVKRVGTLAG----SQAGAMGKVATYFAQALARRIY
MtDELLA 167 VRLVHTLMACAEAIQQKNLKLAEALVKHISLLAS----LQTGAMRKVASYFAQALARRIY
SlDELLA 197 VRLVHTLMACAEAVQQENLTLADQLVRHIGILAV----SQSGAMRKVATYFAEALARRIY
HvSLN1 228 IRLVHALLACAEAVQQENLSAAEALVKQIPLLAA----SQGGAMRKVAAYFGEALARRVF
TaRHT-B1 231 IRLVHALLACAEAVQQENFSAAEALVKQIPLLAA----SQGGAMRKVAAYFGEALARRVF
ZmD8 241 IRLVHALLACAEAVQQENFSAAEALVKQIPMLAS----SQGGAMRKVAAYFGEALARRVY
OsSLR1 239 IRLVHALLACAEAVQQENFAAAEALVKQIPTLAA----SQGGAMRKVAAYFGEALARRVY
AtrDELLA1 189 IRLVHTLMACAEAVQQENMNAAEALVKQIGMLAV----SQAGAMRKVATFFAEALARRIF
AtrDELLA2 130 IRLIHLLMSCAGSVERGEREIALKLVQEMRLLLCR---NITGVIGKVAVFFVDALFWRLS
PtRGA1 222 IRVVHLLMGCAEAIQRNNLKVASDLVREIRMTVNS---APCGAMDKVASHFVEALARRIC
CrDELLAa 396 IKLVHLLMACAEAIQNNALAAAVDMVREIKRLAS----STRGTMSKVANYFVESLARCIY
CrDELLAb 408 IKLVHLLMACAEAIQNDELAAAVDMVREIKRLAS----CTSGAMSKIASYFAESLSQRIY
SkDELLA 193 VQLVHLLLACADAVQRREIPAAGDMARKLRSMLAGGAADSSGAMGRVAAHFVEGLCRRIF
SmDELLAa 140 VRLVHLLLACANAVQRGDLAAAGDMVAQLRILVAH-PSSSSSAMARVATQFVEALSRRIQ
EsDELLA 183 VQLVHSLLACAESIQRGNLILAEETLHRIQMLAL----P-PGPMGKVATHFIDALNRRIY
TauDELLA 210 VQLVHSLLGCAEAIQRGNLNLAEQTLHRIQLLGL----P-PGPMGKVATHFIDALARRVY
HcDELLA 203 VQLVHSLLACAEAIQRGNLKLAEETLHRMQLLGL----P-PGPMGKVATHFIDALARRVY
SfaDELLA 203 VQLVHSLLACAEAIQRGNLKLAEQTLHRMQVLGL----P-PGPMGKVATHFIDALVRRVY
PpDELLAa 182 IQLVHSLLACAESIQRGNLSFAEETLRRIELLSL----P-PGPMGKVATHFIGALTRRIY
PpDELLAb 181 VRLVHSLLACAESIQRGNLNLAEQTLRRIQLLSL----P-PGPMGKVATHFIDALTCRIY
SfDELLAa 219 VQLVHSLLACAEAVQHGDLVRAEETVRHIQLLAS----P-PGPMGKVAAHFIEALTRRIY
MpDELLA 194 VRLVHLLLACAEAVQRSDVRMAEDTVRRIQMLAT----PQRGPMGKVAAHFVEALARRIF
AaDELLA 367 VRLVHLLVTCAQAVHSNDMVRADETVRQIQDLAYLSR-GSTGPMEKVAVHFVDALVRRIY
ApDELLA 334 VRLVHLLVTCAQAVHSNDMVRADETVRQIQDLAYLSR-GSTGPMEKVAVHFVDALVRRIY

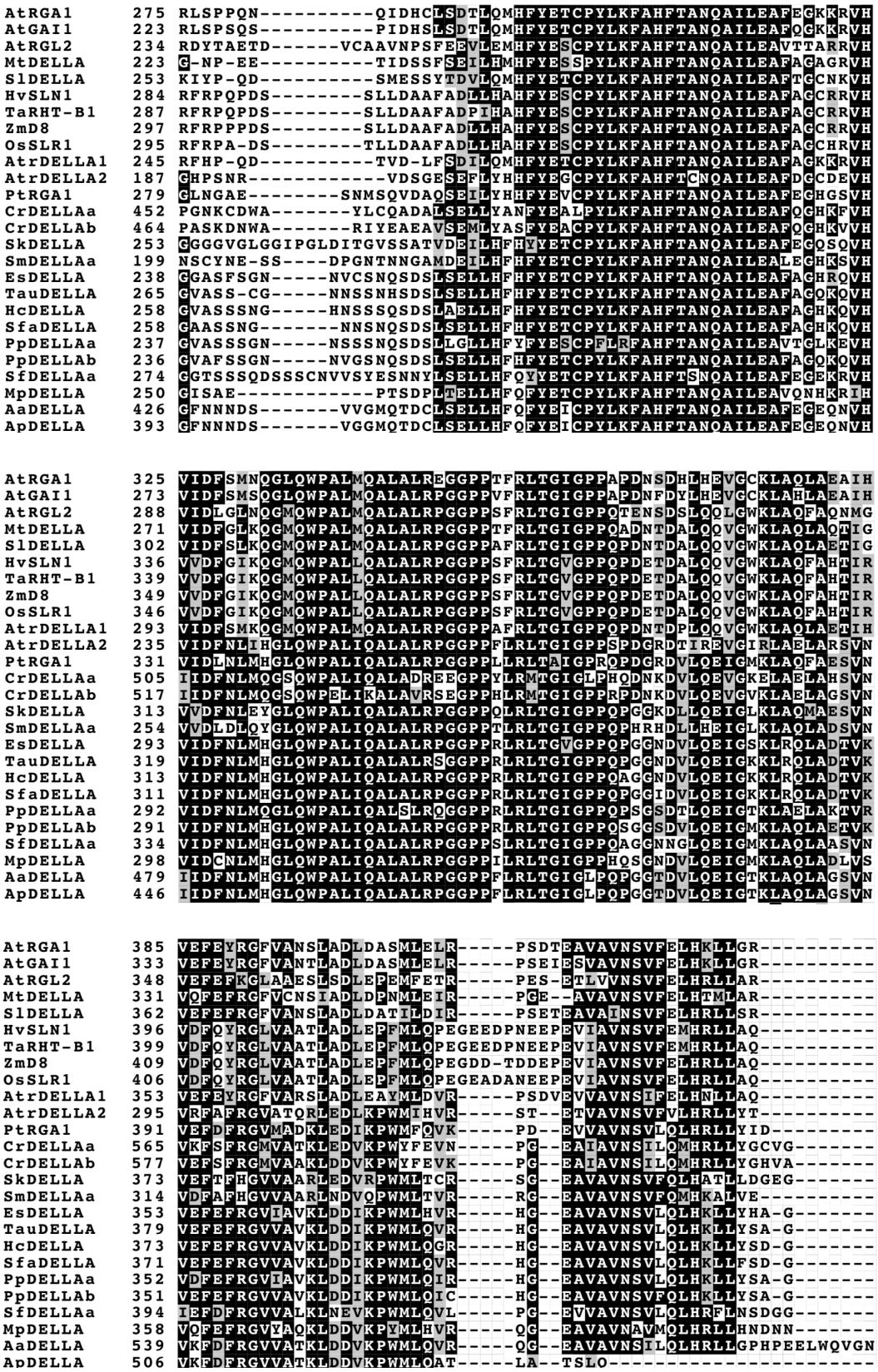
AtRGA1 275 RLSPPQN----------QIDHCLSDTLQMHFYETCPYLKFAHFTANQAILEAFEGKKRVH
AtGAI1 223 RLSPSQS----------PIDHSLSDTLQMHFYETCPYLKFAHFTANQAILEAFQGKKRVH
AtRGL2 234 RDYTAETD------VCAAVNPSFEEVLEMHFYESCPYLKFAHFTANQAILEAVTTARRVH
MtDELLA 223 G-NP-EE----------TIDSSFSEILHMHFYESSPYLKFAHFTANQAILEAFAGAGRVH
SlDELLA 253 KIYP-QD----------SMESSYTDVLQMHFYETCPYLKFAHFTANQAILEAFTGCNKVH
HvSLN1 284 RFRPQPDS--------SLLDAAFADLLHAHFYESCPYLKFAHFTANQAILEAFAGCRRVH
TaRHT-B1 287 RFRPQPDS--------SLLDAAFADPIHAHFYESCPYLKFAHFTANQAILEAFAGCRRVH
ZmD8 297 RFRPPPDS--------SLLDAAFADLLHAHFYESCPYLKFAHFTANQAILEAFAGCRRVH
OsSLR1 295 RFRPA-DS--------TLLDAAFADLLHAHFYESCPYLKFAHFTANQAILEAFAGCHRVH
AtrDELLA1 245 RFHP-QD----------TVD-LFSDILQMHFYETCPYLKFAHFTANQAILEAFAGKKRVH
AtrDELLA2 187 GHPSNR------------VDSGESEFLYHHFYEGCPYLKFAHFTCNQAILEAFDGCDEVH
PtRGA1 279 GLNGAE--------SNMSQVDAQSEILYHHFYEVCPYLKFAHFTANQAILEAFEGHGSVH
CrDELLAa 452 PGNKCDWA-------YLCQADALSELLYANFYEALPYLKFAHFTANQAILEAFQGHKFVH
CrDELLAb 464 PASKDNWA-------RIYEAEAVSEMLYASFYEACPYLKFAHFTANQAILEAFQGHKVVH
SkDELLA 253 GGGGVGLGGIPGLDITGVSSATVDEILHFHYYETCPYLKFAHFTANQAILEAFEGQSQVH
SmDELLAa 199 NSCYNE-SS----DPGNTNNGAMDEILHFHFYETCPYLKFAHFTANQAILEALEGHKSVH
EsDELLA 238 GGASFSGN-----NVCSNQSDSLSELLHFHFYETCPYLKFAHFTANQAILEAFAGHRQVH
TauDELLA 265 GVASS-CG-----NNSSNHSDSLSELLHFHFYETCPYLKFAHFTANQAILEAFAGQKQVH
HcDELLA 258 GVASSSNG-----HNSSSQSDSLAELLHFHFYETCPYLKFAHFTANQAILEAFAGHKQVH
SfaDELLA 258 GAASSNG-------NNSNQSDSLSELLHFHFYETCPYLKFAHFTANQAILEAFAGHKQVH
PpDELLAa 237 GVASSSGN-----NSSSNQSDSLLGLLHFYFYESCPFLRFAHFTANQAILEAVTGLKEVH
PpDELLAb 236 GVAFSSGN-----NVGSNQSDSLSELLHFHFYETCPYLKFAHFTANQAILEAFAGQKQVH
SfDELLAa 274 GGTSSSQDSSSCNVVSYESNNYLSELLHFQYYETCPYLKFAHFTSNQAILEAFEGEKRVH
MpDELLA 250 GISAE----------PTSDPLTELLHFQFYETCPYLKFAHFTANQAILEAVQNHKRIH
AaDELLA 426 GFNNNDS-------VVGMQTDCLSELLHFQFYEICPYLKFAHFTANQAILEAFEGEQNVH
ApDELLA 393 GFNNNDS-------VGGMQTDCLSELLHFQFYEICPYLKFAHFTANQAILEAFEGEQNVH
AtRGA1 325 VIDFSMNQGLQWPALMQALALREGGPPTFRLTGIGPPAPDNSDHLHEVGCKLAQLAEAIH
AtGAI1 273 VIDFSMSQGLQWPALMQALALRPGGPPVFRLTGIGPPAPDNFDYLHEVGCKLAHLAEAIH
AtRGL2 288 VIDLGLNQGMQWPALMQALALRPGGPPSFRLTGIGPPQTENSDSLQQLGWKLAQFAQNMG
MtDELLA 271 VIDFGLKQGMQWPALMQALALRPGGPPTFRLTGIGPPQADNTDALQQVGWKLAQLAQTIG
SlDELLA 302 VIDFSLKQGMQWPALMQALALRPGGPPAFRLTGIGPPQPDNTDALQQVGWKLAQLAETIG
HvSLN1 336 VVDFGIKQGMQWPALLQALALRPGGPPSFRLTGVGPPQPDETDALQQVGWKLAQFAHTIR
TaRHT-B1 339 VVDFGIKQGMQWPALLQALALRPGGPPSFRLTGVGPPQPDETDALQQVGWKLAQFAHTIR
ZmD8 349 VVDFGIKQGMQWPALLQALALRPGGPPSFRLTGVGPPQPDETDALQQVGWKLAQFAHTIR
OsSLR1 346 VVDFGIKQGMQWPALLQALALRPGGPPSFRLTGVGPPQPDETDALQQVGWKLAQFAHTIR
AtrDELLA1 293 VIDFSMKQGMQWPALMQALALRPGGPPAFRLTGIGPPQPDNTDPLQQVGWKLAQLAETIH
AtrDELLA2 235 VIDFNLIHGLQWPALIQALALRPGGPPFLRLTGIGPPSPDGRDTIREVGIRLAELARSVN
PtRGA1 331 VIDLNLMHGLQWPALIQALALRPGGPPLLRLTAIGPRQPDGRDVLQEIGMKLAQFAESVN
CrDELLAa 505 IIDFNLMQGSQWPALIQALADREEGPPYLRMTGIGLPHQDNKDVLQEVGKELAELAHSVN
CrDELLAb 517 IIDFNLMQGSQWPELIKALAVRSEGPPHLRMTGIGPPRPDNKDVLQEVGVKLAELAGSVN
SkDELLA 313 VVDFNLEYGLQWPALIQALALRPGGPPQLRLTGIGPPQPGGKDLLQEIGLKLAQMAESVN
SmDELLAa 254 VVDLDLQYGLQWPALIQALALRPGGPPTLRLTGIGPPQPHRHDLLHEIGLKLAQLADSVN
EsDELLA 293 VIDFNLMHGLQWPALIQALALRPGGPPRLRLTGVGPPQPGGNDVLQEIGSKLRQLADTVK
TauDELLA 319 VIDFNLMHGLQWPALIQALALRSGGPPRLRLTGIGPPQPGGNDVLQEIGKKLRQLADTVK
HcDELLA 313 VIDFNLMHGLQWPALIQALALRPGGPPRLRLTGIGPPQAGGNDVLQEIGKKLRQLADTVK
SfaDELLA 311 VIDFNLMHGLQWPALIQALALRPGGPPRLRLTGIGPPQPGGIDVLQEIGKKLRQLADTVK
PpDELLAa 292 VIDFNLMQGLQWPALIQALSLRQGGPPRLRLTGIGPPQPSGSDTLQEIGTKLAELAKTVR
PpDELLAb 291 VIDFNLMHGLQWPALIQALALRPGGPPRLRLTGIGPPQSGGSDVLQEIGMKLAQLAETVK
SfDELLAa 334 VIDFNLMHGLQWPALIQALALRPGGPPSLRLTGIGPPQAGGNNGLQEIGMKLAQLAASVN
MpDELLA 298 VIDCNLMHGLQWPALIQALALRPGGPPILRLTGIGPPHQSGNDVLQEIGMKLAQLADLVS
AaDELLA 479 IIDFNLMHGLQWPALIQALALRPGGPPFLRLTGIGLPQPGGTDVLQEIGTKLAQLAGSVN
ApDELLA 446 IIDFNLMHGLQWPALIQALALRPGGPPFLRLTGIGLPQPGGTDVLQEIGTKLAQLAGSVN
AtRGA1 385 VEFEYRGFVANSLADLDASMLELR-----PSDTEAVAVNSVFELHKLLGR----------
AtGAI1 333 VEFEYRGFVANTLADLDASMLELR-----PSEIESVAVNSVFELHKLLGR----------
AtRGL2 348 VEFEFKGLAAESLSDLEPEMFETR-----PES-ETLVVNSVFELHRLLAR----------
MtDELLA 331 VQFEFRGFVCNSIADLDPNMLEIR-----PGE--AVAVNSVFELHTMLAR----------
SlDELLA 362 VEFEFRGFVANSLADLDATILDIR-----PSETEAVAINSVFELHRLLSR----------
HvSLN1 396 VDFQYRGLVAATLADLEPFMLQPEGEEDPNEEPEVIAVNSVFEMHRLLAQ----------
TaRHT-B1 399 VDFQYRGLVAATLADLEPFMLQPEGEEDPNEEPEVIAVNSVFEMHRLLAQ----------
ZmD8 409 VDFQYRGLVAATLADLEPFMLQPEGDD-TDDEPEVIAVNSVFELHRLLAQ----------
OsSLR1 406 VDFQYRGLVAATLADLEPFMLQPEGEADANEEPEVIAVNSVFELHRLLAQ----------
AtrDELLA1 353 VEFEYRGFVARSLADLEAYMLDVR-----PSDVEVVAVNSIFELHNLLAQ----------
AtrDELLA2 295 VRFAFRGVATQRLEDLKPWMIHVR-----ST--ETVAVNSVFVLHRLLYT----------
PtRGA1 391 VEFDFRGVMADKLEDIKPWMFQVK-----PD--EVVAVNSVLQLHRLLYID---------
CrDELLAa 565 VKFSFRGMVATKLEDVKPWYFEVN-----PG--EAIAVNSILQMHRLLYGCVG-------
CrDELLAb 577 VEFSFRGMVAAKLDDVKPWYFEVK-----PG--EAIAVNSILQMHRLLYGHVA-------
SkDELLA 373 VEFTFHGVVAARLEDVRPWMLTCR-----SG--EAVAVNSVFQLHATLLDGEG-------
SmDELLAa 314 VDFAFHGVVAARLNDVQPWMLTVR-----RG--EAVAVNSVFQMHKALVE----------
EsDELLA 353 VEFEFRGVIAVKLDDIKPWMLHVR-----HG--EAVAVNSVLQLHKLLYHA-G-------
TauDELLA 379 VEFEFRGVVAVKLDDIKPWMLQVR-----HG--EAVAVNSVLQLHKLLYSA-G-------
HcDELLA 373 VEFEFRGVVAVKLDDIKPWMLQGR-----HG--EAVAVNSVLQLHKLLYSD-G-------
SfaDELLA 371 VEFEFRGVVAVKLDDIKPWMLQVR-----HG--EAVAVNSVLQLHKLLFSD-G-------
PpDELLAa 352 VDFEFRGVIAVKLDDIKPWMLQIR-----HG--EAVAVNSVLQLHKLLYSA-G-------
PpDELLAb 351 VEFEFRGVVAVKLDDIKPWMLQIC-----HG--EAVAVNSVFQLHKLLYSA-G-------
SfDELLAa 394 IEFDFRGVVALKLNEVKPWMLQVL-----PG--EVVAVNSVLQLHRFLNSDGG-------
MpDELLA 358 VQFEFRGVYAQKLDDVKPYMLHVR-----QG--EAVAVNAVMQLHRLLHNDNN-------
AaDELLA 539 VKFDFRGVVATKLDDVKPWMLQVR-----QG--EAVAVNSILQLHRLLGPHPEELWQVGN
ApDELLA 506 VKFDFRGVVATKLDDVKPWMLQAT-----LA--TSLQ----------

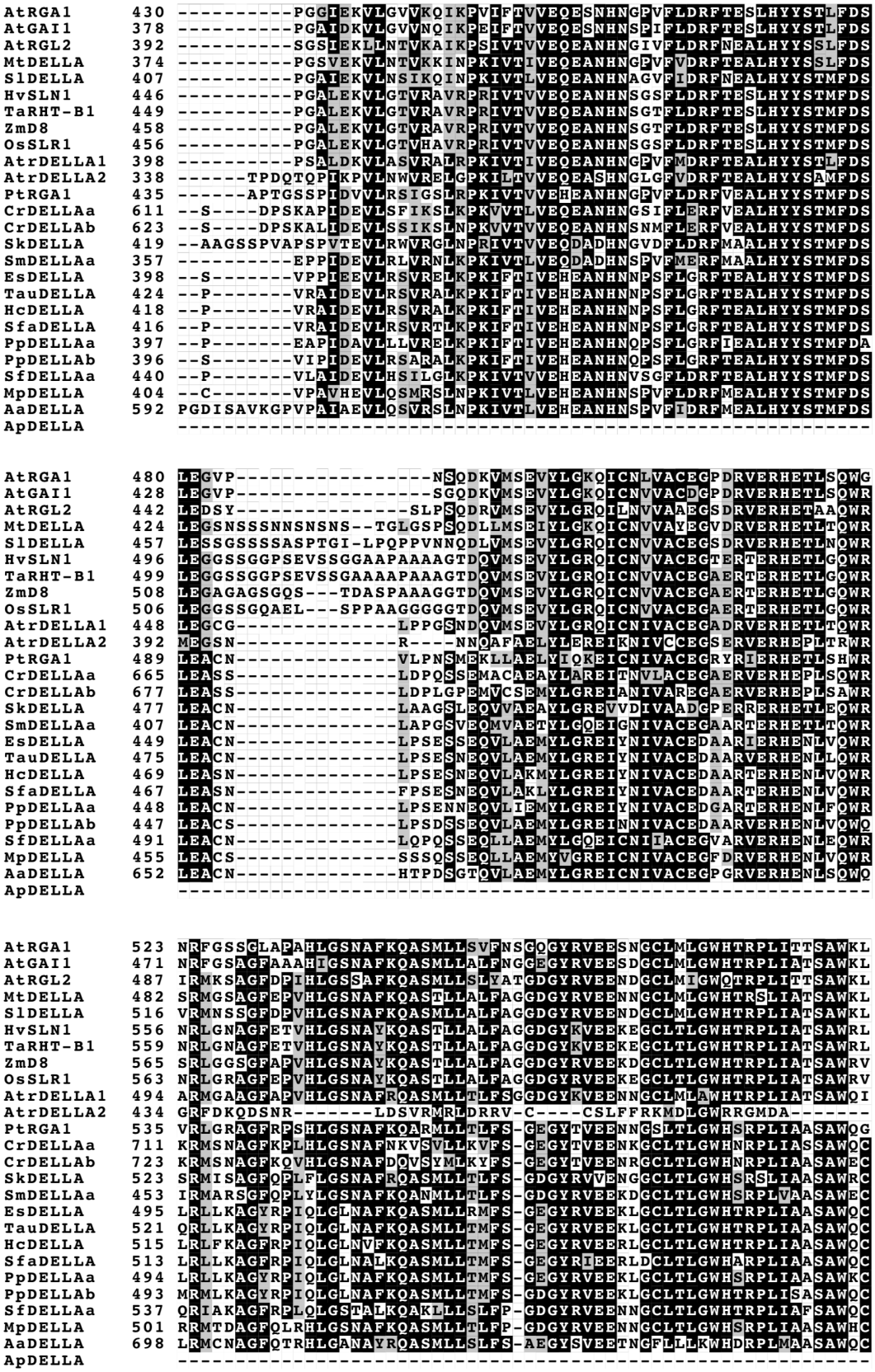
AtRGA1 430 ----------PGGIEKVLGVVKQIKPVIFTVVEQESNHNGPVFLDRFTESLHYYSTLFDS
AtGAI1 378 ----------PGAIDKVLGVVNQIKPEIFTVVEQESNHNSPIFLDRFTESLHYYSTLFDS
AtRGL2 392 ----------SGSIEKLLNTVKAIKPSIVTVVEQEANHNGIVFLDRFNEALHYYSSLFDS
MtDELLA 374 ----------PGSVEKVLNTVKKINPKIVTIVEQEANHNGPVFVDRFTEALHYYSSLFDS
SlDELLA 407 ----------PGAIEKVLNSIKQINPKIVTLVEQEANHNAGVFIDRFNEALHYYSTMFDS
HvSLN1 446 ----------PGALEKVLGTVRAVRPRIVTVVEQEANHNSGSFLDRFTESLHYYSTMFDS
TaRHT-B1 449 ----------PGALEKVLGTVRAVRPRIVTVVEQEANHNSGTFLDRFTESLHYYSTMFDS
ZmD8 458 ----------PGALEKVLGTVRAVRPRIVTVVEQEANHNSGTFLDRFTESLHYYSTMFDS
OsSLR1 456 ----------PGALEKVLGTVHAVRPRIVTVVEQEANHNSGSFLDRFTESLHYYSTMFDS
AtrDELLA1 398 ----------PSALDKVLASVRALRPKIVTIVEQEANHNGPVFMDRFTEALHYYSTLFDS
AtrDELLA2 338 ------TPDQTQPIKPVLNWVRELGPKILTVVEQEASHNGLGFVDRFTEALHYYSAMFDS
PtRGA1 435 ------APTGSSPIDVVLRSIGSLRPKIVTVVEHEANHNGPVFLDRFVEALHYYSTMFDS
CrDELLAa 611 --S----DPSKAPIDEVLSFIKSLKPKVVTLVEQEANHNGSIFLERFVEALHYYSTMFDS
CrDELLAb 623 --S----DPSKALIDEVLSSIKSLNPKVVTVVEQEANHNSNMFLERFVEALHYYSTMFDS
SkDELLA 419 --AAGSSPVAPSPVTEVLRWVRGLNPRIVTVVEQDADHNGVDFLDRFMAALHYYSTMFDS
SmDELLAa 357 ----------EPPIDEVLRLVRNLKPKIVTLVEQDADHNSPVFMERFMAALHYYSTMFDS
EsDELLA 398 --S-------VPPIEEVLRSVRELKPKIFTIVEHEANHNNPSFLGRFTEALHYYSTMFDS
TauDELLA 424 --P-------VRAIDEVLRSVRALKPKIFTIVEHEANHNNPSFLGRFTEALHYYSTMFDS
HcDELLA 418 --P-------VRAIDEVLRSVRALKPKIFTIVEHEANHNNPSFLGRFTEALHYYSTMFDS
SfaDELLA 416 --P-------VRAIDEVLRSVRTLKPKIFTIVEHEANHNNPSFLGRFTEALHYYSTMFDS
PpDELLAa 397 --P-------EAPIDAVLLLVRELKPKIFTIVEHEANHNQPSFLGRFIEALHYYSTMFDA
PpDELLAb 396 --S-------VIPIDEVLRSARALKPKIFTIVEHEANHNQPSFLGRFTEALHYYSTMFDS
SfDELLAa 440 --P-------VLAIDEVLHSILGLKPKIVTVVEHEANHNVSGFLDRFTEALHYYSTMFDS
MpDELLA 404 --C-------VPAVHEVLQSMRSLNPKIVTLVEHEANHNSPVFLDRFMEALHYYSTMFDS
AaDELLA 592 PGDISAVKGPVPAIAEVLQSVRSLNPKIVTLVEHEANHNSPVFIDRFMEALHYYSTMFDS
ApDELLA ----------
AtRGA1 480 LEGVP----------NSQDKVMSEVYLGKQICNLVACEGPDRVERHETLSQWG
AtGAI1 428 LEGVP----------SGQDKVMSEVYLGKQICNVVACDGPDRVERHETLSQWR
AtRGL2 442 LEDSY----------SLPSQDRVMSEVYLGRQILNVVAAEGSDRVERHETAAQWR
MtDELLA 424 LEGSNSSSNNSNSNS--TGLGSPSQDLLMSEIYLGKQICNVVAYEGVDRVERHETLTQWR
SlDELLA 457 LESSGSSSSASPTGI-LPQPPVNNQDLVMSEVYLGRQICNVVACEGSDRVERHETLNQWR
HvSLN1 496 LEGGSSGGPSEVSSGGAAPAAAAGTDQVMSEVYLGRQICNVVACEGTERTERHETLGQWR
TaRHT-B1 499 LEGGSSGGPSEVSSGAAAAPAAAGTDQVMSEVYLGRQICNVVACEGAERTERHETLGQWR
ZmD8 508 LEGAGAGSGQS---TDASPAAAGGTDQVMSEVYLGRQICNVVACEGAERTERHETLGQWR
OsSLR1 506 LEGGSSGQAEL---SPPAAGGGGGTDQVMSEVYLGRQICNVVACEGAERTERHETLGQWR
AtrDELLA1 448 LEGCG----------LPPGSNDQVMSEVYLGRQICNIVACEGADRVERHETLTQWR
AtrDELLA2 392 MEGSN----------R----NNQAFAELYLEREIKNIVCCEGSERVERHEPLTRWR
PtRGA1 489 LEACN----------VLPNSMEKLLAELYIQKEICNIVACEGRYRIERHETLSHWR
CrDELLAa 665 LEASS----------LDPQSSEMACAEAYLAREITNVLACEGAERVERHEPLSQWR
CrDELLAb 677 LEASS----------LDPLGPEMVCSEMYLGREIANIVAREGAERVERHEPLSAWR
SkDELLA 477 LEACN----------LAAGSLEQVVAEAYLGREVVDIVAADGPERRERHETLEQWR
SmDELLAa 407 LEACN----------LAPGSVEQMVAETYLGQEIGNIVACEGAARTERHETLTQWR
EsDELLA 449 LEACN----------LPSESSEQVLAEMYLGREIYNIVACEDAARIERHENLVQWR
TauDELLA 475 LEACN----------LPSESNEQVLAEMYLGREIYNIVACEDAARVERHENLLQWR
HcDELLA 469 LEASN----------LPSESNEQVLAKMYLGREIYNIVACEDAARTERHENLVQWR
SfaDELLA 467 LEASN----------FPSESNEQVLAKLYLGREIYNIVACEDAARTERHENLVQWR
PpDELLAa 448 LEACN----------LPSENNEQVLIEMYLGREIYNIVACEDGARTERHENLFQWR
PpDELLAb 447 LEACS----------LPSDSSEQVLAEMYLGREINNIVACEDAARVERHENLVQWQ
SfDELLAa 491 LEACN----------LQPQSSEQLLAEMYLGQEICNIIACEGVARVERHENLEQWR
MpDELLA 455 LEACS----------SSSQSSEQLLAEMYVGREICNIVACEGFDRVERHENLVQWR
AaDELLA 652 LEACN----------HTPDSGTQVLAEMYLGREICNIVACEGPGRVERHENLSQWQ
ApDELLA ----------
AtRGA1 523 NRFGSSGLAPAHLGSNAFKQASMLLSVFNSGQGYRVEESNGCLMLGWHTRPLITTSAWKL
AtGAI1 471 NRFGSAGFAAAHIGSNAFKQASMLLALFNGGEGYRVEESDGCLMLGWHTRPLIATSAWKL
AtRGL2 487 IRMKSAGFDPIHLGSSAFKQASMLLSLYATGDGYRVEENDGCLMIGWQTRPLITTSAWKL
MtDELLA 482 SRMGSAGFEPVHLGSNAFKQASTLLALFAGGDGYRVEENNGCLMLGWHTRSLIATSAWKL
SlDELLA 516 VRMNSSGFDPVHLGSNAFKQASMLLALFAGGDGYRVEENDGCLMLGWHTRPLIATSAWKL
HvSLN1 556 NRLGNAGFETVHLGSNAYKQASTLLALFAGGDGYKVEEKEGCLTLGWHTRPLIATSAWRL
TaRHT-B1 559 NRLGNAGFETVHLGSNAYKQASTLLALFAGGDGYKVEEKEGCLTLGWHTRPLIATSAWRL
ZmD8 565 SRLGGSGFAPVHLGSNAYKQASTLLALFAGGDGYRVEEKDGCLTLGWHTRPLIATSAWRV
OsSLR1 563 NRLGRAGFEPVHLGSNAYKQASTLLALFAGGDGYRVEEKEGCLTLGWHTRPLIATSAWRV
AtrDELLA1 494 ARMGAAGFAPVHLGSNAFRQASMLLTLFSGGDGYKVEENNGCLMLAWHTRPLIATSAWQI
AtrDELLA2 434 GRFDKQDSNR-------LDSVRMRLDRRV-C-----CSLFFRKMDLGWRRGMDA--------
PtRGA1 535 VRLGRAGFRPSHLGSNAFKQARMLLTLFS-GEGYTVEENNGSLTLGWHSRPLIAASAWQG
CrDELLAa 711 KRMSNAGFKPLHLGSNAFNKVSVLLKVFS-GEGYTVEENKGCLTLGWHNRPLIASSAWQC
CrDELLAb 723 KRMSNAGFKQVHLGSNAFDQVSYMLKYFS-GEGYTVEENRGCLTLGWHNRPLIAASAWEC
SkDELLA 523 SRMISAGFQPLFLGSNAFRQASMLLTLFS-GDGYRVVENGGCLTLGWHSRSLIAASAWRC
SmDELLAa 453 IRMARSGFQPLYLGSNAFKQANMLLTLFS-GDGYRVEEKDGCLTLGWHSRPLVAASAWEC
EsDELLA 495 LRLLKAGYRPIQLGLNAFKQASMLLRMFS-GEGYRVEEKLGCLTLGWHTRPLIAASAWQC
TauDELLA 521 QRLLKAGYRPIQLGLNAFKQASMLLTMFS-GEGYRVEEKLGCLTLGWHTRPLIAASAWQC
HcDELLA 515 LRLFKAGFRPIQLGLNVFKQASMLLTMFS-GEGYRVEERLGCLTLGWHTRPLIAASAWQC
SfaDELLA 513 LRLLKAGFRPIQLGLNALKQASMLLTMFS-GEGYRIEERLDCLTLGWHARPLIAASAWQC
PpDELLAa 494 LRLLKAGYRPIQLGLNAFKQASMLLTMFS-GEGYRVEEKLGCLTLGWHSRPLIAASAWKC
PpDELLAb 493 MRMLKAGYRPIQLGLNAFKQASMLLTMFS-GDGYRVEEKLGCLTLGWHTRPLISASAWQC
SfDELLAa 537 QRIAKAGFRPLQLGSTALKQAKLLLSLFP-GDGYRVEENNGCLTLGWHTRPLIAFSAWQC
MpDELLA 501 RRMTDAGFQLRHLGSNAFKQASMLLTLFP-GDGYRVEENNGCLTLGWHSRPLIAASAWHC
AaDELLA 698 LRMCNAGFQTRHLGANAYRQASMLLSLFS-AEGYSVEETNGFLLLKWHDRPLMAASAWQC
ApDELLA ----------

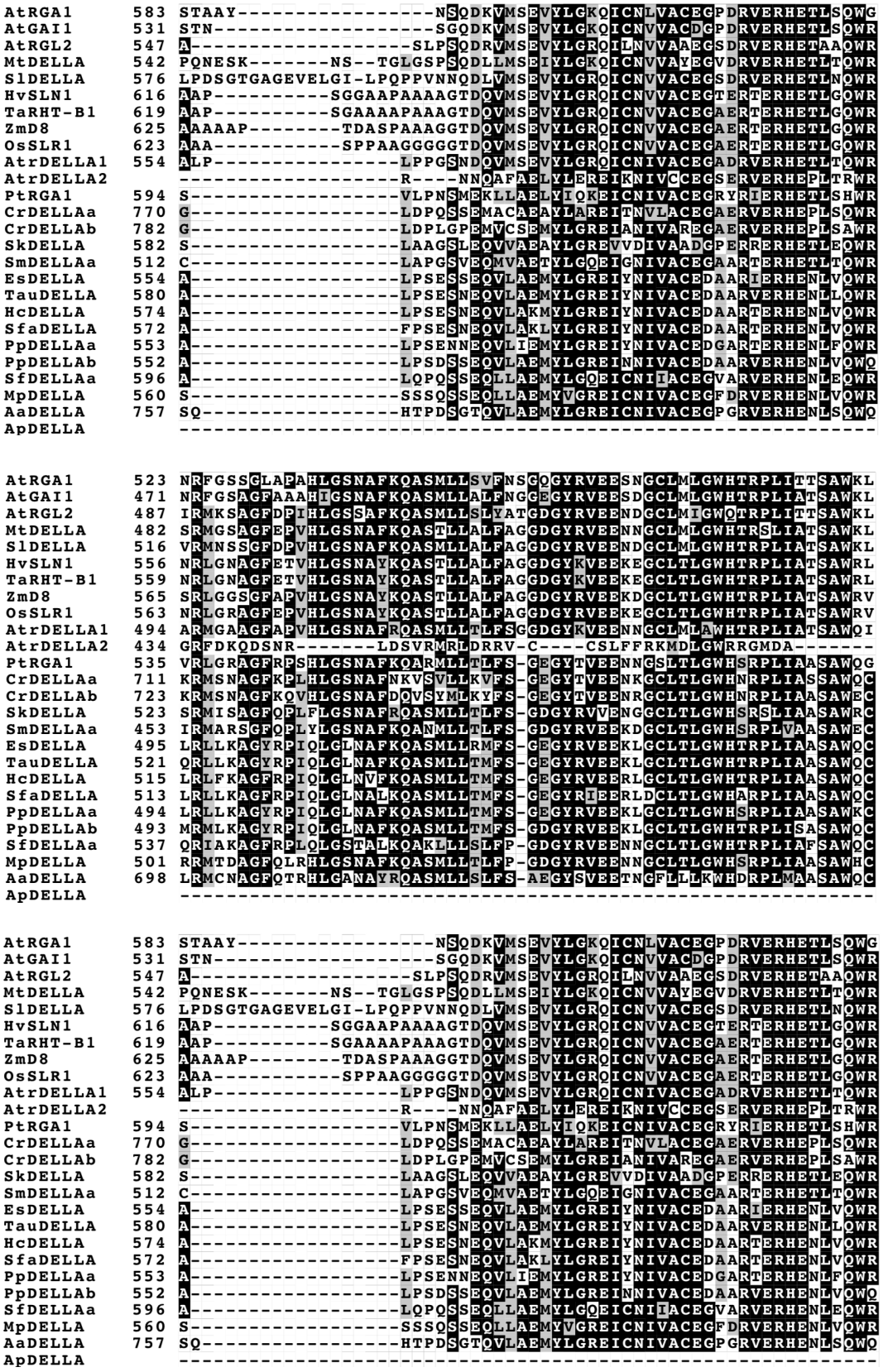
AtRGA1 583 STAAY----------NSQDKVMSEVYLGKQICNLVACEGPDRVERHETLSQWG
AtGAI1 531 STN----------SGQDKVMSEVYLGKQICNVVACDGPDRVERHETLSQWR
AtRGL2 547 A----------SLPSQDRVMSEVYLGRQILNVVAAEGSDRVERHETAAQWR
MtDELLA 542 PQNESK-------NS--TGLGSPSQDLLMSEIYLGKQICNVVAYEGVDRVERHETLTQWR
SlDELLA 576 LPDSGTGAGEVELGI-LPQPPVNNQDLVMSEVYLGRQICNVVACEGSDRVERHETLNQWR
HvSLN1 616 AAP----------SGGAAPAAAAGTDQVMSEVYLGRQICNVVACEGTERTERHETLGQWR
TaRHT-B1 619 AAP----------SGAAAAPAAAGTDQVMSEVYLGRQICNVVACEGAERTERHETLGQWR
ZmD8 625 AAAAAP---------TDASPAAAGGTDQVMSEVYLGRQICNVVACEGAERTERHETLGQWR
OsSLR1 623 AAA----------SPPAAGGGGGTDQVMSEVYLGRQICNVVACEGAERTERHETLGQWR
AtrDELLA1 554 ALP----------LPPGSNDQVMSEVYLGRQICNIVACEGADRVERHETLTQWR
AtrDELLA2 ----------R----NNQAFAELYLEREIKNIVCCEGSERVERHEPLTRWR
PtRGA1 594 S----------VLPNSMEKLLAELYIQKEICNIVACEGRYRIERHETLSHWR
CrDELLAa 770 G----------LDPQSSEMACAEAYLAREITNVLACEGAERVERHEPLSQWR
CrDELLAb 782 G----------LDPLGPEMVCSEMYLGREIANIVAREGAERVERHEPLSAWR
SkDELLA 582 S----------LAAGSLEQVVAEAYLGREVVDIVAADGPERRERHETLEQWR
SmDELLAa 512 C----------LAPGSVEQMVAETYLGQEIGNIVACEGAARTERHETLTQWR
EsDELLA 554 A----------LPSESSEQVLAEMYLGREIYNIVACEDAARIERHENLVQWR
TauDELLA 580 A----------LPSESNEQVLAEMYLGREIYNIVACEDAARVERHENLLQWR
HcDELLA 574 A----------LPSESNEQVLAKMYLGREIYNIVACEDAARTERHENLVQWR
SfaDELLA 572 A----------FPSESNEQVLAKLYLGREIYNIVACEDAARTERHENLVQWR
PpDELLAa 553 A----------LPSENNEQVLIEMYLGREIYNIVACEDGARTERHENLFQWR
PpDELLAb 552 A----------LPSDSSEQVLAEMYLGREINNIVACEDAARVERHENLVQWQ
SfDELLAa 596 A----------LQPQSSEQLLAEMYLGQEICNIIACEGVARVERHENLEQWR
MpDELLA 560 S----------SSSQSSEQLLAEMYVGREICNIVACEGFDRVERHENLVQWR
AaDELLA 757 SQ----------HTPDSGTQVLAEMYLGREICNIVACEGPGRVERHENLSQWQ
ApDELLA ----------
AtRGA1 523 NRFGSSGLAPAHLGSNAFKQASMLLSVFNSGQGYRVEESNGCLMLGWHTRPLITTSAWKL
AtGAI1 471 NRFGSAGFAAAHIGSNAFKQASMLLALFNGGEGYRVEESDGCLMLGWHTRPLIATSAWKL
AtRGL2 487 IRMKSAGFDPIHLGSSAFKQASMLLSLYATGDGYRVEENDGCLMIGWQTRPLITTSAWKL
MtDELLA 482 SRMGSAGFEPVHLGSNAFKQASTLLALFAGGDGYRVEENNGCLMLGWHTRSLIATSAWKL
SlDELLA 516 VRMNSSGFDPVHLGSNAFKQASMLLALFAGGDGYRVEENDGCLMLGWHTRPLIATSAWKL
HvSLN1 556 NRLGNAGFETVHLGSNAYKQASTLLALFAGGDGYKVEEKEGCLTLGWHTRPLIATSAWRL
TaRHT-B1 559 NRLGNAGFETVHLGSNAYKQASTLLALFAGGDGYKVEEKEGCLTLGWHTRPLIATSAWRL
ZmD8 565 SRLGGSGFAPVHLGSNAYKQASTLLALFAGGDGYRVEEKDGCLTLGWHTRPLIATSAWRV
OsSLR1 563 NRLGRAGFEPVHLGSNAYKQASTLLALFAGGDGYRVEEKEGCLTLGWHTRPLIATSAWRV
AtrDELLA1 494 ARMGAAGFAPVHLGSNAFRQASMLLTLFSGGDGYKVEENNGCLMLAWHTRPLIATSAWQI
AtrDELLA2 434 GRFDKQDSNR-------LDSVRMRLDRRV-C----CSLFFRKMDLGWRRGMDA-------
PtRGA1 535 VRLGRAGFRPSHLGSNAFKQARMLLTLFS-GEGYTVEENNGSLTLGWHSRPLIAASAWQG
CrDELLAa 711 KRMSNAGFKPLHLGSNAFNKVSVLLKVFS-GEGYTVEENKGCLTLGWHNRPLIASSAWQC
CrDELLAb 723 KRMSNAGFKQVHLGSNAFDQVSYMLKYFS-GEGYTVEENRGCLTLGWHNRPLIAASAWEC
SkDELLA 523 SRMISAGFQPLFLGSNAFRQASMLLTLFS-GDGYRVVENGGCLTLGWHSRSLIAASAWRC
SmDELLAa 453 IRMARSGFQPLYLGSNAFKQANMLLTLFS-GDGYRVEEKDGCLTLGWHSRPLVAASAWEC
EsDELLA 495 LRLLKAGYRPIQLGLNAFKQASMLLRMFS-GEGYRVEEKLGCLTLGWHTRPLIAASAWQC
TauDELLA 521 QRLLKAGYRPIQLGLNAFKQASMLLTMFS-GEGYRVEEKLGCLTLGWHTRPLIAASAWQC
HcDELLA 515 LRLFKAGFRPIQLGLNVFKQASMLLTMFS-GEGYRVEERLGCLTLGWHTRPLIAASAWQC
SfaDELLA 513 LRLLKAGFRPIQLGLNALKQASMLLTMFS-GEGYRIEERLDCLTLGWHARPLIAASAWQC
PpDELLAa 494 LRLLKAGYRPIQLGLNAFKQASMLLTMFS-GEGYRVEEKLGCLTLGWHSRPLIAASAWKC
PpDELLAb 493 MRMLKAGYRPIQLGLNAFKQASMLLTMFS-GDGYRVEEKLGCLTLGWHTRPLISASAWQC
SfDELLAa 537 QRIAKAGFRPLQLGSTALKQAKLLLSLFP-GDGYRVEENNGCLTLGWHTRPLIAFSAWQC
MpDELLA 501 RRMTDAGFQLRHLGSNAFKQASMLLTLFP-GDGYRVEENNGCLTLGWHSRPLIAASAWHC
AaDELLA 698 LRMCNAGFQTRHLGANAYRQASMLLSLFS-AEGYSVEETNGFLLLKWHDRPLMAASAWQC
ApDELLA ----------
AtRGA1 583 STAAY----------NSQDKVMSEVYLGKQICNLVACEGPDRVERHETLSQWG
AtGAI1 531 STN----------SGQDKVMSEVYLGKQICNVVACDGPDRVERHETLSQWR
AtRGL2 547 A----------SLPSQDRVMSEVYLGRQILNVVAAEGSDRVERHETAAQWR
MtDELLA 542 PQNESK-------NS--TGLGSPSQDLLMSEIYLGKQICNVVAYEGVDRVERHETLTQWR
SlDELLA 576 LPDSGTGAGEVELGI-LPQPPVNNQDLVMSEVYLGRQICNVVACEGSDRVERHETLNQWR
HvSLN1 616 AAP----------SGGAAPAAAAGTDQVMSEVYLGRQICNVVACEGTERTERHETLGQWR
TaRHT-B1 619 AAP----------SGAAAAPAAAGTDQVMSEVYLGRQICNVVACEGAERTERHETLGQWR
ZmD8 625 AAAAAP---------TDASPAAAGGTDQVMSEVYLGRQICNVVACEGAERTERHETLGQWR
OsSLR1 623 AAA----------SPPAAGGGGGTDQVMSEVYLGRQICNVVACEGAERTERHETLGQWR
AtrDELLA1 554 ALP----------LPPGSNDQVMSEVYLGRQICNIVACEGADRVERHETLTQWR
AtrDELLA2 ----------R----NNQAFAELYLEREIKNIVCCEGSERVERHEPLTRWR
PtRGA1 594 S----------VLPNSMEKLLAELYIQKEICNIVACEGRYRIERHETLSHWR
CrDELLAa 770 G----------LDPQSSEMACAEAYLAREITNVLACEGAERVERHEPLSQWR
CrDELLAb 782 G----------LDPLGPEMVCSEMYLGREIANIVAREGAERVERHEPLSAWR
SkDELLA 582 S----------LAAGSLEQVVAEAYLGREVVDIVAADGPERRERHETLEQWR
SmDELLAa 512 C----------LAPGSVEQMVAETYLGQEIGNIVACEGAARTERHETLTQWR
EsDELLA 554 A----------LPSESSEQVLAEMYLGREIYNIVACEDAARIERHENLVQWR
TauDELLA 580 A----------LPSESNEQVLAEMYLGREIYNIVACEDAARVERHENLLQWR
HcDELLA 574 A----------LPSESNEQVLAKMYLGREIYNIVACEDAARTERHENLVQWR
SfaDELLA 572 A----------FPSESNEQVLAKLYLGREIYNIVACEDAARTERHENLVQWR
PpDELLAa 553 A----------LPSENNEQVLIEMYLGREIYNIVACEDGARTERHENLFQWR
PpDELLAb 552 A----------LPSDSSEQVLAEMYLGREINNIVACEDAARVERHENLVQWQ
SfDELLAa 596 A----------LQPQSSEQLLAEMYLGQEICNIIACEGVARVERHENLEQWR
MpDELLA 560 S----------SSSQSSEQLLAEMYVGREICNIVACEGFDRVERHENLVQWR
AaDELLA 757 SQ----------HTPDSGTQVLAEMYLGREICNIVACEGPGRVERHENLSQWQ
ApDELLA ----------